

**EPA-600/4-76-016b**  
**May 1976**

**Environmental Monitoring Series**

# **CONTINUED RESEARCH IN MESOSCALE AIR POLLUTION SIMULATION MODELING: Volume II - Refinements in the Treatment of Chemistry, Meteorology, and Numerical Integration Procedures**



**Environmental Sciences Research Laboratory  
Office of Research and Development  
U.S. Environmental Protection Agency  
Research Triangle Park, North Carolina 27711**

## **RESEARCH REPORTING SERIES**

Research reports of the Office of Research and Development, U.S. Environmental Protection Agency, have been grouped into five series. These five broad categories were established to facilitate further development and application of environmental technology. Elimination of traditional grouping was consciously planned to foster technology transfer and a maximum interface in related fields. The five series are:

1. Environmental Health Effects Research
2. Environmental Protection Technology
3. Ecological Research
4. Environmental Monitoring
5. Socioeconomic Environmental Studies

This report has been assigned to the ENVIRONMENTAL MONITORING series. This series describes research conducted to develop new or improved methods and instrumentation for the identification and quantification of environmental pollutants at the lowest conceivably significant concentrations. It also includes studies to determine the ambient concentrations of pollutants in the environment and/or the variance of pollutants as a function of time or meteorological factors.

May 1976

CONTINUED RESEARCH IN MESOSCALE AIR  
POLLUTION SIMULATION MODELING:  
VOLUME II - REFINEMENTS IN THE TREATMENT  
OF CHEMISTRY, METEOROLOGY, AND  
NUMERICAL INTEGRATION PROCEDURES

S. D. Reynolds  
J. Ames  
T. A. Hecht  
J. P. Meyer  
D. C. Whitney  
M. A. Yocke

Systems Applications, Incorporated  
950 Northgate Drive  
San Rafael, California 94903

68-02-1237

Project Officer

Kenneth L. Demerjian  
Meteorology and Assessment Division  
Environmental Sciences Research Laboratory  
Research Triangle Park, North Carolina 27711

U.S. ENVIRONMENTAL PROTECTION AGENCY  
OFFICE OF RESEARCH AND DEVELOPMENT  
ENVIRONMENTAL SCIENCES RESEARCH LABORATORY  
RESEARCH TRIANGLE PARK, NORTH CAROLINA 27711

## DISCLAIMER

This report has been reviewed by the Office of Research and Development, U.S. Environmental Protection Agency, and approved for publication. Mention of trade names or commercial products does not constitute endorsement or recommendation for use.



# CONTENTS

DISCLAIMER . . . . .	ii
LIST OF AUTHORS. . . . .	vi
LIST OF ILLUSTRATIONS. . . . .	vii
LIST OF TABLES . . . . .	x
LIST OF EXHIBITS . . . . .	xii
I INTRODUCTION . . . . .	1
II CHEMISTRY-RELATED DEVELOPMENT STUDIES. . . . .	4
A. Development of an Automatic Computer Program for the Evaluation of Kinetic Mechanisms . . . . .	5
1. Treatment of Chamber Effects . . . . .	6
2. Computational Considerations . . . . .	8
3. Ease of Changing Reactions . . . . .	9
B. Development of an Improved Kinetic Mechanism for Incorporation in Photochemical Dispersion Models . . . . .	11
1. General Considerations in the Design of a Suitable Mechanism . . . . .	11
2. Elimination of Unimportant Reactions in the General Kinetic Mechanism. . . . .	14
3. Further Modifications To Reduce Computing Requirements . . . . .	29
4. The Present Status of the Mechanism. . . . .	32
C. Development of a Kinetic Mechanism Describing SO <sub>2</sub> Reactions and Sulfuric Acid Formation. . . . .	35
1. The State of the Art of Gas Phase SO <sub>2</sub> Kinetics . . . . .	36
2. The State of the Art Regarding the Oxidation of SO <sub>2</sub> in Solution . . . . .	41
3. Efforts To Test the Gas Phase Reaction Mechanism for SO <sub>2</sub> . . . . .	51
4. Future Examinations of SO <sub>2</sub> Chemistry . . . . .	52
D. Special Considerations Regarding the Treatment of Temperature, Water, and Hydrogen Peroxide in the Airshed Model. . . . .	53

## II CHEMISTRY-RELATED DEVELOPMENT STUDIES (Continued)

1. The Predicted Effects of Changes in Temperature and Water Concentration on Smog Kinetics. . . . .	56
2. Specification of the Initial Concentration of $H_2O_2$ . . . . .	62
3. Spatial and Temporal Variations in Temperature and Water Concentration in the South Coast Air Basin . . . . .	63
E. Treatment of Organics in the Airshed Model. . . . .	73
F. Introduction of the Improved Kinetic Mechanism into the Airshed Model. . . . .	77

## III METEOROLOGY-RELATED DEVELOPMENT ACTIVITIES. . . . . 87

A. Model Sensitivity to the Inclusion of Wind Shear. . . . .	87
1. Wind Velocity Profile . . . . .	89
2. Implementation of the Wind Velocity Profile . . . . .	90
3. Computer Coding . . . . .	91
4. Description of the Experiment . . . . .	91
5. Discussion of the Results . . . . .	92
B. Treatment of Wind Shear in the Airshed Model. . . . .	101
C. Examination of an Algorithm for Deriving Mass-Consistent Wind Fields. . . . .	101
1. The Governing Equations . . . . .	103
2. Tests of the Model. . . . .	106
3. Discussion of the Results . . . . .	110
D. Adoption of an Improved Algorithm for Estimating Turbulent Diffusivities . . . . .	121
E. Modified Treatment of the Inversion Layer in the Airshed Model . . . . .	123

## IV EVALUATION OF ALTERNATIVE TECHNIQUES FOR INTEGRATING THE SPECIES CONTINUITY EQUATIONS. . . . . 126

A. Introduction. . . . .	126
B. Available Methods . . . . .	130
1. The Price Scheme. . . . .	131
2. The Crowley Second- and Fourth-Order Methods. . . . .	132
3. The SHASTA Method . . . . .	133
4. The Galerkin Method . . . . .	135
5. Particle-in-Cell Techniques . . . . .	140
6. The Method of Egan and Mahoney. . . . .	141
C. A Test Problem. . . . .	142

IV	EVALUATION OF ALTERNATIVE TECHNIQUES FOR INTEGRATING THE SPECIES CONTINUITY EQUATIONS (Continued)	
D.	Results . . . . .	146
1.	The Price Scheme. . . . .	148
2.	The Crowley Second- and Fourth-Order Methods. . . . .	148
3.	The SHASTA Method . . . . .	149
4.	The Galerkin Method . . . . .	149
5.	Particle-in-Cell Methods. . . . .	149
6.	The Method of Egan and Mahoney. . . . .	150
7.	Computational Time. . . . .	189
E.	Conclusions . . . . .	190
V	AIRSHED MODEL MODIFICATION FOR MULTIDAY SIMULATION. . . . .	192
A.	Introduction. . . . .	192
B.	Model Refinements . . . . .	194
1.	Treatment of Photochemistry at Night. . . . .	194
2.	Definition of the Modeling Region . . . . .	196
3.	Use of a Grid with Variable Resolution. . . . .	197
4.	Modification of the Finite Difference Equations . . . . .	198
5.	Modification of the Computer Codes. . . . .	200
C.	Multiday Simulation of the Los Angeles Basin. . . . .	201
1.	Preparation of Emissions and Meteorological Results . . . . .	201
2.	Discussion of the Multiday Simulation Results . . . . .	203
D.	Recommendations for Future Work . . . . .	216
	APPENDIX: A USER'S GUIDE TO MODKIN. . . . .	218
	REFERENCES . . . . .	283
	FORM 2220-1. . . . .	288

## AUTHORS

CHAPTER I - Steven D. Reynolds

CHAPTER II - Thomas A. Hecht, David C. Whitney, Jody Ames,  
Steven D. Reynolds

CHAPTER III - Steven D. Reynolds, Mark A. Yocke, Jody Ames

CHAPTER IV - James P. Meyer

CHAPTER V - Steven D. Reynolds, Jody Ames

APPENDIX - David C. Whitney

## ILLUSTRATIONS

1	Concentration-Time Profiles for NO, NO <sub>2</sub> , O <sub>3</sub> , and Propylene at 15°C and 35°C . . . . .	60
2	Predicted Concentration-Time Profiles for NO, NO <sub>2</sub> , O <sub>3</sub> , and Propylene at 0, 50, and 100 Percent Relative Humidity . . . . .	61
3	Locations of Temperature and Relative Humidity Monitoring Sites . . . . .	67
4	Distribution of the Temperature Aloft Above Rialto on 26-27 July 1973 . . . . .	69
5	Temporal Variations in Water Concentration at Five Locations in the Los Angeles Basin . . . . .	71
6	Distribution of the Water Concentration Aloft Above Rialto on 26-27 July 1973 . . . . .	72
7	Predicted and Measured Concentrations for La Habra Using the 15- and 31-Step Kinetic Mechanisms . . . . .	81
8	Predicted and Measured Concentrations for Anaheim Using the 15- and 31-Step Kinetic Mechanisms . . . . .	82
9	Predicted and Measured Concentrations for Pomona Using the 15- and 31-Step Kinetic Mechanisms . . . . .	83
10	Predicted and Measured Concentrations for Pasadena Using the 15- and 31-Step Kinetic Mechanisms . . . . .	84
11	Predicted and Measured Concentrations for Downtown Los Angeles Using the 15- and 31-Step Mechanisms . . . . .	85
12	Predicted and Measured Concentrations for West Los Angeles Using the 15- and 31-Step Mechanisms . . . . .	86
13	The Effect--Expressed as Average Deviation--of Variations in Vertical Wind Shear on NO and NO <sub>2</sub> . . . . .	93
14	The Effect--Expressed as Percentage Deviation--of Variations in Vertical Wind Shear on NO and NO <sub>2</sub> . . . . .	94
15	The Effect--Expressed as Maximum Deviation--of Variations in Vertical Wind Shear on NO and NO <sub>2</sub> . . . . .	95

16	The Effect--Expressed as Percentage Maximum Deviation--of Variations in Vertical Wind Shear on NO and NO <sub>2</sub> . . . . .	96
17	The Effect--Expressed as Average Deviation--of Variations in Vertical Wind Shear on CO and O <sub>3</sub> . . . . .	97
18	The Effect--Expressed as Percentage Deviation--of Variations in Vertical Wind Shear on CO and O <sub>3</sub> . . . . .	98
19	The Effect-Expressed as Maximum Deviation--of Variations in Vertical Wind Shear on CO and O <sub>3</sub> . . . . .	99
20	The Effect-Expressed as Percentage Maximum Deviation--of Variations in Vertical Wind Shear on CO and O <sub>3</sub> . . . . .	100
21	Distribution of O <sub>3</sub> Aloft Between Brackett and Rialto During the Morning of 11 July 1973 . . . . .	124
22	Concentration as a Function of Downwind Distance for the Explicit Price Scheme . . . . .	151
23	Concentration as a Function of Downwind Distance for the Implicit Price Scheme . . . . .	156
24	Concentration as a Function of Downwind Distance for the Crowley Second-Order Scheme . . . . .	161
25	Concentration as a Function of Downwind Distance for the Crowley Fourth-Order Scheme . . . . .	166
26	Concentration as a Function of Downwind Distance for the SHASTA Method . . . . .	171
27	Concentration as a Function of Downwind Distance for the Galerkin Method . . . . .	176
28	Concentration as a Function of Downwind Distance for the Particle-in-Cell (Smoothed) Methods . . . . .	181
29	Concentration as a Function of Downwind Distance for the Egan and Mahoney Method. . . . .	186
30	Comparison of Predicted and Measured Hourly Averaged CO Concentrations at Downwind Los Angeles . . . . .	205
31	Comparison of Predicted and Measured Hourly Averaged CO Concentrations at Long Beach. . . . .	206
32	Comparison of Predicted and Measured Hourly Averaged CO Concentrations at West Los Angeles . . . . .	207



33	Comparison of Predicted and Measured Hourly Averaged CO Concentrations at Burbank . . . . .	208
34	Comparison of Predicted and Measured Hourly Averaged CO Concentrations at Reseda . . . . .	209
35	Comparison of Predicted and Measured Hourly Averaged CO Concentrations at Whittier . . . . .	210
36	Comparison of Predicted and Measured Hourly Averaged CO Concentrations at Azusa . . . . .	211

## TABLES

1	The Reactions Ranked by Amount of Uncertainty . . . . .	18
2	Individual Area and Sensitivity Indices. . . . .	23
3	The Reactions Ranked by Sensitivity . . . . .	24
4	Characteristics of the Smog Chamber Runs . . . . .	27
5	Values of T, H, and M Before and After Removal of the Six Reactions. . . . .	29
6	A Lumped Kinetic Mechanism for Photochemical Smog . . . . .	33
7	Type of Mathematical Representation Required to Predict Concentrations of Species in the General Mechanism . . . . .	35
8	The Effect of Different Catalysts on SO <sub>2</sub> Oxidation . . . . .	47
9	Activation Energies of Reactions in the General Mechanism . . . . .	57
10	Ground-Level Air Temperatures in the Los Angeles Basin on 28-30 June 1974. . . . .	65
11	Ground-Level Relative Humidities in the Los Angeles Basin on 28-30 June 1974 . . . . .	66
12	Rate Constants for O, OH, and O <sub>3</sub> Attack on Various Hydrocarbons .	74
13	Hourly Averaged Wind Speed and Direction in the Los Angeles Basin on 29 September 1969 at 6:00 a.m. PST . . . . .	107
14	Hourly Averaged Wind Speed and Direction in the Los Angeles Basin on 29 September 1969 at 3:00 p.m. PST . . . . .	108
15	Mixing Depths in the Los Angeles Basin on 29 September 1969 at 6:00 a.m. and 3:00 p.m. PST . . . . .	109
16	Predicted Changes in Wind Speed and Direction for Case 1 . . . . .	111
17	Predicted Changes in Wind Speed and Direction for Case 2 . . . . .	112
18	Predicted Changes in Wind Speed and Direction for Case 3 . . . . .	113
19	Predicted Changes in Wind Speed and Direction for Case 4 . . . . .	114

20	Predicted Changes in Wind Speed and Direction for Case 5 . . . . .	115
21	Predicted Changes in Wind Speed and Direction for Case 6 . . . . .	116
22	Predicted Changes in Wind Speed and Direction for Case 7 . . . . .	117
23	Predicted Changes in Wind Speed and Direction for Case 8 . . . . .	118
24	Conditions Represented in Tables 16 through 23 . . . . .	119
25	Values of Diffusivity and Peclet Number for Three Case Studies . .	147
26	Kinetic Constants for Each Case . . . . .	147
27	Computing Time Required for Alternative Solution Methods . . . . .	189
28	Organization of Multiday Input . . . . .	202
29	Predicted and Measured Hourly Averaged CO Concentrations at the End of the 29 to 30 September Nighttime Period . . . . .	213
30	Multiday Ground-Level CO Concentration Map at 5 a.m. PST on 30 September 1969 . . . . .	214
31	Single-Day Ground-Level CO Concentration Map at 5 a.m. PST on 30 September 1969 . . . . .	215
32	Predicted and Measured Hourly Averaged CO Concentrations for the Last Hour of the Multiday Simulation . . . . .	216
A-1	Input Card Format for MODKIN . . . . .	221

## EXHIBITS

A-1	Listing of Main Program MODKIN . . . . .	236
A-2	Listing of Subroutine LMPCAL . . . . .	250
A-3	Listing of Subroutine DIFSUB . . . . .	253
A-4	Listing of Subroutine DIFFUN . . . . .	262
A-5	Listing of Subroutine MATINV . . . . .	266
A-6	Listing of Subroutine PEDERV . . . . .	268
A-7	Listing of Subroutine PLOT . . . . .	269
A-8	Sample MODKIN Input . . . . .	273
A-9	Sample MODKIN Output--Selected Pages . . . . .	275

## I INTRODUCTION

The SAI urban airshed model was originally developed for the Environmental Protection Agency (EPA) under Contracts CPA 70-148 and 68-02-0339. Two series of reports, entitled "Development of a Simulation Model for Estimating Ground-Level Concentrations of Photochemical Pollutants" and "Further Development and Evaluation of a Model for Estimating Ground-Level Concentrations of Photochemical Pollutants," describe our models development and evaluation studies. In concept, the model formulation was general, based on mass conservation relationships for a reactive species in a turbulent fluid. To implement the model, however, we assumed that we could do the following:

- > Use the gradient transport hypothesis to represent pollutant transport by turbulence.
- > Neglect turbulence influences on the net rate of chemical reactions.
- > Neglect subgrid-scale concentration variations and their effect on reaction rates.

Volume III discusses this threefold assumption. In addition, we made several assumptions with regard to the treatment of various parameters in the model. For example, we assumed that a 15-step kinetic mechanism could be used to represent the chemical reaction processes. The nature of these assumptions reflects not only the time and funding constraints on our work then, but also the current understanding of the physical and chemical processes that occur in the urban atmosphere. In this Volume, we discuss efforts carried out under the present contract to refine further various aspects of the model and its usage.

Basically, our model refinement activities have focused on four areas:

- > Chemistry-related model development activities.
- > Meteorology-related model development activities.
- > An evaluation of alternative techniques for integrating the species continuity equations.
- > Airshed model modification for multiday simulation.

Each of these areas is the subject of a chapter in this volume.

Chapter II discusses our efforts to improve the treatment of chemical parameters in the model. Specifically, we began with a 39-step generalized kinetic mechanism and, by eliminating unimportant reactions, by invoking the steady-state assumption, and by combining reaction steps we derived a 31-step mechanism suitable for incorporation in the airshed model. In addition, we examined  $\text{SO}_2$  chemistry and developed an interim 10-step reaction mechanism for describing both homogeneous and heterogeneous reactions. Although this mechanism has yet to be validated using smog chamber data, it does provide a starting point for treating  $\text{SO}_2$  chemistry in the airshed model. We also determined the sensitivity of the kinetic model predictions to variations in temperature, water concentration, and  $\text{H}_2\text{O}_2$  concentration. These results provide guidance with regard to the appropriate treatment of the spatial and temporal variations of these parameters in the airshed model. Finally, the chapter describes our experience to date in using the new 31-step mechanism in an actual simulation of a smoggy day in the Los Angeles basin.

Chapter III describes our efforts to improve the treatment of meteorological parameters in the model. We examined the impact on the model predictions of wind shear--an effect previously neglected in the model. Upon finding that wind shear has a significant influence, we extended the capabilities of the model to treat this parameter. In addition, we developed a methodology to derive improved diffusivity relationships (discussed more fully in Volume III) and examined an algorithm for rendering three-dimensional wind fields mass consistent. We gave special consideration to the treatment of elevated temperature inversions, especially with respect to possible importance of pollutant exchange between the stable inversion layer and the turbulent mixed layer as the inversion is eroded by surface heating.

Chapter IV presents our evaluation of alternative techniques for integrating the species continuity equations. Because the governing equations of the photochemical dispersion model are nonlinear, numerical techniques



must be employed to obtain approximate solutions. Since we must attempt to solve large systems of coupled, nonlinear partial differential equations, we have to be careful to choose an appropriate numerical procedure. The two most important concerns influencing this choice are the following:

- > Accurate representation of the horizontal advective transport of pollutants.
- > Efficient solution of large systems of nonlinear equations.

For this contract effort, we restricted our attention to the first of these areas. We carried out a comparative study of various alternative techniques that have appeared in the literature and that, if implemented in the airshed model, would represent a means for minimizing truncation error propagation effects. The methods examined include finite difference, particle-in-cell, and finite element schemes. We applied each method to the same test problem, and we compared the numerical results with analytical solutions.

Chapter V summarizes our efforts to modify the airshed model for multi-day simulations. In previous photochemical modeling studies, multiday simulations have been ignored. Model applications have usually been limited to the simulation of daytime conditions. For example, a model run might start at some point in the morning preceding the rush hour and extend into the afternoon to model the buildup of  $O_3$ . Accurate nighttime simulations are hindered by the typically small size of wind speeds then and the lack of available measurements aloft. However, multiple-day simulations may prove to be extremely useful. For example, in the evaluation of an emission control strategy that is to be carried out in some future year, the model user must carefully choose the initial pollutant concentration distribution to be employed in the simulation. If a multiple-day run is made, the influence of the initial concentrations on the predictions for the second and subsequent days will not be as pronounced as it is on the first day. Furthermore, multiday simulations may uncover errors in the treatment of emission, meteorological, or chemical parameters that would otherwise remain unnoticed in a relatively short term simulation. Chapter V concludes with a presentation of the results of a 34-hour simulation of the Los Angeles basin for CO using the SAI model.

## II CHEMISTRY-RELATED DEVELOPMENT STUDIES

Thomas A. Hecht  
David C. Whitney  
Jody Ames  
Steven D. Reynolds

One of the distinguishing characteristics of models capable of estimating photochemical pollutant concentrations is that chemical reaction processes must be represented accurately. Two pollutants treated in such models for which air quality standards have been established, namely  $\text{NO}_2$  and  $\text{O}_3$ , are not emitted from sources in appreciable quantities. These pollutants are formed in the atmosphere as the products of numerous reactions involving  $\text{NO}$ , hydrocarbons, and a variety of free radical species. Because of the inherent complexity of the overall reaction processes, care must be exercised to incorporate in a photochemical dispersion model a tractable kinetic mechanism which embodies as much chemical reaction as possible.

In this chapter we discuss efforts to improve the treatment of the atmospheric chemical reaction processes in the SAI airshed model. Previously, these processes were represented by a 15-step mechanism developed by Hecht and Seinfeld (1971). Since this mechanism was developed, however, additional efforts have been undertaken to design improved mechanisms. One of the most promising mechanisms to appear in the literature is that reported by Hecht et al. (1973). This mechanism consists of 39 reaction steps and treats four classes of hydrocarbons (paraffins, olefins, aromatics, and aldehydes). In general, this new mechanism seems to represent an advance of such importance as to warrant its incorporation in the airshed model.

In the course of reviewing modeling needs with respect to atmospheric chemistry, a number of issues were raised. These topics, which we address in this chapter, include the following:

- > Development of a computer program to facilitate the evaluation of kinetic mechanisms.
- > Compaction of the 39-step hydrocarbon/ $\text{NO}_x$ / $\text{O}_3$  mechanism to reduce its impact on computing time in the airshed model.

- > Development of an interim mechanism for  $\text{SO}_2$  reactions and sulfuric acid formation suitable for incorporation in the airshed model.
- > Examination of spatial and temporal variations in temperature, water, and  $\text{H}_2\text{O}_2$  concentration in an urban airshed such as the South Coast air basin to provide guidance with respect to the treatment of these parameters in regional models.
- > Evaluation of alternative means for treating organics in the airshed model.
- > Experience gained in the use of the new kinetic mechanism to perform an actual airshed simulation of the Los Angeles Basin.

Each of these issues is discussed in the succeeding sections of this chapter.

#### A. DEVELOPMENT OF AN AUTOMATIC COMPUTER PROGRAM FOR THE EVALUATION OF KINETIC MECHANISMS

Once a set of reactions for the formation of photochemical smog has been proposed, it is necessary to demonstrate that the mechanism is correct; i.e., that it is able to account for, within experimental error, the actual concentration of each species present in the reaction mixture at any point during the time span of the reaction. In its simplest form, this evaluation process involves the formulation and solution of the set of coupled differential equations that describe the variation in the formation and consumption of each species in the reaction mixture as a function of time. This set of equations can be expressed as follows:

$$\frac{dy_i}{dt} = \sum_{j=1}^J R_{f,i,j} - \sum_{k=1}^K R_{c,i,k} \quad , \quad (1)$$

where

$y_i$  = the concentration of species  $i$ ,

$t$  = time,

$R_{f,i,j}$  = the rate of formation of species  $i$  in reaction  $j$  of the set of  $J$  reactions in which species  $i$  is formed,

$R_{c,i,k}$  = the rate of consumption of species  $i$  in reaction  $k$  of the set of  $K$  reactions in which species  $i$  is consumed.

The concentrations thus calculated can be compared with those measured experimentally in the reaction mixture.

Unfortunately, the real world presents experimental, computational, and operational obstacles to the pursuit of this simple validation scheme. First, for the integrity of the reaction mixture to be preserved, the mixture must be contained in some sort of reaction chamber, which in turn gives rise to two side effects: leaks (intentional, as in sampling, or unintentional) and wall reactions. Second, when the most efficient computer codes are used, the time needed to solve the coupled differential equations increases as the square of the number of species increases. Moreover, certain sets of rates lead all too often to systems of "stiff" equations, for which the solution times can become quite large. Finally, the urge always exists to "improve" a reaction mechanism, no matter how closely it approximates the experimental data; the computer code must allow these changes to be performed with a minimum amount of effort. In dealing with these realities, the researcher is called upon to display his mettle and to tax his ingenuity. The approaches we used in this study are described in the following subsection.

## 1. Treatment of Chamber Effects

With few exceptions, reaction chambers are not completely airtight. Under normal operating conditions, this does not create a serious problem, since almost all chambers are maintained at atmospheric pressure, and since the small amount of interchange by diffusion can usually be ignored. However, a problem

does arise when samples are removed from the chamber for analysis. Since the species that comprise smog exist in the atmosphere in minute (1 to 1000 ppb) concentrations, sample sizes on the order of a few liters are commonly needed to obtain enough material for an accurate analysis. Moreover, samples must be withdrawn fairly frequently during the reaction to monitor species concentrations that are changing rapidly. As a result, it is not unusual for 10 to 20 percent of the chamber volume to be withdrawn through sampling procedures. The reaction simulation technique must take this "dilution" of the reaction medium into account.

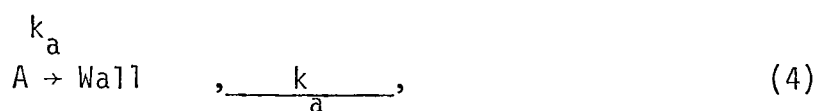
In the ideal case, the gas used to replace the samples being withdrawn is inert with respect to the reaction (e.g., pure nitrogen in a smog system), or it contains only reactive species whose concentrations are so large--relative to the amounts consumed or produced by the reactions--that they can be assumed to be constant throughout the reaction (e.g., oxygen or water vapor in "clean" air). In this case, it is sufficient to apply a "dilution factor" to the concentrations of all the species (inert diluent) or to those that do not remain constant (clean air diluent). If samples of an approximately constant size are removed at reasonably uniform time intervals, the dilution factor can be considered to be a constant,  $Q$ , and the equation for the rate of change of the concentration of species  $i$  becomes

$$\frac{dy_i}{dt} = \sum_{j=1}^J R_{f_{i,j}} - \sum_{k=1}^K R_{c_{i,k}} - y_i Q \quad . \quad (2)$$

In some chamber experiments, however, the incoming medium is just the natural atmosphere in the laboratory, which may contain concentrations of pollutant species as high as or higher than those being followed in the reaction chamber. Moreover, it may be desirable in some cases to inject pollutants or pollutant precursors deliberately into the chamber to simulate the effect of fresh emissions on the reacting mixture. As long as the concentration of species  $i$ ,  $y_{in}$ , in the incoming medium is known, the effect of such inflowing species on the rate equation can be easily expressed:

$$\frac{dy_i}{dt} = \sum_{j=1}^J R_{f_{i,j}} - \sum_{k=1}^K R_{c_{i,k}} - (y_i - y_{in}) Q \quad (3)$$

Unfortunately, wall effects cannot be handled as neatly. Wall absorption is best determined by placing the species in question, A, in a "nonreactive" environment within the chamber and following its decay with time. One can then include within the reaction mechanism an equation such as



with an appropriate rate constant.

Heterogeneous catalysis by the reactor walls is even more troublesome. However, by determining reaction rates at several different surface-to-volume ratios for the reactor (e.g., through the use of "artificial" walls to partition the chamber), the rate constants for the homogeneous and heterogeneous reactions can be obtained, and both reactions can be included in the mechanism.



## 2. Computational Considerations

As mentioned earlier, the computer time required to solve a set of differential equations increases at least as does the square of the number of equations to be solved (or, in the present case, as does the square of a number of distinct chemical species that appear in the reaction mechanism). Thus, any techniques that can be used to decrease the number of species concentrations that actually require coupled differential equations for their solution should be applied. Such techniques include the assumption of constant concentration; the uncoupling of product-only species; the invocation of the steady-state approximation; and the aggregation, or "lumping," of species that yield similar products. The last two techniques are the subjects of further discussion in Sections B and E and are thus not treated here.



Certain species that appear in the reaction mechanism either are present at truly constant concentrations (e.g., the reactor walls) or have concentrations so high--relative to the amounts of that species formed or consumed during the reaction--that they remain essentially constant with respect to time (e.g., oxygen). Since the change in concentration for these species is only negligibly different from zero, they can be excluded from the differential equation process.

A second category of species that need not be included in the set of coupled differential equations is those that appear in the reaction mechanism only as products (e.g.,  $\text{CO}_2$  or  $\text{HNO}_3$ ). The rate of formation of these product species is, to be sure, represented by the following equation:

$$\frac{dy_i}{dt} = \sum_{j=1}^J R_{f,i,j} \quad . \quad (7)$$

However, the presence of this species has no effect on the rate of formation or depletion of any other species; thus, the differential equation describing its formation can be uncoupled from the set of all differential equations and solved independently, at a significant savings in overall computer time.

### 3. Ease of Changing Reactions

Most computer codes used in the simulation of reaction kinetics incorporate, in one form or another, the features described above. The major advantage offered by the present program is the ease of preparation and, particularly, the ease of alteration of the mechanism and its associated species concentrations. The user need know nothing about computer programming or the solution of differential equations, and very little about chemical reaction mechanisms, to obtain meaningful results from the program.

On the first line of input, the user specifies the run identification, the number of reactions in the mechanism to be studied, how many of these are lumped reactions, the number of each of the various types of species described in the previous subsection, and an indication of whether the reaction rates should be printed. The second line continues this specification of parameters with an indication of the frequency of printout, the time step sizes, and the dilution factor.

The user then submits his reaction mechanism, one reaction per line, restricted only by one requirement on ordering: The lumped reactions must appear last. Each reaction appears as an ordinary chemical equation, with a list of reactants, a list of products, and a rate constant. The products can have coefficients (either fractions or integers), but the reactants cannot--each reactant molecule must be entered separately. The user can choose any four-letter mnemonic he wishes for the species names.

If there are any lumped reactions, the sets of individual reactions comprising each "lump" are then entered. Their formulation is exactly the same as that of the lumped reaction, except that the name of each species that contributes to the composition of the lump appears in place of the lumped species as the first reactant.

The user then provides the list of species and their initial concentrations--one per line. The order of their types must be the same as that given on the initial parameter line, but no particular order is required within each species type.

Should any of the species be present in the gas flowing into the reaction chamber, their concentrations in the inflowing stream and, if needed, the time and new values of any change in this concentration are entered next. Finally, the user can request concentration-time plots of any species. If desired, these plots can contain experimental points with which those points calculated by the proposed mechanism can be compared.

To change a rate constant or chemical reaction, the user need merely alter the corresponding input line. New reactions can be added by insertion; old ones can be removed by deletion. A similarly easy process can be used to change an initial species concentration or to add or remove species names from the list. Species can be transferred among species types (e.g., differential to steady-state) by a single interchange of lines.

A complete user's guide to the computer program is included in Appendix A. This appendix provides detailed information on each of the features described above, descriptions and listings of all of the computer routines, and sample inputs and outputs.

## B. DEVELOPMENT OF AN IMPROVED KINETIC MECHANISM FOR INCORPORATION IN PHOTOCHEMICAL DISPERSION MODELS

### 1. General Considerations in the Design of a Suitable Mechanism

The selection of a chemical mechanism for inclusion in an atmospheric diffusion model depends substantially on two factors:

- > The accuracy of prediction of the chemistry module.
- > The computing time required to evaluate the mathematical equations representing the mechanism.

From the standpoint of developing a chemical transformation model, the second factor is subordinate to the first. After a reliable mechanism has been developed, it can be condensed in several ways to reduce the computing time necessary to obtain predictions--for example, by eliminating unimportant reactions, by combining species that react in the same ways and at similar rates into a general grouping, and by invoking the steady-state approximation where applicable.

Depending on the degree to which these compaction measures are applied, the resultant mechanism can be assigned one of three broad categories: detailed mechanisms, lumped general mechanisms, or parametric models. A detailed mechanism consists entirely of elementary reactions. Because there are hundreds of different organics in the atmosphere, such a mechanism requires an extremely large number of mathematical equations to represent the chemical transformations. Although a detailed mechanism is ultimately the most accurate (in the limit if all rate constants and reactions are known), it is unsuitable for atmospheric modeling because of the second criterion listed above. A lumped general mechanism results when reactants and reactions of the same type are combined into general classes and reactions and those that clearly do not contribute to the predictions are eliminated from a detailed mechanism. A lumped general mechanism strikes a balance between detail of representation and compactness of form. The elimination of reactions that significantly affect predicted concentrations would oversimplify the mechanism to the point where it could not

provide accurate predictions unless corrective measures were taken. In particular, adjustable coefficients would have to be incorporated, forming a parametric model. For such a model, the values of the adjustable parameters are selected to minimize the discrepancies between experimental data and calculated values.

When we first began to develop a photochemical airshed model two types of chemical mechanisms were available for use. The first, a detailed model for propylene, was unsuitable because it was too narrow in scope. Its predictions for the atmosphere would have almost certainly been unreliable. The second was a parametric model, the Hecht-Seinfeld 15-reaction mechanism, for which values of the adjustable parameters had been determined for several hydrocarbon-NO<sub>x</sub> systems using smog chamber data. These hydrocarbons included propylene, iso-butylene, toluene, and n-butane; binary mixtures of propylene and n-butane, propylene and ethane, and toluene and n-butane; and auto exhaust. Thus, to the extent that the atmosphere could be represented as a surrogate consisting of these species, the parametric mechanism could be expected to provide reasonably accurate predictions over the range of initial conditions explicitly used in selecting values of the parameters. Moreover, the mechanism was mathematically compact. The predicted time-varying behavior of the pollutants could be obtained at every time step through the solution of only four differential equations and six algebraic equations. Given a choice of these two mechanisms, we selected the parametric model for incorporation in the airshed model because it came closest to meeting our two criteria.

The compact mechanism is far from ideal, however. Recent experimental studies have demonstrated the key roles of OH and HO<sub>2</sub> reactions in smog formation, reactions whose importance is understated in the mechanism. Other studies have shown that O and CO are less important than we thought at the time we formulated the model. And one limitation that is particularly discomforting is the narrow range over which values of the adjustable parameters are valid. This last shortcoming would limit the accuracy of the results obtained from the atmospheric dispersion model in such applications as the evaluation of alternative emission control strategies.

The mechanism most suitable for use in atmospheric models is a lumped general mechanism. Under EPA Contract 68-02-0580, we recently undertook the development of such a general kinetic mechanism. In this mechanism, we incorporated state-of-the-art knowledge of the reaction processes, and we provided for the rapid and straight forward modeling of organic species not explicitly evaluated using smog chamber data.

In the new kinetic mechanism, the inorganic reactions common to all organic-NO<sub>x</sub> systems are treated in great detail. We introduced generality into the model by lumping similar types of organics and free radicals into several new classes. In particular, olefins, aromatics, paraffins, and aldehydes constitute four separate classes of organics. We segregated organic free radicals into alkoxy, peroxyalkyl, and peroxyacyl subgroupings. Using propylene-NO<sub>x</sub>, n-butane-NO<sub>x</sub>, and propylene-n-butane-NO<sub>x</sub> smog chamber data over a wide range of HC/NO<sub>x</sub> ratios, we evaluated the model and showed that its predictions of the dependence of peak ozone on the initial concentrations of hydrocarbon and oxides of nitrogen qualitatively agree with experimental observations. Seinfeld et al. (1973) discussed the rationale and formulation of this lumped kinetic mechanism, and Hecht et al. (1973) and Hecht et al. (1974) presented initial and secondary evaluation results using the mechanism.

This new mechanism appears to be more accurate than the Hecht-Seinfeld mechanism that we previously employed in the atmospheric simulation model. In addition, we can easily extend the new mechanism to new organics that have not been explicitly evaluated (the values of the adjustable parameters do not need to be determined). Unfortunately, the computing time that is initially required to carry out a simulation with the new mechanism is much higher than that needed for the Hecht-Seinfeld model. At the outset of this project, representation of the chemistry of a system consisting of a paraffin, an olefin, and NO<sub>x</sub> in air (no aromatics or CO) required 36 reactions and the solution of 16 differential equations and 4 algebraic equations to obtain predictions. Such mathematical complexity would certainly be excessive if the mechanism were imbedded in the airshed model, where the kinetics must be evaluated at every grid point for every time step. We therefore set out to reduce the computing time necessary to obtain predictions from the mechanism.

We approached the problem of long computational time requirements from two directions. Initially, we sought to condense the mechanism to the smallest number of reactions required for accurate predictions. We identified critical reactions by means of a sensitivity analysis, and we subsequently eliminated insensitive reactions from the model. We also found that taking a flexible posture toward solving the representative rate expressions resulted in time savings. Our experience in working with the kinetic mechanism showed that computation time increased approximately linearly with the number of reactions, but quadratically with the number of coupled differential equations. Thus, we identified and verified species for which the pseudo-steady-state approximation is valid; this step permitted the replacement of three coupled differential equations by three coupled algebraic equations. Next, we took advantage of the fact that differential equations describing the concentrations of species that are formed as a result of chemical reactions but do not themselves enter into reactions can be solved independently of reacting species. We separated these so-called uncoupled species from the coupled species, eliminating three coupled differential equations, but adding three uncoupled differential equations.\* Finally, we eliminated one species from the mechanism by algebraic manipulation, thus reducing the number of coupled algebraic equations by one.

Since the computing time was the single greatest hindrance to our incorporating the improved kinetic mechanism in the airshed model, we focused a great deal of attention on this problem. As a result, we condensed the mechanism in both its physical and mathematical structure to a form that is amenable to diffusion modeling. We discuss the details, methodology, and results of this program below.

## 2. Elimination of Unimportant Reactions in the General Kinetic Mechanism

During the period in which we first formulated and subsequently modified the lumped kinetic mechanism to achieve satisfactory predictions, we added and deleted several reactions. However, we made no attempt to eliminate unimportant

---

\* Appendix A discusses the concept of coupled and uncoupled species.



reactions. Under EPA Contract 68-02-0580, we recently completed a sensitivity analysis of the kinetic mechanism; we used the results of this study to help us select possible reactions for elimination. Our goal in the sensitivity study was primarily to identify the "critical parameters" in the model, that is, those whose uncertainties most greatly influence the reliability of predictions. In essence, we calculated the rate of change in predictions with changes in the value of each rate constant, holding all other rate constants fixed at their standard values as a measure of sensitivity. Rate constants for which the measure has a high value correspond to sensitive reactions. Low values indicate insensitive reactions that may not have to be included in the model to make accurate predictions. Before proceeding with a discussion of our results, we describe the procedures and methods that we used in the sensitivity analysis.

The sensitivity study focused on a binary hydrocarbon-NO<sub>x</sub> system (EPA Run 352) in which the initial concentrations were as follows:

<u>Species</u>	<u>Concentration (ppm)</u>
NO <sub>2</sub>	0.07
NO	0.27
Propylene	0.265
n-Butane	3.29

We chose this particular experiment for several reasons:

- > Both high and low reactivity hydrocarbons were present initially.
- > The initial concentrations of total hydrocarbons and oxides of nitrogen were typical of those found in a polluted atmosphere.
- > The accumulation of ozone reached an asymptotic level during the experiment.
- > We had the run modeled with reasonable success in our evaluation study.

We performed the sensitivity analysis in the following manner. Using the nominal (or base) values for all parameters reported by Hecht et al. (1973) (see Tables 14 and 16 in that reference), we obtained base concentration-time profiles for propylene, n-butane, NO, NO<sub>2</sub>, and O<sub>3</sub> by integrating the governing rate equations with each parameter at its nominal value. We then increased (and subsequently decreased) one of the parameters by a fixed percentage, holding all other parameters at their nominal values. We integrated the equations twice, once for each of the two new settings (+50 percent and -50 percent) of the selected input parameter. Repeating this process for each rate constant, we carried out, for n parameters, integrations for a base case and 2n parameter variations. Finally, for each of the 2n + 1 integrations, we determined the values of the sensitivity measures or "decision variables." We compared the magnitudes of the decision variables for each variation in a parameter with those computed for the base case, and ranked the sensitivities of the parameters by tabulating the magnitudes of the differences.

a. Measurement of Sensitivity

Central to a sensitivity analysis of a mathematical model is the meaningful quantification of changes in model predictions that result from perturbing the input parameters one at a time. As the measure of sensitivity for each parameter, we chose the absolute area between the concentration-time profile for the given parameter, with all parameters held at their base values, and the profile generated when the i-th parameter was perturbed by a fixed percentage. We denote these parameters as A<sub>NO<sub>2</sub></sub>, A<sub>NO</sub>, A<sub>O<sub>3</sub></sub>, A<sub>O<sub>1</sub>ef</sub> (propylene), and A<sub>para</sub> (n-butane). Since Hecht et al. (1973) discussed these criteria in some detail, we review their appropriateness only briefly here.

The five indices (A<sub>NO<sub>2</sub></sub>, A<sub>NO</sub>, A<sub>O<sub>3</sub></sub>, A<sub>O<sub>1</sub>ef</sub>, and A<sub>para</sub>) constitute continuous measurements of sensitivity determined experimentally over the entire period of simulation for each species. Mathematically, we represent this relationship as follows:

$$|A| = \int_0^{400 \text{ min}} |C_i(p,t) - C_i(p + \%p,t)| dt \quad ,$$

where

- $|A|$  = the absolute area between the concentration-time profile predicted for the  $i$ -th species, with all parameters at their base values, and the profile obtained when one parameter is perturbed by a fixed percentage.
- $C$  = the concentration of the  $i$ -th chemical species.
- $i$  = the species index-- $\text{NO}_2$ ,  $\text{NO}$ ,  $\text{O}_3$ , olefin, paraffin.
- $p$  = the parameter that is being perturbed.
- $\%$  = the percentage perturbation in  $p$  divided by 100.

If the perturbation of a given parameter greatly alters the time history of the  $i$ -th chemical species, indicating high sensitivity to that parameter,  $|A_i|$  will have a large value. But if the concentration-time trace remains essentially unchanged, the predictions of the model will be insensitive to variations in the parameter under evaluation, and  $|A_i|$  will be small.

To facilitate the comparison and ranking of their sensitivities, we varied all parameters in turn by the same fixed percentage. Some of the input parameters are very poorly characterized, having associated uncertainties of up to an order of magnitude, whereas the values of other parameters are known within an uncertainty of 10 percent. The comparative table of rate constants [Table 16 in Hecht et al. (1973)] suggests that a representative "degree of precision" among the several alternative experimental determinations or theoretical estimates available for any particular parameter is on the order of 50 percent. Therefore, we used that percentage as the magnitude of perturbation for the sensitivity calculations. However, because the precision bounds of the rate constant values for individual reaction rate constants vary greatly, our choice of the "range of perturbation" was arbitrary. The significance of the 50 percent figure rests only on its approximate division of the very uncertain from the less uncertain parameters. Table 1 ranks the reactions by the amount of uncertainty. (We define the uncertainty bound for a rate constant as the range within which the "true value" of the constant can be presumed to fall with confidence.)

Table 1

THE REACTIONS RANKED BY AMOUNT  
OF UNCERTAINTY

<u>Reaction</u>	<u>Percent Uncertainty</u>
1. $\text{N}_2\text{O}_5 + \text{H}_2\text{O}$	$\pm 100 \%$
2. $\text{NO} + \text{HNO}_3$	100
3. $\text{HNO}_2 + \text{HNO}_3$	100
4. $\text{NO} + \text{NO}_2 + \text{H}_2\text{O}$	100
5. $\text{HNO}_2 + \text{HNO}_2$	100
6. $\text{HNO}_2 + \text{h}\nu$	100
7. $\text{OH} + \text{NO}_2$	100
8. $\text{OH} + \text{NO} + \text{M}$	100
9. $\text{RO}_2 + \text{NO}$	100
10. $\text{RCO}_3 + \text{NO}$	100
11. $\text{RCO}_3 + \text{NO}_2$	100
12. $\text{HO}_2 + \text{HO}_2$	100
13. $\text{HO}_2 + \text{RO}_2$	100
14. $\text{RO}_2 + \text{RO}_2$	100
15. $\text{RO} + \text{NO}_2$	80
16. $\text{ALD} + \text{h}\nu$	70
17. $\text{RO} + \text{NO}$	65
18. $\text{OLEF} + \text{OH}$	45
19. $\text{O} + \text{NO}_2 + \text{M}$	40
20. $\text{O}_3 + \text{NO}_2$	40
21. $\text{NO}_3 + \text{NO}$	40

Table 1 (Concluded)

<u>Reaction</u>	<u>Percent Uncertainty</u>
22. PARA + OH	$\pm 40\%$
23. ALD + OH	40
24. RO + O <sub>2</sub>	40
25. PARA + O	35
26. HO <sub>2</sub> + NO	30
27. OLEF + O <sub>3</sub>	30
28. O + NO <sub>2</sub>	25
29. NO <sub>2</sub> + hv	20
30. O <sub>3</sub> + NO	20
31. NO <sub>3</sub> + NO <sub>2</sub>	20
32. H <sub>2</sub> O <sub>2</sub> + hv	20
33. OLEF + O	20
34. O + NO + M	15
35. O + O <sub>2</sub> + M	10
36. N <sub>2</sub> O <sub>5</sub>	5

The small amount of experimental data available upon which to base our estimates limited the procedure we followed to estimate the uncertainty bound for each rate constant. In essence, we calculated the percentage deviation of the highest and lowest expected values of each rate constant, having surveyed the literature to find independent determinations of these rate constants. Thus, the so-called estimate of uncertainty bounds is, in fact, simply an indication of the degree of agreement (or more precisely, the disagreement) among a number of independent determinations of the same rate parameter. In three situations, this "definition" does not apply:

- > If only a single determination was made for a given rate constant, the uncertainty bound is an indication of the precision of the experiment.
- > Since photolysis rate constants (e.g.,  $k_1$ ) must be determined *in situ* for a smog chamber experiment, the bounds are an indication of the reliability of the experimental method.
- > The uncertainty estimate for  $k_{37}$  ( $\text{HO}_2 + \text{HO}_2$ ) was taken from Lloyd (1974), who reviewed the reactions of the  $\text{HO}_2$  radical.

Because of the imprecision of these estimates, we assumed that the uncertainty bounds were symmetric about the nominal value. Therefore, although we estimated the uncertainties associated with several parameters to be  $\pm 100$  percent, the true upper bound may be considerably higher.

#### b. Results of the Sensitivity Analysis

For the purpose of ranking the parameters by sensitivity, we averaged the values of the area indices calculated for plus and minus percentage variations in the parameters to obtain a single characteristic value. Although this procedure facilitated ranking, some information was lost in the process. Because each of the measures of sensitivity is based on the difference between nominal

and perturbed concentration-time profiles, the magnitude of each difference, in general, depends upon the degree of perturbation (e.g., 10, 25, 50 percent). Because the equations governing the kinetics are nonlinear, the values of the sensitivity measures typically are not identical for plus and minus perturbations in a given parameter. But, in examining the values of the "area" sensitivity measures for plus and minus perturbations, we found them to agree sufficiently well to justify using their average values to rank the parameters.

Since we were interested chiefly in quantifying the overall sensitivity (or insensitivity) associated with each reaction in the model, the use of an indicator based on the changes in the predictions of several species was appropriate. Thus, we combined the five area sensitivity measures into a single scalar, which we term the "sensitivity." We defined the synthesized sensitivity measure for each rate constant as follows:

$$\text{Sensitivity}_j = \sum_{i=1}^5 \frac{w_i A_{ij}}{A_{\max_i}},$$

where

- $i$  = 1, 2, 3, 4, and 5 refer to the average area sensitivity measures for  $\text{NO}_2$ ,  $\text{NO}$ ,  $\text{O}_3$ , olefin, and paraffin, respectively.
- $j$  = the number of the reaction rate constant in the kinetic mechanism.
- $w_i$  = the weighting of the individual measure in the combined sensitivity scalar. (We weighted each of the five measures equally because, in developing and evaluating the general kinetic mechanism, we were interested in predicting the concentration-time behavior of each of these species with equal accuracy. However, we might have chosen different weights if our goals were different. For example, to predict oxidant and  $\text{NO}_x$  for evaluating alternative emission control strategies, we might have weighted  $\text{O}_3$ ,  $\text{NO}$ , and  $\text{NO}_2$  more heavily.)

$A_{ij}$  = the average area measurement determined for the  $i$ -th criterion and the  $j$ -th reaction.

$A_{\max i}$  = the maximum value of the  $i$ -th criterion observed for any of the reactions. (Dividing by the maximum value scales each of the arrays of the five individual area measurements between zero and one.)

Table 2 presents the values of this "sensitivity" index (seventh column), along with the values of the five averaged individual area indices. Table 3 ranks the reactions according to the combined sensitivity. As Table 3 shows, the following rate constants, presented in the order of decreasing sensitivity, display the greatest overall sensitivity:

<u>Rate Constant</u>	<u>Identification</u>
$k_1$	$\text{NO}_2$ photolysis
$k_{28}$	Oxidation of n-butane by OH
$k_{20}$	Oxidation of NO by $\text{HO}_2$
$k_3$	Reaction of $\text{O}_3$ with NO
$k_{16}$	Photolysis of $\text{HNO}_2$
$k_{23}$	Oxidation of propylene by $\text{O}_3$
$k_{29}$	Photolysis of aldehydes
$k_{24}$	Reaction of OH with propylene

Just as there are critical parameters in the model whose values must be determined with certainty, some parameters are almost insensitive. Large variations in the magnitude of these parameters result in small changes in model predictions. By identifying those reactions that contribute minimally to the total predicted response, the sensitivity analysis provides the basis for eliminating reactions from the mechanism. Removal, of course, is subject to further limited individual testing of each reaction over a range of initial conditions and bounds of uncertainty.



Table 2

## INDIVIDUAL AREA AND SENSITIVITY INDICES

NO.	A(NO2)	A(NO)	A(O3)	A(OLEF)	A(PARA)	SENSITIVITY.
1	4.0999994E 00	3.0100000F-01	4.8099991E 01	5.9399996E 00	1.1099999E 01	6.0233879E-01
2	2.9399997E-01	1.5199995E-01	5.8699995E-01	3.7799996E-01	7.1099997E-01	4.2636652E-02
3	3.5400000E 00	2.3799998E-01	4.2899994E 01	4.4599991E 00	9.1799994E 00	5.0078332E-01
4	9.4299972E-02	5.8300000E-02	1.5199995E-01	3.4999996E-02	6.1699998E-02	1.0480803E-02
5	1.9699997E-01	4.7399998E-02	6.3000000E-01	2.5999997E-02	3.0299997E-01	1.5842065E-02
6	9.4299972E-02	5.8399998E-02	1.4699996E-01	3.4299999E-02	6.0699999E-02	1.0441024E-02
7	3.4399996E 00	1.5199995E-01	1.2000000E 01	7.7999997E-01	1.9899998E 00	1.8804300E-01
8	3.5099993E 00	9.3699992E-02	5.2399998E 00	2.8599995E-01	5.9499997E-01	1.2817216E-01
9	3.1999998E 00	8.8999987E-02	4.5699997E 00	2.4199998E-01	4.9599999E-01	1.1538500E-01
10	3.4799995E 00	9.3499959E-02	5.1799994E 00	2.8399998E-01	5.8999997E-01	1.2708902E-01
11	2.6999998E 00	9.5499992E-02	3.5699997E 00	1.3000000E-01	3.6199999E-01	9.5649123E-02
12	2.2599993E 00	7.1199954F-02	4.1699991E 00	3.0299997E-01	1.2500000E 00	9.8682284E-02
13	9.9599999E-01	5.7499997E-02	8.6199999E-01	2.6499998E-02	4.8899996E-01	3.8531106E-02
14	2.4799995E 00	1.2599993E 00	4.0699997E 00	1.4899998E 00	2.2900000E 00	2.7009088E-01
15	1.6799994E 00	7.2599995E-01	3.0799999E 00	1.0999994E 00	2.0199995E 00	1.7816830E-01
16	5.0799999E 00	1.9299994E 00	7.5000000F 00	2.7999992E 00	5.1599998E 00	4.7975492E-01
17	3.7799997E 00	1.0499992E 00	6.8199987E 00	2.3799992E 00	5.4899998E 00	3.4641325E-01
18	2.5599995E 00	1.1999998E 00	3.9299994E 00	1.4499998E 00	2.0299997E 00	2.6154286E-01
19	0.0	0.0	0.0	0.0	0.0	0.0
20	8.4699993E 00	6.4899999E-01	2.1699997E 01	3.2799997E 00	6.7199993E 00	5.1467425E-01
21	1.3699999E 00	8.7499976E-02	1.4699993F 00	2.3099995E-01	2.0499992E 00	7.3833704E-02
22	3.2299995E-01	1.2799996E-01	5.9899998E-01	3.0100000E-01	1.6999996E-01	3.3491254E-02
23	6.9899998E 00	4.5400000E-01	4.1199999E 00	7.1099997E 00	1.1199999E 00	4.4005167E-01
24	2.2399998E 00	8.2699996E-01	7.7199993E 00	5.4199991E 00	5.0999994E 00	3.7242830E-01
25	0.0	0.0	0.0	0.0	0.0	0.0
26	0.0	0.0	0.0	0.0	0.0	0.0
27	8.2799971E-02	4.9599998E-02	8.6899996E-02	1.6500000E-02	7.9099953E-02	8.6847395E-03
28	5.6199999E 00	1.5999994E 00	1.2500000E 01	1.8799996E-01	2.0699997E 01	5.5576986E-01
29	6.6099997E 00	8.7399995E-01	1.7000000E 01	2.4799995E 00	4.3899994E 00	4.2951244E-01
30	1.5799999E 00	7.5099945E-02	8.6499996E 00	1.3499994E 00	7.7999992E 00	1.9439411E-01
31	1.0400000E 00	7.9399943E-02	3.2099991E 00	1.7299998E-01	1.1399996E-01	5.2100249E-02
32	9.1899997E-01	1.7499995E-01	7.7599993E 00	7.1499997E-01	3.2099998E-01	9.5314741E-02
33	1.0499992E 00	1.1099994E-01	8.6499996E 00	7.3699999E-01	3.3099997E-01	9.6192002E-02
34	6.1299998E-01	3.4599996E-01	3.5400000E 00	6.9699997E-01	1.0299997E 00	9.4606638E-02
35	3.8299996E-01	1.2399995E-01	2.2699995E 00	4.0099996E-01	6.1999995E-01	4.8602294E-02
36	1.7699999E-01	1.0799998E-01	4.5599997E-01	1.2899995E-01	1.6499996E-01	2.2490099E-02
37	4.1499996E 00	2.7099997E-01	1.0200000E 01	1.4799995E 00	3.3099995E 00	2.4209946E-01
38	2.0400000E-01	5.8300000E-02	4.3599999E-01	1.7199997E-02	4.1499998E-02	1.3556119E-02
39	3.1699997E-01	6.2099997E-02	9.4499999E-01	2.5099996E-02	7.1799994E-02	1.9249547E-02

Table 3  
THE REACTIONS RANKED BY SENSITIVITY

Reaction	Sensitivity
1. $\text{NO}_2 + h\nu$	0.60
2. $\text{PARA} + \text{OH}$	0.56
3. $\text{HO}_2 + \text{NO}$	0.51
4. $\text{O}_3 + \text{NO}$	0.50
5. $\text{HNO}_2 + h\nu$	0.48
6. $\text{OLEF} + \text{O}_3$	0.44
7. $\text{ALD} + h\nu$	0.43
8. $\text{OLEF} + \text{OH}$	0.37
9. $\text{OH} + \text{NO}_2$	0.35
10. $\text{NO} + \text{NO}_2 + \text{H}_2\text{O}$	0.27
11. $\text{OH} + \text{NO}$	0.26
12. $\text{HO}_2 + \text{HO}_2$	0.24
13. $\text{ALD} + \text{OH}$	0.19
14. $\text{O}_3 + \text{NO}_2$	0.19
15. $\text{HNO}_2 + \text{HNO}_2$	0.18
16. $\text{NO}_3 + \text{NO}$	0.13
17. $\text{N}_2\text{O}_5$	0.13
18. $\text{NO}_3 + \text{NO}_2$	0.12
19. $\text{NO} + \text{HNO}_3$	0.10
20. $\text{RCO}_3 + \text{NO}_2$	0.10
21. $\text{N}_2\text{O}_5 + \text{H}_2\text{O}$	0.10
22. $\text{RCO}_3 + \text{NO}$	0.10

Table 3 (Concluded)

<u>Reaction</u>	<u>Sensitivity</u>
23. $RO + O_2$	0.09
24. $H_2O_2 + hv$	0.07
25. $RO_2 + NO$	0.05
26. $RO \pm NO_2$	0.05
27. $O + O_2 + M$	0.04
28. $HNO_2 + HNO_3$	0.04
29. $OLEF + O$	0.03
30. $RO + NO$	0.02
31. $RO_2 + RO_2$	0.02
32. $O + NO_2$	0.02
33. $HO_2 + RO_2$	0.01
34. $O + NO + M$	0.01
35. $O + NO_2 \pm M$	0.01
36. $PARA + O$	0.01

Reactions that could potentially be removed from the mechanism, based on the results of the sensitivity analysis, appear in the lower portion of Table 3. These reactions included the oxygen atom oxidation of the species tabulated below:

<u>Species</u>	<u>Reaction</u>
Paraffins	$k_{27}$
NO	$k_4$
NO <sub>2</sub> in the presence of a third body (M)	$k_6$
NO <sub>2</sub> second order reaction	$k_5$
Olefins	$k_{22}$

Other candidates included the following:

<u>Species</u>	<u>Reaction</u>
HNO <sub>2</sub> -HNO <sub>3</sub>	$k_{13}$
RO-NO	$k_{36}$
RO <sub>2</sub> -HO <sub>2</sub>	$k_{38}$
RO <sub>2</sub> -RO <sub>2</sub>	$k_{39}$

Finally, we included among the candidates for potential elimination the reaction between NO and HNO<sub>3</sub> ( $k_{12}$ ). After carrying out the sensitivity calculations, we learned that the experimental value of this rate constant was several orders of magnitude less than our earlier estimate; this change sharply decreased the sensitivity of the reaction.

### c. Elimination of Insensitive Reactions

We based the tentative conclusions reached thus far largely on the averaged sensitivity criteria characterizing a single set of initial reactant concentrations. If we were to repeat the calculations using only half the initial hydrocarbon and twice the initial NO<sub>x</sub> used in the present study, we would expect to

find the order of parameter ranking to be somewhat different than that given in Table 3. Thus, we had to scrutinize each reaction carefully prior to its elimination; our criterion for elimination was that the reaction be "insensitive" (a term defined quantitatively shortly) over the range of initial concentrations of interest, as well as over the uncertainty bounds of the reaction rate constant (Table 1).

We chose three EPA smog chamber runs as a representative set of initial concentrations and ratios over which to evaluate the reactions for possible removal. As shown in Table 4, two of these runs are binary hydrocarbon systems; in the other experiment, propylene was the only hydrocarbon present. These three runs span a total hydrocarbon-to- $\text{NO}_x$  initial ratio of 0.7 to 10.5 and a reactive hydrocarbon-to- $\text{NO}_x^*$  initial ratio of 0.2 to 0.8. Air quality data obtained in Los Angeles indicate that the ratios for polluted air there are often within these ranges. (In the atmosphere, the ratio can vary with both location and time of day.)

Table 4  
CHARACTERISTICS OF THE SMOG CHAMBER RUNS

EPA Run	Concentrations (ppm)				Total [HC]/[ $\text{NO}_x$ ]	High Reactivity [HC]/[ $\text{NO}_x$ ]
	[n-butane] <sub>0</sub>	[propylene] <sub>0</sub>	[NO] <sub>0</sub>	[NO <sub>2</sub> ] <sub>0</sub>		
329	--	0.24	0.29	0.06	0.7	0.7
333	3.40	0.23	1.25	0.08	2.7	0.2
352	3.29	0.26	0.27	0.07	10.5	0.8

We considered reactions to be "insensitive" if, upon their removal individually and as a group, the remaining set of reactions was able to predict the following within 10 percent of the values predicted by the complete mechanism:

---

\* Defined as propylene.

- > The time to the  $\text{NO}_2$  peak (T)
- > The height of the  $\text{NO}_2$  peak (H)
- > The magnitude of the ozone peak (M).

These three scalars, all of which can be easily quantified, are of interest because the onset of formation of many secondary products formed in the atmosphere accompanies the peak concentration of  $\text{NO}_2$  and because the intensity of smog is often associated with the ozone and  $\text{NO}_2$  concentrations. Thus, T, H, and M constitute three major indicators of smog formation and severity. Although the choice of the 10 percent range was arbitrary, this value is lower than the uncertainty bounds associated with the experimental chamber data used to evaluate and "tune" the model. Thus, we felt that the choice was reasonable.

Consideration of the sensitivity values associated with each rate constant led us to select 10 reactions for possible removal from the mechanism. Of these, we found that only six could actually be eliminated based on the criteria cited above:

<u>Species</u>	<u>Reaction</u>
$\text{O} + \text{NO}$	$k_4$
$\text{O} + \text{NO}_2 + \text{M}$	$k_6$
$\text{NO} + \text{HNO}_3$	$k_{12}$
$\text{HNO}_2 + \text{HNO}_3$	$k_{13}$
$\text{RO}_2 + \text{HO}_2$	$k_{38}$
$\text{RO}_2 + \text{RO}_2$	$k_{39}$

As shown in Table 5, the values of T, H, and M after removal of these six reactions were within 10 percent of the values before the reactions were eliminated. Several other reactions could have been removed for one or two of the EPA runs, but not for all three. However, since their elimination would have limited the applicability of the kinetic mechanism to a narrower range of initial concentrations and ratios, we did not drop them.

Table 5

VALUES OF T, H, AND M BEFORE AND AFTER  
REMOVAL OF THE SIX REACTIONS

EPA Run	Time to the NO <sub>2</sub> Peak (T) (minutes)		Concentration (ppm)			
			Height of the NO <sub>2</sub> Peak (H)		Magnitude of the Ozone Peak (M)	
	Before	After	Before	After	Before	After
329	87	86	0.25	0.25	0.39	0.40
333	285	281	0.75	0.70	0.40	0.41
352	65	70	0.25	0.25	0.50	0.52

The conclusions we reached during this study were based on the lumped general mechanism. If this mechanism proves to be fundamentally inadequate, the sensitivity calculations should be repeated with the corrected mechanism, and reactions that we eliminated should be examined again to judge their sensitivity in the environment of the corrected mechanism.

### 3. Further Modifications To Reduce Computing Requirements

Although the elimination of unnecessary reactions saves computing time, the condensation discussed thus far focused primarily on giving prominence to the important reactions in the mechanism. Significantly greater reductions in computing time can be obtained by varying the mathematical representation of the chemical mechanism. From a purist's point of view, a series of differential rate equations most accurately represents changes in the concentrations of reactants with time. (Ideally, one would solve these equations analytically. We used numerical methods to solve the equations on the computer, but these techniques were evaluated using test systems of equations for which analytical solutions were available.) Over the years, scientists have used the following approximations and simplifications to facilitate the solution of complex kinetic systems:

- > Recognizing the fundamental mathematical difference between the differential equations of species that are produced but do not enter into reactions and those of species that do react. The differential equations for reactants are often mathematically coupled and must therefore be solved simultaneously. If these coupled species have vastly different characteristic times of reaction, the equations become "stiff" numerically and must be solved using very small time steps to preserve accuracy. In contrast, the differential equations for species that do not react are not coupled and can be solved accurately one at a time using a method as simple as Simpson's rule.
- > Applying the steady-state approximation. If the concentration of a species equilibrates rapidly (relative to many other species in the system), one can assume that the summation of the rate terms for formation and consumption of the species is identically zero. This assumption reduces the differential equation to an algebraic equation.
- > Combining second-order reactions into higher order reactions. In some special cases, two or more reactions can be combined into a single reaction, with the elimination of an intermediate as well.

The following subsections summarize the results of applying each of these techniques to the lumped kinetic mechanism.

#### a. Treatment of Uncoupled Species

In a system containing propylene, n-butane,  $\text{NO}_x$ , and air, four species form that do not react subsequently: nitric acid, peroxyacylnitrates, organic nitrites, and organic nitrates. Because these products do not enter into reactions with other species present in the system, we can uncouple and solve the differential equations for each of the four species independently.

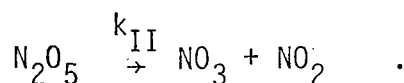
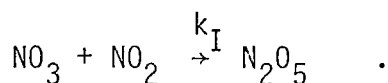


b. Invocation of the Steady-State Approximation

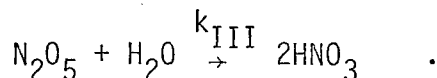
In earlier work, we demonstrated the validity of the steady-state approximation for O, OH, RO, and NO<sub>3</sub> (Hecht et al., 1973). Recently, we justified the application of the approximation to obtain predictions of the concentrations of HO<sub>2</sub>, N<sub>2</sub>O<sub>5</sub>, RO<sub>2</sub>, and RCO<sub>3</sub>. To demonstrate the validity of the approximation for any given species, we compared the concentration-time profile for the species predicted by an algebraic description with that predicted by a differential expression. In so doing, we found that the profiles generated using the two mathematical representations agreed to within 0.1 percent for these species. Thus, we eliminated four additional coupled differential equations, which were replaced by four coupled algebraic equations.

c. Combination of Reactions into a Single Higher Order Reaction

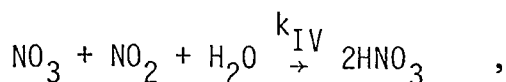
The species N<sub>2</sub>O<sub>5</sub> exists in equilibrium with NO<sub>2</sub> and NO<sub>3</sub>:



The only important reaction of N<sub>2</sub>O<sub>5</sub> other than Reaction II is hydrolysis to form nitric acid, a stable product in the mechanism:



If we assume that N<sub>2</sub>O<sub>5</sub> is in a steady-state (we have established the validity of this assumption) we can combine these reactions into the single third-order reaction:



having the rate constant

$$k_{IV} = \frac{k_I k_{III}}{k_{II} + k_{III} H_2O} \quad .$$

The combination of these three reactions eliminates  $N_2O_5$  as a species, thereby saving one algebraic equation and removing a net total of two reactions from the mechanism.

#### 4. The Present Status of the Mechanism

As a result of the procedures described thus far, we added nine reactions to the mechanism. Thus, a total of 31 reactions are necessary to represent the chemistry of a system of paraffins, olefins,  $NO_x$ , CO and air. In addition, to facilitate usage of the mechanism in the airshed model, we included two additional reactions involving O and OH reactions with aromatics. It is to be understood, however, that this is an interim treatment of the chemistry involving aromatics and is subject to revision at such time as a more suitable mechanism is developed. Table 6 presents the revised mechanism. Of the 25 species included in the mechanism, 10 are represented by coupled differential equations, 7 by algebraic equations, and 4 are constant, as shown in Table 7. Although the computing time associated with individual sets of initial conditions varies because of changes in the stiffness of the system of equations, we found that incorporating the changes presented here reduced the required computing time by approximately 50 percent over that required previously (Hecht et al. 1973). This saving is significant enough to justify the replacement of the simplified 15-step mechanism by the more accurate lumped kinetic mechanism as the kinetics module in the airshed dispersion model.

Table 6  
A LUMPED KINETIC MECHANISM FOR PHOTOCHEMICAL SMOG

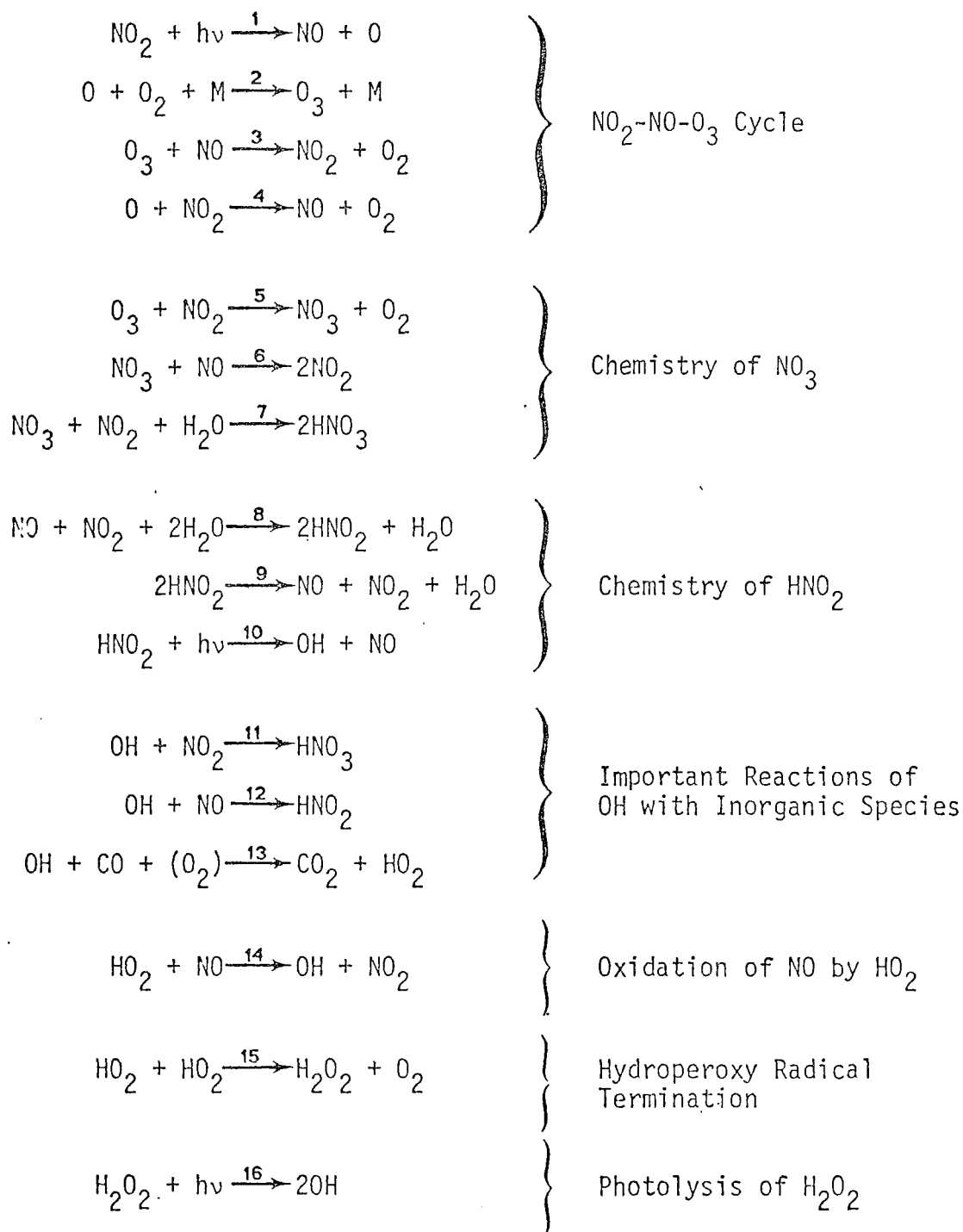
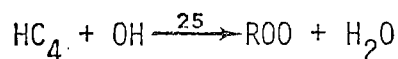
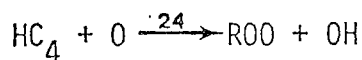
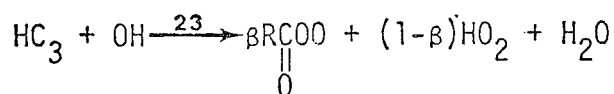
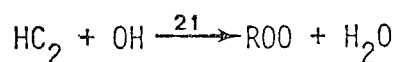
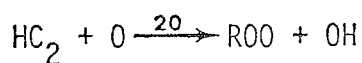
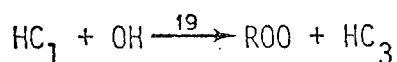
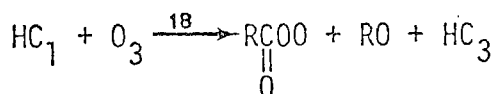
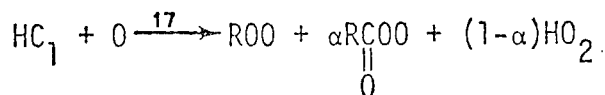


Table 6 (Concluded)



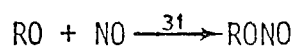
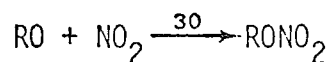
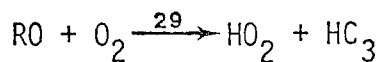
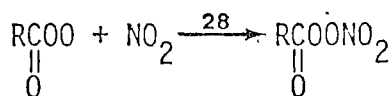
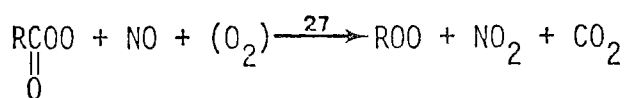
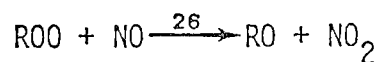
Organic Oxidation  
Reactions

$\text{HC}_1$  = Olefins

$\text{HC}_2$  = Paraffins

$\text{HC}_3$  = Aldehydes

$\text{HC}_4$  = Aromatics



Reactions of Organic  
Free Radicals with  $\text{NO}$ ,  
 $\text{NO}_2$ , and  $\text{O}_2$

Table 7  
TYPE OF MATHEMATICAL REPRESENTATION REQUIRED TO PREDICT  
CONCENTRATIONS OF SPECIES IN THE GENERAL MECHANISM

<u>Coupled Differential Equations</u>	<u>Uncoupled Differential Equations</u>	<u>Steady-State Algebraic Equations</u>	<u>Constant</u>
$\text{NO}_2$	$\text{HNO}_3$	O	M
NO	PAN	$\text{NO}_3$	$\text{O}_2$
$\text{O}_3$	$\text{RNO}_2$	OH	$\text{H}_2\text{O}$
$\text{HNO}_2$	$\text{RNO}_3$	$\text{HO}_2$	$\text{CO}_2$
$\text{H}_2\text{O}_2$		RO	
CO		$\text{RO}_2$	
Olefins		$\text{RCO}_3$	
Paraffins			
Aldehydes			
Aromatics			

#### C. DEVELOPMENT OF A KINETIC MECHANISM DESCRIBING $\text{SO}_2$ REACTIONS AND SULFURIC ACID FORMATION

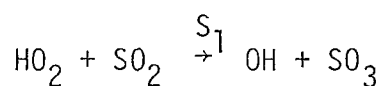
During the past decade, air pollution investigators have focused a substantial amount of scientific attention on  $\text{SO}_2$ , the precursor of sulfuric acid and sulfate, because of its effects on visibility and health. They observed that the oxidation of gaseous  $\text{SO}_2$  occurs both through reactions with gas phase oxidants and through reactions with liquid aerosol droplets. They demonstrated that the addition of  $\text{SO}_2$  to a reactor in which atmospheric concentrations of organics and  $\text{NO}_x$  in air are being irradiated (i.e., a smog simulation experiment)

results in a substantial decrease in visibility due to the formation of a sulfuric acid aerosol. And they established that  $\text{SO}_2$  is oxidized in fog. In this section, we review current knowledge and speculation concerning the oxidation of  $\text{SO}_2$  through reactions that occur in the gas phase and in solution. Since Bufalini (1971) has extensively reviewed the oxidation of  $\text{SO}_2$  in polluted air, our discussion focuses primarily on more recent results. We conclude this section with a discussion of our efforts to model a set of dynamic organic- $\text{NO}_x$ - $\text{SO}_2$  smog chamber experiments and a summarization of our future plans to simulate the chemistry of  $\text{SO}_2$ .

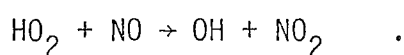
### 1. The State of the Art of Gas Phase $\text{SO}_2$ Kinetics

Until recently, air pollution  $\text{SO}_2$  research focused primarily on the qualitative and semi-quantitative characterization of the interaction of  $\text{SO}_2$  with components of smog. Scientists have been particularly interested in evaluating the effect of  $\text{SO}_2$  on oxidant levels and visibility in simulated smog (irradiated mixtures of organics,  $\text{NO}_x$ ,  $\text{SO}_2$ , and air); they have used environmental chambers extensively for this purpose. In these experiments, they observed that the concentration of  $\text{SO}_2$  slowly diminishes with time. However, most of the early (prior to 1970) experiments were not controlled carefully enough to allow an accurate estimate to be made of the rate of  $\text{SO}_2$  oxidation due to gas phase chemical reactions. Variations in relative humidity, the reactivity of chamber surfaces, and the accuracy of the analytical instrumentation all served to introduce imprecision into the data. And, by their very nature, smog chamber experiments provide minimal insight into the actual individual reactions by which  $\text{SO}_2$  is oxidized in smog. Observations are limited to macroscopic changes in the concentrations of the major reactants and products with time. The results of recent chamber experiments and detailed kinetic studies of elementary reactions have provided sufficient insight so that we can now postulate a provisional mechanism for the oxidation of  $\text{SO}_2$  by homogeneous gas phase reactions. We discuss this 10-step mechanism briefly below.

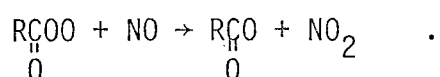
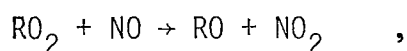
Experimental studies have indicated that peroxy radicals, diradicals, and hydroxyl radicals are the most potent gas phase oxidizing agents with respect to  $\text{SO}_2$  in photochemical smog. Davis et al. (1973) obtained a preliminary measurement of the rate constant for the reaction



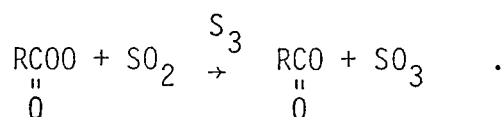
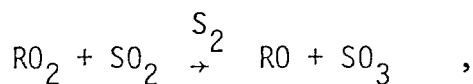
of  $0.45 \text{ ppm}^{-1} \text{ min}^{-1}$ . The observed rate is sufficiently high to suggest that the  $\text{HO}_2$ - $\text{SO}_2$  reaction is important at about the time that  $\text{NO}_2$  reaches its maximum values and  $\text{O}_3$  begins to accumulate. Studies of  $\text{SO}_2$  in smog simulation experiments have shown that this is the time at which the oxidation rate of  $\text{SO}_2$  is greatest.  $\text{HO}_2$  is, of course, generally regarded as the principal oxidant of  $\text{NO}$ :



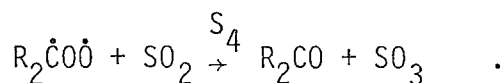
Because of the functional similarity of peroxyalkyl and peroxyacyl radicals to  $\text{HO}_2$ , it does not seem unreasonable to presume that these three species would undergo the same chemical reactions with a given reductant. Both  $\text{RO}_2$  and  $\text{RCO}_3$  apparently oxidize  $\text{NO}$  through a reaction similar to the  $\text{HO}_2$ - $\text{NO}$  reaction:



Although the rate constants for these reactions are not known yet, the reactions are thought to proceed more rapidly than the  $\text{HO}_2$ - $\text{NO}$  reaction. We feel that, because of the analogies between the structure and behavior of  $\text{HO}_2$ ,  $\text{RO}_2$ , and  $\text{RCO}_3$ , the last two species oxidize  $\text{SO}_2$  at a rate somewhat faster than that of  $\text{HO}_2$ . We therefore estimate that  $k_{\text{S}_2} = k_{\text{S}_3} = 1 \text{ ppm}^{-1} \text{ min}^{-1}$ :

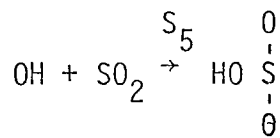


Cox and Penkett (1972) observed that  $SO_3$  forms with reasonable rapidity when a system containing  $O_3$ , olefin, and  $SO_2$  react, and they postulated that diradicals, products of the  $O_3$ -olefin reaction, are the species that oxidize  $SO_2$ :



Since diradicals apparently form in smog only as a result of  $O_3$ -olefin reactions, this reaction, depending on its rate, may be less important than Reactions  $S_1$  through  $S_3$  in polluted air, where normally less than 20 percent of the organics are olefinic. O'Neal and Blumstein (1973) recently reconsidered the mechanism of the  $O_3$ -olefin reaction, and they feel that the intermediate complex of the reaction may decompose to form free radicals, including H. A hydrogen atom formed in this manner could combine with  $O_2$  to form  $HO_2$ , which is known to oxidize  $SO_2$  (Reaction  $S_1$ ). Thus, in the Cox and Penkett experiments,  $HO_2$ , rather than a diradical, may have been the species generated by the  $O_3$ -olefin reaction that oxidized  $SO_2$ . Consequently, Reaction  $S_4$  is very speculative.

Recent measurements of the  $OH$ - $SO_2$  rate constant have suggested that the reaction

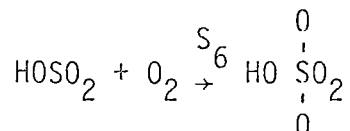


may be an important loss mechanism for  $SO_2$  in photochemical smog. Cox (1974) obtained a value of  $850 \text{ ppm}^{-1} \text{ min}^{-1}$  under atmospheric conditions, and Castleman et al. (1974) found the value to be  $600 \text{ ppm}^{-1} \text{ min}^{-1}$ .

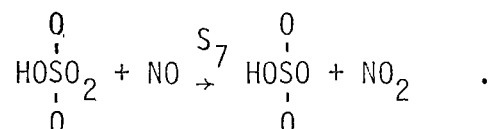


One can only speculate as to subsequent reactions of  $\text{HOSO}_2$  in smog [see, for example, Smith and Urone (1974) and references therein]. We offer one possible reaction scheme here, which is largely an analogy to reactions of organic free radicals.

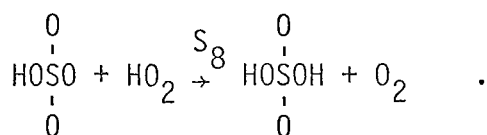
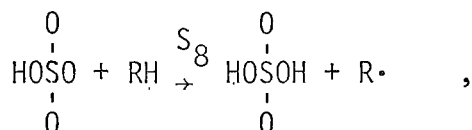
We assume that  $\text{O}_2$  adds to the  $\text{HOSO}_2$  radical



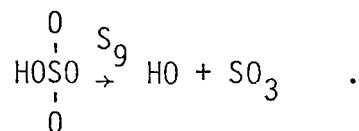
and that this peroxy radical can oxidize nitric oxide:



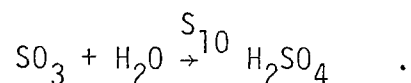
The  $\text{HOSO}_3$  might abstract a hydrogen atom from an organic molecule or from an  $\text{HO}_2$  radical, forming  $\text{H}_2\text{SO}_4$  directly:



Or the  $\text{HOSO}_3$  might undergo a unimolecular decomposition reaction to form OH and  $\text{SO}_3$ :

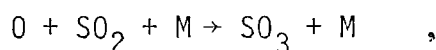


Sulfur trioxide is, of course, the anhydride of sulfuric acid:



Although we can set forth other reactions for the  $\text{HSO}_x$  radicals describing their behavior in the presence of  $\text{NO}_2$  and other reactive species, we cannot substantiate such reactions (including  $\text{S}_7$  through  $\text{S}_{10}$ ) with the results of experiments that have been carried out to date.

Although we did not include several reactions in the core mechanism ( $\text{S}_1$  through  $\text{S}_{10}$ ) for the oxidation of  $\text{SO}_2$ , some comments about them are in order. The  $\text{O-SO}_2$  reaction, for example,



has a reasonably high rate constant but is, nevertheless, slow because of the extremely low concentration of oxygen atoms in smog. The direct photolysis of  $\text{SO}_2$  in otherwise clean air results in the slow disappearance of  $\text{SO}_2$ , but the rate of  $\text{SO}_2$  loss is not comparable to the rates observed in polluted air.

Wilson and Levy (1969) showed that  $\text{NO}_2$  reacts very slowly with  $\text{SO}_2$ . Calvert (1975) determined upper limits for the rates of reaction of  $\text{NO}_3$  and  $\text{N}_2\text{O}_5$  with  $\text{SO}_2$  of  $10^{-5} \text{ ppm}^{-1} \text{ min}^{-1}$  and  $6 \times 10^{-8} \text{ ppm}^{-1} \text{ min}^{-1}$ , respectively. Consequently, both of the reactions are of negligible importance in photochemical smog. In addition, Calvert found, in agreement with others, that the  $\text{O}_3\text{-SO}_2$  reaction is very slow, having a rate constant of about  $10^{-8} \text{ ppm}^{-1} \text{ min}^{-1}$ . In summary, each of this last group of reactions results in the slow oxidation of  $\text{SO}_2$  to  $\text{SO}_3$ . Although we could have included in the core  $\text{SO}_2$  mechanism, the results of kinetic studies of these reactions suggest that their combined contribution to the total predicted loss rate of  $\text{SO}_2$  is minor.

Because kineticists have studied in detail only two of the ten elementary reactions included in the mechanism for the gas phase oxidation of  $\text{SO}_2$  the mechanism has an extremely high level of uncertainty. EPA is presently funding investigations of some of these reactions; therefore, more accurate values

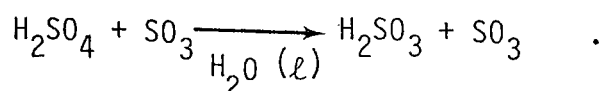
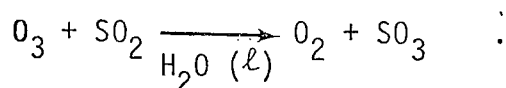
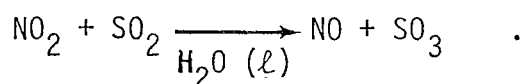
of the corresponding rate constants may be forthcoming in the near future. Despite the uncertainty, we attempted to test this mechanism using smog chamber data. (Section C-3 describes these efforts.) However, we found that the chamber data were inadequately characterized in many important respects and, consequently, were unusable.

## 2. The State of the Art Regarding the Oxidation of SO<sub>2</sub> in Solution

A large percentage of the volume of aerosol particles consists of water. Gas phase borne SO<sub>2</sub> can dissolve in these particles, especially in the environment of a stack plume, where the SO<sub>2</sub> concentration is often high. Once SO<sub>2</sub> is dissolved, both direct and catalyzed reactions apparently lead to the oxidation of SO<sub>2</sub> to sulfate. However, it is not now possible to assess the relative importance of these competitive pathways under conditions of photochemical smog formation. Certainly, the contribution of these two types of reactions to the total SO<sub>2</sub> oxidation rate in solution depends on such factors as aerosol size, oxidant concentration, catalyst concentration, species of oxidant present, catalyst species present, and other chemical species in the droplet that might enter into reactions with the oxidants or the catalysts. In this section, we identify possible important direct and catalyzed reactions in solution and attempt to explain the mechanisms of these reactions.

### a. Reactions of SO<sub>2</sub> in Solution with Oxidants Produced in the Gas Phase

Investigators have studied the reactions of SO<sub>2</sub> in solution with three products of photochemical smog: NO<sub>2</sub>, O<sub>3</sub>, and H<sub>2</sub>SO<sub>4</sub>.



The first of these reactions (Wilson et al., 1972) and the last (Gerhard and Johnstone, 1955) proceed very slowly. Ozone and  $\text{SO}_2$ , however, react rapidly in the presence of liquid water, and the reaction probably occurs in solution (Wilson and Levy, 1969). The rate of this aqueous reaction contrasts sharply with that of the gas phase  $\text{O}_3$ - $\text{SO}_2$  reaction, which is extremely slow. Thus, the reaction between  $\text{SO}_2$  and  $\text{O}_3$  could be significant in aerosol particles, and measurement of the rate constant of the reaction in a simulated atmospheric environment is important.

b. Direct and Catalyzed Reactions of  $\text{SO}_2$  with Metal Ions in Solution

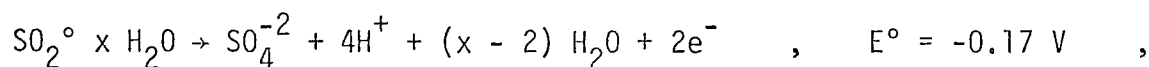
As reported in the literature,  $\text{SO}_2$  is slowly oxidized when dissolved in water (probably through a direct reaction with dissolved oxygen); however, the presence of metal ions, such as  $\text{Mn}^{+2}$ ,  $\text{Fe}^{+2}$ ,  $\text{Fe}^{+3}$ ,  $\text{Ni}^{+2}$ , and  $\text{Cu}^{+2}$ , in the solution accelerates the oxidation rate of  $\text{SO}_2$  substantially (Urone and Schroeder, 1969; Bufalini, 1971). The metal ions can interact chemically with  $\text{SO}_2$  in either or both of two ways: through direct reaction with  $\text{SO}_2$  or through catalysis of the (dissolved) air oxidation of  $\text{SO}_2$ . We now turn to a discussion of each of these classes of reactions.

Direct Oxidation-Reduction Reactions Between Metal Ions and  $\text{SO}_2$ . An examination of half-cell potentials provides a straightforward means of evaluating whether a given reaction is expected to occur on the basis of purely thermodynamic considerations. In the context of this discussion, we are particularly interested in learning whether oxidation-reduction couples (i.e., reactions) between  $\text{SO}_2$  and metal ions result in the oxidation of  $\text{SO}_2$  to  $\text{SO}_3$  (or  $\text{SO}_4^{=}$ ) and the reduction of metal ions to some lower oxidation state.

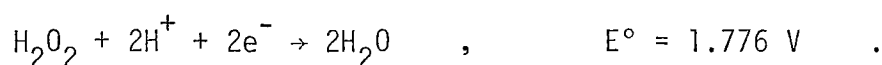
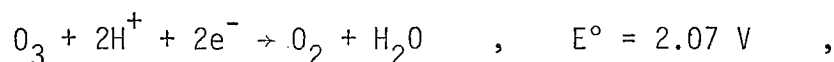
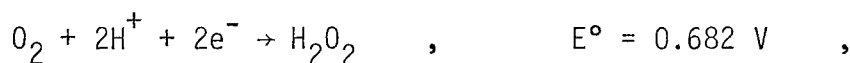
We first observe that according to predictions,  $\text{O}_2$ ,  $\text{O}_3$ , and  $\text{H}_2\text{O}_2$  should all oxidize  $\text{SO}_2$ . Noting that the  $\text{SO}_2$ - $\text{SO}_4^{=}$  half-reaction is:

---

\* We used reduction potentials for these calculations; thus, for a reaction couple to be favored, the combined potential must be positive.



we see that  $\text{SO}_2$  is oxidized as a result of any of the following half-reactions:



The coupled potentials are, therefore, positive by 0.51 V, 1.90 V, and 1.61 V, respectively.

Of the five metal cations known to "oxidize"  $\text{SO}_2$ , only two would be predicted to enter into direct reaction with  $\text{SO}_2$  on the basis of thermodynamic considerations alone:  $\text{Fe}^{+3}$  and  $\text{Cu}^{+2}$ . Their respective half-cell potentials are



Direct reactions between  $\text{SO}_2$  and  $\text{Mn}^{+2}$ ,  $\text{Fe}^{+2}$ , and  $\text{Ni}^{+2}$  are extremely unfavored. Their respective half-cell potentials are:

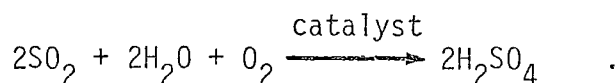


These data indicate that for the direct oxidation of  $\text{SO}_2$  by  $\text{Mn}^{+2}$ ,  $\text{Fe}^{+2}$ , and  $\text{Ni}^{+2}$  to occur, one would have to apply 2.54 V, 0.58 V, and 0.40 V, respectively, of energy to the reacting system.

Theoretical results such as these should, of course, be subjected to experimental scrutiny. In fact, experimenters have observed the direct reactions between  $\text{SO}_2$  and  $\text{O}_2$ ,  $\text{O}_3$ , and  $\text{H}_2\text{O}_2$ , in a water solution that are predicted to take place on the basis of thermodynamic principles. The two cations  $\text{Fe}^{+3}$  and  $\text{Cu}^{+2}$  are known to accelerate the rate of oxidation of  $\text{SO}_2$ . However, it has not yet been shown (to our knowledge) that the mechanism of oxidation of  $\text{SO}_2$  by  $\text{Fe}^{+3}$  and  $\text{Cu}^{+2}$  is direct. The isolation of  $\text{Fe}^{+2}$  and  $\text{Cu}$  as products of reactions in an aqueous solution of  $\text{SO}_2$ ,  $\text{Fe}^{+3}$ , and  $\text{Cu}^{+2}$  would, for example, constitute acceptable evidence for the direct oxidation mechanism. (It is important to remember the limitations of these electrochemical cell calculations. Although half-cell potentials provide a means of predicting the direction of a chemical reaction, they do not in any way indicate the rate at which the reaction will proceed.)  $\text{Mn}^{+2}$ ,  $\text{Fe}^{+2}$ , and  $\text{Ni}^{+2}$  do not enter into a direct reaction with  $\text{SO}_2$  unless energy is supplied to the system; thus, their roles in the oxidation process must be catalytic or indirect.

Catalytic Oxidation of  $\text{SO}_2$ . Catalytic oxidation may well be the principal process for  $\text{SO}_2$  conversion under conditions of high humidity and high particulate concentration, such as those that exist in plumes from power plants. Gartrell et al. (1963) reported, for example, that the rate of  $\text{SO}_2$  oxidation in a smoke plume was quite low for relative humidities less than 70 percent, but it increased markedly for higher humidities. In one case, they measured a rate of  $\text{SO}_2$  conversion of 55 percent in 108 minutes. Although such a rate is too high to be accounted for by a photochemical mechanism [a conclusion based on early studies of the photochemical oxidation of  $\text{SO}_2$  by Gerhard and Johnstone (1955)], it is similar to that expected of oxidation in solution in the presence of a catalyst. Since the metal sulfates (and chlorides) emitted in a plume from a coal-burning process are potential catalysts for the liquid phase oxidation of  $\text{SO}_2$ , a reasonable explanation for this process is that these particles act as condensation nuclei, producing droplets of metal salt solution, which then act as loci for the  $\text{SO}_2$  conversion.

The atmospheric catalytic oxidation of  $\text{SO}_2$  involves both water and dissolved  $\text{O}_2$ ,<sup>\*</sup> and it requires the presence of a catalyst:

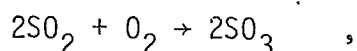


Catalysts for this reaction include several metal salts, such as sulfates and chlorides of manganese and iron, which usually exist in air as suspended particulate matter. At high humidities, these particles act as condensation nuclei or undergo hydration to become solution droplets. The oxidation process then proceeds by absorption of both  $\text{SO}_2$  and  $\text{O}_2$  by the liquid aerosol, with a subsequent chemical reaction in the liquid phase.

Early experiments conducted by Johnstone and Coughanowr (1958) and Johnstone and Moll (1960), in which they measured  $\text{SO}_2$  oxidation in droplets of  $\text{MnSO}_4$ , confirmed the basic catalytic mechanism. In addition, studies performed by Junge and Ryan (1958) of the oxidation of  $\text{SO}_2$  in bulk catalyst solutions yielded valuable information on the effects of solution acidity on the rate of  $\text{SO}_2$  oxidation.

Recently, Cheng et al. (1971) reported laboratory results involving the catalytic oxidation of  $\text{SO}_2$  in aerosol drops containing metal salts. They developed an aerosol-stabilizing technique in which aerosol particles were deposited on inert supporting Teflon beads in a fluidized bed. This deposition process altered neither the physical shape nor the chemical properties of the aerosol. After packing the Teflon beads with the deposited aerosol particles into a flow reactor, in which the catalytic oxidation of  $\text{SO}_2$  occurred, the experimenters passed a mixture of  $\text{SO}_2$  and humid air through the reactor. The  $\text{SO}_2$  concentrations at the reactor entrance ranged from 3 to 18 ppm. To monitor the progress of the oxidation, Cheng et al. continuously measured the  $\text{SO}_2$  concentration at the reactor exit. They identified reaction products by analyzing the reactor contents at the completion of an experiment.

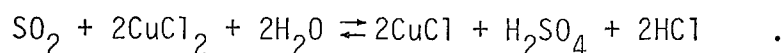
<sup>\*</sup>The rate of the direct reaction of  $\text{SO}_2$  with  $\text{O}_2$ ,



is too slow at room temperature to be of importance in the atmospheric oxidation of  $\text{SO}_2$ .

The  $\text{SO}_2$  conversion progressed in three stages. During the initial period, all of the influent  $\text{SO}_2$  was converted; none appeared at the reactor exit. A transitional period followed, in which the  $\text{SO}_2$  conversion rate decreased from the initial maximum value to a steady value. From then on, a steady-state conversion of  $\text{SO}_2$  took place. The three-stage process can be related to the change in solubility of  $\text{SO}_2$  in a water solution as the solution becomes more acidic. The initially rapid conversion of  $\text{SO}_2$  apparently results from the high rate of dissolution of gaseous  $\text{SO}_2$  into liquid catalyst drops. The increase in sulfuric acid in the drops soon affects the initial stage of rapid conversion. Because  $\text{H}_2\text{SO}_4$  in a dilute concentration undergoes complete dissociation to  $\text{HSO}_4^-$  and  $\text{H}^+$ , the added  $\text{H}^+$  concentration diminishes the solubility of  $\text{SO}_2$ . Finally, as the solution acid concentration exceeds a certain level, the high  $\text{H}^+$  concentration prevents further dissociation of  $\text{H}_2\text{SO}_4$ , and the solubility of  $\text{SO}_2$  becomes constant. In this final stage, the rate of conversion of  $\text{SO}_2$  to sulfate equals the rate at which  $\text{SO}_2$  is absorbed in the drops.

Although  $\text{NaCl}$ ,  $\text{CuSO}_4$ ,  $\text{MnCl}_2$ , and  $\text{MnSO}_4$  all exhibited the same general behavior, each salt differed in effectiveness as a catalyst for the oxidation of  $\text{SO}_2$ . Table 8 shows the steady-state conversions found by Cheng et al. (1971). In the case of  $\text{CuCl}_2$ , Cheng et al. found that, rather than acting as a catalyst,  $\text{CuCl}_2$  reacted directly with  $\text{SO}_2$  according to the following reaction:



Although the conversion of  $\text{SO}_2$  proceeded even at very low relative humidities (less than 40 percent), it did so slowly. Above about 70 percent relative humidity, which is the level at which the transition from solid crystals surrounded by a layer of water to actual solution drops takes place, the rate of conversion increased dramatically.

The individual steps in the liquid-phase catalytic oxidation of  $\text{SO}_2$  are as follows:



- > The gas-phase diffusion of  $\text{SO}_2$  to the drops,
- > The diffusion of  $\text{SO}_2$  from a drop's surface to the interior,
- > The catalytic reaction in the interior.

Under steady-state conditions, the slowest of these three steps limits the overall rate of  $\text{SO}_2$  conversion. If the gas phase diffusion of  $\text{SO}_2$  to the drops is the controlling step, then the rate of  $\text{SO}_2$  conversion should depend on the gas velocity in the system. If the liquid-phase diffusion of  $\text{SO}_2$  controls the conversion rate, then the rate can be expected to be independent of the type of catalyst. In varying the gas flow rate through their reactor, Cheng et al. found that the overall rate of  $\text{SO}_2$  conversion was unaffected. Since, as the results in Table 8 show, these rates clearly depend on the type of catalyst, the rate-controlling step is the chemical reaction itself. Foster (1969) reached similar conclusions.

Table 8  
THE EFFECT OF DIFFERENT CATALYSTS ON  $\text{SO}_2$  OXIDATION

<u>Catalyst</u>	<u>Weight (mg)</u>	<u>Mean Resi- dence Time (min)</u>	<u>Influent <math>\text{SO}_2</math> Concentrations (ppm)</u>	<u>Fraction Conversion</u>	<u>Effective- ness Factor</u> *
NaCl	0.36	1.7	14.4	0.069	1.0
$\text{CuSO}_4$	0.15	1.7	14.4	0.068	2.4
$\text{MnCl}_2$	0.255	0.52	3.3	0.052	3.5
$\text{MnSO}_4$	0.51	0.52	3.3	0.365	12.2

\* The catalytic effectiveness of the various materials was compared with that of NaCl. Thus, the effectiveness factor is the product of the ratio of the weight of the catalyst in the reactor, the ratio of the reactor mean residence time, and the ratio of the reaction conversion of  $\text{SO}_2$  in the reactor. The effectiveness factor for  $\text{MnSO}_4$ , for example, is:

$$1.0 \cdot \left( \frac{0.36}{0.51} \right) \left( \frac{1.7}{0.52} \right) \left( \frac{0.365}{0.069} \right) = 12.2$$

For steady-state conversion in the atmosphere, Cheng et al. derived the following first-order rate expression from their data for  $\text{MnSO}_4$ :

$$R_{\text{SO}_2} = 0.67 \times 10^{-2} [\text{SO}_2] \quad ,$$

where  $R_{\text{SO}_2}$  is the micrograms of  $\text{SO}_2$  converted per minute per milligram of  $\text{MnSO}_4$ ,  $[\text{SO}_2]$  is the gas phase concentration of  $\text{SO}_2$  in micrograms per cubic meter, and the constant factor is for drops containing 500 ppm of  $\text{MnSO}_4$ . The factor can be altered for other catalysts using Table 8. We can compute the rate of conversion of  $\text{SO}_2$  for conditions typical of natural fog in an urban atmosphere:

- >  $(\text{SO}_2) = 0.1$  ppm.
- > The average diameter of the fog droplets is  $15 \mu$ .
- > Half the fog droplets contain a catalyst capable of oxidizing  $\text{SO}_2$  to  $\text{H}_2\text{SO}_4$ . The catalyst concentration within these droplets is equivalent to 500 ppm  $\text{MnSO}_4$ .
- > The fog concentration is 0.2 gram of  $\text{H}_2\text{O}$  per cubic centimeter of air.

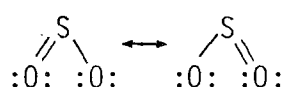
Under these assumptions, the equivalent catalyst concentration is 50 micrograms of  $\text{MnSO}_4$  per cubic meter of air, and the rate of conversion of  $\text{SO}_2$  is 2 percent per hour. Typical concentrations of catalyst metals are tabulated below:

<u>Catalyst</u>	<u>Concentration (<math>\mu\text{g m}^{-3}</math>)</u>
Mn	10
Cu	10
Zn	58
Fe	74
Pb	17

Thus, the conditions of the sample calculation are reasonable for actual air.

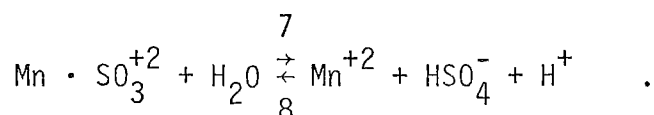
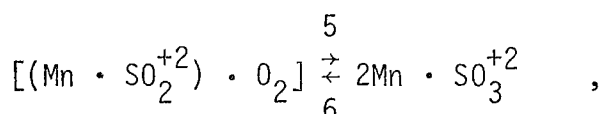
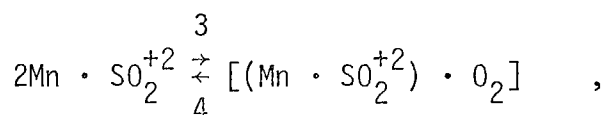
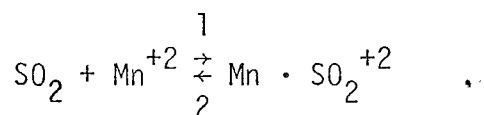
The detailed mechanism of the catalized oxidation of  $\text{SO}_2$  is not yet known; however, the first step in the process may involve the association of a reactant with the catalyst. If the catalyst is a transition metal cation, the reactant apparently enters into a coordination complex with the cation; thus, the reactant occupies a position in the ligand field of the metal. Matteson et al. (1969) observed that catalyst potency toward the oxidation of  $\text{SO}_2$  tends to decrease as the number of possible sites at which  $\text{SO}_2$  can complex on the metal ion decreases. Thus, the configuration of the ligand field (e.g., square planar, octahedral) of a given metal ion strongly influences the catalytic behavior of the ion.

If the first step in catalysis is, indeed, the coordination of  $\text{SO}_2$  with the cation, the rate of displacement of other ligands in the ligand field by  $\text{SO}_2$  must be examined. Some species form much stronger coordination bonds with transition metal ions than others do. For example, carbon monoxide poisoning of the blood results because the binding energy of CO to the iron in hemoglobin is much greater than that of  $\text{O}_2$ . Consequently,  $\text{O}_2$  cannot displace the CO from the iron, and the body rapidly depletes the blood of  $\text{O}_2$ .  $\text{SO}_2$  can, in principle, coordinate with transition metals, since it contains unshared electrons--a general characteristic of ligands:



(Other ligands include, for example,  $\text{H}_2\text{O}$ , NO, and CO.) But, if, as a result of this mechanism involving transition metal cations,  $\text{SO}_2$  is to be catalytically oxidized in aerosols, it must be able to displace other ligands from the catalyst. Because of the high concentration of water and the presumably low relative concentrations of  $\text{SO}_2$  and catalysts in aerosols, the tendency for  $\text{SO}_2$  to displace water from the ligand field must be especially great. Thus, an experimental investigation of the rate of  $\text{H}_2\text{O}$  displacement by  $\text{SO}_2$  in the principal catalysts for  $\text{SO}_2$  oxidation is clearly needed.

One explanation of the catalytic oxidation of  $\text{SO}_2$  in solution is the series of four equilibria proposed by Matteson et al. (1969):



Matteson et al. made three crucial assumptions in this mechanism:

- >  $\text{SO}_2$  coordinates rapidly with  $\text{Mn}^{+2}$  (Step 1)
- > The association of  $\text{Mn} \cdot \text{SO}_2^{+2}$  complexes is likely (Step 3)
- > Oxygen transfer to the  $[(\text{Mn} \cdot \text{SO}_2^{+2})_2 \cdot \text{O}_2]$  complex occurs (Step 5).

Although Matteson et al. did not address these issues in formulating their mechanism, the series of reactions provides a construct for further experimental and theoretical inquiries.

It is not possible now to ascertain the extent to which the oxidation of  $\text{SO}_2$  in solution competes with the gas phase reactions. Very little data pertaining to the kinetics of the reactions between  $\text{SO}_2$  and dissolved salts exist that can be incorporated in a predictive model. Understanding the role of  $\text{SO}_2$

in the atmosphere and, indeed, the formulation of effective  $\text{SO}_2$  control strategies will critically depend on the fundamental investigation of the types of reactions discussed in this section. Without quantitative data upon which to build a model, predictions are of little significance.

### 3. Efforts To Test the Gas Phase Reaction Mechanism for $\text{SO}_2$

Shortly after the inception of the project, we received the results of a series of smog chamber experiments from EPA to use to test the 10-step mechanism described in Section C-1 as a possible explanation for the oxidation of  $\text{SO}_2$  in the gas phase. The experiments were carried out in a dynamic flow reactor, and propylene,  $\text{NO}_x$ ,  $\text{SO}_2$ , and air were used as reactants. To simulate the system, we added the  $\text{SO}_2$  reactions (Reactions  $\text{S}_7$  through  $\text{S}_{10}$ ) to a general mechanism for smog (Hecht et al., 1974). We had previously performed extensive tests of the organic- $\text{NO}_x$ -air reactions using propylene- $\text{NO}_x$ -air data obtained in the same smog chamber operated in a static mode.

Unfortunately, we found that the dynamic  $\text{SO}_2$  experiments were unsuitable for modeling for two reasons. First, the concentration of  $\text{SO}_2$  in the inlet tube fluctuated substantially during an irradiation, but the inlet concentrations were not measured often enough to permit an accurate inflow profile of  $\text{SO}_2$  to be generated. Second, the oxidation reactions of  $\text{SO}_2$  are quite slow relative to the majority of other chemical transformations of interest in this particular chemical system (e.g., the oxidation of NO and organics, and the formation of  $\text{O}_3$ ). The net effect of these two characteristics of the system was that the fluctuations in the inlet tube  $\text{SO}_2$  concentrations masked any loss of  $\text{SO}_2$  due to chemical reactions.

The mechanism evaluation procedure, therefore, became more a test of the adequacy with which the mixing and flow characteristics of the chamber were modeled than of the accuracy of the mechanism. In view of the substantial uncertainties in the inflow data, even very good agreement between the predictions and the data would not be sufficient to demonstrate the validity of the mechanism. Consequently, we suspended our efforts to test the  $\text{SO}_2$  mechanism

until more carefully controlled smog chamber data become available. A new experimental study involving organics,  $\text{NO}_x$ , and  $\text{SO}_2$  is now in progress; we summarize that program in the following section.

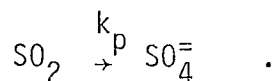
#### 4. Future Examinations of $\text{SO}_2$ Chemistry

Under the direction of Dr. Arthur Levy, investigators at Battelle Memorial Laboratory are presently conducting a series of organic- $\text{NO}_x$ - $\text{SO}_2$ -air experiments using propylene (nine runs) and toluene (six runs) as the reactive organic. Under another EPA contract, we expect to employ these data to test the  $\text{SO}_2$  mechanism proposed in Section C-1. The use of these data offers several advantages:

- > The experiments are being conducted under static conditions. Consequently, we will not have to contend with fluctuations in inflow reactant concentrations as an additional variable in evaluating the model.
- > The chamber is still in operation (the chamber used for the experiments mentioned in Section C-1 has been disassembled). Thus, any chamber effects that were not yet measured can still be determined, if needed, for the model testing exercises.
- > Dr. Levy's group at Battelle has considerable experience and expertise in studying  $\text{SO}_2$  in smog chambers. Therefore, the new  $\text{SO}_2$  data will almost certainly be the best that are currently obtainable.

The evaluation of a mechanism describing the oxidation of  $\text{SO}_2$  in solution or in aerosols is more difficult. To our knowledge, no systematic experimental study of this process suitable for model testing has yet been carried out. Until the oxidation rate of  $\text{SO}_2$  in systems containing aerosol particles has been determined as a function of particle size (volume, surface area), composition and concentration of reactants in the particle, pH of the particle, and concentration of  $\text{SO}_2$  in the gas phase, it will be difficult to propose with any confidence a physical model for the oxidation of  $\text{SO}_2$  in solution. As a temporary

measure, it may be possible to develop a parametric model in which the oxidation of  $\text{SO}_2$  in particles is described by the first-order reaction



The parameter  $k_p$  can then be estimated from the following:

- > Observations of the  $\text{SO}_2$  oxidation rate in droplets under well-controlled conditions, such as those used in the experiments of Cheng et al. (1971).
- > Knowledge of the composition of atmospheric aerosols.

Although a parametric mechanism is necessarily simplistic, combined with the gas phase mechanism, it may be sufficient to predict the atmospheric conversion of  $\text{SO}_2$  to sulfate within the uncertainty bounds of aerometric measurements. We expect to analyze the methods for selecting values of  $k_p$  during Contract 68-02-0580.

#### D. SPECIAL CONSIDERATIONS REGARDING THE TREATMENT OF TEMPERATURE, WATER, AND HYDROGEN PEROXIDE IN THE AIRSHED MODEL

In the process of reviewing previous airshed modeling exercises, as well as considering some of the possible difficulties that might arise in the use of the latest version of the SAI model, we identified the following three questions that seemed to need further clarification:

- > To what extent should temperature effects on reaction rate constants be considered in the model?
- > How important are the spatial and temporal variations in water concentration?
- > Will the model predictions be sensitive to the initial concentration distribution of hydrogen peroxide?

In an attempt to answer these questions, we carried out various sensitivity studies using the kinetic mechanism, and we reviewed available measurements for some of these parameters in one of the most severe and persistent photochemical air pollution regions--the South Coast air basin of California.

It is well known that reaction rate constants are a function of temperature. This effect is commonly expressed using the Arrhenius relationship:

$$k(T) = A \exp\left(-\frac{E_a}{RT}\right) ,$$

where

$k$  = the rate constant,

$A$  = a constant (sometimes referred to as the frequency factor),

$E_a$  = the so-called activation energy for the reaction,

$R$  = the gas constant,

$T$  = the absolute temperature.

Given  $k$  at some temperature  $T_0$  and the activation energy, the value of  $k$  at any other temperature can be estimated from

$$k(T) = k(T_0) \exp\left[-\frac{E_a}{R}\left(\frac{1}{T} - \frac{1}{T_0}\right)\right] . \quad (8)$$

Thus, we do not need to determine  $b$ . In the computer programs, we input  $T_0$  and the values of  $E_a$  and  $k(T_0)$  for each chemical reaction. Then  $k$  can be calculated at any other temperature  $T$  using Eq. (8).

Although the algorithm outlined above is not difficult to incorporate in the model, there is some question of the extent to which spatial and temporal variations in temperature must be considered. For example, complete specification of the temperature as a function of  $x$ ,  $y$ ,  $z$ , and time would require significant amounts of additional computer storage, not to mention the extra



effort required of the user to assemble sufficient data to estimate the complete temperature field. Thus, we undertook a study to examine the sensitivity of the kinetic mechanism to variations in temperature that might be found in an urban airshed. These results can be used as a guide for determining under what conditions spatial and temporal features of the temperature field must be considered in the model.

Similar questions arise concerning the distribution of water in the gas phase over an urban area, especially a region like the South Coast air basin, in which there are coastal areas as well as inland valleys. We note that though spatial variations of relative humidity are significant in this airshed, it is important to examine the variations in water concentration because this is the parameter entering the kinetic rate expressions. Thus, to determine the extent to which provisions for treating spatial and temporal variations in water concentration should be included in the model, we examined the sensitivity of the mechanism to variations in water concentration.

Finally, incorporation of the 31-step mechanism (excluding  $\text{SO}_2$  chemistry) in the model will require the user to specify initial and boundary concentrations of  $\text{HNO}_2$  and  $\text{H}_2\text{O}_2$ , two pollutants that are rarely measured routinely in most urban areas. To obtain a rough estimate of the concentrations of these pollutants, we can assume that each is in chemical equilibrium; thus, from the kinetic mechanism, we can write

$$[\text{HNO}_2] = \frac{-k_{10} + \left\{ k_{10}^2 + 8k_9 \left( 2k_8[\text{NO}][\text{NO}_2][\text{H}_2\text{O}]^2 + k_{12}[\text{OH}][\text{NO}] \right) \right\}^{1/2}}{4k_9},$$

$$[\text{H}_2\text{O}_2] = \frac{k_{15}[\text{HO}_2]^2}{k_{16}}.$$

If a simulation is to start somewhat before dawn, use of the above relationships would be tantamount to assuming that chemical equilibrium had been approached during the preceding nighttime period. Although this assumption may be reasonable for  $\text{HNO}_2$ , we note that the  $\text{H}_2\text{O}_2$  photolysis rate constant,  $k_{16}$ , would be

essentially zero at night. In fact, from the mechanism we see that there is no "sink" for  $\text{H}_2\text{O}_2$  other than the photolysis reaction. Thus, the use of the equilibrium assumption for  $\text{H}_2\text{O}_2$ , especially at night, does not seem desirable. To examine this issue further, we carried out simulation runs using the mechanism to ascertain its sensitivity to the initial  $\text{H}_2\text{O}_2$  conditions. In the following sections, we discuss the results obtained from these sensitivity studies involving temperature, water, and  $\text{H}_2\text{O}_2$ .

#### 1. The Predicted Effects of Changes in Temperature and Water Concentration on Smog Kinetics

To determine what effect changes in temperature or water concentration have on the concentration predictions, we carried out simulations of a smog chamber experiment using the new kinetic scheme incorporated in the airshed model. The base values used were those of EPA Run 333:

- >  $[\text{NO}]_0 = 1.25 \text{ ppm},$
- >  $[\text{NO}_2]_0 = 0.08 \text{ ppm},$
- >  $[\text{C}_3\text{H}_6]_0 = 0.23 \text{ ppm},$
- >  $[\text{n-C}_4\text{H}_{10}]_0 = 3.41 \text{ ppm},$
- >  $[\text{H}_2\text{O}]_0 = 16,000 \text{ ppm},$
- >  $T = 25^\circ\text{C}.$

For each simulation run, we changed only one parameter from the base values.

We performed the simulations for two different temperatures,  $15^\circ\text{C}$  and  $35^\circ\text{C}$ , with all other factors kept the same. We calculated the rate constants at the new temperatures from the base values of the rate constants ( $25^\circ\text{C}$ ) and from measured or estimated reaction activation energies, as shown in Table 9 (Garvin and Hampson, 1974; Demerjian et al., 1974; Johnston et al., 1970). Because the majority of the reactions in the mechanism are thermal and because they have small positive activation energies, raising the temperature accelerated the conversion of  $\text{NO}$  to  $\text{NO}_2$  and decreased the time to the onset of  $\text{O}_3$

Table 9

## ACTIVATION ENERGIES OF REACTIONS IN THE GENERAL MECHANISM

Reaction	$E_A$ kcal mole <sup>-1</sup>	Reference
$\text{NO}_2 + h\nu \xrightarrow{1} \text{NO} + \text{O}$	0	Estimate
$\text{O} + \text{O}_2 + \text{M} \xrightarrow{2} \text{O}_3 + \text{M}$	-1	Garvin and Hampson (1974)
$\text{O}_3 + \text{NO} \xrightarrow{3} \text{NO}_2 + \text{O}_2$	2.4	Garvin and Hampson (1974)
$\text{O} + \text{NO}_2 \xrightarrow{4} \text{NO} + \text{O}_2$	0.6	Garvin and Hampson (1974)
$\text{O}_3 + \text{NO}_2 \xrightarrow{5} \text{NO}_3 + \text{O}_2$	4.9	Garvin and Hampson (1974)
$\text{NO}_3 + \text{NO} \xrightarrow{6} 2\text{NO}_2$	1.4	Johnston et al. (1974)
$\text{NO}_3 + \text{NO}_2 + \text{H}_2\text{O} \xrightarrow{7} 2\text{HNO}_3$	-1.9*	Davis (1974)
$\text{NO} + \text{NO}_2 + 2\text{H}_2\text{O} \xrightarrow{8} 2\text{HNO}_2 + \text{H}_2\text{O}$	0	Demerjian et al. (1974)
$2\text{HNO}_2 \xrightarrow{9} \text{NO} + \text{NO}_2 + \text{H}_2\text{O}$	9	Demerjian et al. (1974)
$\text{HNO}_2 + h\nu \xrightarrow{10} \text{OH} + \text{NO}$	0	Estimate
$\text{OH} + \text{NO}_2 \xrightarrow{11} \text{HNO}_3$	-2.2	Garvin and Hampson (1974)
$\text{OH} + \text{NO} \xrightarrow{12} \text{HNO}_2$	-2.2	Garvin and Hampson (1974)
$\text{OH} + \text{CO} + (\text{O}_2) \xrightarrow{13} \text{CO}_2 + \text{NO}_2$	0.15	Davis (1974)
$\text{HO}_2 + \text{NO} \xrightarrow{14} \text{OH} + \text{NO}_2$	2	Estimate
$\text{HO}_2 + \text{HO}_2 \xrightarrow{15} \text{H}_2\text{O}_2 + \text{O}_2$	0	Estimate
$\text{H}_2\text{O}_2 + h\nu \xrightarrow{16} 2\text{OH}$	0	Estimate

\* The value of  $E_A$  listed for this composite reaction we determined from the values of  $E_A$  for the three equivalent reactions:

Reaction	$E_A$	Reference
$\text{NO}_3 + \text{NO}_2 \longrightarrow \text{N}_2\text{O}_5$	-2	Demerjian et al. (1974)
$\text{N}_2\text{O}_5 \longrightarrow \text{NO}_2 + \text{NO}_3$	19.4	Garvin and Hampson (1974)
$\text{N}_2\text{O}_5 + \text{H}_2\text{O} \longrightarrow 2\text{HNO}_3$	0	Estimate

Table 9 (concluded)

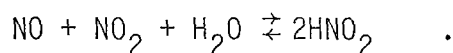
Reaction	$E_A$ kcal mole <sup>-1</sup>	Reference
$HC_1 + O \xrightarrow{17} ROO + \alpha \underset{\text{O}}{\underset{\parallel}{RCOO}} + (1-\alpha)HO_2$	0.1 <sup>§</sup>	Garvin and Hampson (1974)
$HC_1 + O_3 \xrightarrow{18} \underset{\text{O}}{\underset{\parallel}{RCOO}} + RO + HC_3$	3.8 <sup>§</sup>	Garvin and Hampson (1974)
$HC_1 + OH \xrightarrow{19} ROO + HC_3$	1 <sup>§</sup>	Estimate
$HC_2 + O \xrightarrow{20} ROO + OH$	5†	Estimate
$HC_2 + OH \xrightarrow{21} ROO + H_2O$	1†	Estimate
$HC_3 + h\nu \xrightarrow{22} \beta ROO + (2-\beta)HO_2$	0	Estimate
$HC_3 + OH \xrightarrow{23} \beta \underset{\text{O}}{\underset{\parallel}{RCOO}} + (1-\beta)HO_2 + H_2O$	0	Estimate
$HC_4 + O \xrightarrow{24} ROO + OH$	--	--
$HC_4 + OH \xrightarrow{25} ROO + H_2O$	--	--
$ROO + NO \xrightarrow{26} RO + NO_2$	1	Estimate
$RCOO + NO + (O_2) \xrightarrow{27} ROO + NO_2 + CO_2$	0	Estimate
$RCOO + NO_2 \xrightarrow{28} \underset{\text{O}}{\underset{\parallel}{RCOONO_2}}$	0	Estimate
$RO + O_2 \xrightarrow{29} HO_2 + HC_3$	6	Garvin and Hampson (1974)
$RO + NO_2 \xrightarrow{30} RONO_2$	0	Estimate
$RO + NO \xrightarrow{31} RONO$	0	Estimate

§ Estimated  $E_A$  for propylene

† Estimated  $E_A$  for n-butane

accumulation, as expected. Conversely, lowering the temperature noticeably slowed the smog formation process. Figure 1 presents concentration-time profiles for NO, NO<sub>2</sub>, O<sub>3</sub>, and propylene for each of these two runs.

We carried out similar runs at two extreme conditions of relative humidity--0 and 100 percent--at the base temperature (25°C). These percentages correspond to 0 and 32,000 ppm of H<sub>2</sub>O, respectively. Figure 2 shows a comparison of the predicted concentration-time profiles for these two cases with the profile for the base case. Increasing the water concentration accelerated the conversion of NO to NO<sub>2</sub>, whereas a complete elimination of water dramatically slowed down the overall smog kinetics. Both of these effects are attributable to changes in the production rate and equilibrium level of nitrous acid, governed by the reactions



Because it is virtually impossible--even with pumping and baking--to obtain a water concentration of 0 ppm in existing smog chambers, we carried out one final run at 3.2 ppm of H<sub>2</sub>O. The concentration-time profile obtained under these conditions differed from those of the completely dry run by less than 2 percent after six hours of simulation time.

In urban areas, ambient temperatures and water concentrations change considerably during the day and from one day to the next. Thus, the results of these simulation runs suggest that it may be necessary to account for variations in temperature and water concentration when modeling urban photochemical smog. Toward this end, smog chamber experiments conducted at various constant levels of temperature and water concentration would be most useful in ascertaining the effects of variations of these two parameters on smog kinetics.

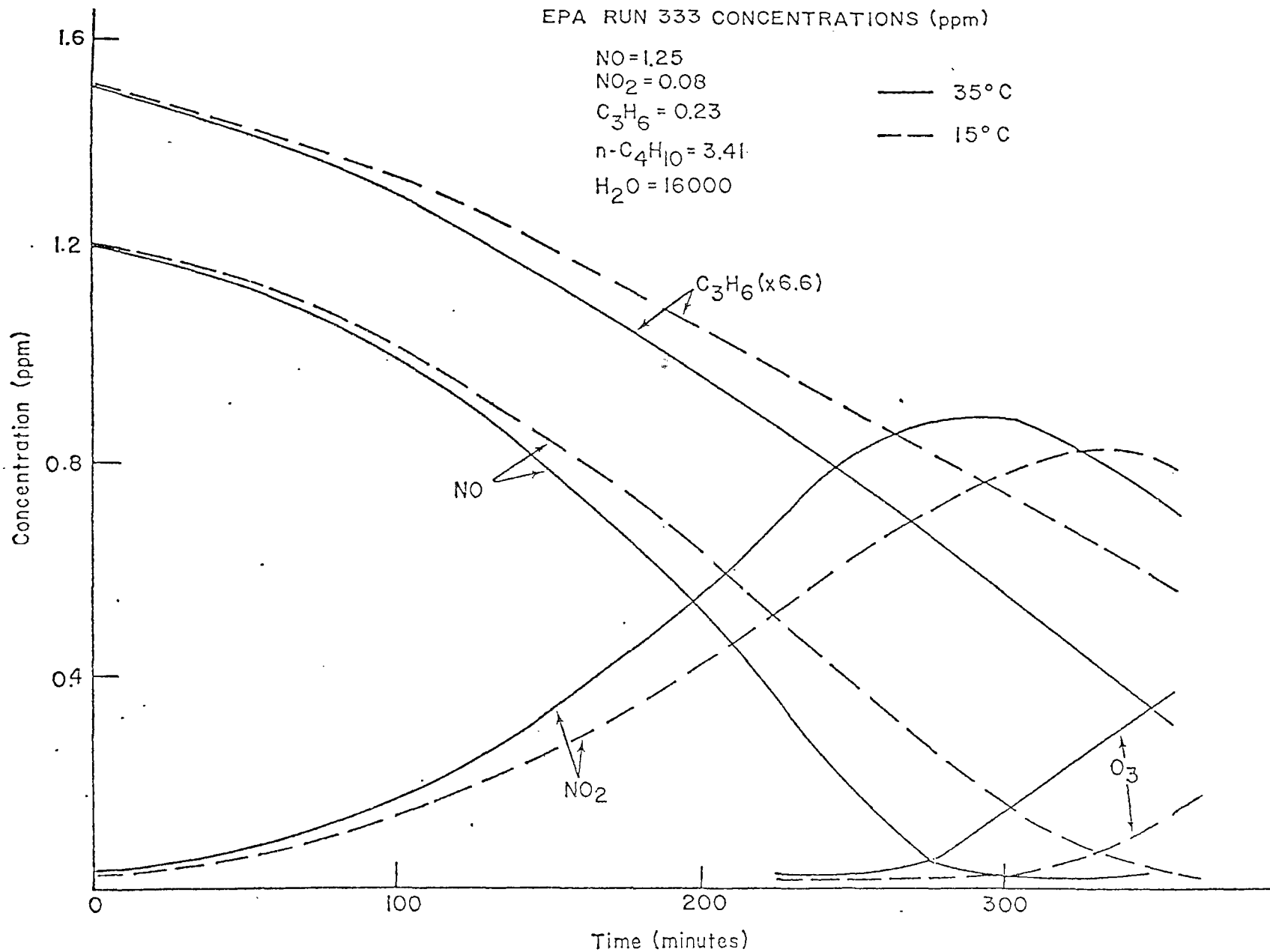


FIGURE 1. CONCENTRATION-TIME PROFILES FOR NO,  $\text{NO}_2$ ,  $\text{O}_3$ ,  
AND PROPYLENE AT 15°C AND 35°C

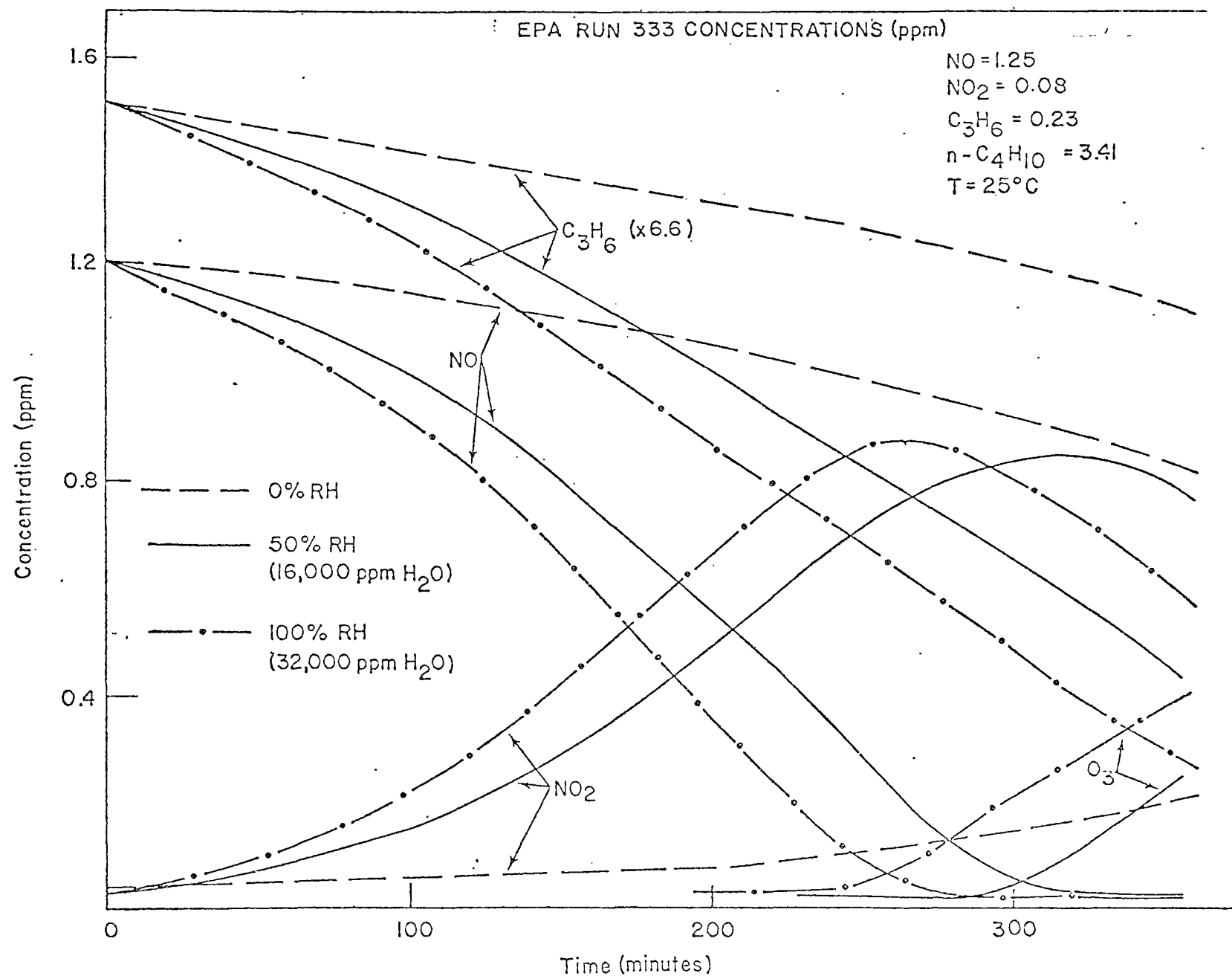


FIGURE 2. PREDICTED CONCENTRATION-TIME PROFILES FOR NO, NO<sub>2</sub>, O<sub>3</sub>, AND PROPYLENE AT 0, 50, AND 100 PERCENT RELATIVE HUMIDITY

## 2. Specification of the Initial Concentration of $\text{H}_2\text{O}_2$

With the implementation of the new kinetic scheme in the airshed model, we must now specify the emission rate and the initial and boundary concentrations of a new reactant,  $\text{H}_2\text{O}_2$ . To ascertain the accuracy with which these parameters must be determined, we carried out kinetic simulations of EPA Chamber Run 333 (under the initial conditions listed in Section D-1) at three different initial  $\text{H}_2\text{O}_2$  concentrations: 0, 0.01, and 0.1 ppm.

The concentration-time profiles obtained for the case in which  $[\text{H}_2\text{O}_2]_0 = 0.01$  ppm did not differ appreciably from those for the base case, in which  $[\text{H}_2\text{O}_2]_0 = 0$  ppm. The small initial  $\text{H}_2\text{O}_2$  concentration resulted in a five-minute reduction in the time to the  $\text{NO}_2$  peak (305 versus 310 minutes) and a small increase in  $\text{O}_3$  at 360 minutes (0.32 versus 0.30 ppm).

In contrast, the effect on the predictions of the presence of 0.1 ppm of  $\text{H}_2\text{O}_2$  initially was far more visible. The conversion of  $\text{NO}$  to  $\text{NO}_2$  was accelerated considerably, and the  $\text{NO}_2$  peaked at 264 minutes. As a result of the substantial reduction in the time to the  $\text{NO}_2$  peak,  $\text{O}_3$  accumulated to 0.46 ppm before the simulation was terminated at 360 minutes.

For similar simulations of another smog chamber experiment (EPA Run 349), the initial conditions were as follows:

- >  $[\text{NO}]_0 = 0.31$  ppm,
- >  $[\text{NO}_2]_0 = 0.03$  ppm,
- >  $[\text{propylene}]_0 = 0.44$  ppm,
- >  $[\text{n-butane}]_0 = 3.25$  ppm,
- >  $[\text{H}_2\text{O}]_0 = 16,000$  ppm,
- >  $T = 25^\circ\text{C}$ .

In these simulations, a maximum in the  $\text{O}_3$  concentration did occur, and the results indicate that the asymptotic ozone level is not affected appreciably (less than 2 percent) by the initial presence of as much as 0.1 ppm of  $\text{H}_2\text{O}_2$ .



However, the  $\text{H}_2\text{O}_2$  did serve to reduce the time that elapsed before the maximum was reached. For example, the predicted  $\text{O}_3$  maximum occurred at 194 minutes for EPA Run 349 when the initial charge contained 0.1 ppm of  $\text{H}_2\text{O}_2$ , compared with 225 minutes when  $\text{H}_2\text{O}_2$  was absent initially.

On the basis of these simulations, we feel that an effort should be made to construct an emissions inventory for  $\text{H}_2\text{O}_2$  only if the sources of such emissions would lead to an ambient hydrogen peroxide concentration of more than 0.01 ppm. Should  $\text{H}_2\text{O}_2$  sources contribute less than this amount, the error incurred by neglecting these sources would be very small, especially prior to the formation of the  $\text{NO}_2$  peak and at the  $\text{O}_3$  asymptote.

With regard to the specification of initial and boundary concentrations in the airshed model, the sensitivity runs indicate that care should be exercised in specifying  $\text{H}_2\text{O}_2$  concentrations when they are on the order of 0.1 ppm or larger. Data presented by Bufalini et al. (1972) suggest that  $\text{H}_2\text{O}_2$  in the South Coast air basin may reach levels as high as 0.18 ppm during a very smoggy day. However, early morning and late afternoon levels were reported to be about 0.01 to 0.02 ppm, thus indicating that overnight carry-over effects may not be too significant. We hasten to add that these observations are based on a very limited number of ambient air measurements. Additional measurements of the diurnal behavior of  $\text{H}_2\text{O}_2$  in an urban airshed would be useful.

### 3. Spatial and Temporal Variations in Temperature and Water Concentration in the South Coast Air Basin

Having shown in Section D-1 that the kinetic mechanism is somewhat sensitive to changes in temperature and water concentration, we carried out a limited effort to examine the extent of these variations in an actual airshed. We chose the South Coast air basin for this study for two reasons. First, photochemical smog is particularly severe in this region. Second, we expected that the spatial and temporal variations in temperature and water concentration found here would be as large as those found in most other airsheds where the model might be applied.

During the summer, an onshore flow of moist marine air generally keeps coastal areas relatively cool [temperatures in the 70s to 80s ( $^{\circ}\text{F}$ )]. By the time the air has traveled to the inland valleys, however, significant heating has taken place, and the temperature often exceeds  $100^{\circ}\text{F}$ . In addition, relative humidities near the coast are usually higher than those measured inland. Of course, since water concentration is the parameter of interest, the effect of temperature on relative humidity must be considered.

Tables 10 and 11 present hourly ground-level temperature and relative humidity data for three smoggy days in June 1974. The station location associated with each code number is as follows:

<u>Number</u>	<u>Station Name</u>
13W	Lennox
21W	Long Beach
41W	Burbank
61W	Ontario
75W	Downtown Los Angeles

Figure 3 shows the location of each station. Lennox and Long Beach are representative of coastal locations, whereas Downtown Los Angeles, Burbank, and Ontario are representative of inland communities.

To examine variations in temperature and relative humidity with height above the terrain, we reviewed some of the measurements recently reported by Blumenthal et al. (1974). They measured the three-dimensional distribution of pollutants and meteorological parameters throughout the South Coast air basin using a fully instrumented fixed-wing aircraft. We chose to examine a two-day period--26-27 July 1973--for which numerous aircraft spirals were made, both during the day and at night.

Table 10  
GROUND-LEVEL AIR TEMPERATURES IN THE LOS ANGELES BASIN ON 28-30 JUNE 1974

JOB NUMBER =GANTABLS		AIR POLLUTION CONTROL DISTRICT - COUNTY OF LOS ANGELES																											
PROGRAM =GANTABLS																													
DATE: 07/19/74		TEMPERATURE / AT HOUR / IN DEGREES FAHRENHEIT																											
STA		HOUR PST																											
		0	1	2	3	4	5	6	7	8	9	10	11	12	13	14	15	16	17	18	19	20	21	22	23	AVE	N	MAX	
13W								64	70	75	77	76	77	78	79	79	79	79	76	75	69					75.2	14	80	
21W								65	70	75	81	84		90	93	92	92	90	88	84	77					83.2	13	96	
41W								68	74	79	85	92	97	99	99	99	98	96	95	89	85					89.6	14	99	
61W								67	75	83	88	93	98	103	105	106	106	102	98							93.7	12	106	
75W								67	70	74	79	86	93	96	89	89	88	88	87	86	84					84.0	14	96	
STA		HOUR PST																											
		0	1	2	3	4	5	6	7	8	9	10	11	12	13	14	15	16	17	18	19	20	21	22	23	AVE	N	MAX	
13W								63	65	69	71	69	72	72	72	72	72	70	67	64	63					68.6	14	73	
21W								64	65	68	70	72	73	74	77	77	76	75	72	73	68					71.7	14	79	
41W								65	70	74	79	84	86	86	87	89	88	84	83	80	75					80.7	14	89	
61W								65	69	77	81	86	92	95	97	95	93	92	88	84	77					85.1	14	97	
75W								67	69	72	74	76	80	81	81	83	85	83	80	78	73					77.3	14	85	
STA		HOUR PST																											
		0	1	2	3	4	5	6	7	8	9	10	11	12	13	14	15	16	17	18	19	20	21	22	23	AVE	N	MAX	
13W								62	62	63	66	69	69	71	71	70	71	70	67	65	64					67.1	14	72	
21W								63	63	64	64	68	70	71	71	72	72	69	67	67	66					67.6	14	74	
41W								62	63	66	70	74	76	79	80	78	79	78	75	71	67					72.7	14	80	
61W								57	58	61	67	77	82	85	87	88	87	83	81	76	70					75.6	14	88	
75W								66	66	66	70	72	76	77	78	77	77	75	75	74	70					72.8	14	78	

Table 11  
GROUND-LEVEL RELATIVE HUMIDITIES IN THE LOS ANGELES BASIN ON 28-30 JUNE 1974

JOB NUMBER =GAMTABS		AIR POLLUTION CONTROL DISTRICT - COUNTY OF LOS ANGELES																											
PROGRAM =GAMTABS																													
DATE: 07/19/74		RELATIVE HUMIDITY / AT HOUR / IN PERCENT																											
STA		HOUR PST																											
		0	1	2	3	4	5	6	7	8	9	10	11	12	13	14	15	16	17	18	19	20	21	22	23	AVE	N	MIN	
13W								87	76	60	58	58	52	48	44	44	44	42	48	50	63					55.3	14	42	
21W								65	59	50	36	43		32	31	31	24	26	29	31	40					38.5	13	26	
41W								37	40	31	28	17	12	12	19	19	13	14	14	19	17					20.9	14	12	
61W								38	30	27	23	20	13	10	10	10	11	11	13							18.0	12	10	
75W								65	61	56	51	39	35	32	48	46	43	40	39	38	38					45.1	14	32	
STA		HOUR PST																											
		0	1	2	3	4	5	6	7	8	9	10	11	12	13	14	15	16	17	18	19	20	21	22	23	AVE	N	MIN	
13W								90	90	78	73	76	68	66	66	68	68	73	81	84	87					76.3	14	66	
21W								75	73	65	63	59	57	55	52	50	52	52	57	55	65					59.3	14	50	
41W								43	46	43	38	36	40	42	40	30	31	42	38	46	56					40.8	14	30	
61W								47	47	36	35	25	17	16	21		25	28	34	36	50					32.1	13	16	
75W								82	80	73	69	65	54	60	57	54	56	60	65	68	80					65.9	14	54	
STA		HOUR PST																											
		0	1	2	3	4	5	6	7	8	9	10	11	12	13	14	15	16	17	18	19	20	21	22	23	AVE	N	MIN	
13W								90	90	87	78	70	70	64	66	66	66	68	76	81	84					75.4	14	64	
21W								73	73	70	70	61	57	57	59	57	57	63	65	65	68					63.9	14	57	
41W								81	74	70	63	60	58	52	51	54	51	51	53	61	68					60.8	14	51	
61W								100	100	93	76	54	44	36	32	32	34	41	46	54	66					57.7	14	32	
75W								83	82	81	76	70	62	62	63	62	68	67	70	77	80					71.6	14	62	

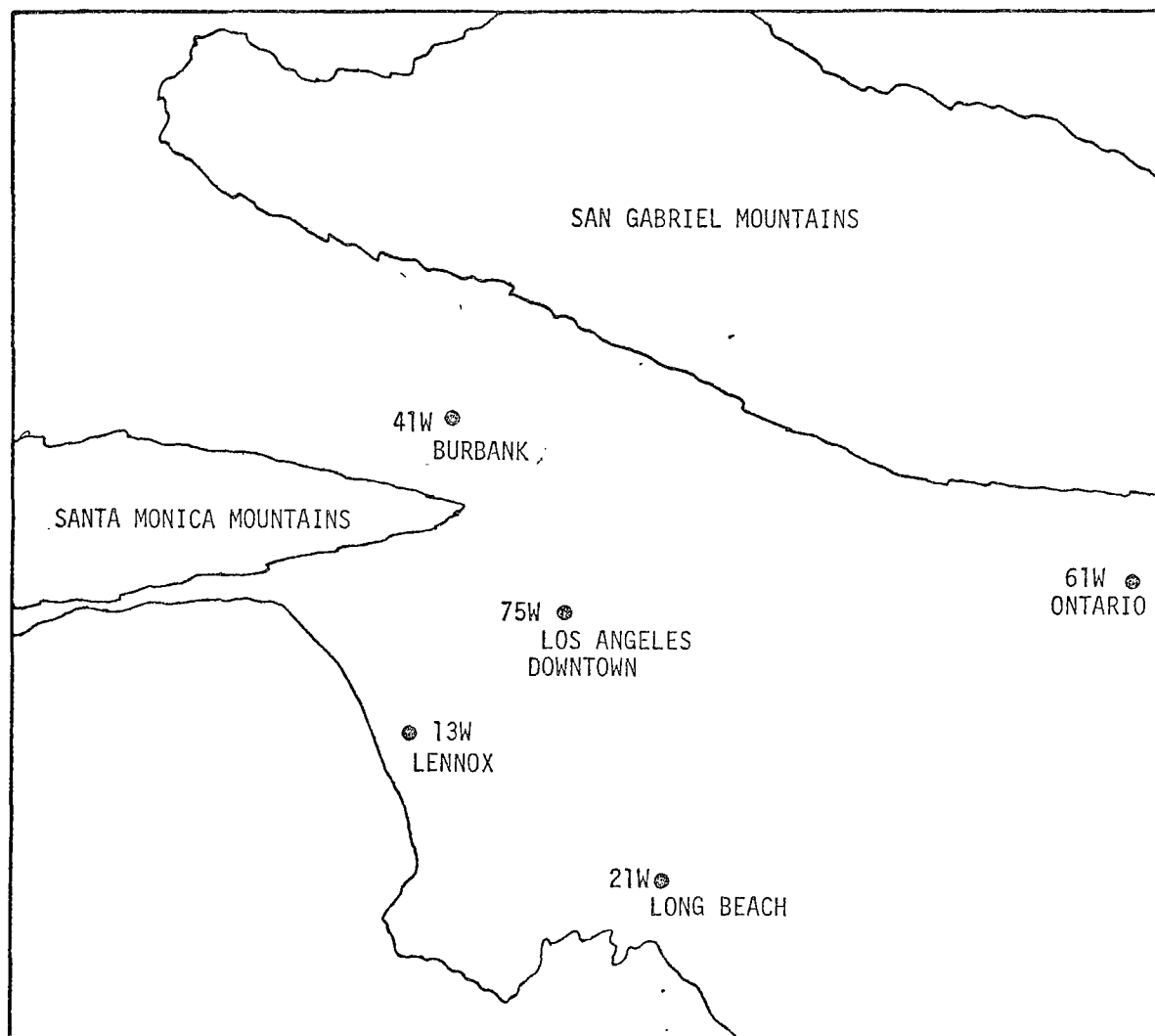


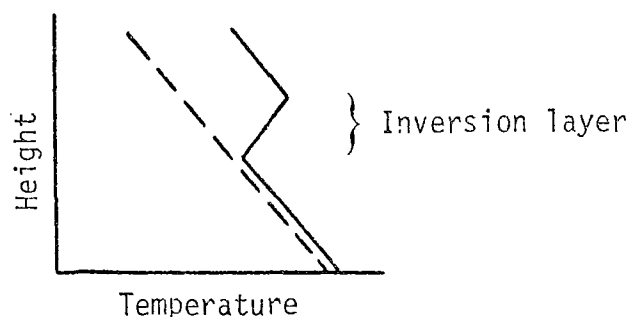
FIGURE 3. LOCATIONS OF TEMPERATURE AND RELATIVE HUMIDITY MONITORING SITES

From the data presented in Table 10, we note that the maximum difference in temperature at any hour during the day and the variation in average air temperatures across the basin for each of the three days are as follows:

<u>Day</u>	<u>Maximum Spatial Temperature Difference</u>		<u>Average Spatial Temperature Difference</u>	
	<u>°C</u>	<u>°F</u>	<u>°C</u>	<u>°F</u>
June 28	15	27	10	18.5
June 29	14	25	9	16.5
June 30	10	18	5	8.5

Thus, spatial variations in temperature of as much as 15°C may exist in the Los Angeles area during the middle of the day. However, on the average, the variations in temperature are somewhat smaller.

To show temperature variations aloft, we plotted in Figure 4 temperature profiles above Rialto, California, at five times on 26-27 July 1973. The 13:07 sounding on July 26 exhibits a temperature difference of about 9°C. If adiabatic conditions had persisted, we would have expected the temperature gradient to be  $-0.01^{\circ}\text{C m}^{-1}$ . Thus, over a 1000m interval, the temperature difference would be 10°C, which is approximately the amount observed at Rialto at 13:07. As illustrated below, when an elevated inversion layer is present, the temperature differences in this situation may be smaller than those that would exist under adiabatic conditions:



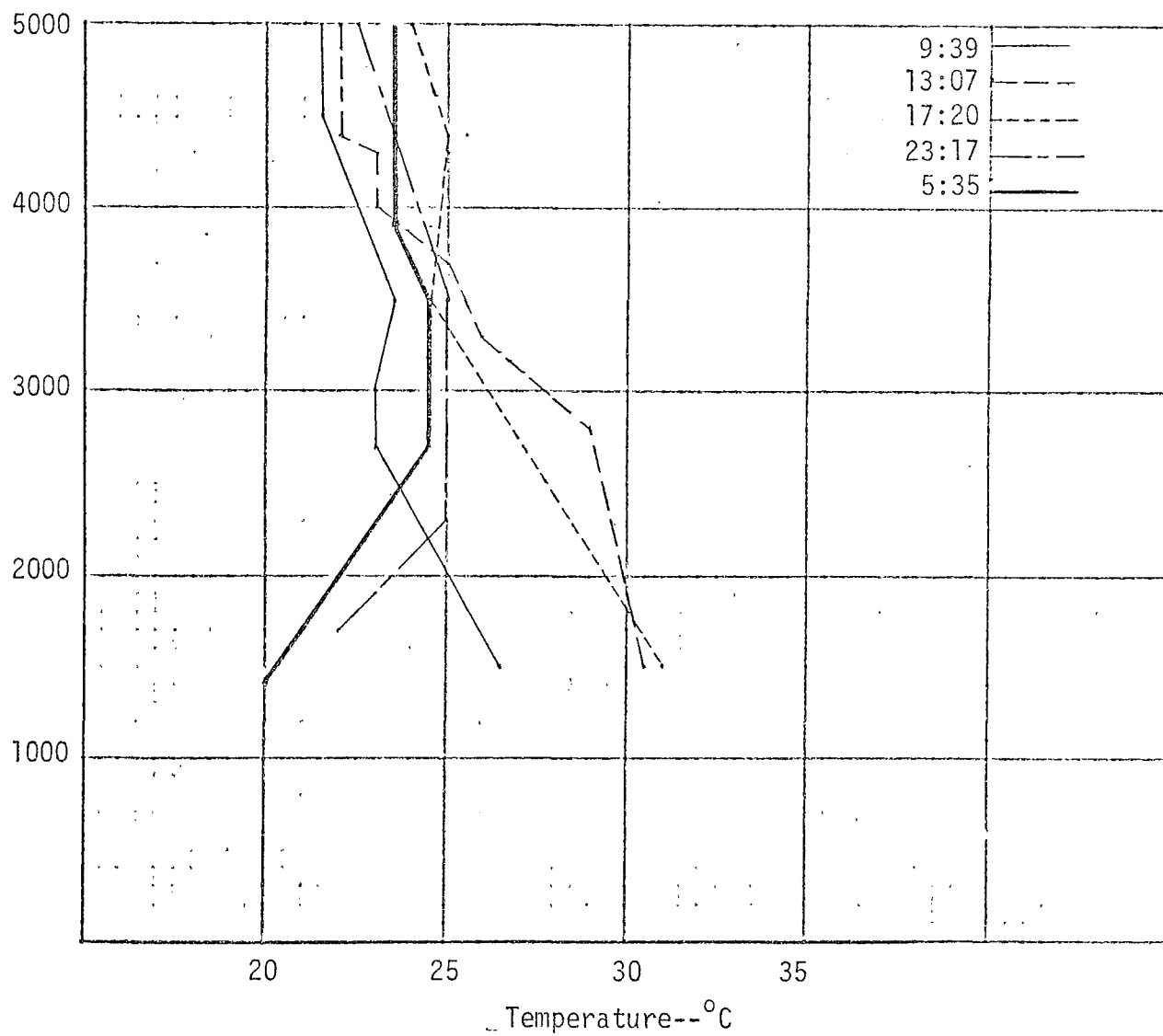


FIGURE 4. DISTRIBUTION OF THE TEMPERATURE ALOFT  
ABOVE RIALTO ON 26-27 JULY 1973

For a modeling region extending to, say, 1000m in height above the terrain, vertical temperature differences may be as large as horizontal variations.

In considering the distribution of water in the basin, we must first convert relative humidity measurements to water concentration in ppm. Using the definition of relative humidity, we can calculate the concentration of water,  $[H_2O]$ , in ppm from the following formula:

$$[H_2O] = \frac{RH \times P(T)}{760} \times 10^4 \quad ,$$

where

RH = relative humidity (in percent),

P = vapor pressure of water (in mm Hg) at temperature T.

Figure 5 illustrates the temporal variation of water concentration at the five ground stations on 28 June 1974. The two coastal locations tend to exhibit similar behavior, as do the two inland locations. Concentrations at the Downtown Los Angeles site seem to be more characteristic of those found near the coast than those observed farther inland. In general, the spatial variation in water concentration is about 7000 to 11,000 ppm.

Examining the temperature and humidity profiles observed at Rialto on 26-27 July 1973, we calculated vertical profiles of water concentration for five times during this two-day period. These profiles are illustrated in Figure 6. The maximum variation in concentration measured on these days was about 8000 ppm, as shown in the 17:20 profile for July 26.

In the analyses described above, we found that spatial variations in temperature and water concentration in the Los Angeles basin can be as large as 15°C and 11,000 ppm, respectively. Of course, since only a very limited number of days were examined, it is highly probable that even greater variations frequently occur. Considering the sensitivity results presented in Section D-1 and the variations in temperature and water concentration cited above, it is



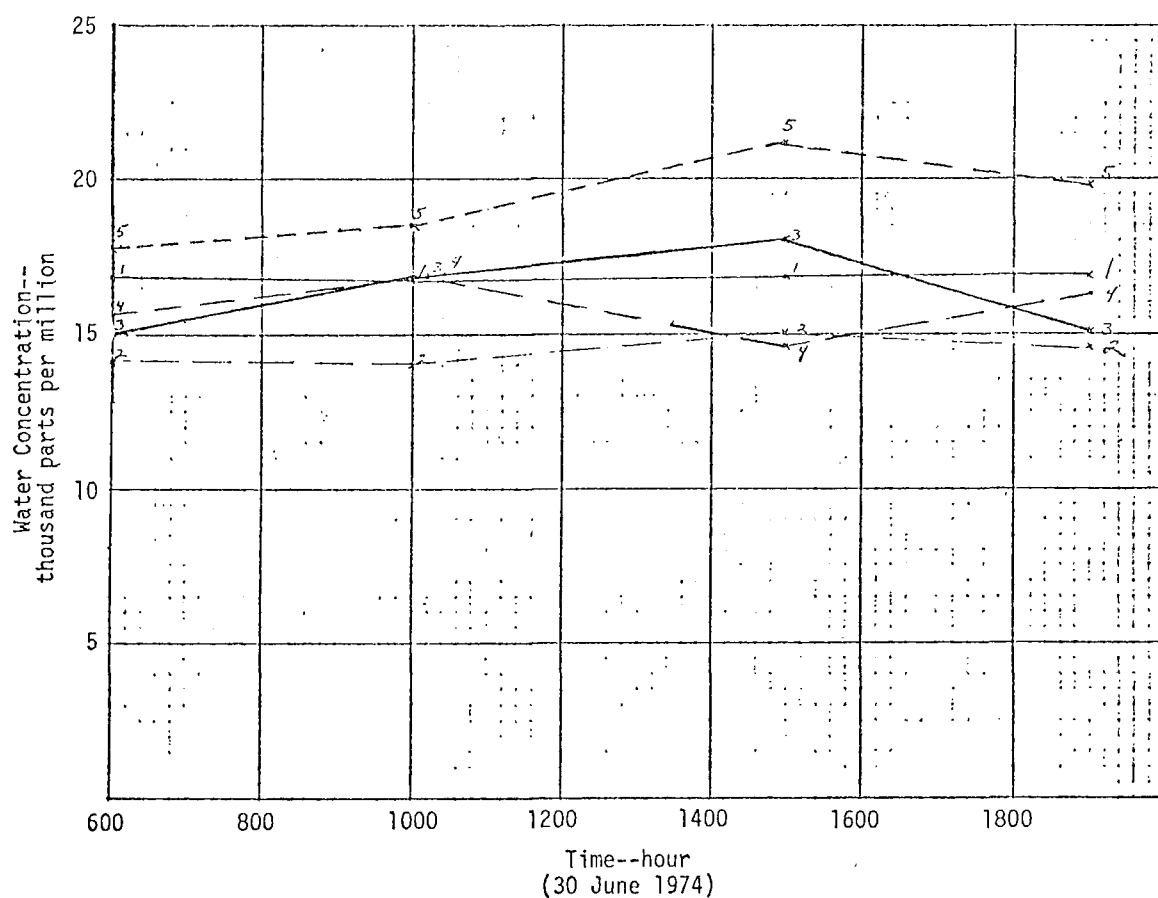
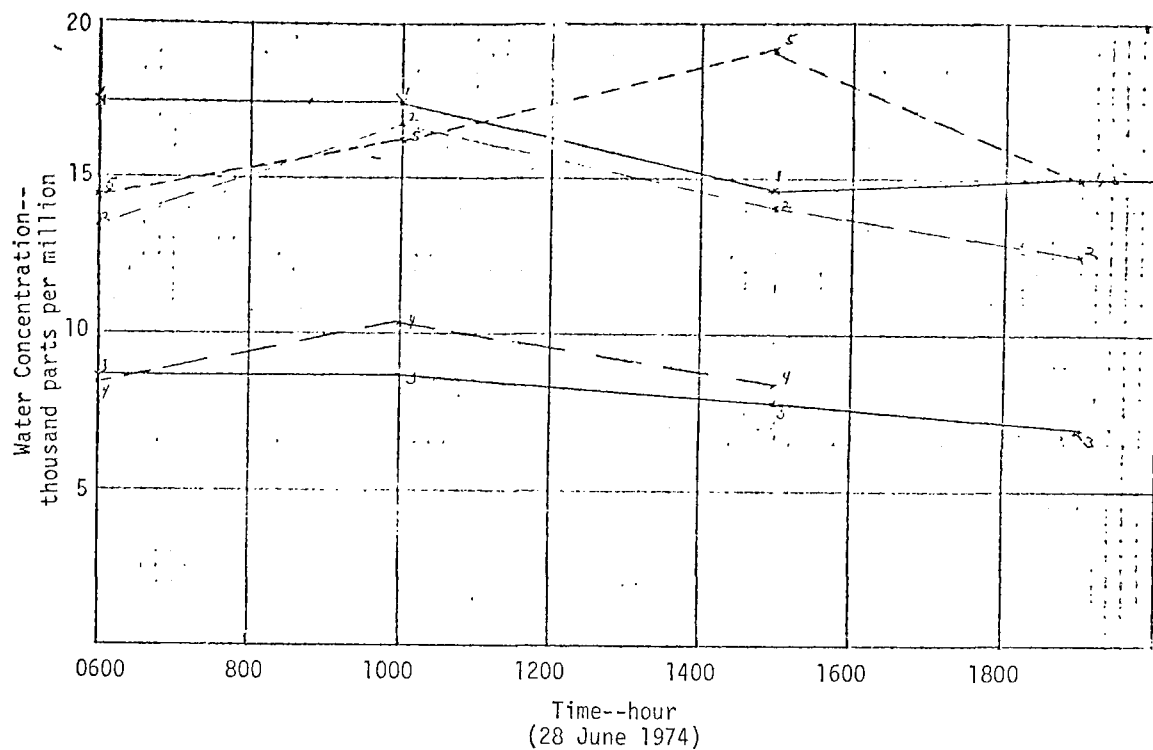


FIGURE 5. TEMPORAL VARIATIONS IN WATER CONCENTRATION  
AT FIVE LOCATIONS IN THE LOS ANGELES BASIN

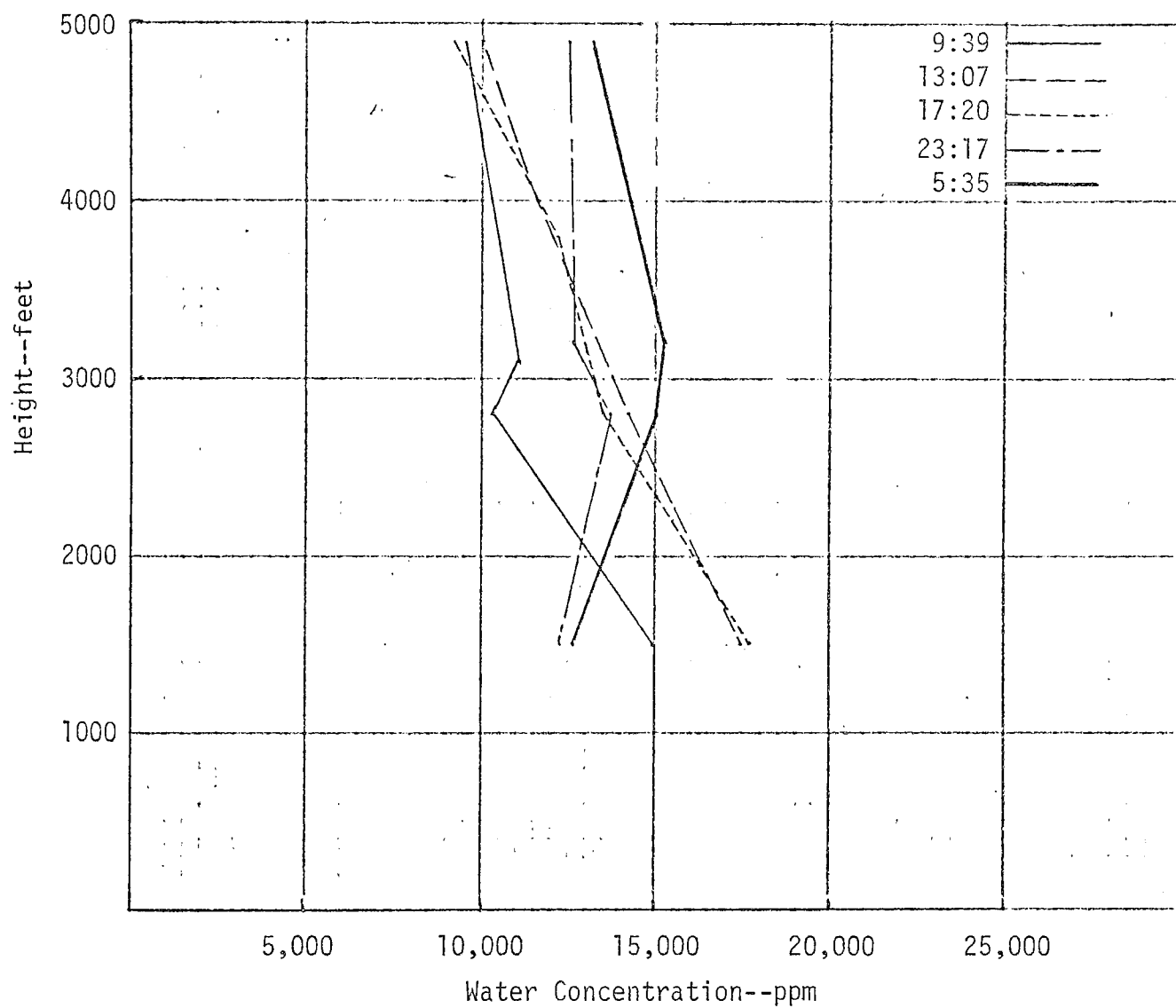


FIGURE 6. DISTRIBUTION OF THE WATER CONCENTRATION ALOFT  
ABOVE RIALTO ON 26-27 JULY 1973

difficult to conclude that these variations can be completely ignored. Therefore, we recommend that future studies be carried out using the airshed model itself to test various alternative strategies for treating temperature and water. Such strategies might include treating temperature or water concentrations as functions of

- > Time only
- > z and time
- > x, y, and time
- > x, y, z, and time.

Toward this end we have included provisions in the computer codes to allow the user to input temperature and relative humidity fields that vary in both space and time.

#### E. TREATMENT OF ORGANICS IN THE AIRSHED MODEL

Use of the kinetic mechanism discussed in Section B-1 requires that the organic species be grouped into four classes: paraffins, olefins, aromatics, and aldehydes. To treat a mixture of numerous organics, such as those found in the atmosphere, "average" rate constants must be estimated for O, OH, and O<sub>3</sub> attack, as appropriate, for each of the four organic groups. In general, specification of a single set of average rate constants that are invariant in space and time is possible only if the individual members of each particular group are of similar reactivity (neglecting spatial and temporal temperature effects). Table 12 presents rate constants for O, OH, and O<sub>3</sub> attack on various hydrocarbons. Because of the abundance of methane in the atmosphere and the wide disparity in reactivities of various paraffins, we conducted a study to ascertain the best treatment of this hydrocarbon group in the airshed model.

We considered four strategies for grouping paraffins:

- (1) One reactive group including all paraffins.
- (2) Two reactive groups--C<sub>1</sub> through C<sub>3</sub> low reactive; C<sub>4</sub>, C<sub>5</sub>, ... high reactive.
- (3) Two groups--C<sub>1</sub> through C<sub>3</sub> nonreactive; C<sub>4</sub>, C<sub>5</sub>, ... reactive.
- (4) Two groups--methane nonreactive; C<sub>2</sub>, C<sub>3</sub>, ... reactive.

Strategy 3 has been employed in previous applications of the airshed model.

Table 12

RATE CONSTANTS FOR O, OH, AND O<sub>3</sub> ATTACK ON VARIOUS HYDROCARBONS

Hydrocarbon	O		OH		O <sub>3</sub>	
	Rate Constant	Reference	Rate Constant	Reference	Rate Constant	Reference
<b>Paraffins</b>						
Methane	$1.8 \times 10^{-2}$	Herron and Huie (1969)	$1.6 \times 10$	Greiner (1967)		
Ethane	1.37	Herron and Huie (1969)	$4.5 \times 10^2$	Greiner (1967)		
Propane	$1.23 \times 10$	Heicklen (1967)	$1.8 \times 10^3$	Greiner (1967)		
Butane	$3.2 \times 10$	Herron and Huie (1969)	$5.72 \times 10^3$	Greiner (1967)		
Isobutane	8.8	Wright (1965)	$5.12 \times 10^3$	Greiner (1967)		
n-pentane	$8.5 \times 10$	Herron and Huie (1969)	$5.81 \times 10^3$	Greiner (1967)		
Isopentane	$1.9 \times 10^2$	Herron and Huie (1969)	$6.76 \times 10^3$	Greiner (1967)		
2,2-dimethylbutane	$3.0 \times 10^2$	Herron and Huie (1969)	$2.80 \times 10^3$	Greiner (1967)		
Cyclopentane	$2.9 \times 10^2$	Herron and Huie (1969)	$1.11 \times 10^4$	Greiner (1967)		
2,3-dimethylbutane	$1.5 \times 10^2$	Heicklen (1967)	$8.2 \times 10^3$	Greiner (1967)		
2-methylpentane	$2.2 \times 10^2$	Estimate	$8.41 \times 10^3$	Greiner (1967)		
3-methylpentane	$2.2 \times 10^2$	Estimate	$8.41 \times 10^3$	Greiner (1967)		
n-hexane	$1.36 \times 10^2$	Herron and Huie (1969)	$7.16 \times 10^3$	Greiner (1967)		
Methylcyclopentane	$1.3 \times 10^2$	Estimate	$6.87 \times 10^3$	Greiner (1967)		
2,4-dimethylpentane	$3.3 \times 10^2$	Estimate	$1.13 \times 10^4$	Greiner (1967)		
2-methylhexane	$2.5 \times 10^2$	Estimate	$1.06 \times 10^4$	Greiner (1967)		
3-methylhexane	$2.5 \times 10^2$	Estimate	$1.06 \times 10^4$	Greiner (1967)		
2,2,4-trimethylpentane	$2.5 \times 10^2$	Herron and Huie (1969)	$7.34 \times 10^3$	Greiner (1967)		
n-heptane	$1.91 \times 10^2$	Herron and Huie (1969)	$8.81 \times 10^3$	Greiner (1967)		
Methylcyclohexane	$1.6 \times 10^2$	Estimate	$8.5 \times 10^3$	Greiner (1967)		
2,4-dimethylhexane	$3.7 \times 10^2$	Estimate	$1.30 \times 10^4$	Greiner (1967)		

Table 12 (Concluded)

Hydrocarbon	O		OH		O <sub>3</sub>	
	Rate Constant	Reference	Rate Constant	Reference	Rate Constant	Reference
2,5-dimethylhexane	$3.7 \times 10^2$	Estimate	$1.30 \times 10^4$	Greiner (1967)		
2,3,4-trimethylpentane	$1.8 \times 10^2$	Herron and Huie (1969)	$1.58 \times 10^4$	Greiner (1967)		
n-octane	$2.5 \times 10^2$	Herron and Huie (1969)	$1.28 \times 10^4$	Greiner (1967)		
n-nonane	$2.0 \times 10^2$	Estimate	$1.21 \times 10^4$	Greiner (1967)		
n-decane	$2.6 \times 10^2$	Estimate	$1.38 \times 10^4$	Greiner (1967)		
Olefins						
Ethylene	$7.72 \times 10^2$	Cvetanovic (1963)	$2.13 \times 10^3$	Morris and Niki (1971)	$3.8 \times 10^{-3}$	Wei (1963)
Propylene	$4.41 \times 10^3$	Cvetanovic (1963)	$2.13 \times 10^4$	Morris and Niki (1971)	$1.6 \times 10^{-2}$	Wei (1963)
Butenes	$4.41 \times 10^3$	Cvetanovic (1963)	$5.12 \times 10^4$	Morris and Niki (1971)	$1.3 \times 10^{-2}$	Wei (1963)
1-pentene			$5.33 \times 10^4$	Morris and Niki (1971)	$1.3 \times 10^{-2}$	Wei (1963)
Trans-2-pentene			$1.13 \times 10^6$	Morris and Niki (1971)	$5.0 \times 10^{-2}$	Wei (1963)
Cis-2-pentene	$1.69 \times 10^4$	Cvetanovic (1963)	$1.13 \times 10^6$	Morris and Niki (1971)	$4.1 \times 10^{-2}$	Wei (1963)
2-methyl-2-butene	$6.03 \times 10^4$	Cvetanovic (1963)	$1.49 \times 10^6$	Morris and Niki (1971)		
Cyclopentene	$2.35 \times 10^4$	Cvetanovic (1963)				
1-hexene	$5.00 \times 10^3$	Cvetanovic (1963)			$1.5 \times 10^{-2}$	Wei (1963)
Cis-2-hexene					$4.1 \times 10^{-2}$	Wei (1963)
1-heptene					$1.21 \times 10^{-2}$	Cadle (1952)
Aldehydes						
Formaldehyde	$4.41 \times 10^2$	Estimate	$1.92 \times 10^4$	Morris and Niki (1971)		
Acetaldehyde	$4.41 \times 10^2$	Estimate	$1.92 \times 10^4$	Morris and Niki (1971)		
Propionaldehyde			$3.84 \times 10^4$	Morris and Niki (1971)		
Aromatics						
Toluene	$1.1 \times 10^2$	Estimate				
M-xylene	$4.4 \times 10^2$	Estimate		Estimate		
p-xylene						

To test these schemes, we performed smog chamber simulations for a mixture of paraffins,  $\text{NO}_x$ , and CO having proportions typical of those found in the Los Angeles atmosphere in 1969. For comparison, we carried out a baseline simulation in which each paraffin was treated as an individual reactive species in the mechanism. Thus, we compared the predictions for Strategies 1 through 4 with those for the baseline case to determine the errors introduced by each lumping scheme.

Initial conditions for the simulation runs were derived from air quality measurements taken at Commerce, California, on 30 September 1969 by Scott Research Laboratories. In particular, we used the following concentrations, which were measured at 8 a.m. on that day:

<u>Species</u>	<u>Concentration (ppm)</u>
CO	10.0
NO	0.4
$\text{NO}_2$	0.1
$\text{H}_2\text{O}$	$1.6 \times 10^4$
$\text{C}_1^+$	4.213
$\text{C}_2^+$	0.476
$\text{C}_1\text{-C}_3$	3.944
$\text{C}_4^+$	0.269

The predicted values of NO,  $\text{NO}_2$ , and  $\text{O}_3$  after 12 hours of irradiation were as follows:

<u>Strategy</u>	<u>Predicted Concentration (ppm)</u>		
	<u>NO</u>	<u><math>\text{NO}_2</math></u>	<u><math>\text{O}_3</math></u>
Baseline	0.05	0.30	0.05
1	0.04	0.30	0.07
2	0.05	0.30	0.05
3	0.09	0.28	0.03
4	0.05	0.30	0.05

These results indicate that Strategies 2 and 4 led to the best agreement with the baseline case. Since Strategy 2 uses two reactive species, whereas Strategy 4 involves only one, we plan to treat the paraffin class according to Strategy 4 to minimize computing costs.

Thus, five organic classes are considered in the airshed model: non-reactive hydrocarbons (methane and acetylene), nonmethane paraffins, olefins, aromatics, and aldehydes. We recommend that future studies be carried out to ascertain whether the olefins should be treated as a single lumped species or as several lumped species. In addition, it may be possible to combine the aromatics with the nonmethane paraffins, since both groups have similar reactivities and may produce similar products (according to the mechanism given in Section B-1).

#### F. INTRODUCTION OF THE IMPROVED KINETIC MECHANISM INTO THE AIRSHED MODEL

In Sections B and C, we delineate efforts aimed at developing improved mechanisms for describing the chemical interactions of hydrocarbons,  $\text{NO}_x$ ,  $\text{O}_3$ , and  $\text{SO}_2$ . With regard to the  $\text{HC-NO}_x\text{-O}_3$  system, the generalized mechanism discussed in Section B represents a significant improvement over the 15-step mechanism previously employed in the airshed model. Thus, we have incorporated the expanded mechanism into the model. In addition, we have implemented in the model the  $\text{SO}_2$  mechanism described in Section C, even though the mechanism has yet to be validated using smog chamber data. In the present section, we discuss our efforts to use the improved kinetic mechanism in an actual airshed simulation.

Installation of the new mechanism in the airshed model required that numerous changes be made in the computer codes. Particular difficulties arose because the number of species that must be followed in the airshed model increased from 6 to 12 ( $\text{NO}$ ,  $\text{NO}_2$ ,  $\text{O}_3$ ,  $\text{H}_2\text{O}_2$ ,  $\text{HNO}_2$ , nonmethane paraffins, olefins, aromatics, aldehydes,  $\text{SO}_2$ ,  $\text{CO}$  and unreactive hydrocarbons). Moreover, the programs were to be exercised on the CDC 7600 computer, which has only a limited amount of small core memory, at Lawrence Berkeley Laboratory. Thus, we

restructured the programs somewhat to make efficient use of available small core memory, as well as the more abundant amounts of extended core memory. After the coding changes were made, we checked the programs by running several test cases.

To gain some experience in using the new mechanism in airshed simulations, we decided to exercise the model using meteorological and emissions inputs derived in previous model evaluation efforts. We felt that using the same meteorological and emissions inputs, to the extent possible would provide a means for ascertaining how sensitive the model predictions were to the change in the kinetic mechanism itself. Because of our previous experience in simulating the Los Angeles basin on 29 September 1969, we chose that day for our initial model application effort.

Before the simulations could be carried out, we first had to compute new splits for hydrocarbon emissions and initial and boundary concentrations. Previously, available hydrocarbon emissions and air quality data were divided into two groups--reactive and unreactive hydrocarbons. To use the new mechanism, we revised the categories to reflect the new definition of the five organic classes--nonmethane paraffins, olefins, aromatics, aldehydes, and nonreactive hydrocarbons (methane and acetylene).

Organics are emitted from a variety of sources in the Los Angeles basin, including motor vehicles, refineries, and numerous other stationary sources. Although the organic composition of automobile emissions has been documented by several investigators, very little information is available for use in establishing guidelines for estimating the composition of the stationary source emissions. For the purposes of this study, we assumed that the composition of stationary source emissions is the same as that for automobiles. Although we recognize that this is not necessarily a good assumption, our main objective was simply to make "reasonable" estimates of the emission splits to exercise the model. A more refined inventory can be derived using the results of a recent study of organic emission control strategies carried out by Trijonis and Arledge (1975). Unfortunately, their results were not available in time for inclusion in this study.



Using organic composition data derived from tests of 10 automobiles reported by the Bureau of Mines (1973), we estimated the following mass emission splits:

<u>Group</u>	<u>Mass Split (percent)</u>
Nonmethane paraffins	29
Olefins	30
Aromatics	23
Aldehydes*	5
Nonreactive hydrocarbons	18

Thus, we added previous estimates of reactive and nonreactive hydrocarbon emissions to estimate the spatial and temporal distribution of total hydrocarbon emissions. Then, we multiplied the emission splits cited above by the total hydrocarbon emissions in each grid cell to estimate the distribution of emissions for each of the five classes.

We calculated initial and boundary concentrations using our previous estimates of reactive and nonreactive hydrocarbon concentrations in conjunction with gas chromatographic analyses of ambient air in the basin for 29 September 1969 reported by Scott Research Laboratories (1970). We derived the following relationships:

$$[\text{Olefins}] = 0.211[C_R],$$

$$[\text{Paraffins}] = 0.414[C_R] + 0.057[C_{NR}],$$

$$[\text{Aromatics}] = 0.376[C_R] + 0.003[C_{NR}],$$

$$[\text{Aldehydes}] = 0.04 \text{ ppm},$$

$$[\text{Nonreactive hydrocarbons}] = 0.94[C_{NR}],$$

where  $[C_R]$  and  $[C_{NR}]$  are the original estimates of reactive and nonreactive hydrocarbon concentrations, respectively.

---

\* Aldehyde emissions are estimated to be about 5 percent of the total hydrocarbon emissions. Since aldehydes were not included in the original SAI inventory for Los Angeles, the total percentage adds up to 105 percent. Thus, we increased the total organic emissions by 5 percent to reflect the additional aldehyde emissions.

Figures 7 through 12 illustrate some of the predictions obtained from the SAI model using the 31-step kinetic mechanism and the emissions and air quality inputs described above. These figures also show the predictions from the analogous simulation in which the 15-step mechanism was employed. In general, the most obvious characteristic of these results is that the  $O_3$  production seems to have been accelerated, leading to higher predicted  $O_3$  levels. However, in many instances the  $NO_2$  predictions are in better agreement with the measurements, especially during the late morning and early afternoon.

It is difficult to make any assessment now of the enhanced reliability of the model resulting from the incorporation of the new 31-step mechanism. However, considering the nature of the available model inputs used in this study, the results are encouraging. We recommend that a greater effort be expended in future work to assemble an appropriate organic emissions inventory. Furthermore, the enhanced production of  $O_3$  observed in the results presented here may be caused in part by inaccuracies in the treatment of aldehyde photolysis or NO removal in the mechanism. We assumed that aldehyde photolysis is proportional to that for  $NO_2$ . However, shifts in the UV spectrum throughout the day may invalidate this assumption. Finally, NO may be removed too rapidly in the mechanism, thus, allowing  $O_3$  levels to build up prematurely. These issues can be resolved only by subjecting the model to a comprehensive evaluation. We recommend that such an undertaking be considered in the near future.

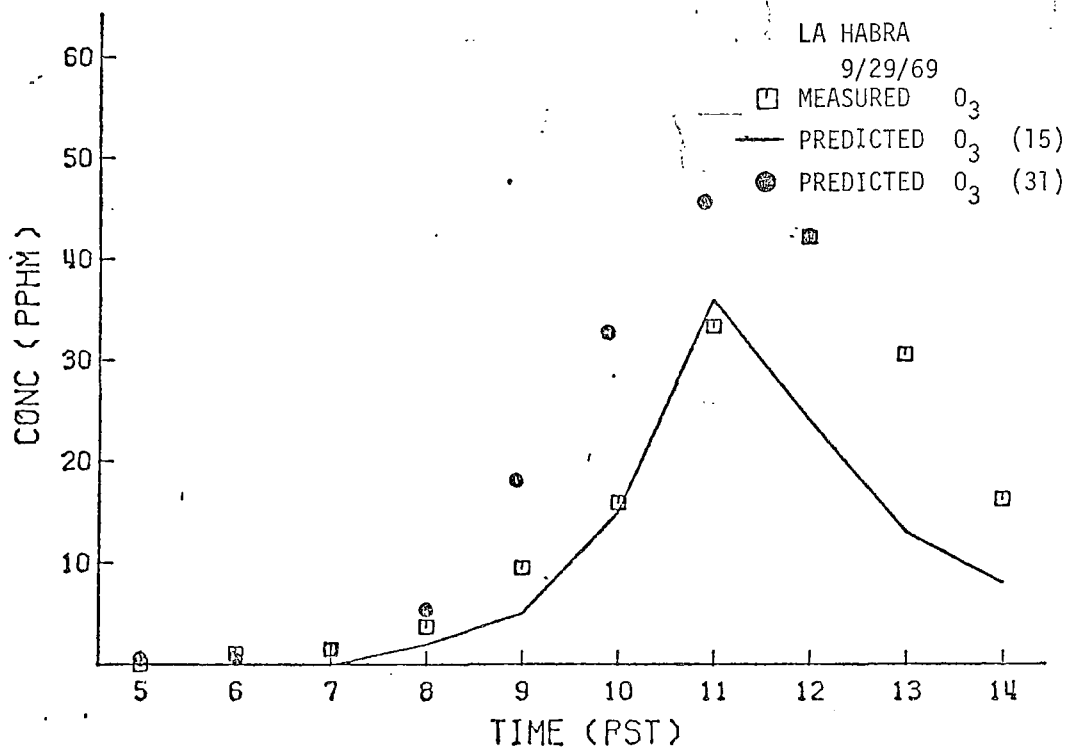
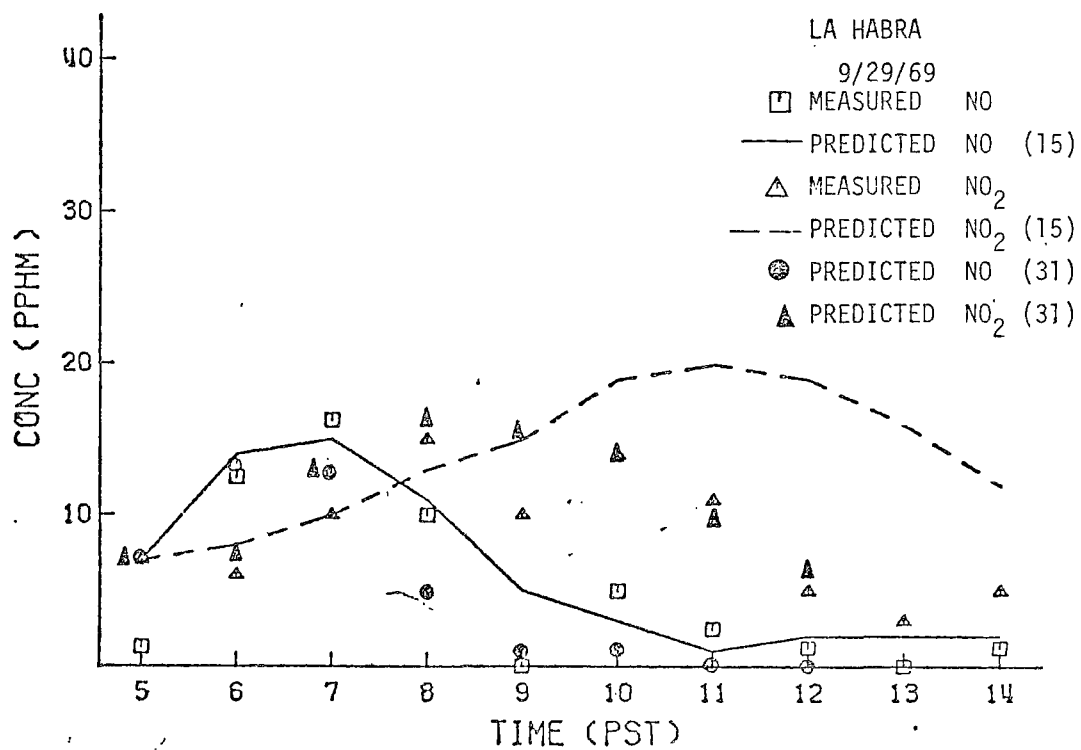


FIGURE 7. PREDICTED AND MEASURED CONCENTRATIONS FOR LA HABRA  
USING THE 15- AND 31-STEP KINETIC MECHANISMS

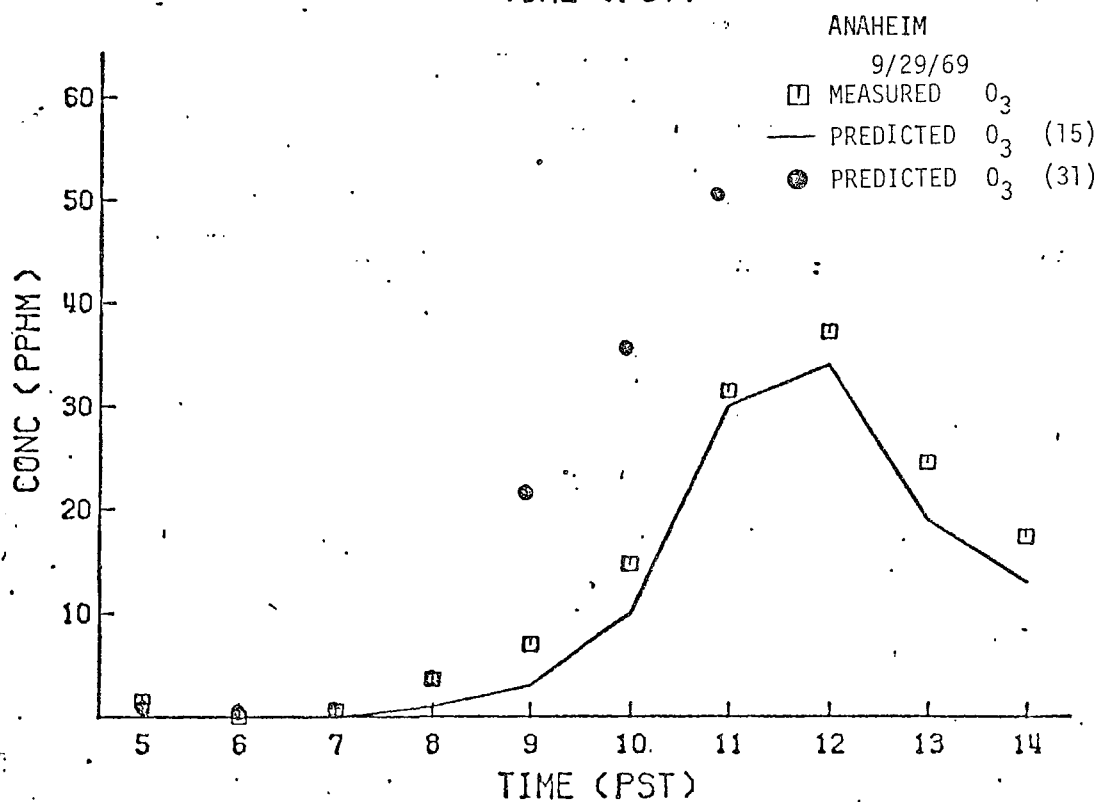
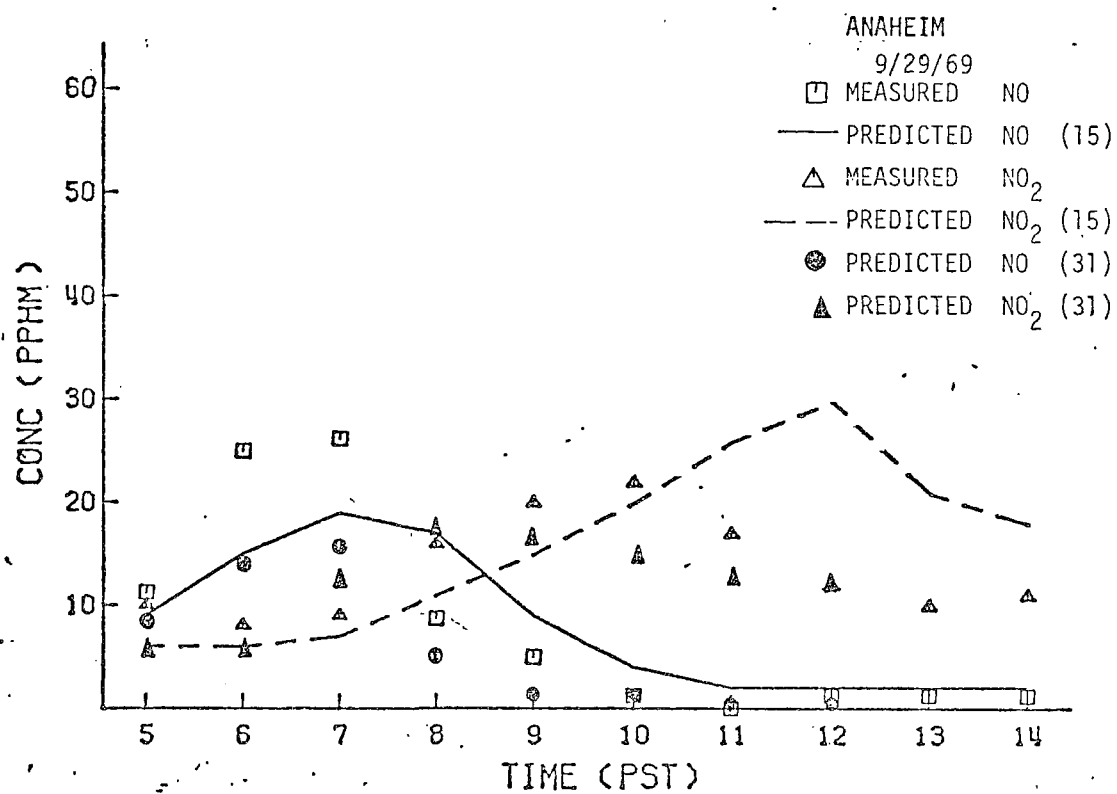


FIGURE 8. PREDICTED AND MEASURED CONCENTRATIONS FOR ANAHEIM  
USING THE 15- AND 31-STEP KINETIC MECHANISMS

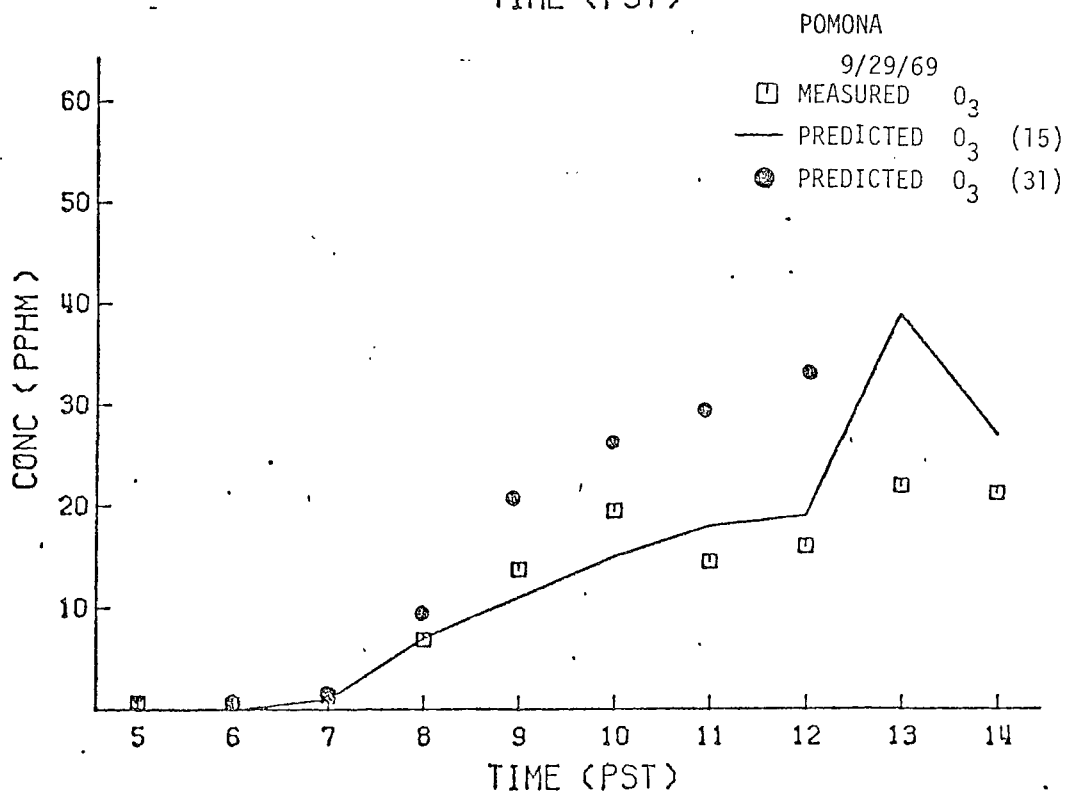
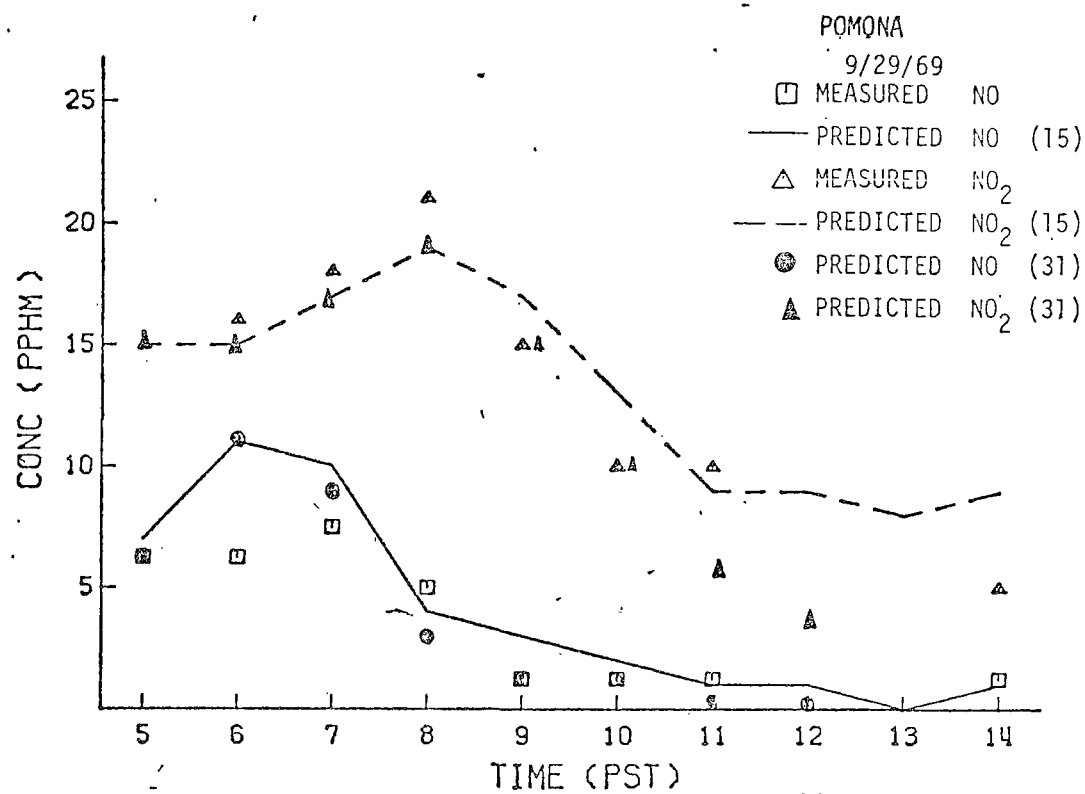


FIGURE 9. PREDICTED AND MEASURED CONCENTRATIONS FOR POMONA  
USING THE 15- AND 31-STEP KINETIC MECHANISMS

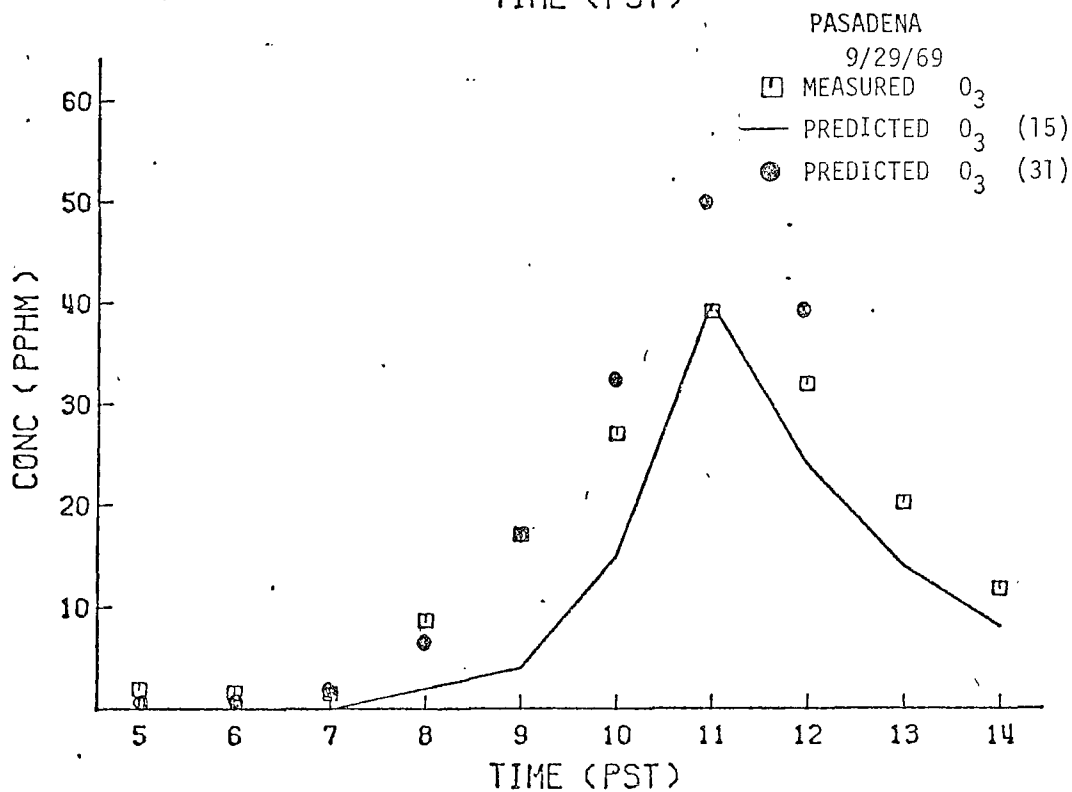
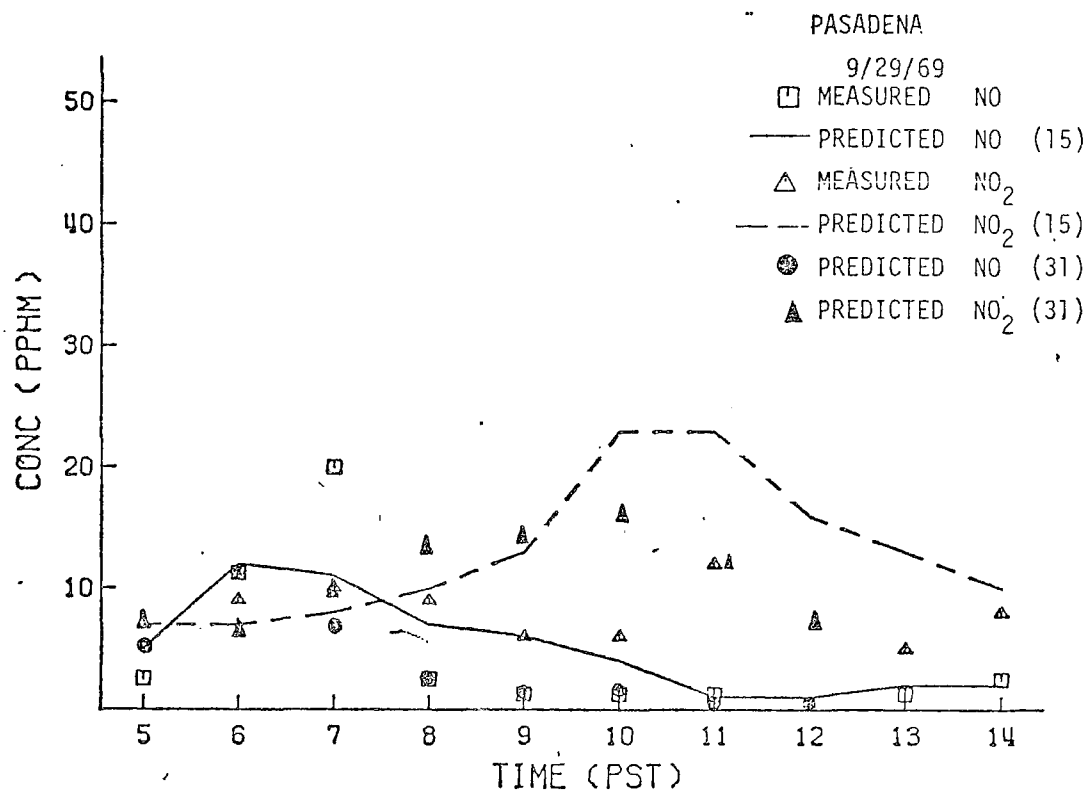


FIGURE 10. PREDICTED AND MEASURED CONCENTRATIONS FOR PASADENA  
USING THE 15- AND 31-STEP KINETIC MECHANISMS

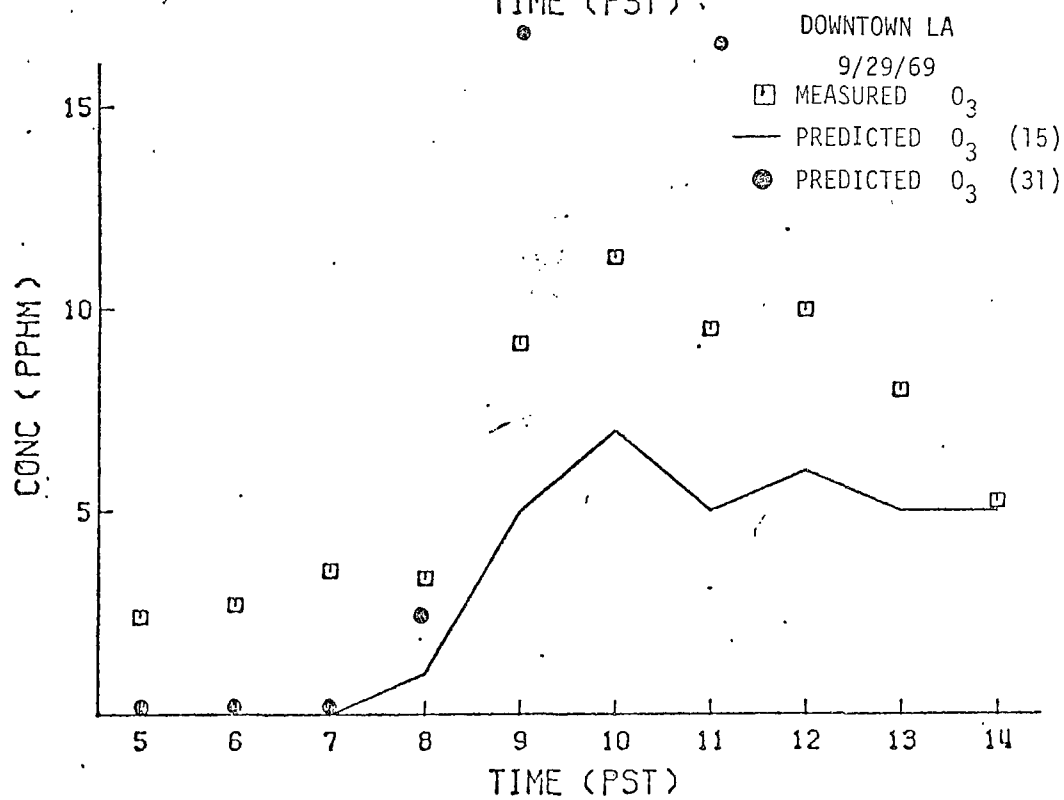
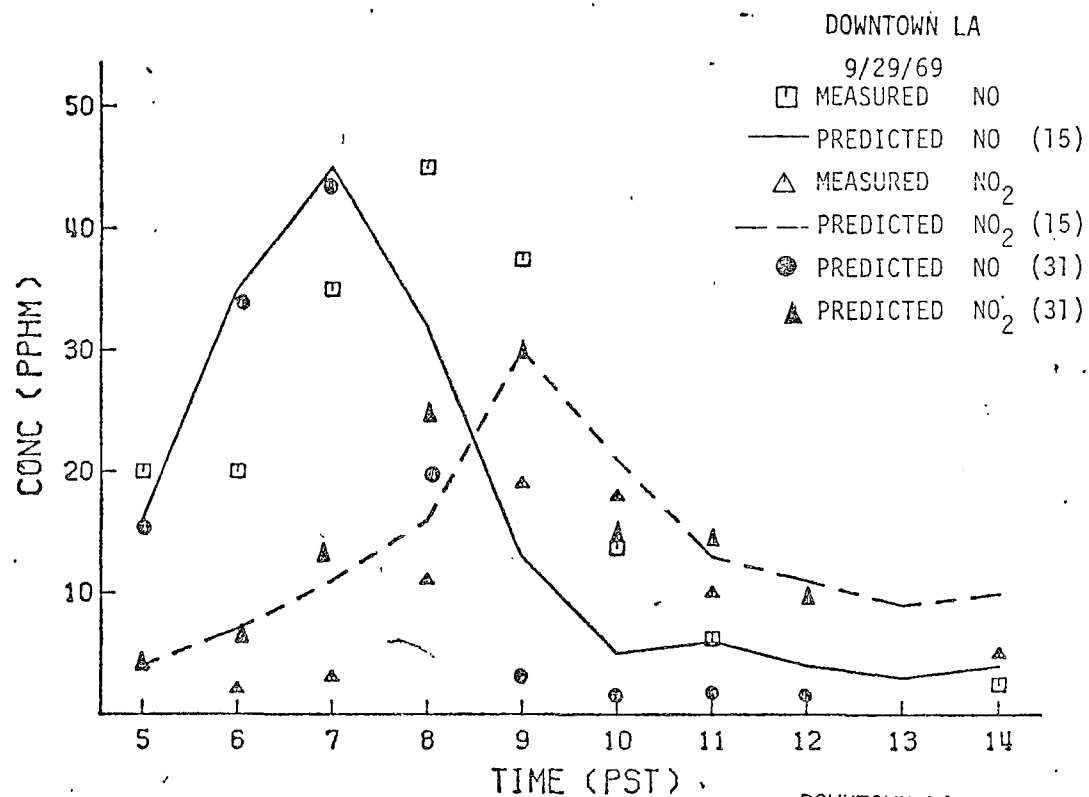


FIGURE 11: PREDICTED AND MEASURED CONCENTRATIONS FOR DOWNTOWN LOS ANGELES USING THE 15- AND 31-STEP MECHANISMS

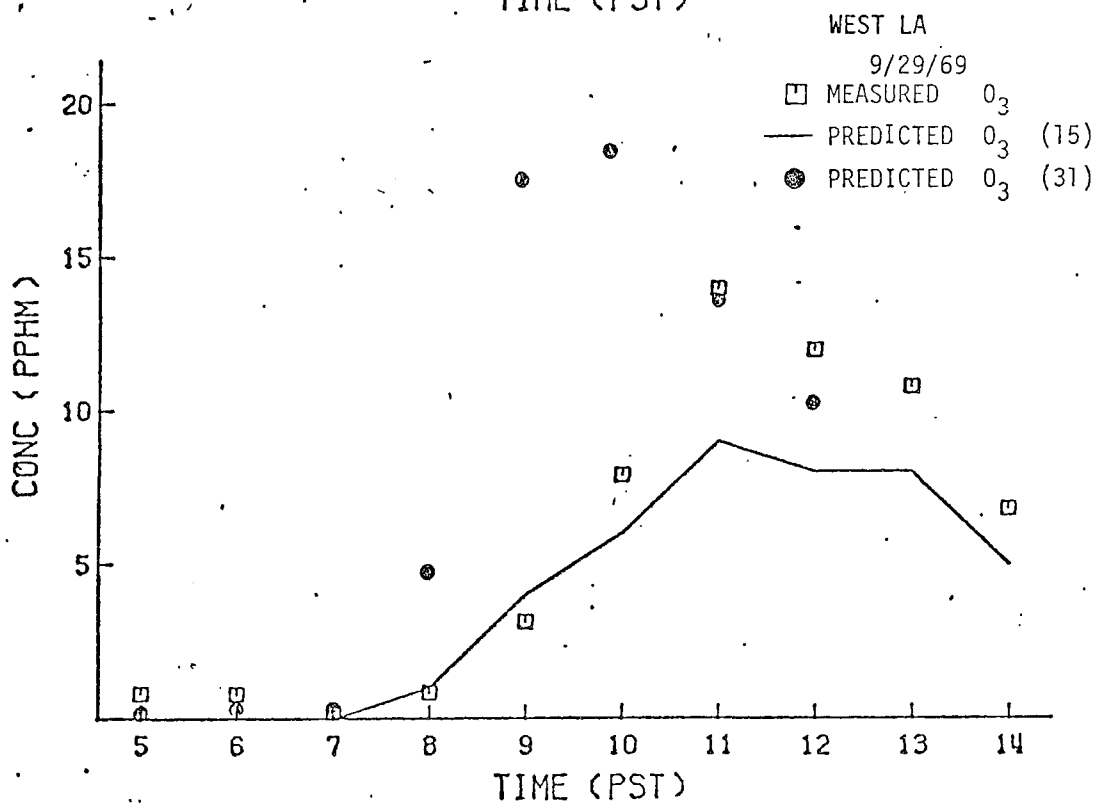
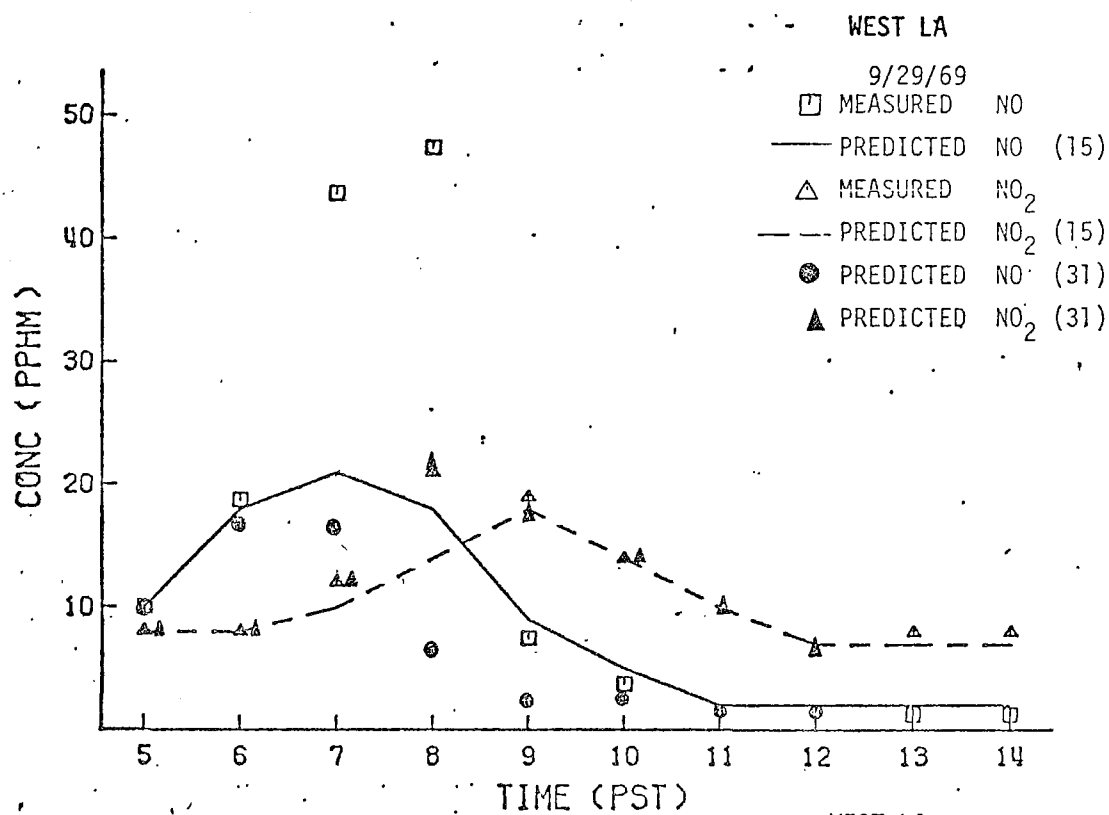


FIGURE 12. PREDICTED AND MEASURED CONCENTRATIONS FOR WEST LOS ANGELES USING THE 15- AND 31-STEP MECHANISMS



### III METEOROLOGY-RELATED DEVELOPMENT ACTIVITIES

Steven D. Reynolds  
Mark A. Yocke  
Jody Ames

In our previous model development and application efforts, we made several assumptions about the treatment of meteorological parameters. Among these, the most notable are the following:

- > Wind shear effects can be neglected.
- > A diffusivity algorithm that is solely a function of wind speed and height can be used.
- > The base of an elevated inversion layer is a suitable choice for the top of the modeling region.

However, these assumptions clearly introduce inaccuracies. First, the wind flow field is fully three-dimensional and should be treated accordingly. Second, the magnitude of the turbulent diffusivity depends on atmospheric stability and surface roughness, as well as on wind speed and height. Third, significant quantities of pollutants trapped in an elevated inversion layer may be injected into the mixed layer as the stable layer is eroded by surface heating effects. Moreover, ground-based inversions frequently occur at night. Thus, further consideration needs to be given to the definition of the modeling region and the treatment of inversion layers in the model. In the following sections, we discuss our efforts to improve the treatment of wind fields, diffusivities, and inversions in the airshed model.

#### A. MODEL SENSITIVITY TO THE INCLUSION OF WIND SHEAR

The results of model sensitivity studies reported in Volume I indicate the importance of accurately specifying the wind speed and direction throughout the region of interest. In this section, we discuss additional sensitivity studies that were carried out to assess the importance of characterizing wind shear effects. The results of this effort will be useful for establishing (1) the need to extend our existing meteorological algorithms to treat

wind shear and (2) the extent to which vertical wind soundings should be taken over urban areas.

Accurate specification of winds aloft is usually hampered in a grid model by a dearth of appropriate measurements. Since the full three-dimensional structure of the wind field must be input to the model, particular attention must be given to this aspect of model usage. The following are four possible means for establishing the complete wind field:

- (1) Assumption of a "flat" velocity profile, where the estimated ground-level wind speeds and directions are assumed to be invariant with height (i.e., wind speeds and directions are a function only of  $x$ ,  $y$ , and  $t$ ).
- (2) Calculation of the winds aloft by scaling the ground-level winds according to the findings of previous wind shear studies (i.e., assumption of a form for the wind shear, such as a power law profile).
- (3) Interpolation for the wind speeds and directions using actual wind soundings aloft.
- (4) Prediction of the wind flow field using a numerical simulation model.

The first alternative, which is the simplest, is useful for establishing the basic characteristics of the flow field. Previous SAI simulations have used this approach. For more refined estimates of the wind field when no measurements aloft are available, the second technique can be used. The last two alternatives afford the best means of specifying winds aloft, provided that--for Alternative 3--the measurement network is sufficiently dense and that--for Alternative 4--the model has been validated. At present, Alternatives 2 and 3 appear to represent the best means for accurately specifying winds aloft.

An important step in procuring a data base for describing the upper level winds is being made in the RAPS program for St. Louis. One aspect of this comprehensive data gathering study will be the regular monitoring of winds aloft

at two to four sites in this metropolitan area. Using the surface wind data in conjunction with the upper wind measurements, one should be able to estimate with reasonable accuracy the structure of the wind field over this urban area.

To gain some insight into the importance of wind shear effects on the predictions obtained from the photochemical airshed model, we carried out a series of comparative simulations for the Los Angeles basin, using both "flat" and power law wind velocity profiles. Since vertical wind soundings were not available for Los Angeles, we used only the surface-based measurements to generate both wind fields. In the following subsections, we further describe the treatment of wind shear and discuss the results of the simulations.

### 1. Wind Velocity Profile

Variations in horizontal wind with height have been the subject of intensive study in meteorology for years. Assuming neutral stability conditions, von Kármán derived a logarithmic relationship for the mean wind velocity in the sublayer (surface layer) of the atmospheric boundary layer from theoretical considerations (Plate, 1971):

$$\frac{U}{u_*} = \frac{1}{K} \ln\left(\frac{Z}{Z_0}\right) \quad , \quad (9)$$

where

- $U$  = wind speed at height  $Z$ ,
- $u_*$  = the friction velocity,
- $Z_0$  = the roughness parameter,
- $K$  = the von Kármán constant.

Subsequently, this relationship was verified through experiment. For diabatic conditions, Laikhtman (1944) and Deacon (1949) proposed that the expression

$$\frac{U}{u_*} = \frac{1}{K(1-\beta)} \left[ \left( \frac{Z}{Z_0} \right)^{1-\beta} - 1 \right] \quad (10)$$

be used, where  $\beta$  is a function of atmospheric stability.

Within the remainder of the atmospheric boundary layer (i.e., above the sublayer), wind profiles are usually characterized by an empirical power law. Blasius was the first to describe the mean velocity distribution by the following general relationship:

$$\frac{U}{U_R} = \left( \frac{Z}{Z_R} \right)^M, \quad (11)$$

where  $U_R$  is the wind velocity vector at a reference height  $Z_R$ . The exponent  $M$  is a function of ground surface roughness and atmospheric stability. DeMarrais (1959), Davenport (1965), Shellard (1965), and Jones et al. (1971) performed experiments to derive quantitative relationships for  $M$ . On the basis of their findings, they estimated that  $M$  is likely to be within the following range:

$$0.4 > M > 0.2.$$

Because of its applicability over the entire boundary layer, we selected the mean velocity power law relationship [Eq. (11)] as the most suitable available description of the wind speed shear. We chose 0.2 as a representative value of  $M$  for an urban area, such as Los Angeles.

## 2. Implementation of the Wind Velocity Profile

The numerical integration scheme used in the grid model requires that the average wind velocity be specified at each grid cell interface. The integration of Eq. (11) along the vertical axis from the lower cell boundary to the upper, followed by division by the cell depth, yields the expression for the mean horizontal wind velocity over a horizontal cell interface:

$$\bar{u} = \frac{\bar{u}_R}{(Z_t - Z_b) Z_R^M (M + 1)} \left( Z_t^{M+1} - Z_b^{M+1} \right) , \quad (12)$$

where  $Z_t$  is the elevation at the top of the cell and  $Z_b$  is the elevation at the bottom of the cell. Equation (12) can be used to obtain both the x and y components of the mean velocity for each horizontal grid cell interface within the modeling region. Assuming that turbulent atmosphere flow is incompressible, the vertical advective velocity,  $w$ , can be computed from the continuity relationship:

$$\frac{\partial u}{\partial x} + \frac{\partial v}{\partial y} + \frac{\partial w}{\partial z} = 0 . \quad (13)$$

### 3. Computer Coding

To incorporate the wind shear algorithms given by Eqs. (12) and (13), we made appropriate coding changes in the computer programs embodying the airshed model. The result of these alterations was a slight increase in both machine storage requirements and CPU time.

### 4. Description of the Experiment

After we altered the computer codes, we designed an experiment to examine the sensitivity of the airshed model to wind shear effects. To insure that the deviations in predicted concentrations are caused only by dissimilarities in the prescribed wind fields, we made test runs using both the original code (in which a flat profile was assumed) and the newly revised code with  $M$  set equal to zero. From Eq. (12), if  $M = 0$ , we obtain the same flat wind profile as was used in the original formulation of the model. Meteorological and emissions data for Los Angeles on 29 September 1969 served as input data for predicting concentrations of RHC, URHC, NO, NO<sub>2</sub>, O<sub>3</sub>, and CO, using both the modified and unmodified programs for the hours 0500 through 1500 PST. The two programs produced identical predictions, thus indicating that all coding alterations had been implemented properly.

Finally, we ran the modified program using a value for  $M$  of 0.2, and we compared the output of this program with the previous unmodified computations (assuming a flat velocity profile). Figures 13 through 20 show plots of the average and maximum deviations in ground-level concentrations for each species as a function of time. Here, the concentration deviations are defined as the predicted concentrations with wind shear minus the corresponding concentrations predicted when wind shear is neglected.

## 5. Discussion of the Results

An examination of the simulation results reveals the significance of incorporating the power law wind profile in the grid model. Because the velocities are systematically altered through the application of the wind profile algorithm, the computed wind velocities at the inversion base and ground-level heights were increased, relative to the straight profile : values ( $M = 0$ ), by as much as 70 and 20 percent, respectively. The wind velocities averaged over the entire mixing depth were consistently much larger than the uniform profile values. As one would expect, therefore, the results of the sensitivity experiment, which was performed with a 25 percent increase in all wind velocities (see Chapter IV of Volume I), are strikingly similar to those shown here.

A characteristic of both the wind speed and wind shear sensitivity studies is that, when the concentration maps are compared with those generated for the base case, a perceptible translation of concentration isopleths toward the northeast, the prevailing wind direction, is observed. In addition, the majority of maximum concentrations are located in Grid Columns 20 through 25; this result was expected because the translation of concentration isopleths is greatest when the path of travel is longest. The fact that average overall deviations for all species are negative also supports the hypothesis that the net effect of the inclusion of wind shear is similar to that resulting from a simple increase in wind speeds.

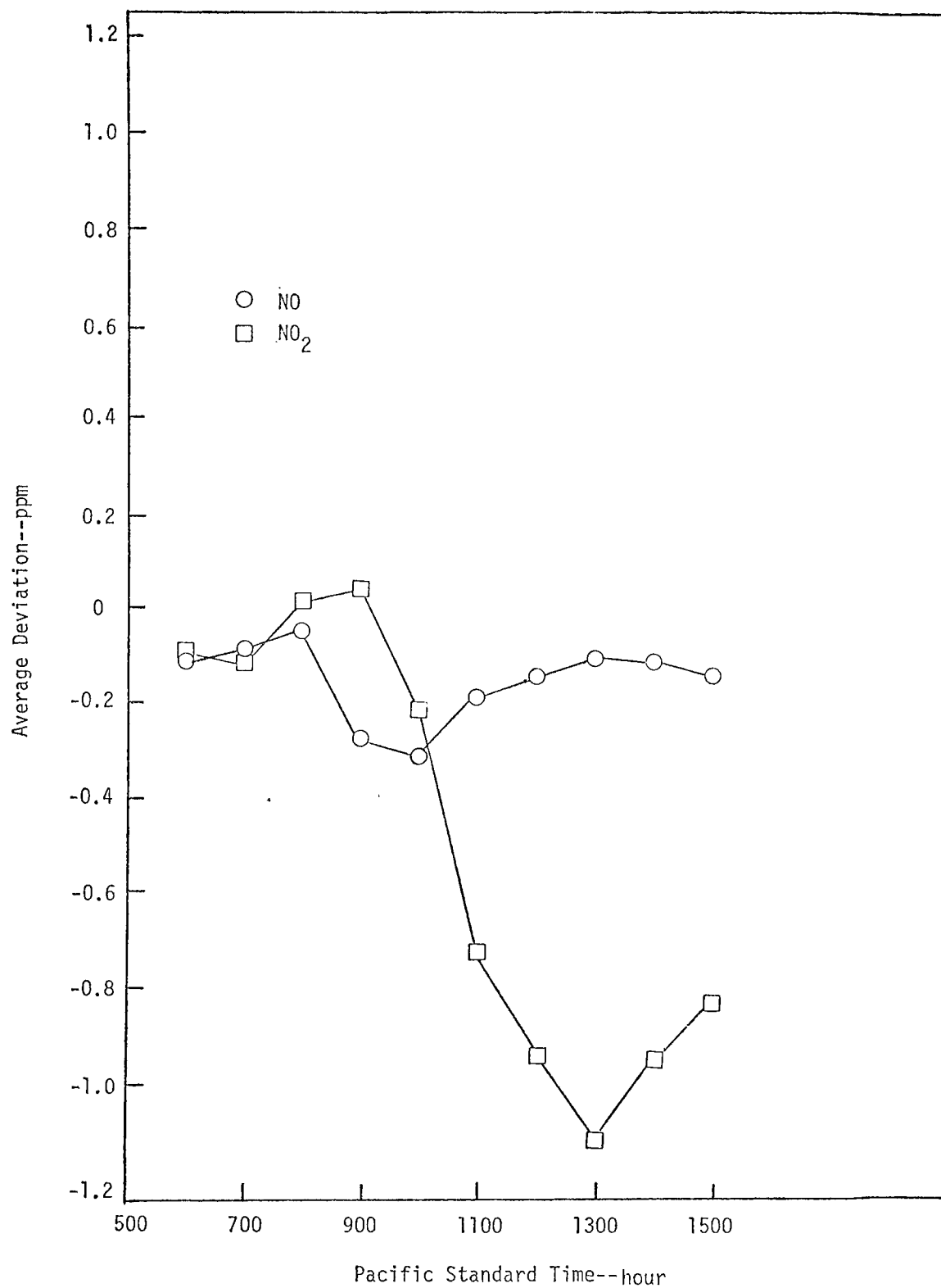


FIGURE 13. THE EFFECT--EXPRESSED AS AVERAGE DEVIATION--OF VARIATIONS IN VERTICAL WIND SHEAR ON NO AND NO<sub>2</sub>

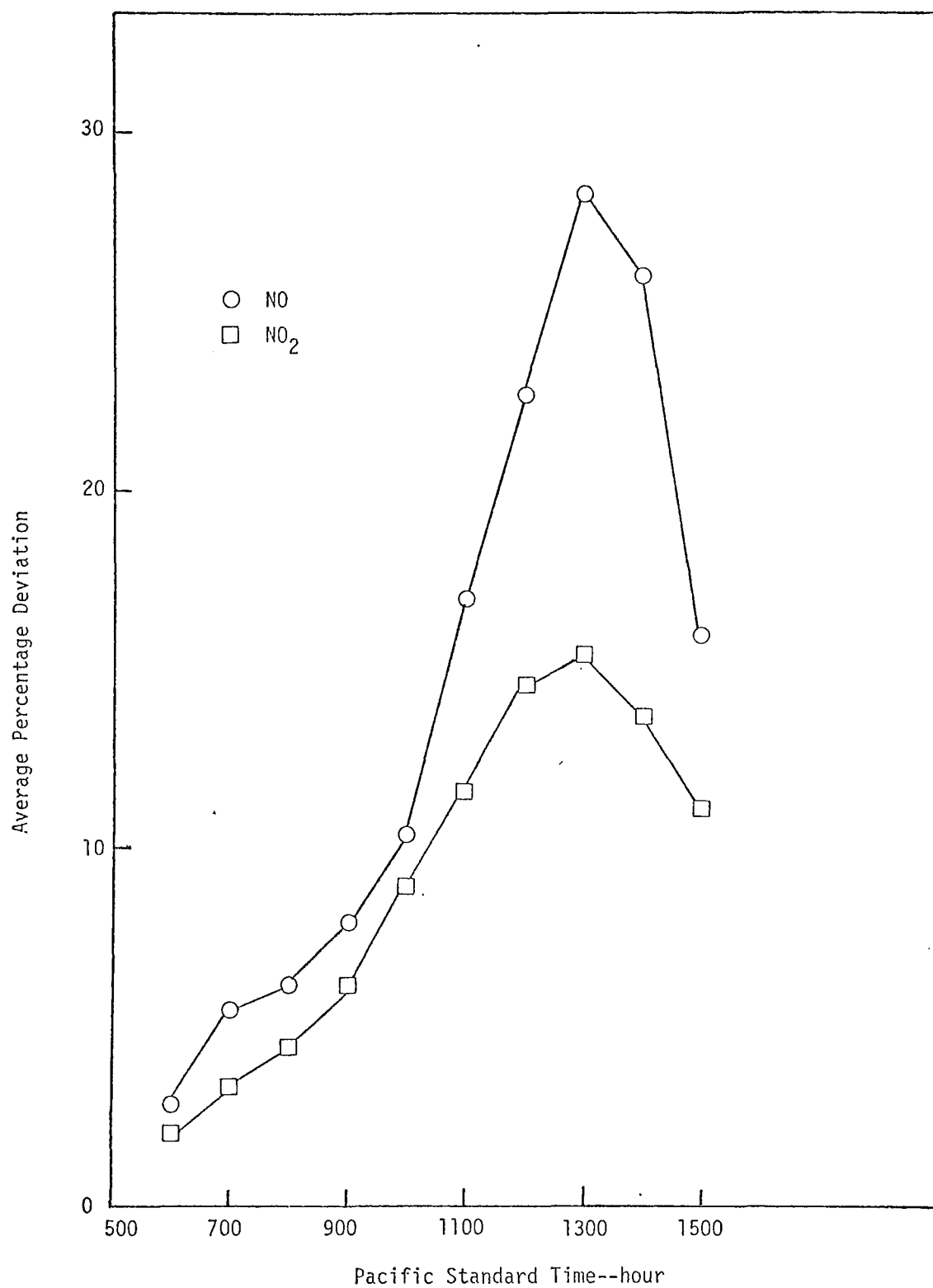


FIGURE 14. THE EFFECT--EXPRESSED AS PERCENTAGE DEVIATION--OF VARIATIONS IN VERTICAL WIND SHEAR ON NO AND NO<sub>2</sub>



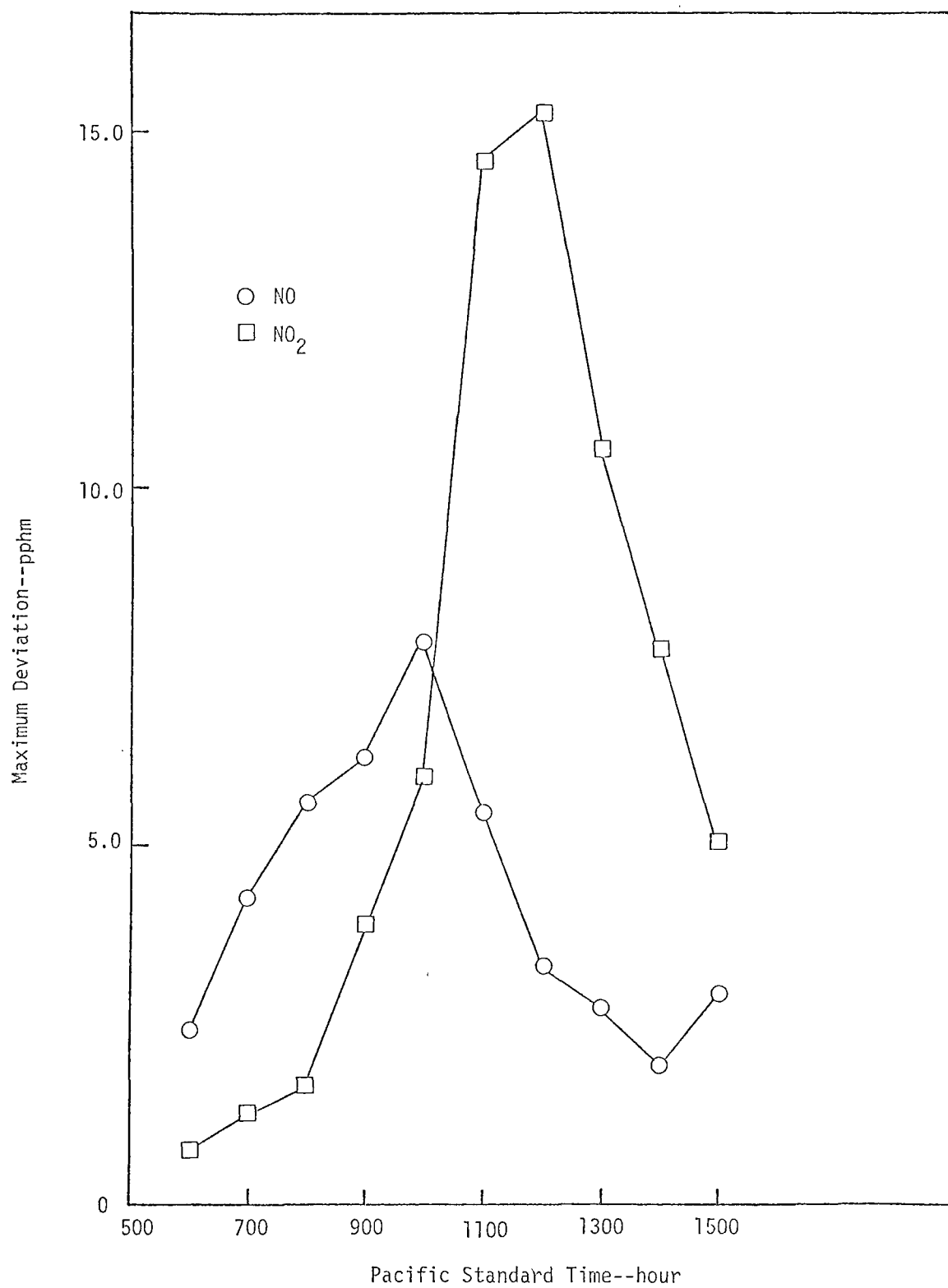


FIGURE 15. THE EFFECT--EXPRESSED AS MAXIMUM DEVIATION--OF VARIATIONS IN VERTICAL WIND SHEAR ON NO AND NO<sub>2</sub>

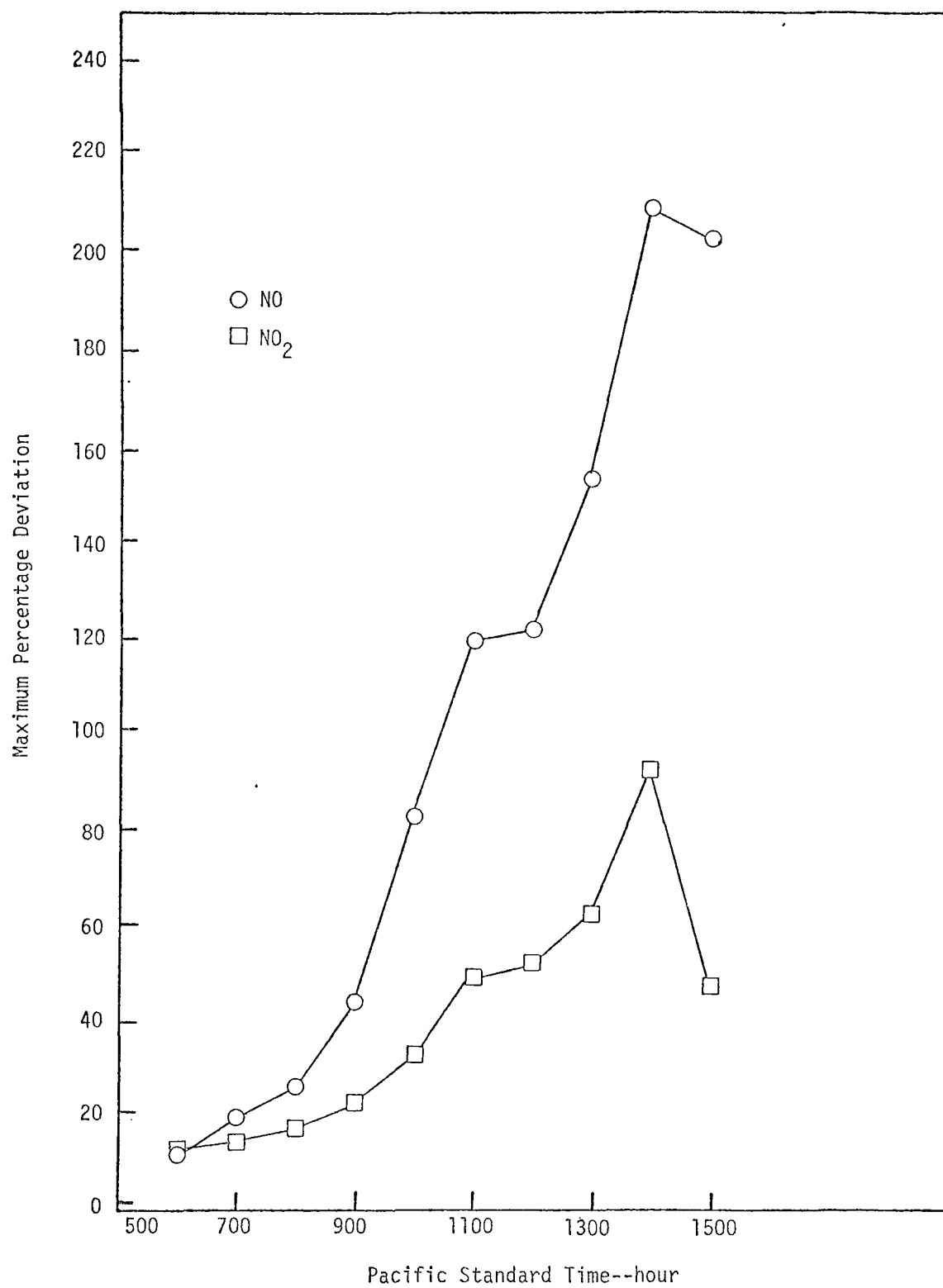


FIGURE 16. THE EFFECT--EXPRESSED AS PERCENTAGE MAXIMUM DEVIATION--OF VARIATIONS IN VERTICAL WIND SHEAR ON NO AND NO<sub>2</sub>

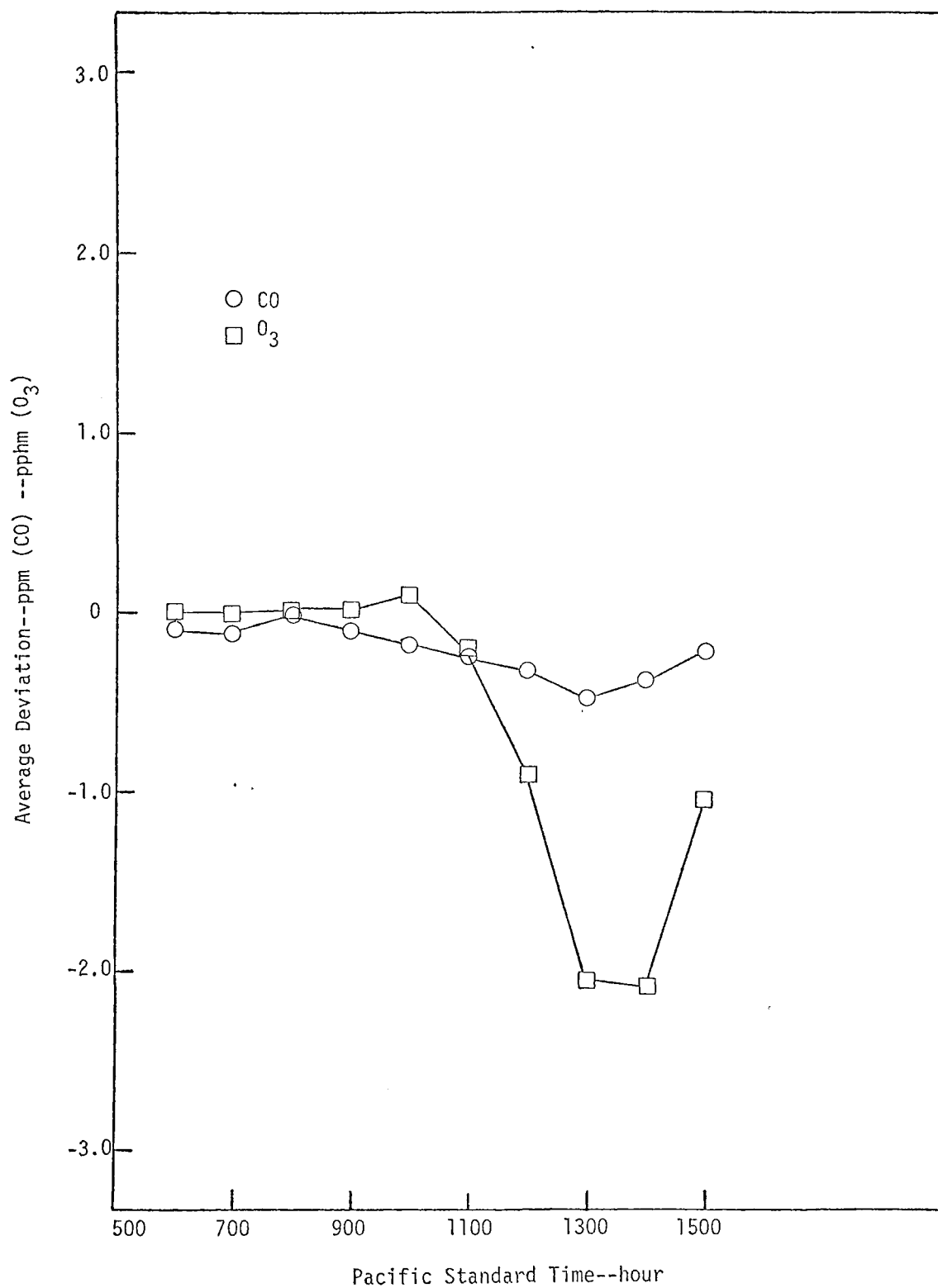


FIGURE 17. THE EFFECT--EXPRESSED AS AVERAGE DEVIATION--OF VARIATIONS IN VERTICAL WIND SHEAR ON CO AND O<sub>3</sub>

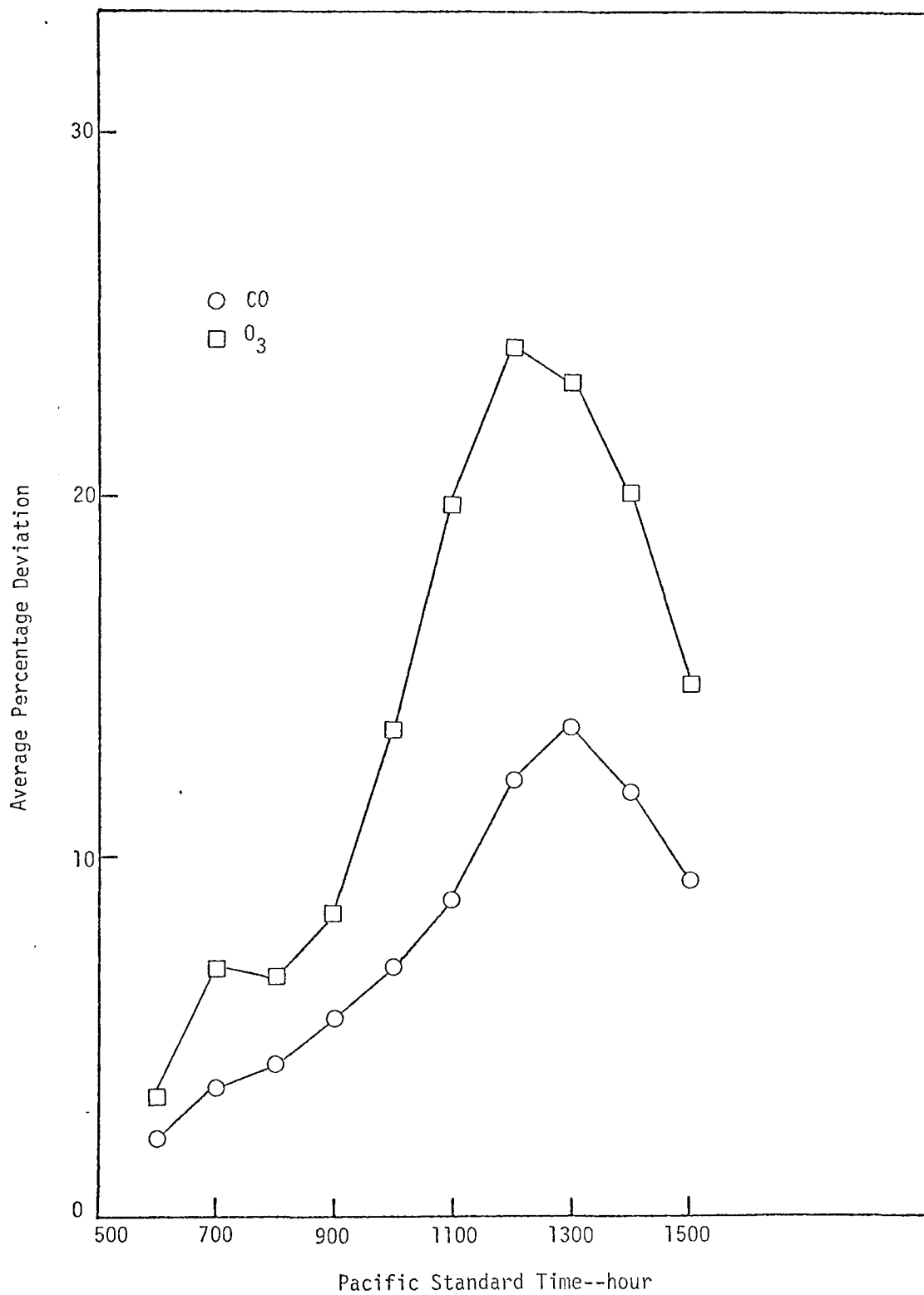


FIGURE 18. THE EFFECT--EXPRESSED AS PERCENTAGE DEVIATION--OF VARIATIONS IN VERTICAL WIND SHEAR ON CO AND O<sub>3</sub>

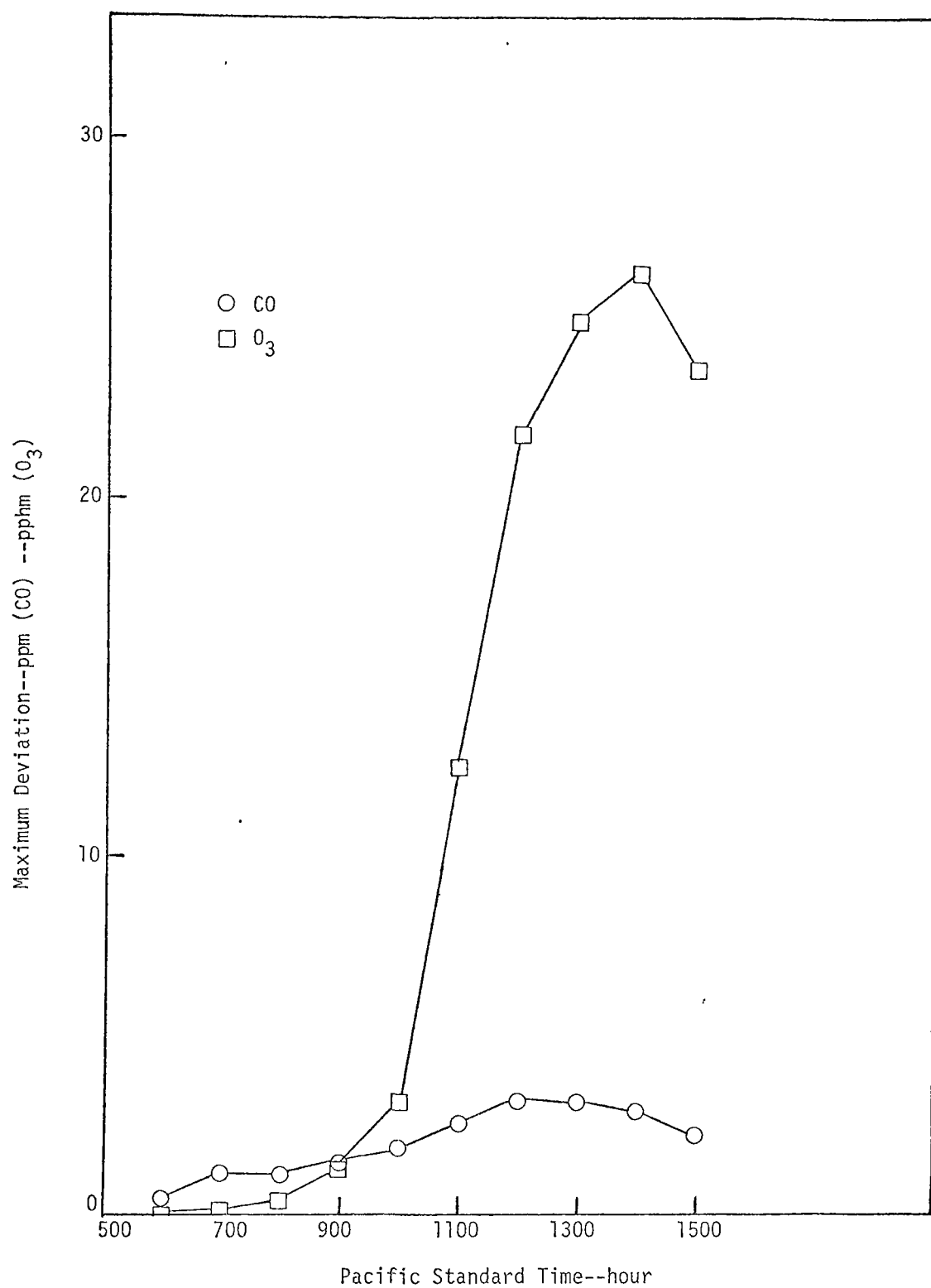


FIGURE 19. THE EFFECT--EXPRESSED AS MAXIMUM DEVIATION--OF VARIATIONS IN VERTICAL WIND SHEAR ON CO AND O<sub>3</sub>

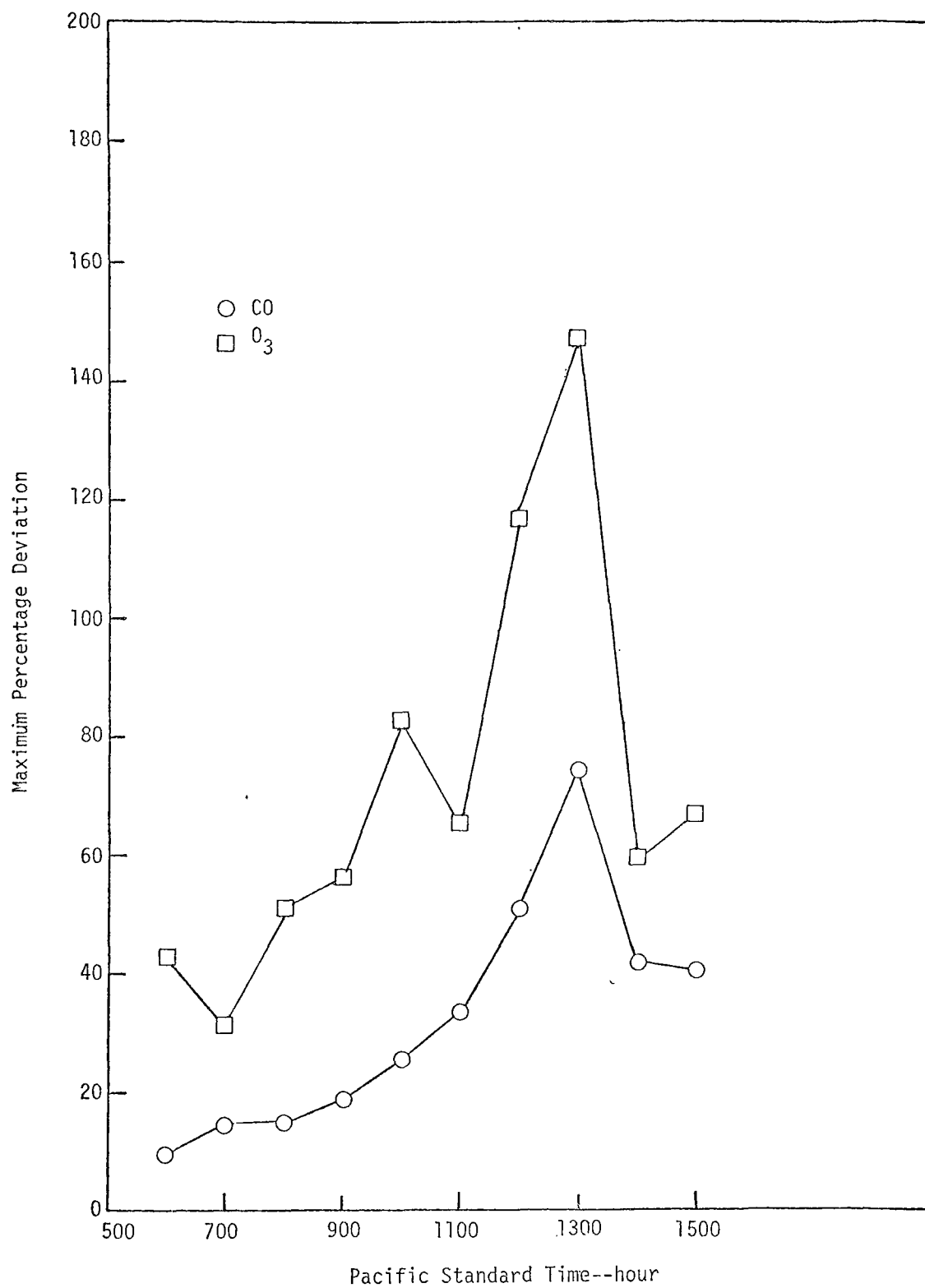


FIGURE 20. THE EFFECT--EXPRESSED AS PERCENTAGE MAXIMUM DEVIATION--OF VARIATIONS IN VERTICAL WIND SHEAR ON CO AND O<sub>3</sub>

The results of this study clearly indicate that wind shear phenomena should be included in the airshed model. Of course, it would be most helpful in the construction of velocity profiles to have wind data taken aloft in cities where the model is to be applied.

#### B. TREATMENT OF WIND SHEAR IN THE AIRSHED MODEL

On the basis of the sensitivity results presented in the previous section, we included provisions in the computer programs for treating a fully three-dimensional wind field. To facilitate usage of either theoretical wind shear relationships or actual wind data aloft, we structured the air quality simulation program to accept the three-dimensional wind field inputs directly from the meteorological data file. The user assembles the wind field inputs by employing the Automated Meteorological Data Preparation Program. Thus, all wind shear algorithms and interpolation routines are embedded in the meteorological data program. By structuring the airshed simulation package in this way, we have enabled changes in the treatment of wind shear to be accomplished without modifying the photochemical dispersion model code.

In many urban areas, sufficient soundings of the winds aloft are seldom available for use in constructing the complete flow field. Therefore, we initiated efforts to derive a set of theoretical wind shear relationships using results obtained from Deardorff's planetary boundary layer model. These relationships are presented and discussed in Chapter II of Volume III. For use in those urban areas where numerous pibal or other suitable data are available, we recommend that an algorithm be developed and installed in the Automated Meteorological Data Preparation Program for the construction of wind fields aloft using the available wind soundings.

#### C. EXAMINATION OF AN ALGORITHM FOR DERIVING MASS-CONSISTENT WIND FIELDS

One of the assumptions commonly invoked in airshed modeling is that the air flow in the planetary boundary layer is incompressible. Under these conditions, the velocity components satisfy the following continuity relationships:

$$\frac{\partial u}{\partial x} + \frac{\partial v}{\partial y} + \frac{\partial w}{\partial z} = 0 \quad , \quad (14)$$

where  $u$ ,  $v$ , and  $w$  are the  $x$ ,  $y$ , and  $z$  components, respectively, of the wind velocity vector. In the SAI model, the  $z$  coordinate is normalized by the depth of the modeling region, in which case Eq. (14) becomes

$$\frac{\partial u \Delta H}{\partial x} + \frac{\partial v \Delta H}{\partial y} + \frac{\partial W}{\partial \rho} = 0 \quad , \quad (15)$$

where

$$\begin{aligned} \rho &= [z - h(x,y)]/[H_t(x,y,t) - h(x,y)], \\ H_t &= \text{the elevation of the top of the modeling region,} \\ h &= \text{the terrain elevation,} \\ \Delta H &= H_t(x,y,t) - h(x,y), \\ W &= w - u[(\partial h/\partial x) + \rho(\partial \Delta H/\partial x)] - v[(\partial h/\partial y) + \rho(\partial \Delta H/\partial y)] \quad . \end{aligned}$$

In typical airshed model applications, estimates of  $u(x,y,z,t)$  and  $v(x,y,z,t)$  are obtained from the available data on wind speed and direction, both at ground level and aloft. Once the horizontal components are specified, Eq. (15) can be solved for  $W$ . Writing this equation in finite difference form, we obtain

$$\begin{aligned} W_{i,j,k+\frac{1}{2}} &= W_{i,j,k-\frac{1}{2}} - \frac{\Delta \rho}{\Delta x} \left[ (u \Delta H)_{i+\frac{1}{2},j,k} - (u \Delta H)_{i-\frac{1}{2},j,k} \right] \\ &\quad - \frac{\Delta \rho}{\Delta y} \left[ (v \Delta H)_{i,j+\frac{1}{2},k} - (v \Delta H)_{i,j-\frac{1}{2},k} \right] \quad , \quad (16) \end{aligned}$$

where the integer triple  $(i,j,k)$  designates the center of a grid cell. Equation (15) is solved subject to the constraint of

$$W = 0 \quad (17)$$



at  $\rho = 0$ , which simply states that either the wind speed is zero at the ground or the wind is flowing parallel to the terrain. By first estimating the horizontal wind components and subsequently solving Eq. (15) for  $W$ , we insure that the net flux of air into each grid cell is zero.

One difficulty associated with the wind field methodology described above is that nonzero vertical velocities may be calculated at the top of the modeling region. Thus, pollutants may be advected out of the modeling region, even though a stable capping inversion layer is present. This situation is somewhat contrary to the usual belief that an elevated inversion layer suppresses vertical transport, although buoyant air parcels may penetrate the stable layer to some extent. It is important to note that the calculated vertical motions are, in part, the result of inaccuracies in the predicted horizontal wind components, especially aloft, where few measurements are generally available.

In previous efforts, we examined means for removing convergence and divergence areas in the flow field aloft (see Roth et al., 1971). However, these attempts to force the vertical velocities to obey some specified constraint, such as a zero velocity at the inversion base, failed to produce acceptable wind fields. In many instances, the algorithms generated horizontal wind speeds aloft in excess of 40 mph. Under the present contract, we revisited this issue of constructing mass-consistent wind fields in light of the findings of recent studies in this area reported in the literature.

## 1. The Governing Equations

The problem that we address here is as follows: Given a set of initial estimates of  $u$  and  $v$  over the modeling region, how should these wind speeds be adjusted to yield vertical wind velocities that not only satisfy Eq. (14), but also obey some imposed constraint. The methodology described below is similar to that given by Fankhauser (1974).

Let  $u_0$  and  $v_0$  designate the initial estimates of the horizontal wind components, which have been obtained through, say, the application of interpolation procedures. The values of  $u$  and  $v$  to be employed in the grid model are obtained by defining a function  $\phi$  in the following manner:

$$u\Delta H = (u\Delta H)_0 + \frac{\partial \phi}{\partial x} \quad , \quad (18)$$

$$v\Delta H = (v\Delta H)_0 + \frac{\partial \phi}{\partial y} \quad . \quad (19)$$

Note that we attempt here to adjust only  $u_0$  and  $v_0$ , not  $\Delta H$ . Substituting Eqs. (18) and (19) into Eq. (15), we obtain

$$\frac{\partial^2 \phi}{\partial x^2} + \frac{\partial^2 \phi}{\partial y^2} = - \frac{\partial W}{\partial \rho} - \frac{\partial (u\Delta H)_0}{\partial x} - \frac{\partial (v\Delta H)_0}{\partial y} \quad . \quad (20)$$

We define the terms on the right-hand side of Eq. (20) as follows:

$$D = - \frac{\partial W}{\partial \rho} \quad , \quad (21)$$

$$D_0 = \frac{\partial (u\Delta H)_0}{\partial x} + \frac{\partial (v\Delta H)_0}{\partial y} \quad . \quad (22)$$

Thus, Eq. (20) becomes

$$\frac{\partial^2 \phi}{\partial x^2} + \frac{\partial^2 \phi}{\partial y^2} = D - D_0 \quad . \quad (23)$$

At this point, recall that from Eq. (17)  $W$  must be zero at the ground. Furthermore, we wish to impose a constraint such as

$$W = W_T \quad (24)$$

at the top of the modeling region. If we set  $W_T = 0$ , then pollutants will not be allowed to advect up into the inversion layer.

Operationally, Eq. (23) is written in finite difference form and is solved on successive layers of grid cells in the x-y plane. Thus, in finite difference notation, Eq. (23) becomes

$$[\nabla^2 \phi]_{i,j,k} = D_{i,j,k} - (D_0)_{i,j,k} \quad , \quad (25)$$

where  $[\nabla^2 \phi]_{i,j,k}$  is the usual five-point difference operator for the Laplacian. Before Eq. (25) can be solved numerically, however, an additional relationship for  $D - D_0$  must be determined, and appropriate boundary conditions must be specified.

In a study carried out by O'Brien (1970), a general objective analysis technique is described for adjusting the divergence and vertical wind speeds associated with wind fields derived from mesoscale rawinsonde data. The essence of this work is that expressions for  $D - D_0$  can be derived on the basis of an assumed form of the errors associated with the values of  $D_0$ . For example, if the errors in  $D_0$  are independent of height, then it can be shown that

$$D_{i,j,k} - (D_0)_{i,j,k} = \frac{[(W_{i,j,k+\frac{1}{2}})_0 - W_T]}{\Delta p(K)} \quad , \quad (26)$$

where  $K$  is the total number of grid cells in the vertical direction. Furthermore, if the errors in  $D_0$  are assumed to be proportional to height above the terrain, then

$$D_{i,j,k} - (D_0)_{i,j,k} = \frac{2k[(W_{i,j,k+\frac{1}{2}})_0 + W_T]}{\Delta p(K)(K+1)} \quad . \quad (27)$$

If numerous ground-level meteorological monitoring sites were scattered over an urban area of interest, and few upper-level soundings were available, then it seems reasonable that the errors in the estimated winds aloft would be somewhat larger than those for winds near the ground. Thus, Eq. (27) may provide a

more satisfactory relationship for  $D - D_0$ . Note that the perturbations to the flow field near the surface are significantly smaller if one uses Eq. (27) than they are if Eq. (26) is used, as demonstrated in the next section.

In specifying boundary conditions, one has two possible choices: the Dirichlet ( $\phi = 0$ ) or the Neumann ( $\partial\phi/\partial n = 0$ ) boundary condition. Physically, the former treatment leaves the  $u$  component of the velocity unaltered along boundaries parallel to the  $x$ -axis and the  $v$  component unaltered on boundaries parallel to the  $y$ -axis. In the latter case, just the opposite is true. Fankhauser (1974) employed the Dirichlet condition in his study, and Liu et al. (1974) report that in simulations using a similar type of model, the results were not significantly influenced by the choice of one formulation over the other.

## 2. Tests of the Model

To test the model described in the previous section, we carried out a study to determine the magnitude of the alterations that would be predicted for the typical wind fields previously used as input to the SAI airshed model. Thus, we rendered the wind fields used in the 29 September 1969 model evaluation study for Los Angeles (see Reynolds et al., 1973) mass consistent; moreover, we constrained the vertical velocity  $W$  to be zero at the base of the inversion layer. We used a  $25 \times 25 \times 5$  grid layout, where  $\Delta x = \Delta y = 2$  miles and  $\Delta p = 0.2$ . Since wind shear was neglected in the Los Angeles study, we considered  $u_0$  and  $v_0$  to be functions only of  $x$ ,  $y$ , and time. Tables 13 through 15 illustrate the nominal wind speeds and directions and mixing depths for 6 a.m. and 3 p.m. on 29 September 1969. These maps served as the inputs to the mass-consistent wind algorithm.

In performing the calculations with the model, we wished to assess the sensitivity of the predictions to (1) the manner in which  $D - D_0$  is approximated [i.e., the use of Eq. (26) or (27) and (2) the choice of either Dirichlet or Neumann boundary conditions. Furthermore, we examined the nature

Table 13  
HOURLY AVERAGED WIND SPEED AND DIRECTION IN THE LOS ANGELES BASIN  
ON 29 SEPTEMBER 1969 AT 6:00 a.m. PST

## (a) Wind Speed

	1	2	3	4	5	6	7	8	9	10	11	12	13	14	15	16	17	18	19	20	21	22	23	24	25
25	1.0	1.0	1.5	2.0	3.0	4.0	5.0	6.0	7.0	8.0	9.0	10.0	11.0	12.0	13.0	14.0	15.0	16.0	17.0	18.0	19.0	20.0	21.0	22.0	23.0
24	1.0	1.0	1.5	2.0	3.0	4.0	5.0	6.0	7.0	8.0	9.0	10.0	11.0	12.0	13.0	14.0	15.0	16.0	17.0	18.0	19.0	20.0	21.0	22.0	23.0
23	1.0	1.0	1.5	2.0	3.0	4.0	5.0	6.0	7.0	8.0	9.0	10.0	11.0	12.0	13.0	14.0	15.0	16.0	17.0	18.0	19.0	20.0	21.0	22.0	23.0
22	1.0	1.0	2.0	3.0	4.0	5.0	6.0	7.0	8.0	9.0	10.0	11.0	12.0	13.0	14.0	15.0	16.0	17.0	18.0	19.0	20.0	21.0	22.0	23.0	24.0
21	1.0	1.5	2.0	3.0	4.0	5.0	6.0	7.0	8.0	9.0	10.0	11.0	12.0	13.0	14.0	15.0	16.0	17.0	18.0	19.0	20.0	21.0	22.0	23.0	24.0
20	1.0	1.5	2.0	3.0	4.0	5.0	6.0	7.0	8.0	9.0	10.0	11.0	12.0	13.0	14.0	15.0	16.0	17.0	18.0	19.0	20.0	21.0	22.0	23.0	24.0
19	1.0	1.5	2.0	3.0	4.0	5.0	6.0	7.0	8.0	9.0	10.0	11.0	12.0	13.0	14.0	15.0	16.0	17.0	18.0	19.0	20.0	21.0	22.0	23.0	24.0
18	1.0	1.5	2.0	3.0	4.0	5.0	6.0	7.0	8.0	9.0	10.0	11.0	12.0	13.0	14.0	15.0	16.0	17.0	18.0	19.0	20.0	21.0	22.0	23.0	24.0
17	1.0	1.5	2.0	3.0	4.0	5.0	6.0	7.0	8.0	9.0	10.0	11.0	12.0	13.0	14.0	15.0	16.0	17.0	18.0	19.0	20.0	21.0	22.0	23.0	24.0
16	2.0	3.0	4.0	5.0	6.0	7.0	8.0	9.0	10.0	11.0	12.0	13.0	14.0	15.0	16.0	17.0	18.0	19.0	20.0	21.0	22.0	23.0	24.0	25.0	26.0
15	3.0	4.0	5.0	6.0	7.0	8.0	9.0	10.0	11.0	12.0	13.0	14.0	15.0	16.0	17.0	18.0	19.0	20.0	21.0	22.0	23.0	24.0	25.0	26.0	27.0
14	4.0	5.0	6.0	7.0	8.0	9.0	10.0	11.0	12.0	13.0	14.0	15.0	16.0	17.0	18.0	19.0	20.0	21.0	22.0	23.0	24.0	25.0	26.0	27.0	28.0
13	5.0	6.0	7.0	8.0	9.0	10.0	11.0	12.0	13.0	14.0	15.0	16.0	17.0	18.0	19.0	20.0	21.0	22.0	23.0	24.0	25.0	26.0	27.0	28.0	29.0
12	6.0	7.0	8.0	9.0	10.0	11.0	12.0	13.0	14.0	15.0	16.0	17.0	18.0	19.0	20.0	21.0	22.0	23.0	24.0	25.0	26.0	27.0	28.0	29.0	30.0
11	7.0	8.0	9.0	10.0	11.0	12.0	13.0	14.0	15.0	16.0	17.0	18.0	19.0	20.0	21.0	22.0	23.0	24.0	25.0	26.0	27.0	28.0	29.0	30.0	31.0
10	8.0	9.0	10.0	11.0	12.0	13.0	14.0	15.0	16.0	17.0	18.0	19.0	20.0	21.0	22.0	23.0	24.0	25.0	26.0	27.0	28.0	29.0	30.0	31.0	32.0
9	9.0	10.0	11.0	12.0	13.0	14.0	15.0	16.0	17.0	18.0	19.0	20.0	21.0	22.0	23.0	24.0	25.0	26.0	27.0	28.0	29.0	30.0	31.0	32.0	33.0
8	10.0	11.0	12.0	13.0	14.0	15.0	16.0	17.0	18.0	19.0	20.0	21.0	22.0	23.0	24.0	25.0	26.0	27.0	28.0	29.0	30.0	31.0	32.0	33.0	34.0
7	11.0	12.0	13.0	14.0	15.0	16.0	17.0	18.0	19.0	20.0	21.0	22.0	23.0	24.0	25.0	26.0	27.0	28.0	29.0	30.0	31.0	32.0	33.0	34.0	35.0
6	12.0	13.0	14.0	15.0	16.0	17.0	18.0	19.0	20.0	21.0	22.0	23.0	24.0	25.0	26.0	27.0	28.0	29.0	30.0	31.0	32.0	33.0	34.0	35.0	36.0
5	13.0	14.0	15.0	16.0	17.0	18.0	19.0	20.0	21.0	22.0	23.0	24.0	25.0	26.0	27.0	28.0	29.0	30.0	31.0	32.0	33.0	34.0	35.0	36.0	37.0
4	14.0	15.0	16.0	17.0	18.0	19.0	20.0	21.0	22.0	23.0	24.0	25.0	26.0	27.0	28.0	29.0	30.0	31.0	32.0	33.0	34.0	35.0	36.0	37.0	38.0
3	15.0	16.0	17.0	18.0	19.0	20.0	21.0	22.0	23.0	24.0	25.0	26.0	27.0	28.0	29.0	30.0	31.0	32.0	33.0	34.0	35.0	36.0	37.0	38.0	39.0
2	16.0	17.0	18.0	19.0	20.0	21.0	22.0	23.0	24.0	25.0	26.0	27.0	28.0	29.0	30.0	31.0	32.0	33.0	34.0	35.0	36.0	37.0	38.0	39.0	40.0
1	17.0	18.0	19.0	20.0	21.0	22.0	23.0	24.0	25.0	26.0	27.0	28.0	29.0	30.0	31.0	32.0	33.0	34.0	35.0	36.0	37.0	38.0	39.0	40.0	41.0

## (b) Wind Direction

	1	2	3	4	5	6	7	8	9	10	11	12	13	14	15	16	17	18	19	20	21	22	23	24	25
25	93	103	103	113	110	123	120	136	141	146	143	149	150	150	150	150	151	151	151	150	150	150	150	150	150
24	89	93	97	106	110	121	127	132	137	142	147	140	148	149	140	146	144	144	144	140	140	140	140	140	140
23	80	85	91	98	112	119	126	132	138	145	147	148	147	146	146	145	143	140	136	136	131	120	120	120	120
22	75	79	84	96	110	110	125	132	139	147	147	148	147	146	142	130	135	133	129	125	120	117	115	113	110
21	76	80	85	95	100	115	121	120	135	142	146	147	147	142	130	135	130	123	120	115	110	107	105	103	100
20	77	81	85	94	105	112	117	124	131	130	146	145	144	139	135	133	128	123	117	110	95	93	92	91	90
19	77	81	86	93	102	109	114	120	126	133	130	142	141	136	133	130	128	120	110	100	95	93	92	91	90
18	70	82	86	92	99	105	110	116	122	129	131	137	135	133	130	127	119	113	106	100	95	93	92	91	90
17	79	83	87	91	97	102	106	111	117	125	126	130	129	130	120	123	110	110	103	98	95	93	92	91	90
16	79	83	87	91	95	99	103	107	112	119	120	123	123	120	126	120	113	108	105	100	95	93	92	91	91
15	80	84	88	92	96	100	104	107	110	113	115	117	117	110	110	117	112	107	104	100	95	93	93	91	91
14	81	84	88	91	94	97	100	103	106	100	113	116	117	118	117	116	111	107	107	101	96	92	90	90	90
13	82	84	87	90	92	94	96	99	102	107	111	115	117	118	110	116	114	105	106	101	97	93	90	90	90
12	83	85	87	89	90	91	93	95	99	103	109	114	117	120	122	122	122	105	102	100	95	93	93	93	93
11	84	85	86	88	88	89	90	91	96	103	100	113	117	120	123	125	125	125	105	96	92	92	92	92	92
10	84	85	86	87	88	89	90	90	96	103	100	113	117	119	123	126	120	122	116	107	98	95	92	91	91
9	85	86	87	88	89	90	92	93	98	103	107	111	115	118	123	126	121	118	111	100	101	99	96	92	92
8	87	88	88	89	90	92	94	96	99	103	107	110	113	118	124	128	130	130	126	100	96	96	92	90	90
7	88	89	90	91	92	94	96	98	100	104	106	109	111	117	124	128	130	130	120	115	110	100	95	91	90
6	90	91	92	93	94	96	98	100	102	104	106	108	110	110	125	125	127	124	113	104	90	93	90	90	90
5	90	91	92	93	94	96	98	100	102	104	106	108	110	111	112	110	119	120	116	109	103	96	92	90	90
4	90	91	92	93	94	96	98	100	102	104	106	108	110	110	110	112	111	111	109	104	104	100	92	90	90
3	90	91	92	93	94	96	98	100	102	104	106	108	110	110	110	110	110	100	106	100	107	92	90	90	90
2	90	91	92	93	94	96	98	100	102	104	106	108	110	110	109	109	111	111	111	105	100	92	90	90	90
1	90	91	92	93	94	96	98	100	102	104	106	108	110	110	109	109	111	111	111	105	100	92	90	90	90

Table 14  
HOURLY AVERAGED WIND SPEED AND DIRECTION IN THE LOS ANGELES BASIN  
ON 29 SEPTEMBER 1969 AT 3:00 p.m. PST

## (a) Wind Speed

	1	2	3	4	5	6	7	8	9	10	11	12	13	14	15	16	17	18	19	20	21	22	23	24	25
25	6.0	6.0	6.0	6.0	6.0	6.0	6.0	6.0	5.0	4.0	4.0	4.0	4.5	4.0	5.0	5.0	5.0	6.0	6.0	7.0	8.0	9.0	9.0	9.0	9.0
24	6.0	6.0	6.0	6.0	6.0	6.0	6.0	6.0	6.0	6.0	6.0	4.0	4.0	4.0	5.0	5.0	6.0	6.0	7.0	8.0	9.0	9.0	9.0	9.0	9.0
23	6.0	6.0	6.0	6.0	6.0	6.0	6.0	6.0	6.0	6.0	6.0	6.0	4.0	4.0	5.0	5.0	6.0	7.0	7.0	8.0	9.0	9.0	9.0	6.0	9.0
22	6.0	6.0	6.0	6.0	6.0	6.0	6.0	6.0	6.0	5.5	5.0	5.0	5.0	5.0	6.0	6.0	7.0	8.0	8.0	9.0	9.0	9.0	9.0	9.0	8.0
21	5.5	6.0	6.0	6.0	6.0	6.0	6.0	6.5	5.5	5.0	5.0	5.0	6.0	7.0	7.0	8.0	9.0	9.0	10.0	10.0	10.0	10.0	9.0	8.0	8.0
20	5.0	6.0	5.5	5.5	5.5	5.5	5.5	5.0	5.0	6.0	6.0	6.0	7.0	8.0	8.0	9.0	10.0	10.0	11.0	11.0	10.0	9.0	8.0	7.0	7.0
19	6.0	6.0	5.0	5.0	5.0	5.0	6.0	6.0	6.0	6.0	6.0	7.0	8.0	9.0	10.0	10.0	11.0	12.0	11.0	10.0	9.0	8.0	7.0	7.0	6.0
18	5.0	6.0	5.0	5.0	5.0	5.0	6.0	6.0	6.0	6.0	7.0	8.0	9.0	10.0	11.0	11.0	12.0	12.0	10.0	9.0	8.0	8.0	7.0	7.0	6.0
17	6.0	5.0	5.0	5.0	5.0	5.0	6.0	7.0	7.0	8.0	9.0	9.0	10.0	12.0	12.0	11.0	10.0	9.0	8.0	6.0	7.0	6.0	6.0	6.0	6.0
16	5.0	5.0	7.0	7.0	7.0	7.0	7.0	8.0	8.0	9.0	10.0	10.0	12.0	11.0	10.0	10.0	9.0	8.0	7.0	7.0	6.0	6.0	6.0	6.0	5.0
15	7.0	7.0	8.0	8.0	9.0	9.0	9.0	8.0	9.0	9.0	10.0	11.0	12.0	11.0	10.0	9.0	9.0	8.0	7.0	7.0	6.0	5.0	5.0	5.0	5.0
14	8.0	8.0	9.0	9.0	9.0	9.0	9.0	9.0	10.0	10.0	11.0	12.0	11.0	10.0	9.0	8.0	8.0	7.0	6.0	6.0	5.0	5.0	5.0	5.0	5.0
13	9.0	9.0	9.0	9.0	9.0	9.0	9.0	9.0	10.0	11.0	12.0	13.0	11.0	10.0	9.0	8.0	8.0	7.0	7.0	6.0	5.0	5.0	5.0	5.0	4.0
12	9.0	9.0	9.0	8.5	8.5	8.5	9.0	9.0	10.0	11.0	13.0	15.0	13.0	11.0	10.0	9.0	8.0	8.0	7.0	6.0	6.0	5.0	5.0	4.0	4.0
11	8.5	8.5	8.5	8.0	8.0	8.0	9.0	10.0	11.0	12.0	14.0	15.0	11.0	10.0	10.0	9.0	9.0	8.0	7.0	6.0	5.0	5.0	4.0	4.0	4.0
10	8.5	8.0	8.0	8.0	8.0	8.0	8.0	9.0	10.0	12.0	13.0	13.0	11.0	10.0	9.0	9.0	8.0	7.0	6.0	5.0	4.0	4.0	4.0	4.0	4.0
9	8.0	8.0	8.0	8.0	8.0	8.0	8.0	8.5	9.0	10.0	11.0	12.0	13.0	11.0	10.0	9.0	8.0	7.0	6.0	5.0	4.0	4.0	4.0	4.0	4.0
8	8.0	8.0	8.0	8.0	8.0	8.0	8.0	8.5	9.0	9.0	10.0	11.0	10.0	9.0	8.0	7.0	6.0	5.5	5.5	4.5	4.5	4.0	4.0	4.0	4.0
7	8.0	8.0	8.0	8.0	8.0	8.0	8.0	8.5	8.5	8.5	9.0	10.0	9.0	8.0	7.0	6.0	5.5	5.5	5.0	5.0	4.5	4.5	4.0	4.0	4.0
6	8.0	8.0	8.0	8.0	8.0	8.0	8.0	8.0	8.0	8.0	8.5	8.5	9.0	8.0	7.0	6.0	5.5	5.0	5.0	5.0	5.0	4.5	4.0	4.0	4.5
5	8.0	8.0	8.0	8.0	8.0	8.0	8.0	8.0	8.0	8.0	8.0	8.0	8.0	7.0	6.0	5.5	5.0	5.0	5.0	5.0	5.0	5.0	4.5	4.0	4.5
4	8.0	8.0	8.0	8.0	8.0	8.0	8.0	7.5	7.0	7.0	7.0	7.0	7.0	6.0	6.0	5.0	5.0	5.0	5.0	5.0	5.0	5.0	5.0	5.0	4.5
3	8.0	8.0	8.0	8.0	8.0	7.5	7.5	7.0	6.0	6.0	6.0	6.0	6.0	6.0	6.0	5.0	5.0	5.0	5.0	5.0	5.0	5.0	5.0	5.0	5.0
2	8.0	8.0	8.0	7.5	7.5	7.0	7.0	6.0	6.0	5.0	5.0	5.0	5.0	5.0	5.0	5.0	5.0	5.0	5.0	5.0	5.0	5.0	5.0	5.0	5.0
1	8.0	8.0	7.5	7.5	7.0	7.0	6.0	6.0	5.0	5.0	5.0	5.0	5.0	5.0	5.0	5.0	5.0	5.0	5.0	5.0	5.0	5.0	5.0	5.0	5.0

## (b) Wind Direction

	1	2	3	4	5	6	7	8	9	10	11	12	13	14	15	16	17	18	19	20	21	22	23	24	25
25	125	115	105	105	99	95	90	85	70	70	65	63	60	53	36	36	36	35	35	35	34	32	30	30	30
24	131	123	110	107	90	94	90	83	70	70	65	60	37	33	36	36	36	36	36	36	35	34	31	30	30
23	126	126	112	110	99	93	90	83	63	63	60	47	30	36	36	36	37	37	37	37	36	33	30	30	30
22	116	116	116	111	100	95	90	80	77	63	55	50	41	40	40	40	39	38	38	36	33	30	30	30	30
21	110	110	110	110	103	93	90	79	73	63	50	40	41	40	43	44	43	39	37	37	36	35	35	35	43
20	90	90	90	90	90	80	87	83	68	65	46	46	40	49	49	49	49	45	45	43	40	40	43	45	50
19	80	80	80	70	70	76	75	70	60	60	46	49	50	53	50	50	50	50	50	44	44	44	45	53	58
18	83	82	80	78	77	75	75	70	53	50	50	50	55	54	53	52	51	50	50	50	50	60	62	65	60
17	88	80	80	78	70	60	60	57	50	50	59	59	67	53	56	56	54	52	50	60	65	65	72	72	73
16	75	75	70	70	63	62	60	60	60	63	60	59	59	50	50	56	56	60	63	65	67	70	72	72	73
15	72	72	70	65	63	65	66	65	64	64	63	62	60	60	59	59	60	63	63	65	65	67	72	72	73
14	70	69	66	65	65	66	66	66	65	65	64	62	62	61	61	60	60	63	63	65	65	70	72	73	73
13	70	69	66	66	66	67	67	66	66	65	64	62	62	62	62	62	62	66	66	68	68	72	73	74	74
12	69	66	66	69	69	68	68	66	66	64	63	62	62	62	64	64	64	68	68	70	70	74	75	75	75
11	70	69	69	70	71	69	68	66	65	64	62	62	62	64	66	68	68	70	72	72	73	74	75	75	75
10	71	71	72	72	70	69	67	66	64	64	62	64	70	66	60	72	72	72	72	72	73	74	75	75	75
9	72	72	72	70	70	68	66	64	64	66	66	66	73	72	72	72	72	72	72	72	73	74	75	75	70
8	72	72	72	72	69	68	68	68	68	70	71	72	72	72	72	72	72	73	73	73	74	74	76	76	76
7	73	73	73	73	73	70	70	70	70	73	72	72	72	72	72	73	73	73	73	73	75	75	76	76	76
6	73	73	73	74	73	73	73	73	73	73	73	73	73	73	73	73	73	73	73	73	76	76	77	77	78
5	74	74	74	75	73	73	73	73	73	73	73	73	73	73	73	73	73	73	74	74	77	77	79	79	80
4	76	76	75	75	75	73	73	73	73	73	73	73	73	73	73	73	73	75	77	79	82	83	83	83	83
3	76	76	75	74	74	73	70	73	73	73	73	73	73	73	73	73	73	75	77	79	82	83	83	83	83
2	75	74	74	73	73	73	73	73	73	73	73	73	73	73	73	73	73	73	73	73	77	79	82	83	83
1	75	74	74	73	73	73	73	73	73	73	73	73	73	73	73	73	73	73	75	77	79	82	83	83	83

Table 15  
MIXING DEPTHS IN THE LOS ANGELES BASIN  
ON 29 SEPTEMBER 1969 AT 6:00 a.m. AND 3:00 p.m. PST  
(a) 6:00 a.m.

	1	2	3	4	5	6	7	8	9	10	11	12	13	14	15	16	17	18	19	20	21	22	23	24	25
25	100	100	100	100	100	100	100	100	100	200	200	200	200	200	200	200	200	200	200	200	200	200	200	200	200
24	100	100	100	100	100	100	100	100	100	150	200	200	200	200	200	200	200	200	200	200	200	200	200	200	200
23	100	100	100	100	100	100	100	100	100	100	150	150	150	200	200	200	200	200	200	200	200	200	200	200	200
22	100	100	100	100	100	100	100	100	100	100	100	100	100	150	220	200	200	200	200	200	200	200	200	200	200
21	100	100	100	100	100	100	100	100	100	100	100	100	100	100	100	100	100	100	100	100	100	100	100	100	100
20	100	100	100	100	100	100	150	150	150	100	100	100	100	100	100	100	100	100	100	100	100	125	150	150	150
19	200	200	200	200	200	200	200	200	200	200	150	140	120	100	100	100	100	100	100	100	100	100	100	100	100
18	300	300	300	300	300	275	250	250	250	225	200	170	150	125	100	100	100	100	100	100	100	100	100	100	100
17	400	400	400	400	375	325	300	300	275	250	225	200	175	150	125	100	100	100	100	100	100	100	100	100	100
16	500	500	500	400	450	410	350	325	300	275	250	225	200	175	150	125	100	100	100	100	100	100	100	100	100
15	500	500	500	500	400	440	410	350	325	300	275	250	225	200	175	150	125	100	100	100	100	100	100	100	100
14	500	500	500	500	500	470	425	375	350	325	300	275	250	225	200	175	150	125	125	125	125	150	200	200	200
13	500	500	500	500	500	480	450	400	375	350	325	300	275	250	230	225	200	150	150	150	150	175	200	200	200
12	500	500	500	500	500	500	490	450	400	375	350	325	300	280	260	270	225	200	175	175	175	200	200	200	200
11	500	500	500	500	500	500	470	460	430	400	375	350	350	350	340	330	250	250	200	200	200	225	225	225	200
10	500	500	500	500	500	500	490	450	450	450	400	400	400	400	400	370	300	300	250	225	225	250	250	250	200
9	500	500	500	500	500	500	500	400	430	430	400	425	430	450	450	450	400	350	330	300	275	250	250	250	200
8	500	500	500	500	500	500	400	350	350	400	450	450	430	475	470	450	400	370	350	325	300	300	300	300	250
7	500	500	500	500	500	500	400	350	350	350	400	490	490	490	480	475	450	400	400	375	350	325	325	325	300
6	500	500	500	500	500	500	500	500	500	500	400	350	400	500	500	500	500	500	450	425	400	375	350	350	350
5	500	500	500	500	500	500	500	500	500	500	500	500	500	500	500	500	500	490	490	400	450	425	400	375	350
4	500	500	500	500	500	500	500	500	500	500	500	500	500	500	500	500	500	490	490	400	460	425	400	400	400
3	500	500	500	500	500	500	500	500	500	500	500	500	500	500	500	500	500	500	500	500	500	480	450	425	400
2	500	500	500	500	500	500	500	500	500	500	500	500	500	500	500	500	500	500	500	500	500	500	400	350	350
1	500	500	500	500	500	500	500	500	500	500	500	500	500	500	500	500	500	500	500	500	500	500	500	500	500

(b) 3:00 p.m.

[illegible]

of the changes in the flow field at two levels on the grid: near the surface and at the top of the modeling region (i.e.,  $k = 1$  and  $k = 5$ )\*. The results of these simulations are presented in Tables 16 through 23. Table 24 summarizes the nature of the inputs and the treatment of the parameters in the wind algorithms corresponding to each table. The predicted changes in wind speed and direction given in these tables are defined as follows:

$$\Delta S = (u^2 + v^2)^{1/2} - (u_0^2 + v_0^2)^{1/2} ,$$

$$\Delta \theta = 57.2958 \left[ \tan^{-1}\left(\frac{u}{v}\right) - \tan^{-1}\left(\frac{u_0}{v_0}\right) \right] ,$$

where  $\Delta S$  and  $\Delta \theta$  are the reported changes in wind speed and direction, respectively.

### 3. Discussion of the Results

Reviewing Tables 16 through 23, we note that wind speed and direction are altered by no more than about 11 mph and  $93^\circ$ , respectively. To place some perspective on these results, we must consider the magnitude of the errors associated with the input wind fields themselves. Typically, the uncertainties in the wind fields employed in airshed simulations are on the order of 2 mph in speed and  $60^\circ$  in direction. For the most part, the predicted perturbations in wind direction are smaller than  $60^\circ$ . However, significant alterations in the wind speed are predicted for the 3 p.m. wind inputs. These predictions are the result of generally higher wind speeds and a greater degree of convergence and divergence in the interpolated wind field.

---

\* Since  $u_0$  and  $v_0$  are considered to be independent of  $z$ , the perturbations calculated using Eq. (26) are the same in each layer of grid cells. Thus, the change in speed and direction is reported only for the bottom layer of cells (i.e.,  $k = 1$ ).



Table 16  
PREDICTED CHANGES IN WIND SPEED AND DIRECTION FOR CASE 1\*  
(a) Wind Speed

	1	2	3	4	5	6	7	8	9	10	11	12	13	14	15	16	17	18	19	20	21	22	23	24	25
25	-0.0	-1.1	-0.0	-0.0	-1.2	-1.0	-0.5	-0.7	-0.3	-0.2	-0.2	-0.1	-0.1	-0.1	-0.2	-0.2	-0.0	-0.3	-0.5	-0.4	-0.4	-0.0	-0.3	0.0	0.0
24	-0.0	-0.0	-0.5	-0.9	-1.1	-0.9	-0.9	-0.6	-0.3	-0.2	-0.2	0.0	-0.0	-0.1	-0.2	-0.2	-0.3	-0.3	-0.2	-0.5	-0.4	-0.0	-0.0	0.1	0.1
23	-0.0	-0.1	-0.0	-1.0	-0.7	-1.1	-0.0	-0.5	-0.1	0.0	0.4	0.0	0.2	-0.0	-0.2	-0.3	-0.5	-0.0	-0.0	-0.0	-0.0	-0.0	-0.1	0.2	0.4
22	0.0	0.1	-0.9	-0.9	-0.0	-1.2	-0.8	-0.5	0.0	0.0	0.7	0.7	0.6	0.0	-0.2	-0.1	-0.4	-0.7	-0.6	-0.8	-0.4	-0.3	-0.4	-0.0	0.2
21	0.2	-0.0	-0.4	-1.2	-1.1	-0.9	-0.0	0.3	0.5	0.7	0.0	0.9	0.3	0.2	0.1	-0.2	-0.6	-1.1	-1.1	-0.7	-0.0	-0.7	-0.4	-0.0	0.2
20	0.0	-0.1	-0.2	-0.0	-0.7	-0.5	-0.2	0.0	1.0	0.0	0.0	0.0	0.1	0.1	0.3	0.2	-0.5	-1.3	-1.4	-1.1	-1.2	-0.9	-0.7	-0.4	0.0
19	0.1	0.1	-0.1	-0.2	-0.2	-0.1	0.3	0.5	-0.3	-0.0	-0.3	-0.3	-0.3	-0.0	-1.2	-1.8	-2.3	-2.1	-1.6	-1.0	-0.0	-0.6	-0.2	0.1	0.1
18	0.1	0.0	-0.0	-0.1	-0.1	0.1	0.4	-0.4	-0.3	-0.4	-0.0	-0.7	-0.9	-1.7	-2.1	-2.0	-2.6	-2.0	-1.2	-1.0	-0.5	-0.4	-0.1	0.0	0.0
17	0.0	0.0	-0.0	-0.1	-0.1	0.0	0.0	-0.3	-0.0	-0.7	-1.0	-1.2	-1.3	-1.0	-1.9	-2.5	-2.3	-1.5	-1.1	-0.0	-0.4	-0.4	0.0	0.1	0.0
16	0.0	-0.0	-0.1	-0.1	-0.0	0.1	0.2	-0.5	-0.4	-1.1	-0.9	-0.0	-1.7	-1.7	-1.0	-1.9	-1.0	-1.1	-0.0	-0.0	0.3	-0.1	0.1	-0.0	-0.0
15	-0.0	-0.0	-0.1	-0.1	-0.1	-0.1	-0.0	0.0	-0.9	-0.7	-0.0	-0.0	-1.3	-1.2	-1.3	-1.0	-1.2	-0.6	-0.5	0.0	0.2	0.0	-0.0	-0.1	-0.0
14	-0.0	-0.1	-0.1	-0.2	-0.2	-0.0	0.3	-0.4	-0.6	-0.6	-0.4	-0.9	-1.4	-1.0	-1.1	-1.3	-0.6	-0.7	0.2	0.2	0.6	0.2	-0.0	-0.0	0.0
13	-0.0	-0.1	-0.1	-0.2	-0.1	0.1	0.1	-0.4	-0.7	-0.5	-1.3	-1.2	-1.2	-0.6	-1.1	-0.6	-0.1	-0.3	0.6	0.7	0.1	-0.1	0.1	0.0	0.0
12	-0.0	-0.1	-0.1	-0.2	-0.1	-0.1	0.1	-0.0	-0.4	-0.7	-1.1	-1.6	-1.4	-0.7	-1.1	-0.6	-0.7	-0.1	-0.5	0.2	0.8	0.4	0.1	0.0	0.0
11	-0.0	-0.1	-0.1	-0.1	-0.1	-0.1	-0.0	0.1	-0.5	-0.9	-1.4	-1.1	-0.7	-0.7	-0.7	-0.0	-0.7	-1.0	-0.5	0.2	0.7	0.3	0.1	0.1	0.0
10	-0.0	-0.1	-0.1	-0.1	-0.2	-0.1	-0.1	0.1	-0.0	-0.6	-1.4	-0.4	-0.2	-0.9	-0.7	-0.5	-0.4	-0.4	0.0	0.0	0.0	0.3	0.0	-0.0	0.0
9	-0.0	-0.1	-0.1	-0.2	-0.2	-0.2	-0.2	-0.1	-0.6	-0.0	-0.0	-0.6	-0.0	-0.6	-0.4	-0.2	-0.1	0.1	0.4	0.2	0.0	0.2	0.0	-0.1	0.0
8	-0.0	-0.1	-0.1	-0.2	-0.2	-0.3	-0.2	-0.3	-0.4	-0.4	-0.7	-0.6	-0.9	-0.7	-0.5	-0.4	-0.0	0.0	0.0	0.2	0.1	0.1	-0.0	-0.0	-0.0
7	-0.0	-0.1	-0.1	-0.2	-0.3	-0.3	-0.3	-0.3	-0.3	-0.4	-0.5	-0.9	-0.0	-0.4	-0.2	0.2	0.3	0.1	-0.0	-0.0	0.0	0.0	0.0	0.0	0.0
6	-0.0	-0.1	-0.1	-0.2	-0.2	-0.3	-0.3	-0.3	-0.3	-0.4	-0.6	-0.6	-0.9	-0.0	-0.2	-0.0	0.1	0.2	0.1	-0.0	-0.0	-0.0	0.0	0.0	0.0
5	-0.0	-0.1	-0.1	-0.2	-0.2	-0.2	-0.3	-0.3	-0.3	-0.4	-0.5	-0.6	-0.5	-0.4	-0.2	-0.0	0.0	0.1	-0.0	-0.1	-0.1	-0.1	-0.0	0.0	0.0
4	-0.0	-0.1	-0.1	-0.2	-0.2	-0.2	-0.3	-0.3	-0.3	-0.4	-0.4	-0.5	-0.4	-0.3	-0.2	-0.1	-0.0	0.0	-0.0	-0.1	-0.1	-0.1	-0.0	0.0	0.0
3	-0.0	-0.1	-0.1	-0.1	-0.2	-0.2	-0.0	-0.3	-0.3	-0.4	-0.4	-0.4	-0.4	-0.3	-0.2	-0.1	-0.0	-0.1	-0.2	-0.2	-0.1	-0.0	0.0	0.0	0.0
2	-0.0	-0.1	-0.1	-0.1	-0.2	-0.2	-0.0	-0.3	-0.3	-0.4	-0.4	-0.4	-0.3	-0.3	-0.2	-0.1	-0.1	-0.1	-0.2	-0.2	-0.2	-0.0	0.0	0.0	0.0
1	-0.0	-0.0	-0.1	-0.1	-0.2	-0.2	-0.0	-0.3	-0.3	-0.4	-0.4	-0.4	-0.3	-0.3	-0.2	-0.2	-0.1	-0.1	-0.2	-0.3	-0.2	-0.1	0.0	0.0	0.0

(b) Wind Direction

	1	2	3	4	5	6	7	8	9	10	11	12	13	14	15	16	17	18	19	20	21	22	23	24	25
25	-2	-2	4	10	19	23	21	20	14	10	9	5	7	9	13	16	20	22	22	23	23	22	11	2	-0
24	0	1	5	10	23	32	30	30	24	17	10	7	8	9	13	16	21	24	24	25	26	30	10	6	2
23	2	2	0	10	22	31	29	30	20	26	22	16	14	13	14	15	17	10	10	16	17	24	22	14	10
22	-1	-1	-2	5	15	26	27	26	25	26	28	26	26	23	19	19	21	20	14	14	16	15	16	13	11
21	-13	-14	-11	-3	1	15	24	24	27	28	29	32	39	39	30	42	40	32	25	19	15	15	15	13	14
20	-21	-22	-21	-11	6	19	27	20	31	29	26	30	33	38	30	34	34	31	23	16	19	10	21	24	21
19	-18	-20	-21	-14	1	12	22	20	10	10	20	21	22	27	21	17	15	9	6	8	7	11	15	10	16
18	-12	-12	-11	-10	-7	-2	3	6	6	8	10	7	7	10	5	2	2	-0	-1	-0	2	5	9	11	9
17	-4	-4	-4	-4	-5	-7	-5	0	0	1	0	-1	-3	-2	-7	-12	-12	-11	-0	-4	-1	3	5	6	3
16	-0	-0	-1	-1	-1	-5	-8	-4	-2	-3	-2	-2	-2	-7	-11	-13	-10	-17	-13	-10	-4	1	2	-1	-1
15	2	0	0	-1	-2	-5	-7	-3	-2	-4	-1	-0	1	-0	-4	-7	-15	-10	-14	-12	-7	-4	-3	-4	-4
14	1	0	0	-0	-0	-0	-1	-1	-0	0	-0	0	0	-0	-1	-2	-0	-15	-17	-15	-11	-6	-6	-6	-5
13	0	0	0	0	1	1	-0	0	1	0	0	-0	-1	-2	-2	-0	-2	-8	-14	-19	-10	-12	-9	-8	-0
12	0	0	0	0	1	0	-1	0	2	0	-1	-3	-4	-5	-5	-6	-0	-3	-6	-14	-16	-14	-13	-11	-11
11	-0	-0	0	0	1	1	-0	0	1	1	2	1	1	-0	-2	-6	-10	-16	-22	-13	-11	-9	-10	-12	-13
10	0	0	0	1	0	-0	-1	-2	-3	0	9	7	5	1	-2	-1	-4	-7	-8	-8	-8	-0	-11	-14	-14
9	0	0	0	0	-0	-2	-4	-6	-3	3	11	10	7	8	6	3	1	6	3	-8	-6	-9	-10	-9	-11
8	-0	-0	-0	-0	-1	-3	-4	-6	-2	4	10	11	8	4	3	1	-4	-2	-5	7	2	-3	-5	-4	-5
7	-1	-1	-1	-1	-1	-0	-0	-3	-3	-0	6	9	11	8	7	5	-0	-1	-0	-7	-10	-0	-7	-4	-4
6	-2	-2	-2	-2	-1	-0	0	-1	-2	-2	1	7	14	17	10	8	1	0	2	2	1	-1	-3	-4	-4
5	-2	-2	-2	-1	-1	-0	0	0	0	-1	0	6	13	15	16	11	5	0	-1	-2	-2	-3	-4	-4	-4
4	-1	-1	-1	-1	-0	-0	0	0	0	0	2	6	9	12	13	10	9	6	4	1	-1	-7	-5	-4	-4
3	-1	-0	-0	-0	-0	-0	0	0	1	3	8	5	7	0	9	8	7	7	6	6	-2	-0	-4	-4	-1
2	-0	-0	-0	-0	-0	0	0	1	1	2	0	4	5	6	6	5	4	0	2	2	3	-1	-3	-3	-3
1	-0	-0	-0	0	0	0	1	1	2	5	8	4	4	4	4	3	2	2	1	2	1	-0	-0	-1	-1

\* See Table 24 for a description of the experimental conditions.

Table 17  
 PREDICTED CHANGES IN WIND SPEED AND DIRECTION FOR CASE 2\*  
 (a) Wind Speed

	1	2	3	4	5	6	7	8	9	10	11	12	13	14	15	16	17	18	19	20	21	22	23	24	25
25	-0.0	.1	-.2	-.2	-.5	-.9	-.2	-.3	-.1	-.1	-.1	-.0	-.0	-.1	-.1	-.1	-.2	-.2	-.3	-.2	-.2	-.3	-.2	-.1	-.1
24	-0.0	.1	-.2	-.3	-.4	-.4	-.4	-.8	-.1	-.1	-.1	.0	-.0	-.0	-.1	-.1	-.2	-.1	.0	-.2	-.1	-.5	-.1	-.1	.0
23	-0.0	.1	-.2	-.4	-.1	-.0	-.3	-.3	-.2	.2	.2	.1	.1	-.0	-.1	-.1	-.2	-.4	-.4	-.2	-.4	-.1	-.1	.1	.1
22	.0	.2	-.5	-.3	-.1	-.6	-.3	-.4	.2	.2	.2	.2	.2	-.0	-.1	.0	-.1	-.3	-.2	-.4	-.2	-.1	-.3	-.0	.0
21	.1	-.0	-.0	-.6	-.4	-.4	-.5	.2	.0	.2	.2	.3	-.1	-.0	-.0	-.2	-.3	-.5	-.5	-.2	-.4	-.3	-.2	-.0	.0
20	.2	-.1	.0	-.4	-.2	-.2	-.2	.4	.0	-.1	.2	-.1	-.1	.1	.1	-.2	-.6	-.6	-.3	-.5	-.4	-.3	-.2	-.0	.0
19	.0	.0	-.0	-.1	-.1	-.0	.1	.3	-.3	.0	-.2	-.1	-.1	-.4	-.3	-.7	-.0	-.0	-.6	-.2	-.3	-.2	-.1	-.0	.0
18	.0	.0	-.0	-.0	-.0	.0	.3	-.3	-.0	-.2	-.3	-.2	-.7	-.7	-.7	-.5	-.0	-.7	-.3	-.4	-.1	-.1	-.0	-.0	.0
17	.0	.0	-.0	-.0	-.1	.3	.0	-.1	-.2	-.2	-.4	-.0	-.4	-.6	-.6	-.9	-.9	-.4	-.5	-.1	-.1	-.3	.3	.0	-.0
16	.0	-.0	-.0	-.0	-.0	.0	.2	-.4	.0	-.0	-.3	-.1	-.0	-.6	-.7	-.7	-.7	-.4	-.1	-.4	.3	-.1	.1	-.0	-.0
15	-.0	-.0	-.0	-.0	-.0	-.0	.0	-.5	-.2	-.3	-.2	-.4	-.4	-.4	-.5	-.4	-.2	-.4	.3	-.0	.2	-.0	-.0	-.0	-.0
14	-.0	-.0	-.0	-.1	-.1	-.0	.2	-.2	-.3	-.2	-.0	-.3	-.6	-.2	-.4	-.5	-.1	-.5	.2	-.1	.3	.1	-.0	-.0	-.0
13	-.0	-.0	-.1	-.1	-.0	.1	.1	-.2	-.4	-.0	-.6	-.4	-.0	-.0	-.5	-.1	.1	-.3	.3	.3	-.1	-.1	.1	.0	.0
12	-.0	-.0	-.0	-.1	-.0	-.0	.1	.1	-.2	-.3	-.4	-.7	-.7	-.1	-.6	-.1	-.4	.1	-.3	.0	.4	.1	.0	.0	.0
11	-.0	-.0	-.0	-.0	-.0	-.0	.2	-.2	-.3	-.6	-.3	-.2	-.2	-.2	-.3	-.3	-.7	-.3	-.1	.4	.1	.0	.0	.0	.0
10	-.0	-.0	-.0	-.0	-.1	-.0	.2	-.4	-.0	-.8	.1	.1	-.4	-.2	-.1	-.1	-.2	.2	.1	.3	.1	.0	-.0	-.0	-.0
9	-.0	-.0	-.0	-.1	-.1	-.1	.0	-.3	-.1	-.3	-.2	-.2	-.2	-.1	.0	.0	.0	.2	-.0	.2	.1	-.0	-.0	-.0	-.0
8	-.0	-.0	-.0	-.1	-.1	-.1	-.1	-.1	-.0	-.3	-.1	-.4	-.3	-.2	-.2	.0	.1	.2	.0	.1	.0	-.0	-.0	-.0	-.0
7	-.0	-.0	-.0	-.1	-.1	-.1	-.1	-.1	-.1	-.1	-.1	-.4	-.3	-.2	-.1	-.1	.2	.1	.0	-.1	-.1	-.0	-.0	-.0	-.0
6	-.0	-.0	-.0	-.1	-.1	-.1	-.1	-.1	-.1	-.1	-.2	-.1	-.5	-.1	-.0	-.0	.0	.1	.0	.0	.0	.0	.0	.0	.0
5	-.0	-.0	-.0	-.1	-.1	-.1	-.1	-.1	-.1	-.1	-.2	-.2	-.2	-.1	-.1	-.0	.0	.0	-.0	-.0	-.0	-.0	-.0	-.0	.0
4	-.0	-.0	-.0	-.1	-.1	-.1	-.1	-.1	-.1	-.1	-.1	-.2	-.1	-.1	-.1	-.0	-.0	.0	.0	-.0	-.0	-.0	-.0	.0	.0
3	-.0	-.0	-.0	-.0	-.1	-.1	-.1	-.1	-.1	-.1	-.1	-.1	-.1	-.1	-.1	-.0	-.0	-.0	-.1	-.1	-.1	-.0	.0	.0	.0
2	-.0	-.0	-.0	-.0	-.1	-.1	-.1	-.1	-.1	-.1	-.1	-.1	-.1	-.1	-.1	-.0	-.0	-.0	-.1	-.1	-.1	-.0	.0	.0	.0
1	-.0	-.0	-.0	-.0	-.1	-.1	-.1	-.1	-.1	-.1	-.1	-.1	-.1	-.1	-.1	-.1	-.1	-.0	-.0	-.1	-.1	-.1	-.0	.0	.0

(b) Wind Direction

	1	2	3	4	5	6	7	8	9	10	11	12	13	14	15	16	17	18	19	20	21	22	23	24	25
25	-2	-3	-0	0	3	7	9	6	2	2	3	6	2	3	4	4	6	5	6	6	5	6	2	0	-0
24	0	0	2	2	5	10	7	9	6	5	8	1	2	2	4	3	0	0	7	9	7	0	4	1	-0
23	1	1	-0	3	4	9	7	9	0	8	9	0	5	4	4	2	4	4	4	8	4	8	0	6	4
22	0	1	0	1	3	7	6	7	7	9	11	10	11	7	6	6	7	7	3	3	5	3	4	3	3
21	-3	-3	-3	-1	-1	2	7	6	7	10	11	11	12	13	11	11	12	11	0	7	4	3	4	4	5
20	-7	-7	-5	-2	2	5	11	11	16	13	8	10	11	14	12	9	9	0	4	3	8	7	0	10	5
19	-6	-7	-7	-3	2	7	11	7	6	5	7	6	5	0	2	1	2	0	1	4	2	3	5	6	5
18	-5	-4	-3	-3	-1	-0	0	1	1	2	4	1	0	2	0	0	1	0	-0	-0	0	1	3	3	7
17	-1	-1	-1	-1	-1	-2	-1	1	0	0	0	-1	-1	-0	-2	-3	-1	-2	-2	-0	-0	1	1	2	0
16	-0	-0	-0	-0	0	-1	-2	-0	-1	-1	-0	-1	-0	-4	-4	-3	-4	-4	-4	-3	-1	1	0	-0	-0
15	1	0	-0	-0	-1	-2	-3	-2	-0	-2	0	-0	2	1	-0	-1	-4	-5	-4	-3	-2	-2	-1	-1	-1
14	0	0	-0	-0	-0	-0	-0	-0	-0	0	0	0	0	0	0	-0	-2	-5	-6	-6	-4	-1	-1	-2	-1
13	-0	0	0	0	0	0	-0	0	0	-1	-0	0	-0	-0	-0	1	0	-1	-3	-6	-7	-4	-2	-2	-2
12	0	0	0	0	0	0	-0	0	0	-0	-1	-2	-2	-3	-3	-3	-3	2	2	-4	-6	-5	-5	-4	-4
11	-0	-0	0	0	0	0	0	0	1	0	1	0	0	-0	-1	-3	-5	-0	-13	-5	-4	-2	-3	-4	-4
10	0	0	0	0	0	0	0	-0	-0	-0	4	3	3	2	0	-1	0	-0	-1	-2	-3	-3	-2	-3	-4
9	0	0	0	0	-0	-0	-1	-2	-0	0	4	2	2	3	3	2	1	6	2	-2	-4	-4	-4	-3	-4
8	-0	-0	0	0	-0	-0	-1	-1	-0	1	3	3	2	0	0	0	-3	-2	-5	7	3	-0	-0	-1	-1
7	-0	-0	-0	-0	-0	-0	-0	-0	-0	1	2	4	1	2	2	-0	-0	-0	-6	-7	-4	-3	-1	-1	-1
6	-1	-1	-1	-1	-0	-0	-0	-0	-1	-0	0	2	4	6	1	3	-0	-0	2	3	1	0	-1	-1	-1
5	-0	-0	-0	-0	-0	-0	0	0	0	0	1	4	4	6	4	1	-0	-2	-2	-1	-0	-1	-1	-1	-1
4	-0	-0	-0	-0	-0	0	0	0	0	0	1	2	3	4	3	4	3	1	0	-0	-4	-2	-1	-1	-1
3	-0	-0	-0	-0	-0	0	0	0	0	1	1	2	2	2	2	2	3	3	3	-2	1	-1	-1	-1	-1
2	-0	-0	-0	-0	0	0	0	0	0	1	1	1	1	2	2	1	0	-0	-0	2	-0	-1	-1	-1	-1
1	-0	-0	-0	0	0	0	0	0	0	1	1	1	1	1	1	0	0	0	0	0	-0	-0	-0	-0	-0

\* See Table 24 for a description of the experimental conditions.

Table 18  
 PREDICTED CHANGES IN WIND SPEED AND DIRECTION FOR CASE 3\*  
 (a) Wind Speed

	1	2	3	4	5	6	7	8	9	10	11	12	13	14	15	16	17	18	19	20	21	22	23	24	25
25	-0.0	-0.2	-0.8	-1.2	-1.7	-1.9	-1.1	-0.8	-0.4	-0.4	-0.0	-0.2	-0.2	-0.2	-0.2	-0.3	-0.3	-0.4	-0.4	-0.4	-0.4	-0.7	-0.4	-0.1	-0.1
24	-0.0	-0.2	-0.9	-1.5	-1.6	-1.0	-0.9	-0.6	-0.2	-0.2	-0.2	0.0	-0.0	-0.1	-0.2	-0.3	-0.4	-0.3	-0.2	-0.5	-0.4	-0.6	-0.2	-0.4	-0.3
23	-0.0	-0.2	-1.0	-1.6	-1.0	-1.2	-0.8	-0.4	0.2	0.0	0.7	0.6	0.4	0.0	-0.2	-0.4	-0.6	-1.0	-1.0	-0.8	-1.0	-0.3	-0.1	-0.3	0.0
22	0.0	-0.6	-1.2	-1.5	-1.3	-1.5	-0.9	-0.3	1.1	1.5	1.4	1.4	1.1	0.2	-0.1	-0.2	-0.5	-0.9	-0.9	-1.1	-0.6	-0.4	-0.4	-0.1	-0.3
21	0.3	-0.0	-0.6	-1.0	-1.0	-1.3	-0.8	0.6	1.1	1.4	1.0	1.0	0.9	0.0	0.0	0.3	-0.1	-0.8	-1.1	-0.9	-1.0	-0.9	-0.0	-0.1	-0.0
20	0.0	0.0	-0.2	-1.2	-1.2	-0.6	-0.1	1.2	1.0	0.6	1.1	0.6	0.6	0.0	0.0	-0.3	-1.2	-1.0	-1.4	-1.6	-1.3	-1.1	-0.5	-0.4	0.0
19	0.3	0.2	-0.0	-0.3	-0.4	-0.1	0.0	0.0	-0.2	-0.0	-0.3	-0.3	-0.3	-0.9	-1.5	-2.5	-3.3	-3.3	-2.6	-1.6	-1.3	-0.9	-0.2	-0.4	-0.4
18	0.2	0.1	-0.0	-0.1	-0.1	0.1	0.4	0.0	-0.0	-0.7	-1.1	-1.2	-1.5	-2.7	-3.3	-3.5	-4.1	-3.3	-2.1	-1.6	-0.0	-0.6	-0.1	-0.2	-0.1
17	0.1	0.0	-0.1	-0.1	-0.1	0.5	0.1	-0.4	-0.8	-1.1	-1.6	-1.9	-2.2	-2.9	-3.2	-3.8	-3.5	-2.4	-1.8	-0.9	-0.6	-0.5	-0.4	-0.2	-0.0
16	0.0	-0.0	-0.1	-0.1	-0.1	0.1	0.3	-0.7	-0.7	-1.7	-1.5	-1.4	-2.5	-2.7	-2.0	-2.9	-2.5	-1.6	-0.0	-0.6	0.3	-0.0	0.1	-0.0	-0.0
15	-0.0	-0.1	-0.1	-0.2	-0.2	-0.1	-0.0	-0.1	-1.3	-1.3	-1.0	-1.4	-2.1	-2.1	-2.2	-2.3	-1.7	-0.7	-0.6	0.0	0.4	0.4	-0.1	-0.1	-0.0
14	-0.0	-0.1	-0.2	-0.3	-0.3	-0.0	0.3	-0.6	-1.0	-1.0	-0.9	-1.4	-2.2	-1.0	-1.9	-2.0	-1.2	-0.8	0.3	0.0	0.4	0.4	-0.1	-0.1	0.0
13	-0.0	-0.2	-0.3	-0.3	-0.2	0.1	0.0	-0.6	-0.7	-1.1	-1.0	-2.0	-2.0	-1.9	-1.2	-1.7	-1.1	-0.3	-0.2	1.0	1.1	0.0	-0.1	-0.2	-0.1
12	-0.0	-0.1	-0.2	-0.3	-0.2	-0.1	0.0	-0.1	-0.7	-1.2	-1.0	-2.4	-2.1	-1.2	-1.6	-1.0	-1.1	-0.3	-0.6	0.4	1.2	0.6	0.2	-0.1	-0.1
11	-0.0	-0.1	-0.2	-0.2	-0.2	-0.2	-0.1	0.1	-0.8	-1.5	-2.2	-1.0	-1.3	-1.1	-1.2	-1.2	-1.0	-1.2	-0.3	0.4	1.1	0.6	0.2	0.2	-0.1
10	-0.0	-0.1	-0.2	-0.2	-0.3	-0.2	-0.1	-0.1	-1.1	-1.2	-2.0	-0.0	-0.6	-1.3	-1.1	-0.0	-0.6	-0.6	0.4	0.8	0.9	0.5	0.1	0.0	-0.1
9	-0.0	-0.1	-0.2	-0.3	-0.3	-0.3	-0.3	-0.9	-0.9	-1.2	-1.0	-1.0	-1.0	-0.7	-0.4	-0.2	0.1	0.6	0.4	0.7	0.4	0.0	-0.1	-0.0	0.0
8	-0.0	-0.1	-0.2	-0.3	-0.4	-0.5	-0.4	-0.6	-0.7	-1.1	-1.0	-1.4	-1.1	-0.8	-0.6	-0.0	0.1	0.5	0.3	0.2	0.1	-0.0	-0.1	-0.0	0.0
7	-0.0	-0.1	-0.2	-0.3	-0.4	-0.5	-0.5	-0.5	-0.6	-0.7	-0.9	-1.3	-1.2	-1.0	-0.6	-0.3	0.3	0.4	0.2	0.0	-0.0	-0.0	0.0	0.0	0.0
6	-0.0	-0.1	-0.2	-0.3	-0.4	-0.5	-0.5	-0.5	-0.5	-0.7	-1.0	-1.0	-1.3	-0.6	-0.2	0.0	0.2	0.2	0.1	-0.0	-0.0	0.0	0.1	0.1	0.1
5	-0.0	-0.1	-0.3	-0.3	-0.3	-0.4	-0.4	-0.5	-0.5	-0.7	-0.9	-0.9	-0.7	-0.0	-0.3	-0.1	0.1	0.1	0.0	-0.1	-0.1	-0.1	-0.0	0.0	0.0
4	-0.0	-0.1	-0.2	-0.3	-0.3	-0.4	-0.4	-0.5	-0.6	-0.7	-0.7	-0.6	-0.6	-0.0	-0.3	-0.2	-0.0	0.0	-0.0	-0.1	-0.2	-0.2	-0.0	0.0	0.0
3	-0.0	-0.1	-0.2	-0.2	-0.3	-0.4	-0.4	-0.5	-0.6	-0.6	-0.7	-0.7	-0.6	-0.5	-0.4	-0.2	-0.1	-0.1	-0.1	-0.3	-0.3	-0.2	-0.0	0.1	0.0
2	-0.0	-0.1	-0.2	-0.2	-0.3	-0.4	-0.4	-0.5	-0.6	-0.6	-0.6	-0.6	-0.6	-0.6	-0.4	-0.3	-0.2	-0.2	-0.2	-0.4	-0.4	-0.3	-0.1	0.1	0.1
1	-0.0	-0.1	-0.2	-0.2	-0.3	-0.4	-0.4	-0.5	-0.5	-0.6	-0.6	-0.6	-0.6	-0.6	-0.5	-0.0	-0.4	-0.3	-0.2	-0.2	-0.4	-0.4	-0.4	-0.1	0.1

(b) Wind Direction

	1	2	3	4	5	6	7	8	9	10	11	12	13	14	15	16	17	18	19	20	21	22	23	24	25
25	-2	-1	13	33	48	49	47	39	27	19	16	11	12	17	23	31	30	40	39	40	42	40	20	4	-3
24	0	2	11	36	61	61	60	54	42	30	10	13	14	16	23	30	37	41	42	44	47	53	01	10	4
23	5	4	1	35	59	61	57	51	46	40	32	24	32	22	25	30	33	36	37	33	35	41	35	22	15
22	-8	-5	-8	16	47	56	52	44	30	36	39	36	37	37	32	34	30	37	30	27	20	20	28	23	10
21	-22	-24	-24	-8	18	35	44	39	05	30	39	40	46	08	59	60	70	72	64	48	36	29	28	25	23
20	-32	-35	-40	-31	16	36	42	39	39	41	39	46	50	56	59	50	64	64	53	36	34	32	33	37	31
19	-20	-32	-35	-30	-1	19	30	30	31	31	33	37	42	51	58	52	45	30	17	15	14	21	26	29	25
18	-19	-19	-19	-17	-13	-4	6	11	13	16	19	16	19	20	30	20	4	-3	-3	-1	4	10	16	18	15
17	-6	-6	-7	-8	-9	-10	-8	-0	1	3	1	-1	-6	-7	-23	-45	-44	-20	-17	-9	-1	5	9	10	9
16	-0	-0	-1	-2	-3	-0	-13	-8	-5	-6	-4	-5	-6	-15	-24	-35	-43	-35	-25	-17	-7	2	8	-1	-2
15	2	1	-0	-1	-4	-7	-10	-7	-4	-6	-2	-1	0	-3	-10	-10	-31	-33	-26	-19	-12	-6	-5	-7	-7
14	2	1	0	-0	-0	-0	-1	-2	-1	6	0	0	0	-2	-4	-6	-18	-20	-27	-24	-17	-10	-11	-11	-10
13	0	0	0	1	1	1	-0	0	2	1	1	-1	-4	-5	-5	-3	-0	-16	-24	-29	-26	-20	-16	-14	-14
12	0	0	0	1	2	0	-1	1	3	1	-1	-0	-6	-8	-9	-11	-14	-9	-15	-22	-23	-21	-20	-18	-10
11	-0	0	1	1	2	1	-0	0	0	1	3	1	2	-0	-4	-10	-16	-24	-32	-19	-16	-14	-17	-20	-21
10	0	0	1	1	1	-0	-2	-5	-6	1	17	17	13	9	2	-3	-4	-0	-12	-13	-13	-13	-14	-19	-23
9	0	0	0	0	-1	-4	-0	-12	-6	7	22	22	16	14	10	4	1	6	3	-4	-9	-13	-15	-13	-17
8	-1	-1	-0	-1	-2	-5	-8	-10	-4	0	22	23	17	11	7	2	-5	-3	-5	7	1	-7	-9	-8	-9
7	-2	-2	-2	-2	-2	-0	-0	-0	-7	-0	14	22	23	17	13	8	0	-1	-1	-9	-12	-12	-11	-7	-6
6	-4	-4	-4	-4	-3	-0	1	-1	-4	-5	2	19	30	32	19	13	3	0	2	1	0	-3	-6	-7	-8
5	-3	-3	-3	-3	-2	-0	0	1	0	-3	1	14	27	29	27	19	9	1	-1	-3	-3	-5	-7	-7	-8
4	-2	-2	-2	-2	-1	-0	0	0	1	1	5	12	19	22	23	18	15	10	6	2	-2	-10	-0	-7	-7
3	-1	-1	-1	-1	-0	-0	0	1	2	5	7	11	14	16	16	15	12	11	10	8	-1	-2	-7	-7	-7
2	-0	-0	-0	-0	-0	0	1	2	5	5	7	9	11	12	12	10	7	5	4	4	5	-2	-5	-6	-3
1	-0	-0	-0	0	0	1	2	0	4	5	7	8	9	9	8	6	4	3	3	3	3	-0	-1	-2	-2

\*See Table 24 for a description of the experimental conditions.

Table 19  
PREDICTED CHANGES IN WIND SPEED AND DIRECTION FOR CASE 4\*

(a) Wind Speed

	1	2	3	4	5	6	7	8	9	10	11	12	13	14	15	16	17	18	19	20	21	22	23	24	25
25	.1	-.0	-.8	-.8	-.4	-.4	-.8	-.6	.1	1.0	1.2	1.6	1.6	1.8	.2	-.1	-.3	-.0	-.2	-.1	.0	-.0	.0	-.1	-.2
24	-.4	-.3	-.4	-.8	-.4	-.4	-.4	-.8	.3	.2	1.2	1.0	.9	.6	-.6	-1.0	-1.0	-.7	-1.0	-.9	-.9	-.4	-1.0	-1.0	-1.2
23	-.4	-.2	-.2	-.1	-.2	-.1	-.0	-.1	-.2	.7	.9	.9	.5	-.8	-1.0	-1.0	-2.2	-1.7	-1.7	-1.9	-1.6	-1.0	.4	-2.1	-2.4
22	-.1	.1	.2	.2	.2	.3	.4	.1	.4	.8	.8	.7	.8	-1.1	-1.4	-2.3	-2.8	-2.3	-2.3	-2.0	-2.0	-2.0	-2.4	-2.3	-2.6
21	.3	.2	.5	.8	.9	.9	.9	.8	.9	1.0	1.2	1.3	.1	-1.2	-1.6	-2.5	-3.2	-2.7	-3.0	-2.6	-2.4	-2.5	-2.0	-1.7	-2.2
20	.7	.6	1.0	1.4	1.6	1.7	1.8	2.0	1.8	1.7	2.1	1.8	1.1	-.4	-1.0	-2.2	-3.1	-2.4	-2.7	-2.5	-1.9	-1.7	-1.4	-1.0	-1.3
19	.6	.9	1.2	1.5	1.9	2.2	2.6	2.5	2.0	2.5	2.4	2.3	1.0	.6	-.9	-1.6	-2.7	-3.2	-2.2	-1.7	-1.5	-1.3	-1.0	-1.2	.4
18	.9	1.2	1.6	2.0	2.5	3.1	3.7	4.1	2.9	3.3	2.9	2.8	2.0	.3	-.9	-2.5	-3.1	-2.0	-1.3	-.8	-1.0	-.4	-.8	-.2	
17	1.3	1.8	2.3	2.8	3.6	4.5	5.6	5.4	4.1	4.0	3.5	3.3	4.1	4.3	2.2	.1	-1.0	-1.7	-1.0	-1.4	1.0	-1.0	-.1	-.2	-.2
16	1.2	2.1	1.9	2.5	3.4	4.2	5.1	4.8	5.0	5.1	4.6	4.3	5.3	4.4	4.2	2.3	.1	-.9	-1.3	-.7	-.0	.0	-.6	.2	.0
15	.9	1.2	1.3	2.6	2.8	3.9	4.3	5.4	4.5	4.7	4.2	4.2	4.1	5.1	4.5	2.7	.3	-.1	-.4	-1.0	-.5	.0	-.2	-.1	.0
14	-.0	.0	1.0	2.1	3.0	3.6	4.0	4.6	4.8	4.2	3.4	3.1	4.2	4.9	3.9	2.9	1.1	.2	.2	-.3	.1	-.1	-.1	.0	.1
13	-.8	.4	1.8	2.0	2.8	3.5	4.1	4.6	3.9	3.2	2.4	1.6	3.5	4.1	3.7	2.9	1.3	.5	-.2	.1	.6	.1	.0	-.1	.5
12	-.4	.2	.9	2.1	2.8	3.6	3.8	4.4	3.0	3.3	1.9	.2	1.0	2.7	2.7	2.3	1.7	.1	.3	.2	.2	.0	.0	.5	.3
11	-.3	.3	.0	1.9	2.6	3.4	4.3	4.1	3.8	3.1	2.4	.5	.7	2.0	2.5	1.7	1.9	.0	.2	.5	.3	.0	.9	.9	.4
10	-.8	.5	1.0	1.6	2.3	3.1	3.8	4.4	4.0	3.5	2.0	1.1	.4	1.6	2.0	2.3	1.2	.4	.2	.9	.5	.7	.4	.4	.4
9	-.2	.3	.9	1.5	2.1	2.9	3.7	4.0	4.1	3.4	2.6	1.9	-.0	1.0	1.7	1.0	1.0	.0	.3	.0	1.0	.7	.6	.5	.0
8	-.1	.3	.8	1.4	1.9	2.5	3.4	4.4	4.3	3.3	3.1	1.9	.0	1.1	1.0	1.7	1.0	1.1	.5	.1	.6	.9	.7	.0	.5
7	-.0	.3	.5	1.0	1.0	2.3	2.9	3.8	3.7	3.1	2.7	2.0	.7	1.2	1.0	1.0	1.0	1.3	.5	.0	.2	.6	.4	.7	.6
6	.0	.3	.5	1.2	1.0	2.0	2.5	3.2	3.4	2.9	2.1	1.0	.9	1.1	1.4	1.6	1.4	.9	.9	.0	.4	.3	.6	.5	.4
5	.1	.8	.7	1.1	1.5	1.0	2.1	2.5	2.6	2.4	2.0	1.0	.9	1.0	1.4	1.3	1.9	1.1	.8	.6	.9	.3	.1	.0	.4
4	.1	.9	.7	1.0	1.3	1.6	1.7	2.2	2.5	2.2	1.0	1.3	.7	1.1	1.1	1.3	1.1	1.0	.8	.6	.4	.3	.2	.1	.4
3	.1	.8	.6	.9	1.0	1.6	1.0	1.0	2.4	2.1	1.7	1.3	.8	.8	1.1	.9	.9	.8	.6	.4	.3	.2	.2	.2	.2
2	.4	.3	.9	.9	.9	1.4	1.2	1.9	1.6	2.1	1.7	1.3	1.0	.8	.8	.8	.7	.6	.5	.3	.1	.1	.1	.1	.1
1	.0	.1	.0	.0	1.1	1.0	1.7	1.4	2.0	1.7	1.5	1.2	.9	.8	.0	.7	.6	.5	.4	.2	.1	-.0	-.0	-.0	.0

(b) Wind Direction

	1	2	3	4	5	6	7	8	9	10	11	12	13	14	15	16	17	18	19	20	21	22	23	24	25
25	-1	1	1	1	0	0	0	0	2	5	7	9	14	20	9	2	-2	-4	-3	-2	-0	1	3	3	1
24	-8	-7	-2	-0	1	2	3	5	8	9	12	17	32	25	15	8	1	1	1	1	3	5	10	6	5
23	-9	-12	-5	-3	0	2	6	10	9	20	26	39	42	34	20	17	9	7	7	1	7	17	12	14	14
22	-4	-5	-9	-4	1	5	9	15	19	20	35	42	47	30	35	24	15	14	11	11	14	17	25	22	23
21	1	0	-2	-3	0	6	11	21	23	33	43	46	49	41	35	26	16	18	15	16	19	23	27	20	21
20	23	21	20	18	15	16	17	21	29	34	40	46	40	33	29	23	17	16	13	15	21	22	23	23	22
19	36	35	33	33	31	31	32	36	36	39	45	30	34	27	26	22	15	11	12	17	20	21	22	16	17
18	39	37	36	34	32	32	32	35	42	44	37	32	25	22	20	17	11	9	13	13	18	10	10	8	9
17	45	43	39	30	30	30	43	42	33	31	25	18	10	16	12	9	4	4	3	3	2	1	0	1	3
16	40	44	37	36	39	39	37	32	27	22	19	15	12	9	5	8	-1	-5	-4	-2	-0	-2	-8	0	-0
15	38	35	32	34	33	30	26	25	21	18	13	8	7	4	1	-2	-8	-11	-0	-6	-3	-1	-3	-1	-2
14	32	30	29	29	27	26	24	22	19	15	10	5	2	0	-3	-5	-11	-13	-14	-13	-7	-7	-6	-6	-4
13	26	24	25	25	23	22	20	19	16	13	9	3	1	-0	-3	-7	-11	-14	-15	-14	-12	-12	-11	-10	-10
12	22	23	22	19	18	18	17	16	13	12	8	4	3	1	-3	-6	-10	-14	-15	-14	-13	-14	-14	-12	-12
11	17	17	17	16	13	13	13	13	11	9	6	2	2	-1	-4	-8	-10	-13	-14	-13	-14	-13	-13	-12	-12
10	13	13	12	11	12	11	10	9	8	6	3	-0	-5	-4	-7	-12	-15	-15	-15	-15	-15	-13	-13	-13	-13
9	9	10	9	11	9	9	9	8	6	1	-1	-4	-9	-9	-11	-12	-15	-15	-16	-16	-16	-15	-15	-15	-16
8	7	7	7	7	8	6	4	2	-0	-4	-9	-12	-12	-11	-12	-13	-15	-15	-15	-14	-14	-15	-17	-17	-16
7	4	4	4	4	3	3	1	-0	-3	-7	-10	-12	-13	-12	-12	-13	-14	-15	-14	-12	-13	-14	-15	-15	-16
6	2	3	3	2	1	-0	-1	-3	-6	-7	-9	-11	-13	-12	-11	-11	-11	-12	-12	-11	-11	-11	-12	-13	-14
5	0	0	0	0	-0	-0	-1	-2	-4	-5	-7	-9	-10	-9	-9	-9	-10	-10	-10	-10	-11	-10	-11	-12	-13
4	-1	-0	-0	-0	-1	-0	-1	-2	-3	-4	-5	-6	-7	-6	-5	-6	-7	-8	-9	-10	-11	-12	-12	-12	-13
3	-1	-1	-1	-0	-0	-0	-1	-1	-2	-3	-3	-4	-4	-2	-3	-3	-4	-5	-6	-7	-8	-9	-9	-9	-9
2	-0	-0	0	0	0	0	0	0	0	0	-1	-1	-1	-0	-0	-0	-1	-1	-2	-3	-3	-4	-5	-5	-6
1	-0	-0	0	1	1	1	2	2	3	3	2	2	1	1	1	1	1	0	0	-0	-0	-1	-1	-1	-1

\*See Table 24 for a description of the experimental conditions;

Table 20  
 PREDICTED CHANGES IN WIND SPEED AND DIRECTION FOR CASE 5\*  
 (a) Wind Speed

	1	2	3	4	5	6	7	8	9	10	11	12	13	14	15	16	17	18	19	20	21	22	23	24	25
25	.2	.0	-.1	-.1	-.2	-.2	-.2	-.4	.6	.5	.4	.5	.4	.4	.0	.0	-.0	-.2	.1	.1	.1	-.1	.0	-.0	-.1
24	-.2	-.1	-.2	-.1	-.2	-.1	-.1	-.4	.2	-.1	.5	.2	.2	.0	-.3	-.4	-.5	-.1	-.3	-.3	-.5	-.1	-.1	-.3	-.4
23	-.2	-.1	-.1	-.0	-.1	-.0	-.0	-.0	-.3	.3	-.2	.2	.1	-.5	-.3	-.6	-.0	-.0	-.6	-.8	-.6	-.7	1.1	-.9	-1.3
22	-.0	.1	.0	.1	.0	.1	.1	-.1	-.0	.2	.0	-.2	-.1	-.7	-.6	-.9	-1.1	-.7	-.8	-.6	-.6	-.7	-1.3	-1.2	-1.0
21	.1	-.1	.1	.2	.2	.3	.1	.2	.2	.1	.1	.1	-.0	-.9	-.8	-1.0	-1.3	-.9	-1.2	-1.0	-1.0	-1.3	-1.0	-.6	-1.0
20	.2	.0	.3	.4	.5	.5	.4	.6	.4	.2	.5	.1	-.1	-.8	-.8	-.8	-1.2	-.7	-1.1	-1.1	-.8	-.6	-.6	-.2	-.6
19	-.0	.1	.2	.3	.4	.5	.6	.5	.5	.5	.4	.3	.2	-.1	-.7	-.6	-1.0	-1.4	-.9	-.6	-.6	-.6	-.3	-.7	-.1
18	.0	.1	.0	.0	.0	.0	1.0	1.1	.0	.0	.0	.0	.0	.0	.0	-.2	-.3	-1.1	-1.4	-.7	-.0	-.3	-.5	.0	-.1
17	.0	.2	.0	.0	.0	.0	1.1	1.6	1.3	.9	1.2	1.0	.9	1.4	1.0	.3	-.2	-.3	-.5	-.6	-.6	1.2	-.7	.1	-.0
16	-.1	.0	-.3	.0	.7	.9	1.4	1.0	1.4	1.6	1.4	1.2	2.0	.9	1.4	.9	-.1	-.3	-.4	-.0	-.4	.2	-.4	.2	.0
15	-.2	.2	-.1	.0	.4	.9	1.0	1.9	1.2	1.6	1.4	1.4	1.0	1.7	1.0	1.1	.2	-.1	-.0	-.5	-.2	.1	-.1	-.0	.0
14	-.3	.1	-.1	.4	.7	.9	1.1	1.4	1.0	1.4	1.1	.8	1.5	1.5	1.4	1.1	.3	.0	.2	-.3	.2	-.1	-.1	-.0	.0
13	-.8	-.1	.2	.0	.7	1.0	1.3	1.5	1.2	1.0	.8	.6	1.4	1.4	1.3	1.1	.3	.3	-.5	.0	.0	.0	-.0	-.2	.3
12	-.3	-.1	.1	.0	.0	1.2	1.1	1.5	1.2	1.2	.0	-.5	.4	1.0	.0	.7	.7	-.2	.1	-.0	-.0	.3	-.2	.3	.1
11	-.2	.0	.1	.0	.0	1.1	1.0	1.3	1.2	1.0	.9	-.3	.0	.0	.9	.3	.0	-.2	-.1	.0	.1	.1	.4	.1	.1
10	-.2	.2	.3	.5	.7	1.0	1.2	1.6	1.3	1.3	.0	.3	-.2	.7	.0	.9	.2	.1	.0	.1	.4	.1	.1	.1	.1
9	-.1	.1	.2	.0	.7	.9	1.3	1.3	1.4	1.1	.0	.0	-.6	.7	.0	.0	.0	.1	.0	.2	.4	.2	.1	.1	.1
8	-.1	.1	.3	.0	.0	1.1	1.6	1.5	1.0	1.2	.7	-.2	.3	.0	.0	.0	.0	.4	.2	-.2	.2	.3	.2	.2	.1
7	-.0	.1	.3	.0	.0	1.0	1.3	1.2	1.0	1.0	.7	-.1	.3	.0	.0	.0	.0	.1	.2	-.0	.3	.0	.3	.3	.1
6	-.0	.1	.3	.0	.0	.7	.9	1.1	1.1	1.0	.6	.7	.0	.3	.4	.6	.0	.2	.4	.2	.1	-.0	.2	.1	.1
5	.0	.1	.2	.4	.5	.6	.7	.0	.0	.6	.5	.1	.3	.0	.4	.5	.3	.2	.2	.1	.1	-.1	.2	.1	.1
4	.0	.1	.2	.3	.4	.5	.5	.7	.9	.7	.6	.4	.1	.4	.4	.5	.4	.3	.2	.2	.1	.1	.1	-.1	.2
3	.0	.1	.2	.3	.3	.5	.9	.5	1.0	.7	.0	.0	.2	.3	.0	.3	.3	.0	.0	.2	.1	.1	.1	.0	.0
2	.0	.1	.0	.0	.2	.0	.8	.0	.4	.9	.0	.4	.0	.3	.0	.3	.2	.2	.2	.1	.0	.0	.0	.0	.0
1	.0	-.0	.3	.1	.0	.2	.7	.8	.0	.0	.5	.4	.8	.8	.3	.2	.2	.2	.1	.1	.0	-.0	-.0	-.0	.0

(b) Wind Direction

	1	2	3	4	5	6	7	8	9	10	11	12	13	14	15	16	17	18	19	20	21	22	23	24	25
25	-3	1	1	0	0	0	0	0	0	1	2	3	4	10	2	0	-0	-1	-1	-1	-0	-0	1	1	0
24	-4	-3	-0	0	0	1	1	1	3	2	4	4	14	0	4	.2	-0	0	0	0	1	1	5	2	1
23	-3	-6	-1	-1	0	0	2	3	1	8	9	16	15	9	8	4	1	3	2	1	2	1	5	1	4
22	-1	-1	-4	-1	0	1	3	5	7	11	13	15	16	9	10	6	3	4	2	3	4	9	6	6	6
21	-1	-1	-2	-4	-2	1	3	6	9	12	16	16	17	12	10	6	2	6	4	5	6	7	0	9	6
20	10	9	9	0	6	5	6	6	11	12	20	18	14	9	8	6	3	4	3	4	7	6	6	6	6
19	15	15	14	14	14	14	15	17	14	15	19	14	13	8	8	7	4	2	2	6	6	7	8	4	.
18	13	13	14	13	13	13	12	14	19	21	16	14	9	9	6	6	4	2	3	4	8	1	3	1	0
17	16	16	14	15	16	17	22	21	14	13	9	6	7	6	4	3	1	1	0	-0	-1	-1	-0	0	0
16	17	17	13	14	17	18	18	15	12	9	8	6	5	3	2	1	-0	-2	-2	-1	0	-1	-0	0	-0
15	13	13	11	14	14	13	11	8	8	5	3	3	1	0	-0	-4	-4	-2	-2	-0	0	-1	-0	-0	-0
14	10	11	11	11	10	10	10	10	7	6	3	1	0	-0	-1	-2	-4	-5	-4	-5	-2	-2	-2	-2	-0
13	8	8	9	9	9	9	0	8	6	5	3	0	0	-0	-1	-2	-4	-5	-5	-5	-4	-1	-3	-3	-1
12	7	9	8	7	7	7	7	7	5	5	3	1	1	1	-1	-2	-3	-5	-4	-5	-4	-4	-5	-4	-4
11	5	5	5	6	4	5	5	5	5	3	2	0	1	-0	-1	-2	-4	-4	-4	-4	-4	-4	-4	-4	-4
10	4	4	3	3	4	4	4	3	3	2	2	-0	-3	-0	-2	-5	-6	-5	-5	-5	-5	-4	-4	-4	-1
9	2	3	3	4	3	3	4	4	3	1	-0	-0	-4	-3	-4	-4	-5	-5	-5	-6	-6	-5	-5	-5	-5
8	2	2	2	2	3	3	2	0	-0	-2	-4	-5	-5	-4	-4	-4	-5	-5	-5	-4	-4	-5	-6	-6	-6
7	1	1	1	1	1	1	0	0	-1	-3	-3	-4	-5	-4	-4	-5	-5	-5	-5	-4	-4	-4	-5	-5	-5
6	1	1	1	0	0	-0	-0	-1	-3	-3	-3	-4	-5	-4	-4	-4	-4	-4	-4	-4	-4	-4	-4	-4	-4
5	0	0	0	-0	-0	-0	-0	-1	-2	-2	-3	-4	-3	-3	-3	-4	-4	-4	-4	-3	-3	-2	-3	-4	-4
4	-0	-0	-0	-0	-0	-0	-0	-1	-1	-1	-2	-2	-3	-2	-2	-2	-2	-2	-2	-3	-4	-4	-5	-4	-4
3	-0	-0	-0	0	-0	0	-0	-0	-0	-1	-1	-1	-1	-1	-1	-1	-1	-1	-1	-2	-2	-2	-3	-3	-3
2	-0	0	0	0	0	0	-0	0	0	0	-0	-1	-1	-0	-0	-0	-0	-0	-0	-0	-1	-1	-1	-1	-2
1	-0	-0	0	0	0	0	0	0	1	1	1	0	0	0	0	0	0	0	0	0	-0	-0	-0	-0	-0

\*See Table 24 for a description of the experimental conditions.

Table 21  
 PREDICTED CHANGES IN WIND SPEED AND DIRECTION FOR CASE 6\*  
 (a) Wind Speed

	1	2	3	4	5	6	7	8	9	10	11	12	13	14	15	16	17	18	19	20	21	22	23	24	25
25	.1	-.1	-.5	-.6	-.7	-.7	-.8	-.9	.1	1.4	2.0	2.7	2.9	2.9	.5	-.2	-.5	-.8	-.8	-.3	-.6	.1	.0	-.1	-.4
24	-.5	-.4	-.6	-.5	-.7	-.6	-.6	-.7	.8	.6	1.9	2.0	1.9	1.2	-.6	-1.6	-1.7	-1.4	-1.6	-1.4	-1.4	-.5	-1.3	-1.7	-1.9
23	-.6	-.2	-.1	-.2	-.3	-.1	.0	-.1	.0	1.2	1.3	2.3	1.6	-.2	-1.0	-2.7	-3.4	-2.0	-2.7	-2.0	-2.5	-2.3	.1	-2.9	-3.5
22	-.1	.3	.4	.4	.4	.6	.8	.5	1.0	1.9	2.3	2.4	1.8	-.3	-1.2	-2.9	-4.0	-3.5	-3.6	-3.1	-3.6	-2.9	-2.8	-3.1	-3.5
21	.8	.4	.9	1.3	1.5	1.6	1.7	1.7	1.9	4.0	3.1	3.6	2.2	-.2	-1.3	-3.1	-4.4	-4.0	-4.3	-3.7	-3.1	-2.9	-2.2	-1.8	-2.4
20	1.3	1.3	1.9	2.0	2.9	3.1	3.4	3.7	3.0	8.0	4.0	4.6	3.4	.9	-.6	-2.7	-4.3	-3.7	-3.8	-3.4	-2.4	-1.9	-1.5	-1.1	-1.5
19	1.9	2.2	2.7	3.2	3.7	4.3	5.0	5.1	4.2	5.2	5.4	5.2	4.3	2.2	-.3	-1.9	-4.0	-4.7	-3.3	-2.4	-1.9	-1.5	-1.2	-1.5	-.6
18	2.6	3.1	3.6	4.2	5.0	5.9	7.0	7.7	6.2	6.7	6.1	5.7	5.5	4.2	1.4	-.9	-3.7	-4.6	-3.1	-1.8	-1.0	-1.4	-.7	-1.1	-.4
17	3.0	4.2	4.9	5.6	6.9	8.0	10.3	10.3	8.0	7.3	6.5	6.1	7.2	7.3	4.2	.6	-1.7	-2.9	-3.0	-2.1	.0	-1.3	-.4	-.3	-.3
16	3.5	4.6	5.9	5.5	7.0	8.3	9.4	9.3	9.1	9.0	8.1	7.6	8.0	7.9	7.0	3.6	.2	-1.5	-2.1	-1.4	-1.1	-.1	-.8	.1	-.9
15	2.1	3.1	3.5	3.4	6.1	7.0	8.2	9.4	0.1	8.1	7.3	7.1	7.2	8.5	7.5	4.4	1.5	-.0	-.7	-1.4	-.7	-.1	-.3	-.2	.9
14	1.2	2.3	2.9	4.6	3.9	6.9	7.4	8.1	7.4	7.1	5.9	5.5	7.0	7.2	6.5	4.7	2.1	.6	.4	-.3	.1	-.2	-.2	.1	.5
13	.0	1.6	2.9	4.2	3.3	6.5	7.4	7.9	6.9	5.7	4.2	3.1	5.7	6.0	6.2	4.7	2.4	1.0	.1	.4	.9	.4	.2	.0	.7
12	.1	1.1	2.3	3.9	5.0	6.3	6.9	7.4	6.6	5.0	3.4	1.1	2.6	4.5	4.5	3.9	2.0	.7	.7	.6	.7	.9	.3	.0	.7
11	-.0	.9	1.9	3.4	4.6	5.9	7.1	7.0	6.6	5.4	3.0	1.3	1.4	3.2	4.0	3.1	2.5	.5	.3	.6	.8	.7	1.0	.8	.1
10	-.3	.7	1.0	2.9	4.1	5.4	6.5	7.3	6.0	5.0	3.5	2.0	1.0	2.6	3.5	3.9	2.4	1.0	.6	.9	1.1	1.2	.9	.9	.8
9	-.1	.0	1.6	2.6	3.7	4.9	6.2	6.9	6.9	5.7	3.3	2.4	.0	2.4	3.0	3.3	3.0	1.3	.7	1.1	1.6	1.2	1.1	1.0	1.0
8	-.1	.0	1.5	2.4	3.3	4.3	5.6	7.2	7.0	5.6	3.0	2.1	1.4	2.1	2.8	3.0	2.9	1.9	1.0	.9	1.1	1.5	1.3	1.2	1.1
7	-.0	.0	1.4	2.2	3.1	3.0	4.9	6.3	6.3	5.2	4.6	3.5	1.8	2.2	2.7	2.7	2.7	2.2	1.3	1.0	.9	1.1	1.0	1.3	1.1
6	.0	.0	1.3	2.0	2.7	3.4	4.2	5.3	5.6	4.8	3.7	3.2	1.9	2.1	2.5	2.8	2.4	1.8	1.6	1.1	.7	.6	1.0	.9	.9
5	.1	.6	1.2	1.8	2.4	3.0	3.6	4.1	4.4	4.0	3.4	2.5	1.7	1.8	2.3	2.3	2.3	1.8	1.4	1.1	.8	.6	.4	.9	.6
4	.2	.6	1.1	1.6	2.2	2.7	3.0	3.7	4.1	3.7	3.0	2.2	1.4	1.7	1.8	2.0	1.8	1.6	1.3	1.0	.8	.6	.4	.3	.4
3	.2	.5	1.0	1.4	1.8	2.6	3.0	3.8	3.5	2.8	2.1	1.6	1.4	1.7	1.6	1.5	1.3	1.0	.7	.5	.4	.4	.4	.4	.4
2	.1	.4	.7	1.0	1.0	2.3	2.2	3.1	2.9	3.4	2.8	2.1	1.6	1.4	1.3	1.2	1.0	.8	.5	.2	.1	.1	.1	.1	.2
1	.1	.8	.9	1.1	1.7	1.8	2.6	2.4	3.2	2.9	2.5	2.0	1.6	1.4	1.3	1.2	1.1	.9	.6	.4	.1	-.0	-.1	.0	.6

(b) Wind Direction

	1	2	3	4	5	6	7	8	9	10	11	12	13	14	15	16	17	18	19	20	21	22	23	24	25
25	-2	0	1	1	1	1	1	1	4	7	10	13	20	28	15	3	-3	-7	-6	-4	-0	2	6	4	3
24	-12	-11	-4	-0	1	3	6	9	13	15	19	26	45	39	20	15	4	2	1	2	5	9	16	12	11
23	-15	-10	-10	-3	0	4	11	16	17	31	38	55	62	87	82	39	22	19	14	14	15	19	30	26	23
22	-7	-9	-13	-7	1	8	14	23	29	41	51	60	68	64	63	51	36	30	24	24	29	35	46	44	50
21	4	2	-1	-2	2	11	10	38	37	47	59	64	71	66	62	54	40	37	32	32	37	43	49	51	49
20	34	31	28	25	23	23	25	31	42	47	63	61	58	52	51	46	39	33	20	30	30	42	43	42	41
19	52	50	46	44	41	41	41	47	49	52	60	52	40	42	43	40	33	24	24	31	37	30	39	31	30
18	55	52	50	47	43	42	41	45	54	56	49	43	35	32	32	29	21	18	24	24	29	19	18	13	17
17	61	50	52	50	49	47	51	51	42	40	32	26	25	22	18	14	9	8	8	8	6	4	2	3	7
16	66	59	51	49	51	49	46	41	35	29	25	21	16	12	7	4	-2	-9	-7	-3	-1	-3	-0	-0	0
15	56	51	47	47	45	40	35	33	20	24	18	12	9	6	2	-3	-13	-18	-15	-12	-6	-3	-5	-3	-3
14	49	46	43	41	38	35	32	29	20	21	13	8	3	1	-4	-8	-16	-22	-23	-21	-13	-12	-11	-10	-3
13	41	38	37	35	33	30	28	26	22	19	13	6	2	-0	-4	-10	-17	-23	-24	-23	-20	-19	-10	-17	-16
12	37	36	33	28	26	24	23	22	10	17	19	7	4	0	-5	-10	-16	-23	-24	-23	-21	-22	-22	-19	-10
11	29	20	26	23	20	19	18	17	15	13	9	4	3	-2	-6	-12	-16	-21	-23	-22	-22	-20	-21	-20	-20
10	22	21	19	17	17	16	14	12	12	8	5	-0	-0	-7	-11	-10	-22	-24	-25	-24	-23	-21	-21	-21	-21
9	16	16	15	16	13	13	12	11	8	2	-2	-7	-14	-14	-17	-19	-23	-24	-25	-25	-23	-23	-23	-23	-23
8	12	12	12	10	11	9	6	3	-0	-6	-12	-17	-19	-18	-18	-19	-22	-23	-23	-22	-21	-23	-23	-25	-25
7	7	7	7	7	5	5	2	-0	-5	-10	-14	-10	-20	-19	-18	-19	-20	-23	-21	-20	-19	-20	-22	-23	-24
6	4	4	4	3	2	0	-1	-4	-8	-10	-14	-17	-19	-18	-17	-17	-19	-19	-18	-18	-10	-10	-20	-20	-22
5	1	1	1	0	-0	-0	-2	-4	-6	-8	-11	-13	-15	-14	-13	-13	-14	-13	-16	-16	-17	-16	-10	-20	-21
4	-2	-1	-1	-1	-1	-1	-2	-3	-5	-6	-8	-10	-11	-9	-8	-9	-10	-12	-13	-13	-17	-13	-19	-19	-20
3	-2	-1	-1	-0	-0	-0	-1	-2	-3	-4	-5	-6	-6	-4	-4	-6	-7	-9	-11	-13	-14	-15	-15	-15	-13
2	-0	-0	-0	0	1	0	0	1	0	0	-1	-2	-1	-0	-0	-1	-1	-2	-4	-5	-6	-7	-8	-9	-3
1	-0	-0	1	1	2	2	3	3	4	5	5	3	3	2	2	2	1	1	0	-0	-1	-1	-2	-2	-2

\*See Table 24 for a description of the experimental conditions.

Table 22  
 PREDICTED CHANGES IN WIND SPEED AND DIRECTION FOR CASE 7\*  
 (a) Wind Speed

	1	2	3	4	5	6	7	8	9	10	11	12	13	14	15	16	17	18	19	20	21	22	23	24	25
25	-0.8	.1	.0	.1	-1.1	-0.6	-0.2	-0.5	-0.5	-0.5	-0.4	-0.8	-0.2	-0.2	-0.1	-0.2	-0.2	-0.4	-0.4	-0.4	-0.7	-0.6	-0.6	-0.1	
24	.1	.8	-0.0	-0.0	-0.4	-0.7	-0.9	-1.0	-0.7	-0.8	-0.7	-0.4	-0.3	-0.3	-0.2	-0.2	-0.0	-0.4	-0.4	-0.7	-0.7	-1.0	-0.3	.2	.0
23	.2	.8	-0.1	-0.5	-0.3	-1.0	-1.0	-0.9	-0.6	-0.8	.1	.1	.1	-0.1	-0.2	-0.3	-0.0	-0.8	-0.8	-0.8	-0.7	-0.2	.2	.9	.4
22	.8	.5	-0.5	-0.5	-0.4	-1.2	-0.9	-0.6	.6	.6	.6	.6	.4	-0.1	-0.2	-0.2	-0.5	-0.8	-0.5	-0.6	-0.1	.2	.2	.9	.7
21	.4	.3	-0.1	-1.0	-0.9	-0.7	-0.5	.7	1.0	.9	.9	.8	.6	.6	.1	-0.1	-0.7	-1.1	-0.6	.3	.3	.2	.3	1.9	.7
20	.2	-0.0	-0.0	-0.7	-0.5	-0.2	.1	1.3	1.4	.9	.6	.6	-0.1	.3	.2	-0.6	-1.5	-1.4	-0.5	-0.0	.6	.6	.7	1.3	.8
19	-0.1	-0.1	-0.1	-0.2	-0.1	.2	.7	1.0	-0.1	.1	-0.3	-0.4	-0.4	-0.9	-1.2	-1.8	-2.4	-1.8	-0.6	.6	1.0	1.2	1.6	1.0	.0
18	-0.1	-0.2	-0.1	-0.1	.1	.4	.7	-0.2	-0.2	-0.4	-0.8	-0.0	-0.9	-1.9	-2.0	-1.7	-2.2	-1.2	.1	.7	1.4	1.5	1.7	1.0	.1
17	-0.1	-0.2	-0.1	-0.1	-0.0	.7	.3	-0.1	-0.5	-0.7	-1.1	-1.3	-1.4	-1.9	-1.8	-1.9	-1.4	-0.2	.6	1.4	1.6	1.6	2.2	1.0	.9
16	-0.1	-0.2	-0.2	-0.1	.0	.8	.5	-0.4	-0.4	-1.2	-1.0	-0.0	-1.8	-1.8	-1.8	-1.3	-0.6	.5	1.3	1.6	2.4	1.7	1.3	1.1	.5
15	-0.1	-0.2	-0.2	-0.2	-0.1	.0	.2	.2	-0.9	-0.7	-0.8	-0.8	-1.4	-1.3	-1.1	-1.0	-0.1	1.2	1.6	2.7	2.5	2.1	1.4	1.2	.6
14	-0.1	-0.2	-0.5	-0.3	-0.2	.1	.5	-0.3	-0.7	-0.6	-0.4	-0.9	-1.5	-1.0	-0.9	-0.9	.2	.1	2.0	2.2	2.6	1.0	1.1	1.0	.5
13	-0.1	-0.2	-0.3	-0.2	-0.1	.2	.2	-0.3	-0.4	-0.7	-0.6	-1.0	-1.4	-1.2	-0.4	-0.8	.0	1.1	1.2	2.4	2.5	1.5	1.6	1.3	.6
12	-0.1	-0.2	-0.2	-0.2	-0.1	.0	.3	.1	-0.4	-0.8	-1.4	-1.9	-1.5	-0.6	-0.9	-0.3	-0.1	.8	.6	1.6	2.4	1.6	1.4	1.3	.6
11	-0.1	-0.2	-0.2	-0.2	-0.1	-0.1	.1	.3	-0.5	-1.1	-1.7	-1.3	-0.7	-0.5	-0.6	-0.5	-0.1	-0.2	.6	1.6	2.2	1.7	1.3	1.2	.0
10	-0.0	-0.1	-0.2	-0.2	-0.1	-0.1	.1	.2	-0.8	-0.8	-1.5	-0.8	-0.1	-0.0	-0.6	-0.2	.1	.3	1.4	1.9	2.0	1.5	1.2	1.3	.7
9	-0.0	-0.1	-0.1	-0.2	-0.2	-0.1	-0.0	-0.6	-0.5	-0.7	-0.5	-0.6	-0.6	-0.2	.2	.0	.9	1.4	1.3	1.7	1.4	1.1	1.2	.7	
8	-0.0	-0.0	-0.1	-0.2	-0.3	-0.3	-0.1	-0.1	-0.2	-0.2	-0.6	-0.5	-0.9	-0.7	-0.3	.0	.6	.0	1.2	1.1	1.1	1.0	.9	1.0	.6
7	-0.0	-0.0	-0.1	-0.2	-0.3	-0.3	-0.1	-0.1	-0.1	-0.2	-0.4	-0.9	-0.7	-0.5	-0.0	.3	.9	1.1	.9	.0	.7	.8	.9	.9	.0
6	-0.0	-0.0	-0.1	-0.1	-0.2	-0.2	-0.1	-0.0	-0.2	-0.5	-0.5	-0.7	-0.1	.3	.6	.6	.9	.7	.6	.6	.7	.8	.8	.4	
5	-0.0	-0.1	-0.1	-0.1	-0.1	-0.1	-0.1	-0.1	-0.1	-0.2	-0.4	-0.4	-0.2	.1	.3	.6	.7	.7	.6	.9	.9	.9	.6	.7	.4
4	-0.0	-0.1	-0.1	-0.1	-0.1	-0.1	-0.1	-0.1	-0.1	-0.1	-0.2	-0.1	.0	.2	.3	.5	.6	.6	.6	.4	.4	.4	.5	.6	.3
3	-0.0	-0.0	-0.0	-0.1	-0.1	-0.1	-0.0	-0.0	-0.0	-0.0	.0	.1	.2	.3	.5	.6	.6	.6	.6	.3	.3	.2	.4	.5	.2
2	-0.0	-0.0	-0.0	-0.0	-0.0	-0.0	.0	.0	.0	.0	.0	.1	.2	.3	.4	.6	.4	.6	.4	.2	.2	.1	.3	.4	.2
1	-0.0	.0	.0	.0	.0	.0	.0	.0	.0	.1	.1	.1	.1	.2	.2	.2	.2	.2	.2	.1	.1	.1	.0	.0	-0.0

(b) Wind Direction

	1	2	3	4	5	6	7	8	9	10	11	12	13	14	15	16	17	18	19	20	21	22	23	24	25
25	-2	1	2	-1	-3	-3	-11	-11	-15	-10	-6	-10	-6	-4	-3	-3	-1	-4	-4	-4	-7	-7	-7	-4	-0
24	0	7	9	2	0	0	-11	-13	-26	-16	-10	-20	-16	-13	-10	-8	-1	-2	-6	-5	-6	-9	-9	-18	-7
23	2	6	5	3	2	7	0	-1	-8	-2	-8	-7	-8	-9	-10	-12	-7	-7	-10	-13	-10	-0	1	-5	-5
22	4	7	3	1	-2	5	6	3	-0	2	6	2	2	-9	-3	-3	-1	-3	-11	-10	-6	-4	-2	-5	-3
21	3	-9	-8	-5	-6	4	9	6	4	7	9	9	12	13	7	8	13	8	-2	-5	-5	-2	-0	-1	-1
20	1	-13	-20	-15	-1	9	17	15	16	18	9	11	12	12	7	7	9	2	-8	-9	-2	0	6	8	2
19	-0	-17	-22	-10	-4	3	13	12	10	0	7	3	0	-0	-17	-17	-14	-17	-16	-10	-8	-4	0	2	0
18	-3	-11	-12	-13	-12	-7	-0	0	-1	0	-1	-8	-14	-17	-35	-40	-30	-24	-10	-14	-9	-5	-2	-0	0
17	-1	-4	-5	-6	-8	-11	-10	-5	-5	-6	-9	-14	-20	-25	-36	-43	-39	-29	-21	-14	-9	-4	-2	-0	0
16	-0	-1	-1	-2	-3	-8	-13	-9	-8	-10	-10	-11	-14	-23	-30	-35	-36	-30	-23	-17	-9	-2	-1	-3	-6
15	0	0	-0	-1	-4	-7	-10	-0	-6	-8	-5	-5	-4	-9	-15	-21	-20	-27	-21	-16	-9	-5	-3	-2	-6
14	0	0	-0	-0	-0	-0	-1	-2	-1	5	-1	-1	-3	-6	-7	-10	-17	-22	-21	-17	-11	-4	-3	-2	0
13	-0	-0	0	1	2	2	0	0	2	1	0	-3	-5	-7	-7	-5	-9	-12	-17	-19	-15	-9	-5	-1	0
12	0	0	0	2	2	1	-0	2	4	1	-1	-5	-6	-0	-10	-11	-14	-7	-9	-14	-12	-9	-6	-3	-1
11	-0	0	1	2	4	3	1	2	2	2	3	1	1	-1	-5	-10	-16	-22	-28	-13	-7	-3	-3	-3	-4
10	0	1	2	3	5	2	0	-1	-3	3	18	15	10	7	0	-4	-3	-0	-9	-8	-4	-3	-1	-2	0
9	0	1	1	2	1	-1	-3	-6	-1	9	20	19	14	11	7	2	0	6	4	-1	-2	-4	-3	-1	-1
8	-0	0	1	1	1	-1	-2	-3	1	11	20	21	16	10	6	1	-5	-4	-5	11	7	1	1	1	0
7	0	0	0	0	1	3	4	0	0	5	14	20	22	15	11	6	-8	-1	0	-4	-5	-2	-1	0	0
6	-0	-1	-1	-0	0	3	5	3	1	2	0	19	26	29	16	12	4	2	5	7	7	5	3	1	0
5	0	-0	-0	0	1	3	4	5	5	4	7	16	25	27	26	19	11	5	3	3	4	4	2	1	0
4	0	0	0	1	2	3	4	5	6	7	10	15	20	23	24	21	19	14	12	9	6	1	2	1	0
3	0	0	0	1	2	3	5	6	7	9	11	15	17	20	21	20	18	18	17	17	7	10	5	2	0
2	0	0	1	2	3	4	5	6	8	9	11	14	16	18	19	19	17	15	13	14	16	14	11	6	0
1	0	0	0	1	1	2	2	0	4	4	5	7	7	9	10	10	9	8	7	7	8	8	9	5	0

\*See Table 24 for a description of the experimental conditions;

Table 23  
 PREDICTED CHANGES IN WIND SPEED AND DIRECTION FOR CASE 8\*  
 (a) Wind Speed

	1	2	3	4	5	6	7	8	9	10	11	12	13	14	15	16	17	18	19	20	21	22	23	24	25
25	.2	.2	.0	.1	-.0	-.0	-.0	-.2	.2	.6	.8	.2	-.2	-.4	-.7	-.3	.1	.3	1.0	1.3	1.6	1.4	1.1	.9	-.0
24	.1	.1	-.0	-.0	-.4	-.3	-.3	-.5	.2	.1	.0	.9	-.0	-.5	-1.0	-2.0	-1.2	-.2	.2	.9	1.2	2.2	1.4	1.3	.3
23	-.2	-.4	-.4	-.3	-.3	-.1	-.1	-.3	-.0	.9	.1	.7	.1	-1.6	-2.1	-3.2	-2.3	-1.6	-1.6	-.9	-.4	2.2	.3	.2	.2
22	-.0	-.0	-.3	-.0	.1	.3	.4	-.0	.9	.9	1.0	.9	.4	-1.3	-2.2	-3.7	-4.3	-3.5	-3.3	-2.6	-2.3	-2.1	-1.9	-1.1	.1
21	-1.0	-1.0	-.3	.0	.9	1.0	1.1	1.0	1.1	1.4	1.0	2.1	.7	-1.4	-2.4	-4.0	-5.1	-4.4	-4.5	-3.0	-3.4	-3.3	-2.6	-1.0	-.7
20	-1.0	-1.4	.1	1.2	1.0	2.2	2.4	2.6	2.0	2.5	3.3	3.0	1.9	-.5	-1.0	-3.7	-5.1	-4.3	-4.4	-4.0	-3.3	-3.0	-2.0	-2.2	-1.1
19	-.6	-.6	.0	1.5	2.3	2.9	3.6	3.6	3.0	3.0	3.9	3.7	2.0	.7	-1.7	-3.1	-4.9	-5.4	-4.1	-3.3	-3.2	-3.1	-3.0	-3.4	-1.6
18	.2	.6	1.3	2.2	3.2	4.2	5.2	5.9	4.7	5.0	4.5	4.2	4.0	2.7	.0	-2.1	-4.5	-5.3	-4.0	-3.0	-2.7	-3.3	-3.0	-3.7	-2.0
17	1.0	2.1	2.7	3.7	5.1	6.6	8.4	9.3	6.3	5.0	5.1	4.0	3.7	3.0	2.9	-.5	-2.4	-3.5	-3.9	-3.2	-.6	-2.0	-2.6	-3.2	-2.2
16	1.7	3.7	2.9	4.4	5.0	6.9	8.1	7.9	7.0	7.5	6.7	6.2	7.3	6.5	5.9	2.7	-.4	-1.9	-2.0	-2.5	-2.6	-2.0	-3.2	-2.0	-2.1
15	1.9	4.1	4.1	5.5	5.9	6.9	7.4	8.4	7.1	7.0	6.3	6.2	6.2	7.4	6.0	3.1	1.1	-.4	-1.2	-2.2	-2.1	-1.9	-2.6	-3.1	-2.2
14	2.2	4.0	4.0	5.7	6.6	7.0	7.1	7.4	6.6	6.2	5.1	4.9	6.4	6.6	6.0	4.2	1.0	.3	.1	-.9	-1.0	-1.9	-2.5	-2.9	-2.3
13	2.4	5.2	5.7	6.1	6.6	7.1	7.6	7.6	6.9	5.0	3.0	2.7	5.1	6.1	5.5	4.2	2.0	.5	-.4	-.4	-.3	-1.4	-2.1	-2.9	-1.7
12	2.7	5.5	5.7	6.4	6.0	7.4	7.4	7.6	6.5	5.2	3.0	.6	2.1	3.9	3.9	3.2	2.2	.0	-.1	-.6	-1.0	-1.2	-2.2	-2.1	-2.1
11	2.9	5.0	5.6	6.2	6.7	7.4	8.1	7.3	6.7	5.3	3.7	1.1	1.0	2.7	3.3	2.3	1.7	-.9	-.0	-.9	-1.1	-1.6	-1.6	-2.3	-2.1
10	2.6	5.7	5.6	5.0	6.3	7.1	7.7	8.1	7.3	6.0	3.7	2.1	.9	2.4	3.0	3.0	1.0	.2	-.3	-.5	-.7	-1.1	-1.0	-2.3	-2.0
9	2.5	5.2	5.2	5.5	5.9	6.6	7.5	7.9	7.7	6.3	4.0	2.9	.9	2.4	2.0	2.9	2.6	.0	-.1	-.1	.0	-.9	-1.6	-2.3	-2.0
8	2.3	4.7	4.8	5.0	5.4	6.0	7.0	8.4	8.1	6.4	5.9	4.2	2.2	2.6	3.0	2.8	2.7	1.4	.2	-.0	-.6	-.8	-1.3	-2.2	-1.9
7	2.0	4.2	4.4	4.6	4.9	5.4	6.1	7.6	7.5	6.2	5.4	4.7	2.9	3.0	3.3	3.0	2.7	1.9	.0	-2.2	-1.2	-1.2	-1.9	-2.2	-1.6
6	1.7	3.6	3.7	4.0	4.3	4.7	5.2	6.4	6.0	5.0	4.9	4.4	3.2	3.1	3.3	3.3	2.6	1.7	1.1	.1	-.9	-1.0	-1.9	-2.6	-1.1
5	1.4	2.9	3.1	3.3	3.6	4.0	4.4	5.0	5.3	5.0	4.0	3.0	3.1	3.1	3.2	3.0	2.9	2.0	1.2	.3	-.4	-1.3	-2.1	-2.2	-1.4
4	1.0	2.2	2.4	2.6	3.0	3.3	3.6	4.3	4.0	4.6	4.2	3.0	2.9	3.1	3.0	3.0	2.7	2.2	1.0	.0	.0	-.7	-1.5	-2.0	-1.0
3	.6	1.4	1.7	1.9	2.1	2.0	2.9	3.3	4.4	4.4	4.1	3.7	3.1	3.0	3.1	2.8	2.6	2.3	1.7	1.0	.3	-.3	-.8	-1.3	-.0
2	.2	.7	.0	1.4	1.0	2.1	2.1	3.0	3.1	4.1	4.2	4.0	3.6	3.3	3.0	2.9	2.7	2.4	1.9	1.3	.6	.1	-.3	-.5	-.3
1	-.0	-.0	.3	.2	.0	.9	1.0	.7	1.4	1.3	1.5	1.6	1.0	1.4	1.3	1.2	1.1	1.0	.0	.6	.4	.2	.1	.0	-.0

(b) Wind Direction

	1	2	3	4	5	6	7	8	9	10	11	12	13	14	15	16	17	18	19	20	21	22	23	24	25
25	0	4	3	1	-0	-1	-2	-5	-6	-0	-7	-5	-0	10	6	3	-0	-2	-4	-6	-6	-6	-3	-2	0
24	-3	-4	0	0	-1	-2	-3	-0	-0	-6	-0	7	29	00	20	7	-3	-6	-0	-9	-0	-5	0	2	4
23	-0	-10	-7	-5	-2	-1	1	5	4	16	25	44	64	40	42	22	4	2	-1	-2	-2	-0	7	6	4
22	3	-3	-13	-9	-3	1	5	13	19	31	42	53	63	58	55	38	17	11	6	5	7	9	16	10	2
21	0	1	-5	-0	-4	3	9	21	20	30	51	68	65	60	55	43	24	19	13	13	16	17	17	6	-5
20	3	10	10	13	12	13	16	22	33	39	56	55	52	45	43	37	26	19	13	14	19	17	9	-7	-10
19	2	21	20	29	20	29	31	37	40	44	52	44	41	34	34	30	21	12	11	13	17	10	-2	-20	-15
18	-0	13	21	24	25	27	20	33	43	47	40	34	26	24	23	20	10	5	9	7	0	-7	-10	-37	-14
17	1	11	16	21	26	29	37	30	51	29	22	16	15	13	0	4	-2	-6	-10	-14	-20	-20	-37	-45	-11
16	2	11	14	21	29	31	31	27	22	17	14	9	6	2	-3	-6	-16	-26	-30	-29	-20	-36	-44	-56	-14
15	4	10	14	22	24	23	21	19	15	12	6	0	-1	-4	-9	-10	-27	-36	-39	-41	-40	-46	-59	-66	-14
14	4	11	15	18	18	10	17	15	12	0	2	-3	-8	-11	-16	-21	-32	-42	-40	-53	-53	-60	-63	-71	-13
13	4	9	13	14	14	10	13	12	9	6	0	-5	-9	-12	-17	-24	-33	-43	-49	-54	-56	-63	-69	-80	-10
12	5	12	11	9	0	9	0	8	5	4	0	-4	-7	-11	-10	-24	-33	-44	-49	-53	-55	-64	-74	-93	-19
11	4	8	7	6	3	4	4	4	2	0	-3	-0	-10	-15	-20	-27	-33	-41	-47	-49	-54	-62	-76	-91	-17
10	4	5	3	2	2	2	1	-0	-1	-4	-7	-14	-22	-22	-27	-35	-40	-46	-51	-55	-60	-67	-77	-86	-13
9	4	4	3	3	0	-0	-1	-4	-10	-16	-21	-30	-31	-34	-37	-43	-40	-56	-61	-66	-71	-70	-80	-16	
8	4	4	2	-0	-0	-2	-5	-9	-13	-20	-27	-33	-36	-36	-38	-40	-45	-49	-54	-57	-60	-65	-72	-81	-14
7	3	2	0	-2	-5	-6	-10	-14	-19	-26	-30	-35	-39	-39	-40	-43	-46	-50	-53	-54	-55	-57	-60	-64	-11
6	3	2	-1	-4	-7	-12	-14	-19	-23	-27	-31	-36	-40	-41	-41	-43	-44	-47	-49	-50	-52	-51	-50	-46	-6
5	2	0	-3	-7	-11	-13	-16	-20	-23	-27	-31	-35	-39	-40	-41	-42	-43	-45	-46	-46	-46	-42	-39	-32	-4
4	1	-1	-5	-9	-13	-10	-18	-22	-25	-29	-32	-36	-39	-40	-40	-41	-42	-43	-44	-42	-40	-33	-22	-3	
3	0	-2	-6	-9	-13	-16	-20	-24	-20	-31	-35	-30	-39	-39	-39	-39	-39	-39	-39	-39	-37	-34	-27	-16	-1
2	0	-2	-6	-10	-14	-10	-22	-26	-30	-34	-30	-41	-41	-40	-38	-37	-37	-36	-35	-34	-31	-26	-20	-11	-0
1	-0	-2	-3	-6	-0	-11	-14	-17	-20	-23	-20	-26	-20	-24	-23	-23	-21	-20	-19	-17	-14	-11	-7	-3	0

\*See Table 24 for a description of the experimental conditions.



Table 24

CONDITIONS REPRESENTED IN TABLES 16 THROUGH 23

Case	Table	Time		D - D <sub>0</sub>		Grid Level		Boundary Conditions	
		6 a.m.	3 p.m.	Eq. (26)	Eq. (27)	k = 1	k = 5	$\partial\phi/\partial n = 0$	$\phi = 0$
1	16	X		X		X		X	
2	17	X			X	X		X	
3	18	X			X		X	X	
4	19		X	X		X		X	
5	20		X		X	X		X	
6	21		X		X		X	X	
7	22	X			X		X		X
8	23		X		X		X		X

In addition to the general observations given above, we can also make the following specific comments:

- > Perturbations obtained at ground level from the use of Eq. (26) to estimate  $D - D_0$  are larger than those generated from the use of Eq. (27) (compare Tables 16 and 17 and Tables 19 and 20). The opposite is true at the top of the region (compare Tables 16 and 18 and Tables 19 and 21).
- > When Eq. (27) is used to estimate  $D - D_0$ , the perturbations aloft are much larger than those predicted at ground level (compare Tables 17 and 18 and Tables 20 and 21).
- > The choice of boundary conditions employed does have some influence on the magnitude of the predicted changes in wind speed and direction. As expected, this influence is greatest near the boundary (compare Tables 18 and 22 and Tables 21 and 23).

To explain the first two observations cited above, we note that the forcing function in Eq. (23) follows the same pattern of behavior. This can be illustrated by considering the ratio of the forcing functions employed in each case. If we let  $\Delta D_{26}(K)$  and  $\Delta D_{27}(1,K)$  represent the values of  $D - D_0$  calculated using Eqs. (26) and (27), respectively, then we can write the ratio of the forcing function corresponding to the comparisons made above as follows:

$$\frac{\Delta D_{26}(K)}{\Delta D_{27}(1,K)} = \frac{K + 1}{2} \quad ,$$

$$\frac{\Delta D_{26}(K)}{\Delta D_{27}(K,K)} = \frac{K + 1}{2K}$$

$$\frac{\Delta D_{27}(1,K)}{\Delta D_{27}(K,K)} = \frac{1}{K} \quad ,$$

where  $K$  is the number of vertical layers of grid cells. In this study,  $K$  has a value of 5.

The experience gained in this brief study indicates that the use of algorithms similar to those given in the previous section provides a viable means of producing mass-consistent wind fields. Although such algorithms are relatively simple to employ, they are deficient in the treatment of momentum and energy balance relationships. However, until complete planetary boundary layer models suitable for predicting flow fields over urban areas can be developed and validated, photochemical modeling efforts will undoubtedly continue to rely on wind fields derived from actual field measurements. Thus, the use of mass-consistent wind algorithms should be considered as an interim means for removing excessive convergence and divergence effects in the flow field. The need for such usage may also be enhanced by the inclusion of wind shear in the airshed model, since the extent of convergence and divergence in the predicted flow field aloft may be larger than that previously experienced near the ground.

In future work, we recommend that mass-consistent wind algorithms be employed in conjunction with interpolation procedures for predicting flow fields over an urban area where a reasonably dense meteorological network has been established. In this way, tests can be designed to evaluate the performance of the methodology. The RAPS study in St. Louis may provide such a data base. In addition, further consideration should be given to the manner in which the quantity  $D - D_0$  is estimated. Examination of the characteristics of flow fields over urban areas may provide some guidance in this matter.

#### D. ADOPTION OF AN IMPROVED ALGORITHM FOR ESTIMATING TURBULENT DIFFUSIVITIES

Pollutants are dispersed through advection and turbulent diffusion. In the horizontal directions, the advective mass flux is usually much larger than the diffusive flux. However, vertical transport is often dominated by turbulent diffusion. The usual means for treating vertical diffusion is through the assumption that the turbulent mass flux,  $F_t$ , is proportional to the gradient of the mean concentration field. That is,

$$F_t = -K_v \frac{\partial \langle c \rangle}{\partial z} \quad , \quad (28)$$

where

$K_v$  = turbulent diffusivity,  
 $\langle c \rangle$  = mean concentration.

Turbulent diffusivities are extremely difficult to measure in the field, and their parameterization has been the subject of numerous studies. Upon reviewing the algorithm we employed in the 1969 validation study to calculate  $K_v$ , discussed in Roth et al. (1971), we found that there was sufficient justification to formulate a new algorithm. This new algorithm includes important atmospheric parameters, heretofore omitted, that are known to have a significant effect on the value of the diffusivity. Specific criticisms of the diffusivity algorithm that we used previously are as follows:

- > The diffusivity is assumed to depend only on the wind speed. Using measured diffusivity data reported by Hosler (1969), Eschenroeder et al. (1972) found that the diffusivity does not correlate well with wind speed alone. This finding is not surprising, since we would expect that, for a given wind speed, the value of  $K_v$  for stable atmospheric conditions would be much less than its value under unstable conditions. Clearly, an algorithm for  $K_v$  must include the effect of atmospheric stability.
- > Surface roughness effects are not explicitly included in the formulation of  $K_v$ . Recent studies by Lissaman (1973) and Ragland (1973) indicate that ground-level pollutant concentrations are significantly influenced by the value of the surface roughness.

In reviewing previous efforts to parameterize the diffusivity reported in the literature, we found that guidelines appear to exist that are sufficiently well developed for use in estimating the value of  $K_v$  in the surface layer (up to about 100 m). However, for the remaining portion of the planetary boundary layer above an urban area, we have not found a definitive treatment of the diffusivity that is both general and simple enough to include in an airshed model. Also of concern is the objective for multiday simulations of defining the vertical extent of the modeling region to include the inversion layer, if present. The "trapping" effect of the elevated temperature inversion would be treated through the use of the vertical diffusivity profile. Thus, a relatively sophisticated treatment of  $K_v$  is required aloft, a region of the planetary boundary layer where few measurements are generally available.

Realizing that a completely satisfying treatment of  $K_v$  may not be attainable at the present time, but also recognizing the need to improve the algorithm previously employed in the SAI airshed model, we initiated efforts to develop an algorithm for  $K_v$  that includes, at a minimum, both atmospheric

stability and surface roughness effects. Several schemes for computing  $K_v$  have been proposed in the literature, including those described by Blackadar (1962), Wu (1965), Hino (1968), Pandolfo et al. (1971), Eschenroeder et al. (1972), Ragland (1973), Bergstrom and Viskanta (1973), and Shir and Shieh (1973). However, each of these approaches is to some extent heuristic, and their validity is somewhat uncertain.

To alleviate the difficulties associated with basing a diffusivity algorithm on field measurements, we developed a methodology that uses the predictions of a sophisticated numerical planetary boundary layer model developed by Deardorff. Although the present  $K_v$  algorithm is applicable for only neutral and slightly unstable atmospheric stability regimes, the methodology can be extended to other regimes. For a more detailed discussion of this algorithm, we refer the reader to Chapter II of Volume III.

#### E. MODIFIED TREATMENT OF THE INVERSION LAYER IN THE AIRSHED MODEL

In previous studies, the modeling region has been defined to extend from the ground level to the base of an elevated temperature inversion. However, a major difficulty arises when using this approach for multiday simulations: A significant amount of pollutants can be reintroduced into the mixed layer from aloft as the inversion is eroded away during each daytime period. Unless the pollutants that are trapped in the inversion on the previous day are retained in the modeling region, it will be difficult to account properly for their reintroduction into the mixed layer on a given day. As an example of the  $O_3$  levels that have been observed aloft, we present in Figure 21 a cross section of the pollutant distribution in a portion of the Los Angeles basin on the morning of 11 July 1973 (Jerskey et al., 1975).

As an alternative definition of the modeling region, we propose to include the portion of the atmosphere bounded below by the terrain and bounded aloft by the top of the inversion layer. All governing equations and coordinate transformations used previously still apply, except that the term  $\Delta H$  should be interpreted as

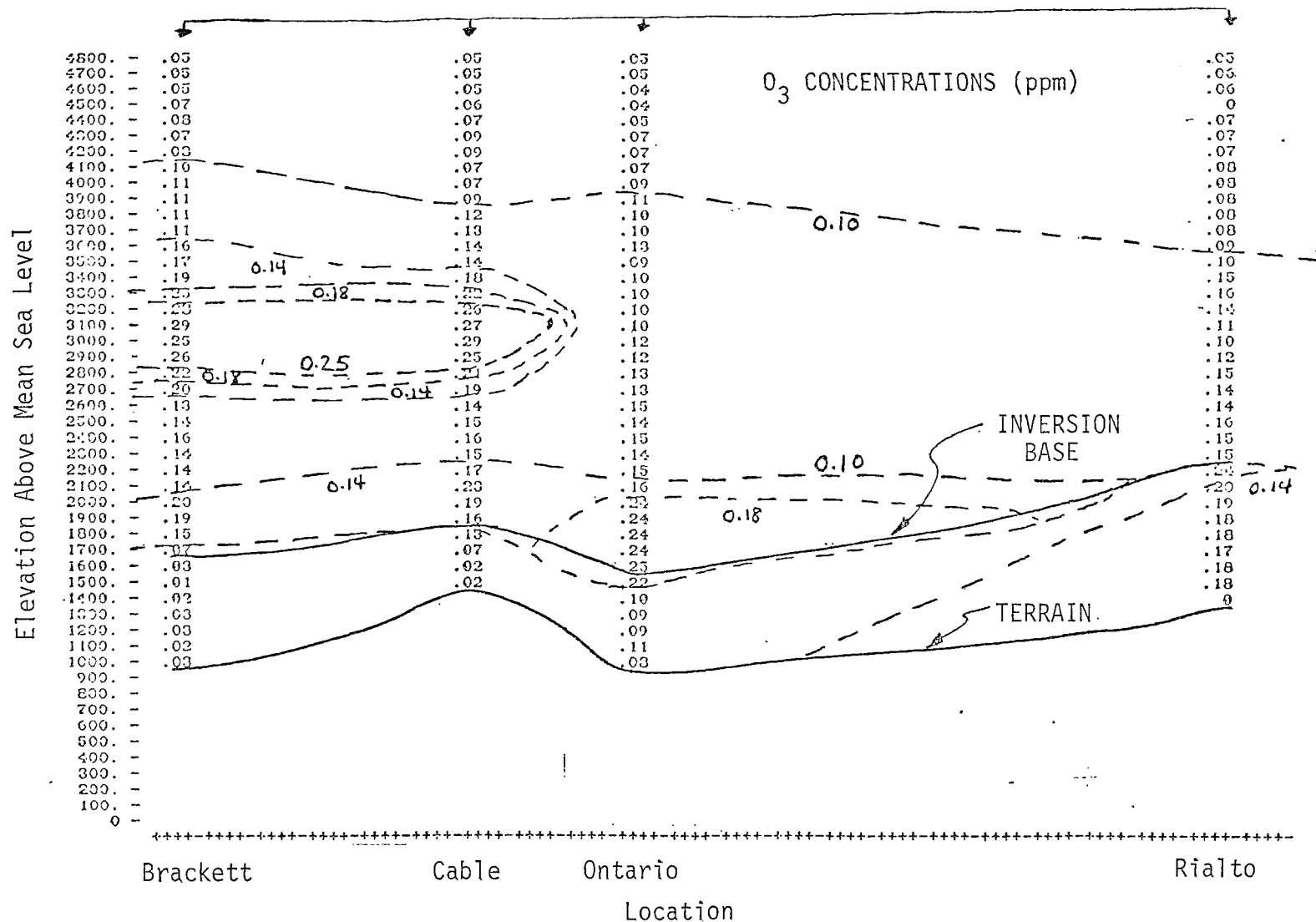


FIGURE 21. DISTRIBUTION OF  $O_3$  ALOFT BETWEEN BRACKETT AND RIALTO DURING THE MORNING OF 11 JULY 1973

$$\Delta H = H_t(x,y,t) - h(x,y) \quad ,$$

where

$H_t(x,y,t)$  = elevation of the top of the inversion layer,  
 $h(x,y)$  = terrain elevation.

The effect of trapping pollutants below the inversion layer can be accounted for through the height dependence of the vertical diffusivity. Whereas relatively large values of  $K_v$  are used in the mixed layer, the values in the stable inversion layer are much smaller, reflecting the suppression of turbulent mixing.

## IV EVALUATION OF ALTERNATIVE TECHNIQUES FOR INTEGRATING THE SPECIES CONTINUITY EQUATIONS

James P. Meyer

### A. INTRODUCTION

In essence, the SAI atmospheric photochemical simulation program is based on the solution of the nonlinear, multidimensional species transport equation

$$\frac{\partial c_i}{\partial t} + \underline{v} \cdot \underline{\nabla} c_i = \underline{\nabla} \cdot K \underline{\nabla} c_i + R_i + S_i \quad , \quad (29)$$

which, for convenience, has been transposed [Reynolds et al. (1973)] into the form

$$\begin{aligned} \frac{\partial (\Delta H c_i)}{\partial \tau} + \frac{\partial}{\partial \rho} (u \Delta H c_i) + \frac{\partial}{\partial \eta} (v \Delta H c_i) + \frac{\partial}{\partial \rho} (w c_i) \\ = \frac{\partial}{\partial \rho} \left( K_H \Delta H \frac{\partial c_i}{\partial \rho} \right) + \frac{\partial}{\partial \eta} \left( K_H \Delta H \frac{\partial c_i}{\partial \eta} \right) + \frac{\partial}{\partial \rho} \left( K_V \Delta H \frac{\partial c_i}{\partial \rho} \right) \\ + R_i \Delta H + S_i \Delta H \quad . \end{aligned} \quad (30)$$

In general, no closed-form analytical solution exists for this highly complex partial differential equation for all possible initial and boundary conditions. Hence, one is forced to resort to approximation techniques, most notably finite difference schemes, to find a solution.



The choice of an appropriate numerical technique for inclusion in the airshed model involves two primary considerations. First, the accuracy of the solution obtained must be such that the error in the predicted concentrations is predominately the result of errors in model inputs rather than errors introduced by the numerical technique itself. Second, the final choice between alternative techniques capable of solving the governing equations to a specified error tolerance should be based on minimizing computing costs. In view of these considerations and the variety of numerical techniques available for solving the equations of interest, care must be taken to choose a method that offers an optimal blend of numerical accuracy and computational efficiency.

Currently, a finite difference approach termed the method of fractional steps [Yanenko (1969)] is employed in the SAI model. The basic feature of this method is that the four-dimensional governing equation in  $(z, n, \rho, \tau)$  is split into three two-dimensional equations in  $(z, \tau)$ ,  $(n, \tau)$ , and  $(\rho, \tau)$ . The details of this analysis are given elsewhere [Reynolds et al. (1973)]. With this type of approach, errors are introduced into the solution in the following ways:

- > Through the introduction of truncation errors caused by the finite differencing of the partial derivatives in the transport equation.
- > Through the decomposition of a three-dimensional equation into a sequence of three two-dimensional equations.

As an example of truncation error effects, Harlow and Amsden (1970) showed that for the one-dimensional advection equation

$$\frac{\partial C}{\partial t} + u \frac{\partial C}{\partial x} = 0 \quad , \quad (31)$$

a numerical solution involving a first-order finite difference approximation introduces an error on the order of

$$u \frac{\delta x}{2} \left( 1 - u \frac{\delta t}{\delta x} \right) \frac{\partial^2 c}{\partial x^2} \quad (32)$$

into the calculation. Since the term  $\partial^2 c / \partial x^2$  appears, this error has been called "numerical diffusion." Its effect is to smooth an initially peaked distribution over a large portion of the modeling area. This reduces the resolution of the solution so much that in extreme cases it becomes nonexistent. In an attempt to reduce the truncation error effects in the SAI model arising from the treatment of the horizontal advection terms, we previously carried out numerical experiments using various second- and fourth-order difference approximations. Although we observed some reduction in truncation error using the higher order methods, many of these techniques also had the undesirable property of producing negative concentrations in the vicinity of steep concentration gradients. We finally selected an uncentered second-order method described by Price et al. (1966), which is somewhat more accurate than the first-order advection approximations, and which, at the same time, presented no difficulties with regard to the prediction of negative concentrations in the initial application of the model to the Los Angeles basin.

In the fractional step technique, the decomposition process for the  $\eta$ ,  $\zeta$ , and  $\rho$  directions introduces a sequence of higher order partial derivatives that would not normally appear in the transport equation. Although the effect of these terms is difficult to quantify a priori, their impact on model predictions can be examined by comparing predicted pollutant concentrations with known analytical solutions of the governing equations. In the discussion presented in Volume I of the validity of the grid and trajectory model concepts, we noted that errors introduced into the grid model predictions by the numerical integration technique can be as large as 50 percent in some situations. These errors are mainly due to the finite

difference treatment of the horizontal advection terms. Thus, the objective of the present study is to test and assess various alternative numerical approximations to the transport terms in the governing equations. In this analysis, our aim is to provide recommendations regarding the course of future efforts to improve the numerical integration procedure employed in the airshed model.

In the work described next, the emphasis was on the development of an analytical solution to the diffusion equation and on a comparison of the analytical results with the corresponding results obtained from various approximate integration schemes. Because of the difficulties involved in developing solutions to the diffusion equation, only a simplified one-dimensional, linear, time-dependent result could be obtained. Thus, we are able to assess the errors associated with various numerical methods for a one-dimensional flow problem in which the pollutant is allowed to undergo a first-order chemical reaction. Clearly, this test situation is not completely representative of a full photochemical airshed simulation. However, numerical techniques incapable of producing sufficiently accurate results in a one-dimensional linear problem cannot be expected to perform better in a multidimensional nonlinear application.

Since it was not possible to carry out the tests for photochemical pollutants, we are unable to assess the effect of inaccuracies introduced in the treatment of the transport terms on error propagation, especially when nonlinear chemical interactions are taking place. In addition, the test results do not illustrate the errors caused by using the fractional step methodology to treat a multidimensional problem. In spite of these limitations, however, we have been able to delineate two numerical methods that seem to represent a significant improvement over the finite difference scheme currently employed in the SAI airshed model.

## B. AVAILABLE METHODS

A variety of methods have been developed to solve partial differential equations. In general, they fall into two categories: finite difference schemes and particle techniques. The former, which are well developed, include the work of Price et al. (1966), Fromm (1969), Crowley (1968), and, more recently, Boris and Book (1973). In contrast, particle-in-cell methods are relatively current; they include the contributions of Sklarew et al. (1971) and Egan and Mahoney (1972).

For the purpose of analysis, a simplified solution of the diffusion equation was developed and the results of this calculation were compared to the results of the suitably programmed approximation schemes. The equation chosen for this work was the one-dimensional transport equation,

$$\frac{\partial c}{\partial t} = D \frac{\partial^2 c}{\partial x^2} - u \frac{\partial c}{\partial x} - kc \quad , \quad (33)$$

in which  $u$ ,  $D$ , and  $k$  were considered constant. The following boundary conditions were imposed:

- > Initially, no material is in the modeling region, i.e.

$$c(0,x) = 0 \quad . \quad (34)$$

- > There is zero concentration gradient at infinity, i.e.,

$$\frac{\partial c}{\partial x}(t,\infty) = 0 \quad . \quad (35)$$

- > There is a uniform concentration at the inlet, i.e.,

$$c(t,0) = 1 \quad . \quad (36)$$

We evaluated the following methods:

- > Price scheme
- > Crowley second- and fourth-order methods
- > SHASTA method
- > Galerkin method
- > Particle-in-cell techniques
- > Egan and Mahoney method.

In the following subsections we briefly describe each method.

### 1. The Price Scheme

Currently, the SAI model uses a method proposed by Price, Varga, and Warren (1966). For the test problem selected, this method has the finite difference form

$$c_j^{n+1} = c_j^n + \frac{K_H \delta t}{(\delta x)^2} \left( c_{j+1}^n - 2c_j^n + c_{j-1}^n \right) - \frac{u \delta t}{2\delta x} \left( 3c_j^n - 4c_{j-1}^n + c_{j-2}^n \right) - k \delta t c_j^n . \quad (37)$$

This approximation has errors that are first order in time  $(\delta t)$  and second order in distance  $(\delta x)^2$ .

Since the solution is explicit in time, definite limits of stability exist. These limits can be developed by assuming that the solution of the transient equation can be written in the complex Fourier form

$$c(t, j\Delta x) = \psi(t) e^{ij\Delta x} , \quad (38)$$

where

$$i = \sqrt{-1} , \quad (39)$$

After considerable algebraic manipulation and stipulation of the requirement

$$\left| \frac{\psi(t + \Delta t)}{\psi(t)} \right| < 1 \quad , \quad (40)$$

we obtain

$$k\delta t < 2 \quad , \quad (41)$$

$$u \frac{\delta t}{\delta x} < 1 \quad , \quad (42)$$

$$u \frac{\delta t}{2\delta x} + K_H \frac{\delta t}{(\delta x)^2} + k \frac{\delta t}{4} < \frac{1}{2} \quad (43)$$

as the conditions required for stability to occur.

## 2. The Crowley Second- and Fourth-Order Methods

To enhance the accuracy of the finite difference approximations used in formulating the advective terms of the governing equations, Crowley (1965) developed both second- and fourth-order centered difference algorithms for these terms. For the test problem, the second-order method has the expansion

$$\begin{aligned} c_j^{n+1} = & \left( \beta - \frac{\alpha}{2} + \frac{\alpha^2}{2} \right) c_{j+1}^n + \left( 1 - 2\beta - \alpha^2 - k\delta t \right) c_j^n \\ & + \left( \beta + \frac{\alpha}{2} + \frac{\alpha^2}{2} \right) c_{j-1}^n \quad , \end{aligned} \quad (44)$$

where

$$\beta = \frac{K_H \delta t}{(\delta x)^2} \quad , \quad (45)$$

$$\alpha = \frac{u \delta t}{\delta x} \quad . \quad (46)$$

The corresponding fourth-order expansion has the form

$$\begin{aligned}
 c_j^{n+1} = & \left( \frac{\alpha}{16} - \frac{\alpha^2}{48} - \frac{\alpha^3}{12} + \frac{\alpha^4}{24} \right) c_{j+2}^n + \left( \beta - \frac{5\alpha}{8} + \frac{7}{12} \alpha^2 + \frac{1}{6} \alpha^3 - \frac{1}{6} \alpha^4 \right) c_{j+1}^n \\
 & + \left( 1 - 2\beta - k\delta t - \frac{27}{24} \alpha^2 + \frac{\alpha^4}{4} \right) c_j^n + \left( \beta + \frac{5\alpha}{8} + \frac{7}{12} \alpha^2 - \frac{1}{6} \alpha^3 - \frac{1}{6} \alpha^4 \right) c_{j-1}^n \\
 & + \left( \frac{-\alpha}{16} - \frac{\alpha^2}{48} + \frac{\alpha^3}{12} + \frac{\alpha^4}{24} \right) c_{j-2}^n \quad . \quad (47)
 \end{aligned}$$

The terms "second order" and "fourth order" refer to the relative amount of error incurred by these expansions; the sizes of such error are  $(\delta x)^2$  and  $(\delta x)^4$ , respectively.

### 3. The SHASTA Method

Instead of relying on conventional finite difference techniques, which occasionally predict negative concentrations--particularly in areas of strong gradients--Boris and Book (1973) developed the SHASTA method, or flux corrected transport algorithm, to model the advective part of the transport equation. This technique is based on the principle of positivity (that is, that the concentration should always be positive) and does not rely on an asymptotic ordering in the equation solution. The algorithm is stable, mass conservative, and essentially second order in regions where the concept of order is meaningful.

Conceptually, the algorithm consists of two stages: a transport step and a subsequent antidiffusion step. During the first stage, the material in adjacent cells is advected in a trapezoidal manner such that the total amount of material within the cell is conserved. During the transport process, a certain amount of numerical diffusion is introduced into the calculation. This error is removed in the antidiffusion step.

In mathematical form, the transport stage has the algebraic expression

$$\tilde{c}_j^{n+1} = \frac{1}{2} \phi_-^2 (c_{j-1}^n - c_j^n) + \frac{1}{2} \phi_+^2 (c_{j+1}^n - c_j^n) + (\phi_+ + \phi_-) c_j^n \quad , \quad (48)$$

where

$$\phi_{\pm} = \frac{\frac{1}{2} \mp u_j^{1/2} \frac{\delta t}{\delta x}}{1 \pm \left( u_{j\pm 1}^{1/2} - u_j^{1/2} \right) \frac{\delta t}{\delta x}} \quad , \quad j = 1, \dots, n \quad , \quad (49)$$

and where  $u_j^{1/2}$  refers to the velocity at the  $j$ -th location at time  $t + (\delta t/2)$ . Completion of the antidiffusion step requires the expression

$$c_j^{n+1} = \tilde{c}_j^{n+1} - \frac{1}{8} \left( \tilde{c}_{j+1}^{n+1} - 2\tilde{c}_j^{n+1} + \tilde{c}_{j-1}^{n+1} \right) \quad . \quad (50)$$

To account for cases in which material may be advected either into or out of the modeling region, the SHASTA method applies the following rules at the end points:

- > Left-hand side
  - If  $v_1 > 0$ , then  $c_0$  and  $v_0$ , the upwind boundary conditions, must be specified.
  - If  $v_1 < 0$ , then  $\partial c / \partial x = 0$ , and  $c_0 = c_1$  and  $v_0$  must be specified.
- > Right-hand side
  - If  $v_n > 0$ , then  $\partial c / \partial x = 0$ , and  $c_{n+1} = c_n$  and  $v_{n+1}$  must be specified.
  - If  $v_n < 0$ , then  $c_{n+1}$  and  $v_{n+1}$ , the incoming concentration and velocity, respectively, must be specified.

Since the SHASTA algorithm treats only the advective parts of the continuity equation, the concurrent diffusion and kinetic steps of the governing equation must be treated as subsequent operations. Hence, the system heavily relies on the method of fractional steps.



For the test case, the advective equation has the form

$$\tilde{c}_j^{*n+1} = \frac{1}{2} \phi_-^2 (c_{j-1}^n - c_j^n) + \frac{1}{2} \phi_+^2 (c_{j+1}^n - c_j^n) + (\phi_+ + \phi_-) c_j^n, \quad (51)$$

$$\phi_{\pm} = \frac{1}{2} \mp u \frac{\delta t}{\delta x}, \quad (52)$$

$$c_j^{*n+1} = \tilde{c}_j^{*n+1} - \frac{1}{8} (\tilde{c}_{j+1}^{*n+1} - 2\tilde{c}_j^{*n+1} + \tilde{c}_{j-1}^{*n+1}) \quad (53)$$

The diffusive and kinetic terms become

$$c_j^{n+1} = \beta \tilde{c}_{j+1}^{*n+1} + (1 - 2\beta - k\delta t) \tilde{c}_j^{*n+1} + \beta \tilde{c}_{j-1}^{*n+1}, \quad (54)$$

$$\beta = \frac{K_H \delta t}{(\delta x)^2}. \quad (55)$$

#### 4. The Galerkin Method

Finite element methods represent a significant departure from finite difference techniques as a tool in solving partial differential equations. Unlike finite difference equations, which approximate derivatives at specific locations, finite element techniques approximate functions over an entire domain [Zienkiewicz (1971), Pinder and Gray (1974)].

To develop finite element solutions, one must follow four steps:

- > Subdivide the domain of interest into a finite number of elements defined by node points.
- > Approximate the dependent variables in terms of their unknown node point values within each element. This insures the continuity of the dependent variable across the element.

- > Minimize an appropriate measure of error such that a set of simultaneous equations results.
- > Solve the resulting set of equations for the node point values.

The distinct advantages of finite element techniques are their ability to model arbitrary geometric areas without a loss of convergence and their generally greater stability compared with corresponding finite difference systems.

Two distinct classes of finite element solutions exist. The Rayleigh-Ritz procedure requires the minimization of a function associated with a defining differential equation. Although this is an extremely useful method, often one cannot determine the functional form associated with the differential equation. Thus, the method has limited applicability. A more general, but somewhat less mathematically elegant, approach is the Galerkin technique [Keldysh (1964), McMichael and Thomas (1973)]. This method requires merely that the integral of the approximate solution be orthogonal to each of the basis functions spanning the solution space. For example, the linear differential equation

$$\frac{\partial c}{\partial t} + u \frac{\partial c}{\partial x} - D \frac{\partial^2 c}{\partial x^2} + kc = 0 \quad (56)$$

is written in operator form as

$$L(c) = \left( \frac{\partial}{\partial t} + \frac{u \partial}{\partial x} - \frac{D \partial^2}{\partial x^2} + k \right) c \quad (57)$$

and is assumed to have a solution of the form

$$\hat{c} = \sum_{i=1}^n a_i \phi_i, \quad (58)$$

where there are  $n$  nodes in the domain of  $c$ . Then, the Galerkin procedure requires that

$$\int_V L(\hat{c}) \phi_i \, dv = 0 \quad , \quad i = 1, 2, \dots, n \quad , \quad (59)$$

so that the coefficients  $(a_i)$  can be determined.

As an illustration of the technique, consider the following sample problem:

$$\frac{\partial c}{\partial t} + u \frac{\partial c}{\partial x} - D \frac{\partial^2 c}{\partial x^2} + kc = 0 \quad . \quad (60)$$

Assume a solution of the form

$$\hat{c} = \sum_{i=1}^n a_i(t) \phi_i(x) \quad . \quad (61)$$

Multiply the differential equation by  $\phi_i$ , and integrate the result over its entire domain:

$$\int_0^L \frac{\partial \hat{c}}{\partial t} \phi_i \, dx + u \int_0^L \frac{\partial \hat{c}}{\partial x} \phi_i \, dx - D \int_0^L \frac{\partial^2 \hat{c}}{\partial x^2} \phi_i \, dx + \int_0^L k \hat{c} \phi_i \, dx = 0 \quad , \quad (62)$$

$i=1, \dots, n \quad .$

By using Green's theorem,

$$\int_0^L \frac{\partial^2 \hat{c}}{\partial x^2} \phi_i \, dx = - \int_0^L \frac{\partial \hat{c}}{\partial x} \frac{\partial \phi_i}{\partial x} \, dx + \phi_i \frac{\partial \hat{c}}{\partial x} \Big|_0^L \quad , \quad (63)$$

and by substituting the expanded series into the equation, we obtain

$$\begin{aligned}
& \int_0^L \sum_j^n \frac{\partial a_j}{\partial t} \phi_i \, dx + u \int_0^L \sum_j^n a_j \frac{\partial \phi_j}{\partial x} \phi_i \, dx + D \int_0^L \sum_j^n a_j \frac{\partial \phi_j}{\partial x} \phi_i \, dx + k \int_0^L \sum_j^n a_j \phi_j \phi_i \, dx \\
& = D \phi_i \sum_j^n a_j \frac{\partial \phi_j}{\partial x} \Big|_0^L, \quad i = 1, 2, \dots, n \quad . \quad (64)
\end{aligned}$$

Once the functions  $\phi_i$  are selected, a series of matrix equations result. They are of the form

$$\underline{A} \frac{d\underline{a}}{dt} + \underline{B}\underline{a} = \underline{S}, \quad (65)$$

where

$\underline{A}, \underline{B}$  = coefficient matrices,

$\underline{a}, \underline{S}$  = column vectors.

These equations can be easily solved by using a Crank-Nicholson technique to approximate  $\underline{a}$  between times  $t$  and  $t + \delta t$ . The initial conditions  $\underline{a}_0$  must be specified.

For the work described in this report, we selected chapeau functions of the form

$$\phi_1 = \begin{cases} \frac{-x}{x_1} & , \quad 0 < x < x_1 \\ 0 & , \quad \text{elsewhere} \end{cases} \quad (66)$$

$$\phi_i = \begin{cases} \frac{x - x_{i-1}}{x_i - x_{i-1}} & , \quad x_{i-1} \leq x \leq x_i \\ \frac{x_{i+1} - x}{x_{i+1} - x_i} & , \quad x_i \leq x \leq x_{i+1} \\ 0 & , \quad \text{elsewhere} \end{cases} \quad (67)$$

$$\phi_n = \begin{cases} \frac{x - x_{n-1}}{x_n - x_{n-1}} & , \quad x_{n-1} \leq x \leq x_n \\ 0 & , \quad \text{elsewhere} \end{cases} \quad (68)$$

Correspondingly, the matrices  $\underline{\underline{A}}$  and  $\underline{\underline{B}}$  had the tridiagonal form

$$\underline{\underline{A}} = \frac{\delta x}{6} \begin{bmatrix} 1 & 4 & 1 & 0 & 0 & \dots & 0 \\ 0 & 1 & 4 & 1 & 0 & \dots & 0 \\ 0 & 0 & 1 & 4 & 1 & \dots & 0 \\ 0 & \dots & 0 & \dots & 1 & 4 & 1 \end{bmatrix} , \quad 1 \leq i \leq n-1 \quad (69)$$

$$\underline{\underline{B}} = \begin{bmatrix} -\alpha & \beta & -\gamma & 0 & \dots & 0 \\ 0 & -\alpha & \beta & -\gamma & \dots & 0 \\ \vdots & & & & & \\ 0 & \dots & & -\alpha & \beta & -\gamma \end{bmatrix} , \quad (70)$$

where

$$\alpha = \frac{D}{\delta x} + \frac{u}{2} - \frac{k\delta x}{6} ,$$

$$\beta = \frac{2D}{\delta x} + \frac{2k\delta x}{3} ,$$

$$\gamma = \frac{D}{\delta x} - \frac{u}{2} - \frac{k\delta x}{2} ,$$

while  $\underline{\underline{S}}$  was zero everywhere. The boundary condition yielded the terms

$$a_1 = 1 \quad , \quad (71)$$

$$a_n = a_{n-1} \quad . \quad (72)$$

## 5. Particle-in-Cell Techniques

Harlow and Welch (1965) first developed particle-in-cell methods for use in the analysis of free-surface fluid mechanical problems. Since their initial development, these techniques have been expanded to include such variations as marker-in-cell (MAC) and HYDRO codes.

An interesting adaptation of the particle-in-cell algorithm has been developed by Sklarew (1971) to model mesoscale air pollution problems. In this variant, pollutant particles representing a fixed weight of material are generated in quantities proportional to the ambient pollutant concentration. As time passes, the particle positions are tracked in space by determining the incremental changes in their locations caused by advective and diffusive forces. Sklarew chose to rewrite the species transport equation in the form

$$\frac{\partial c}{\partial t} + \nabla \cdot (\underline{v}c - D\nabla c) = 0 \quad , \quad (73)$$

where

$\underline{v}$  = mean velocity,

$D\frac{\nabla c}{c}$  = diffusive velocity.

With these definitions, it is possible to increment the radial position of each particle during each time step by a corresponding contribution due to mean fluid flow ( $\underline{v}\delta t$ ) and diffusional motion  $[(D\nabla c\delta t)/c]$ .

To account for photochemistry, one must assume that, within each cell, the particle weights can be summed to form a representative cell concentration and that the reaction occurs as if the material is homogeneously distributed throughout the cell. At the end of the reaction sequence, each particle is reweighted proportionally to the change in the cell concentration of the individual species:

$$m_i(t + \Delta t) = m_i(t) \frac{c(t + \Delta t)}{c(t)} \quad , \quad (74)$$

and the transport process is subsequently allowed to occur.

Hotchkiss and Hirt (1972) improved the modeling of the diffusional part of the transport process at Los Alamos. Their contribution was the representation of the diffusive movement as a random particle motion of the form

$$\delta x_{DIFF} = \sqrt{4D\delta t} \psi \quad , \quad (75)$$

where  $\psi$  is a randomly distributed Gaussian variable. Their work indicates that their method results in substantially better agreement than the method of Sklarew in areas of strong concentration gradients near point sources. This modification overcomes the difficulties in computing the finite difference approximation needed by Sklarew in calculating the gradient of the concentration.

Fundamentally, the problem with all particle-in-cell methods is the essential question of exactly what a particle represents and over what area should it be considered to have domain--classically an Eulerian-Lagrangian paradox. A recurrent problem in using this type of analysis is the background noise that must be accommodated when a particle leaves one cell and enters another. This quantum jump can be smoothed to some extent by volume-averaging the particle over the adjacent cells it intercepts. However, such a procedure may well extend the domain of a pollutant into regions that it does not actually represent. To circumvent this problem, one can always increase the number of particles associated with a problem, but at the added expense of dramatically increasing computer storage and computational time.

## 6. The Method of Egan and Mahoney

One of the more interesting developments in the analysis used in air pollution modeling has been the work of Egan and Mahoney (1970, 1971, 1972). In essence, their approach is to follow air parcels as they move within a

grid network, taking into account the zero, first, and second moments of the pollutant distribution. With this type of analysis, it is possible to maintain extremely high resolution and to eliminate almost entirely the numerical diffusion caused by errors associated with approximations for the advection terms.

Unfortunately, the method, which is owned proprietarily by Environmental Research and Technology in Lexington, Massachusetts, is only paraphrased in the open literature. Hence, the analysis presented here is cursory and represents only a superficial evaluation of the utility of this method.

### C. A TEST PROBLEM

To provide a common basis of comparison for each of the methods, we posed the following two-dimensional problem ( $x - t$ ).

Consider a semi-infinite strip extending from zero to infinity over which the species transport equation is assumed to hold and a first-order irreversible reaction occurs:

$$\frac{\partial c}{\partial t} + u \frac{\partial c}{\partial x} = D \frac{\partial^2 c}{\partial x^2} - kc \quad . \quad (76)$$

Specify that all parameters ( $u$ ,  $D$ , and  $k$ ) are constant, and impose the following boundary conditions:

- > Initially no material is in the modeling region, i.e.,

$$c(0,x) = 0 \quad , \quad 0 \leq x \leq \infty \quad . \quad (77)$$

- > There is zero flux of infinity, i.e.,

$$\frac{\partial c}{\partial x} (t,\infty) = 0 \quad . \quad (78)$$



> There is a uniform concentration at the inlet, i.e.,

$$c(t,0) = 1 \quad . \quad (79)$$

To develop a solution, take the Laplace transform of the defining differential equation

$$s\bar{c} + u \frac{d\bar{c}}{dx} = D \frac{d^2\bar{c}}{dx^2} - k\bar{c} \quad . \quad (80)$$

Then rearrange the equation in the form

$$D \frac{d^2\bar{c}}{dx^2} - u \frac{d\bar{c}}{dx} - (k + s)\bar{c} = 0 \quad . \quad (81)$$

Next, solve for  $\bar{c}$ :

$$\bar{c} = A e^{[(Pe/2) - \phi]\lambda} + B e^{[(Pe/2) + \phi]\lambda} \quad , \quad (82)$$

where

$$Pe = \frac{uL}{D} \quad , \quad (83)$$

$$\lambda = \frac{x}{L} \quad , \quad (84)$$

$$\phi = \frac{L \sqrt{u^2 + 4D(k+s)}}{2D} \quad . \quad (85)$$

By imposing the boundary condition

$$\frac{d\bar{c}}{dx} = 0 \quad \text{at } x = \infty \quad , \quad (86)$$

we find that

$$B = 0 \quad (87)$$

and, hence,

$$\bar{c} = A e^{[(Pe/2) - \phi]\lambda} \quad . \quad (88)$$

At the leading edge of the system,

$$\bar{c} = \frac{1}{s} = A \quad \text{at } \lambda = 0 \quad , \quad (89)$$

and the complete solution in transform space becomes

$$\bar{c} = \frac{e^{[(Pe/2) - \phi]\lambda}}{s} \quad . \quad (90)$$

The inversion of this Laplace transform is nontrivial and requires some rather advanced techniques [Mikusinski (1959)]. Once inverted, the solution takes the form

$$c(\lambda, \eta) = \frac{1}{2} \left\{ e^{[(Pe/2) - \psi]\lambda} \left[ 1 + \operatorname{erf}\left(\frac{\psi\eta}{2} - \frac{\lambda}{\eta}\right) \right] + e^{[(Pe/2) + \psi]\lambda} \left[ 1 - \operatorname{erf}\left(\frac{\psi\eta}{2} + \frac{\lambda}{\eta}\right) \right] \right\} \quad , \quad (91)$$

where

$$\eta = \frac{\sqrt{4Dt}}{L} \quad (92)$$

$$\psi = \sqrt{\frac{kL^2}{D} + \left(\frac{Pe}{2}\right)^2} \quad . \quad (93)$$

Later, we will need to know the flux of material entering the system at the origin. To compute this term, we must obtain the derivative

$$\frac{\partial c}{\partial x}(0, t) \quad . \quad (94)$$

Instead of using  $x - t$  space, which involves the derivative of integrals, it is simpler to compute the derivative in  $x - s$  space and invert the obtained transform.

The inversion of the derivative

$$\frac{dc}{dx}(0,s) = \frac{1}{L} \left[ \frac{Pe}{2s} - \frac{\sqrt{\left(\frac{Pe}{2}\right)^2 + \frac{L^2}{D}} (k + s)}{s} \right] \quad (95)$$

is given by

$$\frac{\partial c}{\partial x}(t,0) = \frac{u}{2D} - \left[ \frac{1}{\sqrt{\pi Dt}} e^{-\Omega t} + \sqrt{\frac{\Omega}{D}} \operatorname{erf}(\Omega t) \right], \quad (96)$$

where

$$\Omega = k + \frac{u^2}{4D}. \quad (97)$$

Consequently, the total flux

$$N(0,t) = uc - D \frac{\partial c}{\partial x} \quad (98)$$

is represented by

$$N(0,t) = \frac{u}{2} + \sqrt{\frac{D}{\pi t}} e^{-\Omega t} + \sqrt{\Omega D} \operatorname{erf}(\sqrt{\Omega t}) \quad (99)$$

for a uniform concentration of one at the origin.

During the time interval  $t$  to  $t + \delta t$ , the amount of material entering the first cell,

$$\int_t^{t+\delta t} N(0,t') dt' = Q, \quad (100)$$

can be approximated by

$$Q = u \frac{\delta t}{2} + \sqrt{\frac{D}{\Omega}} \left[ \operatorname{erf}(\sqrt{\Omega(t + \delta t)}) - \operatorname{erf}(\sqrt{\Omega t}) \right] \\ + \frac{D\delta t}{2} \sqrt{\frac{\Omega}{D}} \left[ \operatorname{erf}(\sqrt{\Omega(t + \delta t)}) + \operatorname{erf}(\sqrt{\Omega t}) \right] \quad . \quad (101)$$

Note that at long times the inflow approaches the quantity

$$Q = \left( \frac{u}{2} + \sqrt{D\Omega} \right) \delta t \quad ; \quad (102)$$

and if  $k = 0$ ,

$$Q = u\delta t \quad , \quad (103)$$

and pure advection occurs. One effect of having the reactive term is to enhance the inflow above the purely advective amount.

In Section D, we present figures in which the analytical solution is always represented by continuous curves.

#### D. RESULTS

To test each method under conditions similar to those encountered in atmospheric modeling, we decided to allow the Peclet number ( $uL/D$ ) and the kinetic rate constant to vary over a wide range of values. For each run, the incremental spatial distance was set at 2 miles, and the total length of the region was assumed to be 50 miles. Each hour was subdivided into 12 five-minute segments. In all cases, the free-stream velocity was held at 4 miles per hour, and the diffusivity was allowed to vary as shown in Table 25.

Table 25  
VALUES OF DIFFUSIVITY AND PECLET NUMBER  
FOR THREE CASE STUDIES

<u>Case</u>	<u>Diffusivity (<math>\text{m}^2\text{sec}^{-1}</math>)</u>	<u>Peclet Number</u>
1	200	720
2	700	206
3	2000	72

These runs varied from almost a square wave propagation (Pec = 720) to a smooth diffusion problem (Pec = 72). For each method tested, we executed a series of 12 runs.

The corresponding kinetic values associated with these transport conditions are given in Table 26.

Table 26  
KINETIC CONSTANTS FOR EACH CASE

<u>Case</u>	<u>Kinetic Constant (<math>\text{sec}^{-1}</math>)</u>
1	0
2	$10^{-4}$
3	$10^{-3}$
4	$2 \times 10^{-3}$

These values include the cases of both no reaction ( $k = 0$ ), and a relatively fast reaction ( $k = 2 \times 10^{-3}$ ). Two intermediate reaction rates were also considered.

In the presentation of the data, we included only those cases in which no reaction occurs ( $k = 0$ ;  $Pec = 720, 206$ , and  $72$ ) and those of highest Peclet number ( $Pec = 720$ ,  $k = 10^{-4}$  and  $10^{-3}$ ). We chose these cases because they are somewhat representative of the range of conditions that can occur in mesoscale modeling systems. The following subsections present a brief synopsis of the performance of each numerical scheme. In each figure presenting our results, the analytical solution is given at 3, 6 and 9 hours from the start of the test.

### 1. The Price Method

As used in the SAI model, the Price scheme is inadequate for accurately modeling mesoscale phenomena. In all cases, the method overpredicts the actual ground-level concentration and transposes the wave to the left because of phase shift, as shown in Figures 22 through 23. Although some improvement occurs in cases having high Peclet numbers, this agreement is not substantial enough to reduce dramatically the errors involved. Thus, we rated the method as poor.

### 2. The Crowley Second- and Fourth-Order Methods

The accuracy of prediction can be substantially increased by using either the Crowley second-order or the Crowley fourth-order approximation, as shown in Figures 24 through 25. In cases where an extremely strong concentration gradient appears ( $Pec = 720$ ), the second-order scheme exhibits some rather erratic results near the top of the wave. Aside from such cases, both methods provide essentially the same results.

In the implementation of these methods in actual simulation programs, some observers have noticed that higher order methods occasionally predict negative concentrations in regions having large concentration gradients.

Although this result did not appear in our work, one should keep it in mind as a limitation when using these methods.

### 3. The SHASTA Method

One of the simplest and yet most efficient methods of solving the species transport equation is the SHASTA method. Figure 26 presents its performance results. Not only does the method exhibit a relatively high degree of accuracy, but also, unlike many of the alternative finite difference methods, it never predicts negative results. Thus, it is the best choice available of an explicit solution algorithm.

### 4. The Galerkin Method

Of all the methods tested, the Galerkin technique provided the most accurate results over the widest range of conditions selected in this study, as shown in Figure 27. The predicted results were always within 1 percent of the analytical solution, and for many individual points in the analysis, the results exhibited zero error. Not only could the method be used to model situations in which extremely strong concentration gradients appeared, but also it could accurately treat cases involving very fast reaction schemes. Although the method is implicit and hence iterative in solution, its execution time appears to be comparable to a corresponding implicit Price scheme as currently used on the SAI model.

We thus recommend that this technique be used for cases where high resolution is desirable, even at the expense of increased computing time and programming effort.

### 5. Particle-In-Cell Methods

Accuracy in particle-in-cell methods is a strong function of the number of particles used. In this study, as the particle size was reduced from 80 to 40 to 20 weight units, the average error was reduced from 9.6 to 6.3 to

3.3 percent, respectively. Figure 28 presents the results obtained using this type of method. These methods proved successful at simulating both reactive and nonreactive systems, and they were able to treat steep gradients exceptionally well.

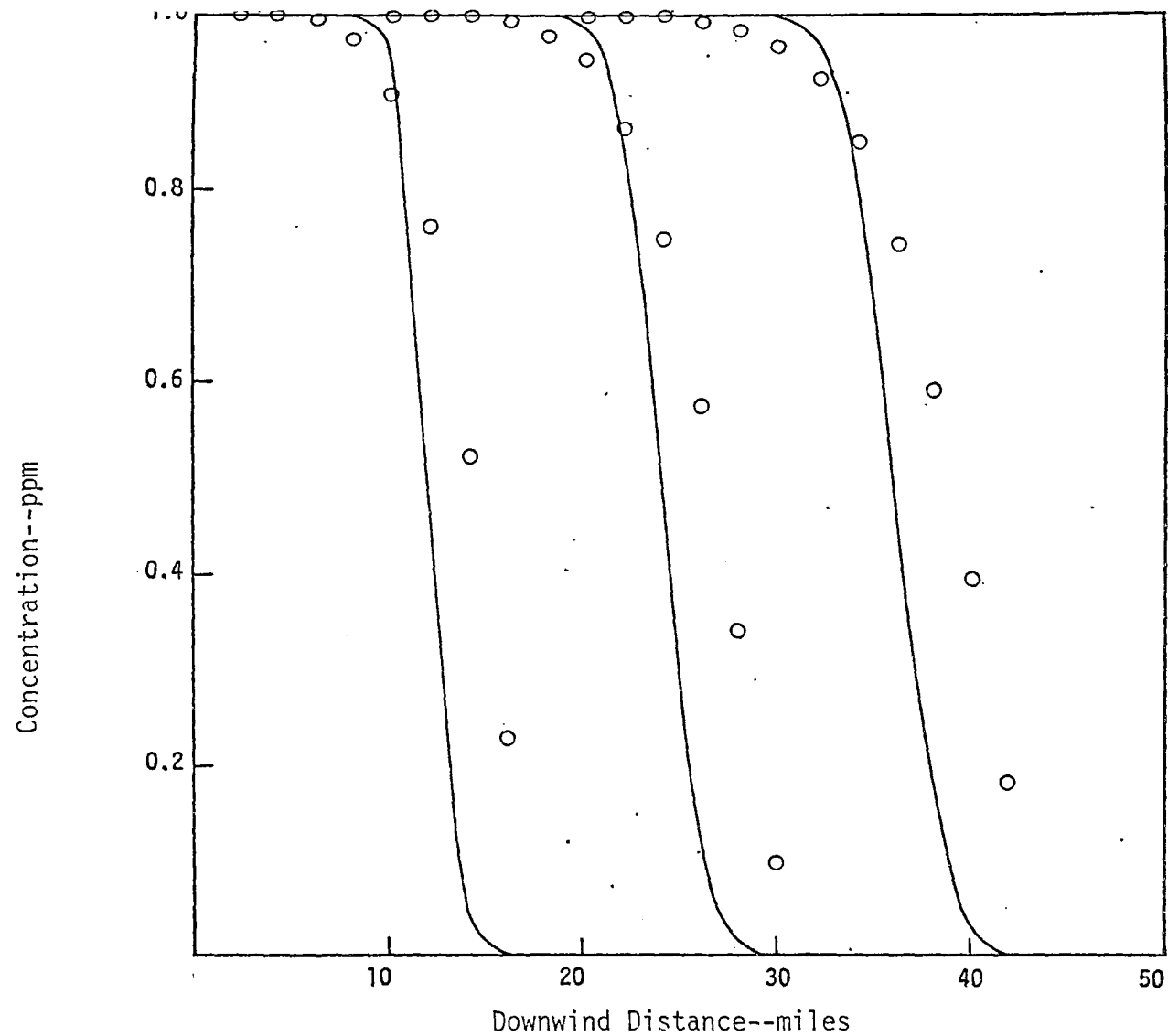
A rather interesting aspect of this analysis is that such techniques show greater accuracy at lower rather than higher Peclet numbers, as would normally be expected to occur. The reason for this phenomenon is probably the following: As the diffusivity is increased, the diffusive component in the Hotchkiss-Hirt analysis displaces the particle by an amount proportional to the square root of the diffusivity. For large values of the diffusion coefficient, this displacement can extend well over several cells. Hence, the method is best applied to those cases in which the diffusivity is less than  $200 \text{ m}^2 \text{ sec}^{-1}$ .

One drawback of particle-in-cell methods is the amount of computing time required to solve a particular problem for a given accuracy. Since a random number must be generated for each particle at each step, computing costs can be exorbitant as the number of particles increases.

## 6. The Method of Egan and Mahoney

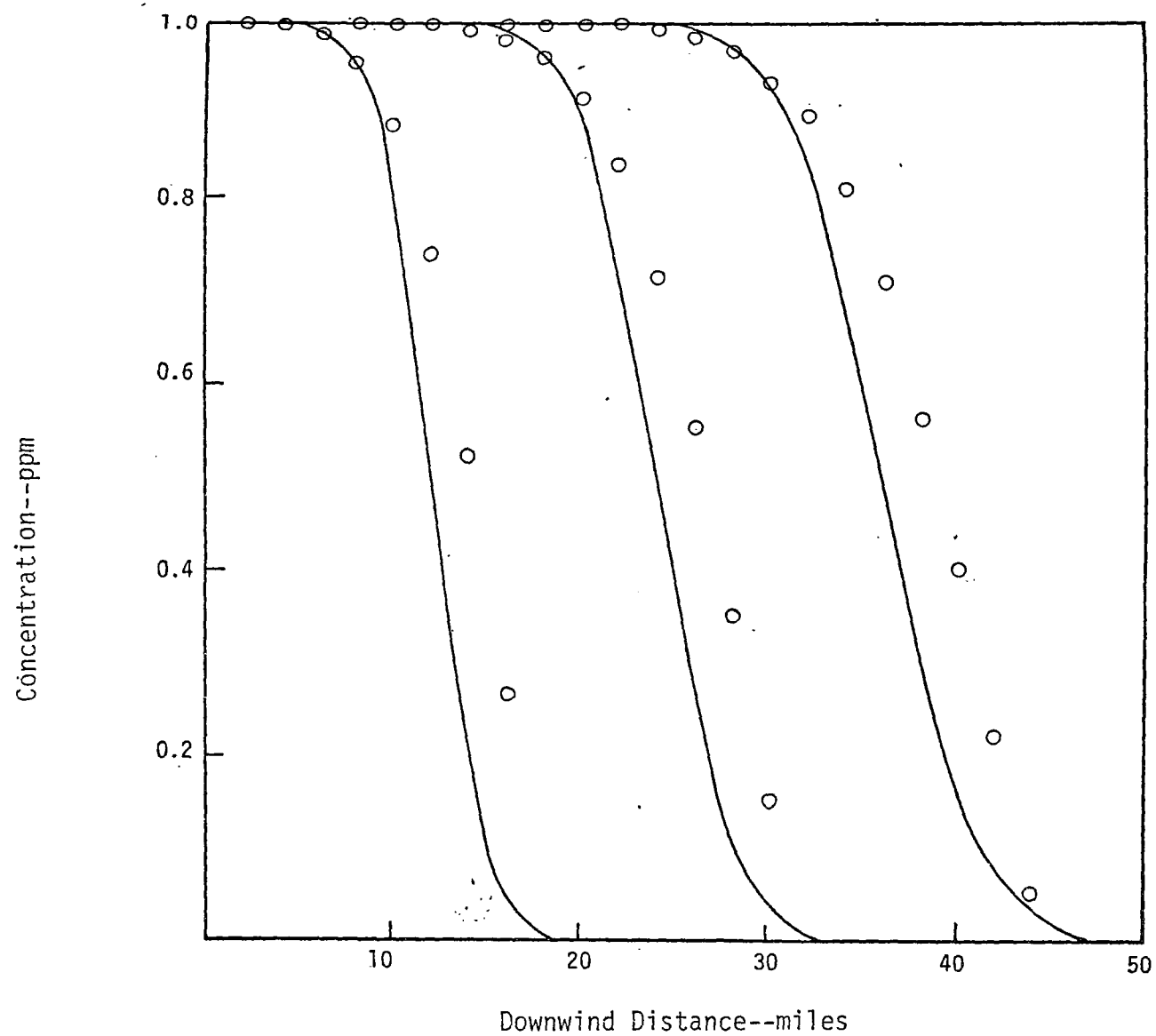
For the strictly advective case, the Egan and Mahoney method generates an extremely accurate solution with virtually no error attributable to numerical diffusion. This accuracy is particularly notable because advective phenomena have been extremely difficult to simulate using computing methods. Figure 29 presents the results obtained using this method. Unfortunately, we could not incorporate the diffusion step in this analysis because of the absence of any clear explanation of the treatment of this process in the open literature. Without this link, it is difficult to form an overall critical appraisal of the technique. In light of this limitation, this method should continue to be investigated as more material becomes available.





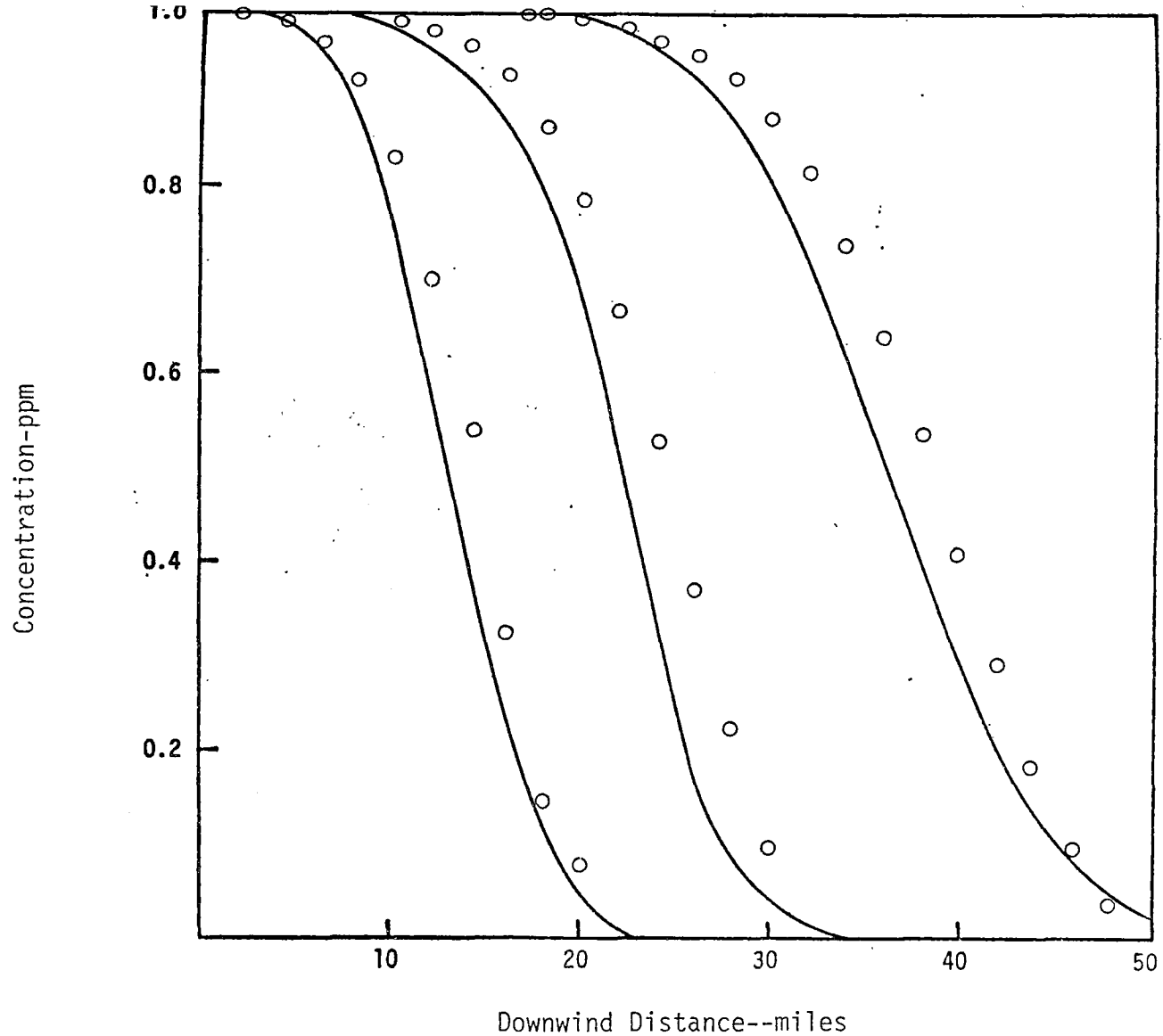
(a)  $Pec = 720$ ,  $k = 0 \text{ sec}^{-1}$

FIGURE 22. CONCENTRATION AS A FUNCTION OF DOWNWIND DISTANCE FOR THE EXPLICIT PRICE SCHEME



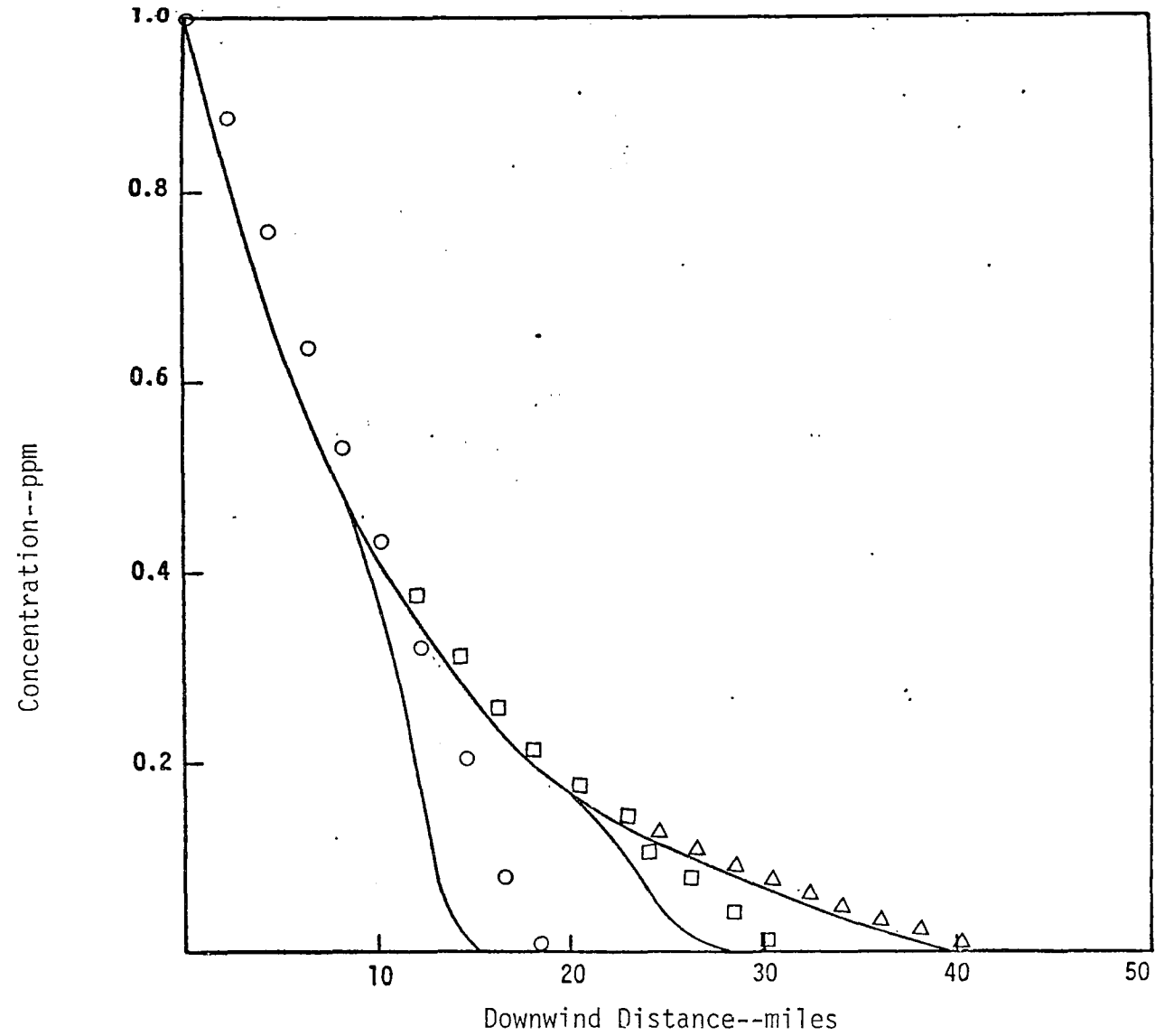
(b)  $Pec = 206$ ,  $k = 0 \text{ sec}^{-1}$

FIGURE 22. CONCENTRATION AS A FUNCTION OF DOWNWIND DISTANCE FOR THE EXPLICIT PRICE SCHEME (Continued)



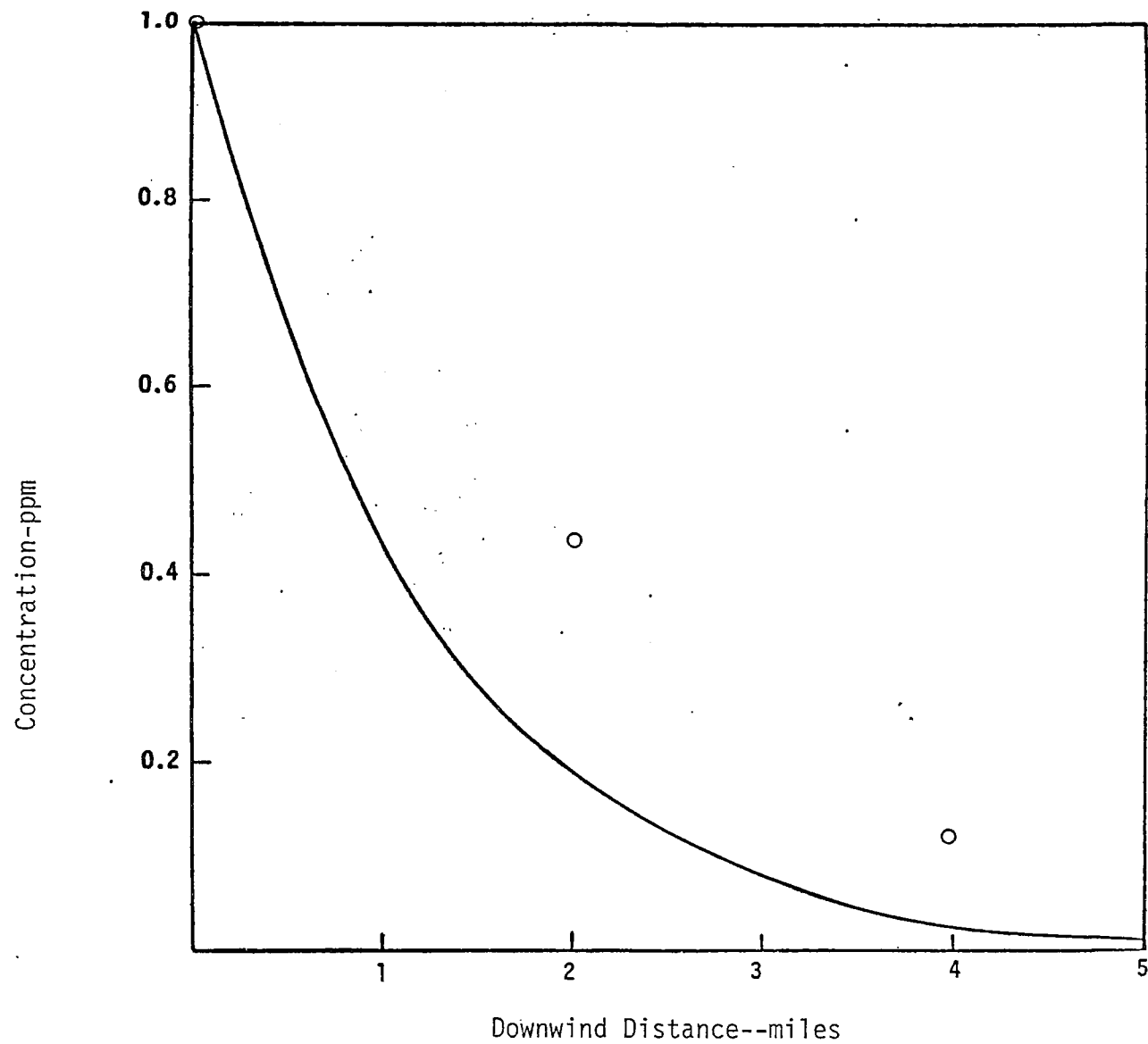
(c) Pec = 72,  $k = 0 \text{ sec}^{-1}$

FIGURE 22. CONCENTRATION AS A FUNCTION OF DOWNWIND DISTANCE FOR THE EXPLICIT PRICE SCHEME (Continued)



(d)  $Pec = 720$ ,  $k = 10^{-4} \text{ sec}^{-1}$

FIGURE 22. CONCENTRATION AS A FUNCTION OF DOWNWIND DISTANCE FOR THE EXPLICIT PRICE SCHEME (Continued)



(e)  $Pec = 720$ ,  $k = 10^{-3} \text{ sec}^{-1}$

FIGURE 22. CONCENTRATION AS A FUNCTION OF DOWNWIND DISTANCE FOR THE EXPLICIT PRICE SCHEME (Concluded)

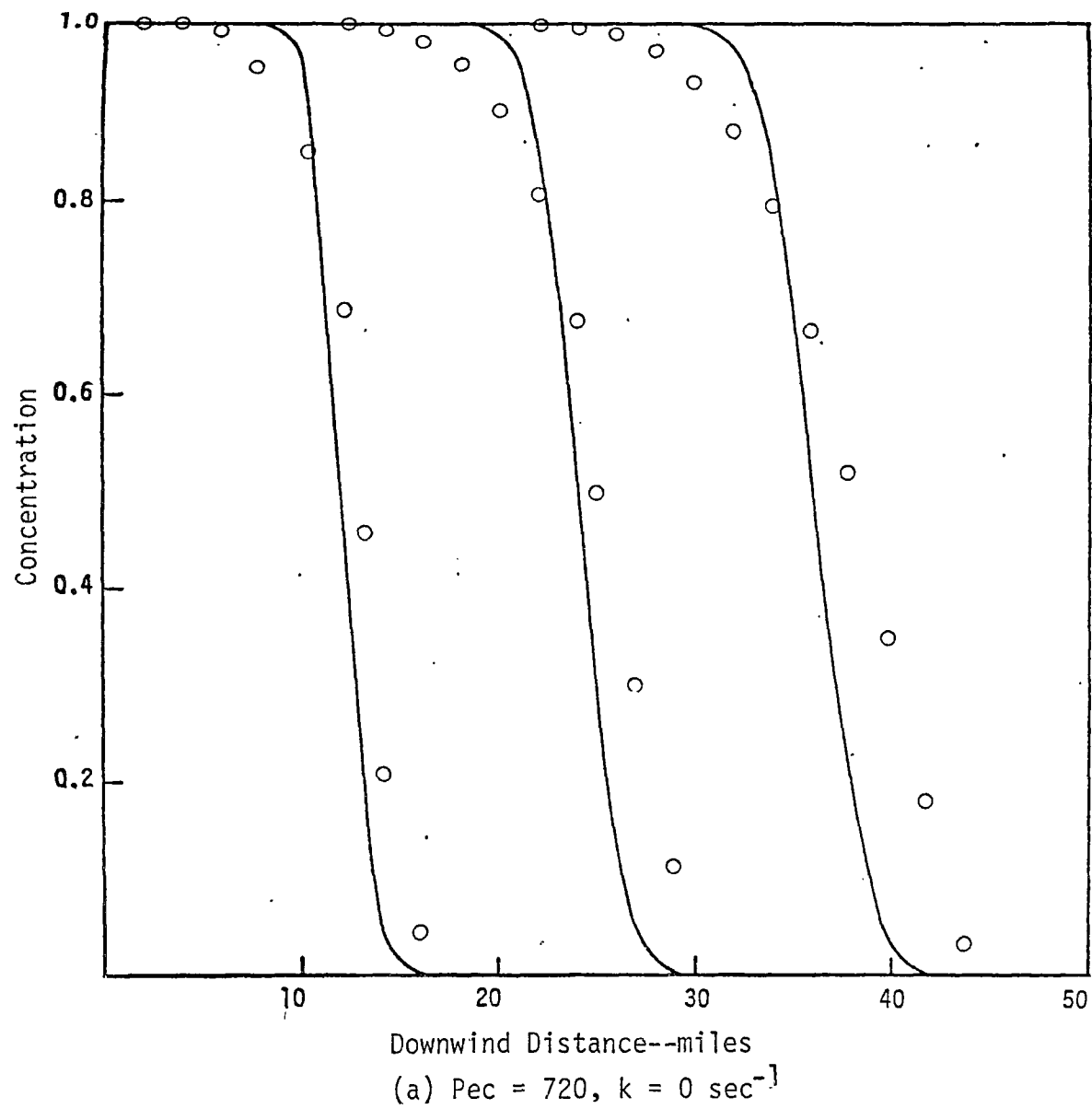


FIGURE 23. CONCENTRATION AS A FUNCTION OF DOWNWIND DISTANCE  
FOR THE IMPLICIT PRICE SCHEME

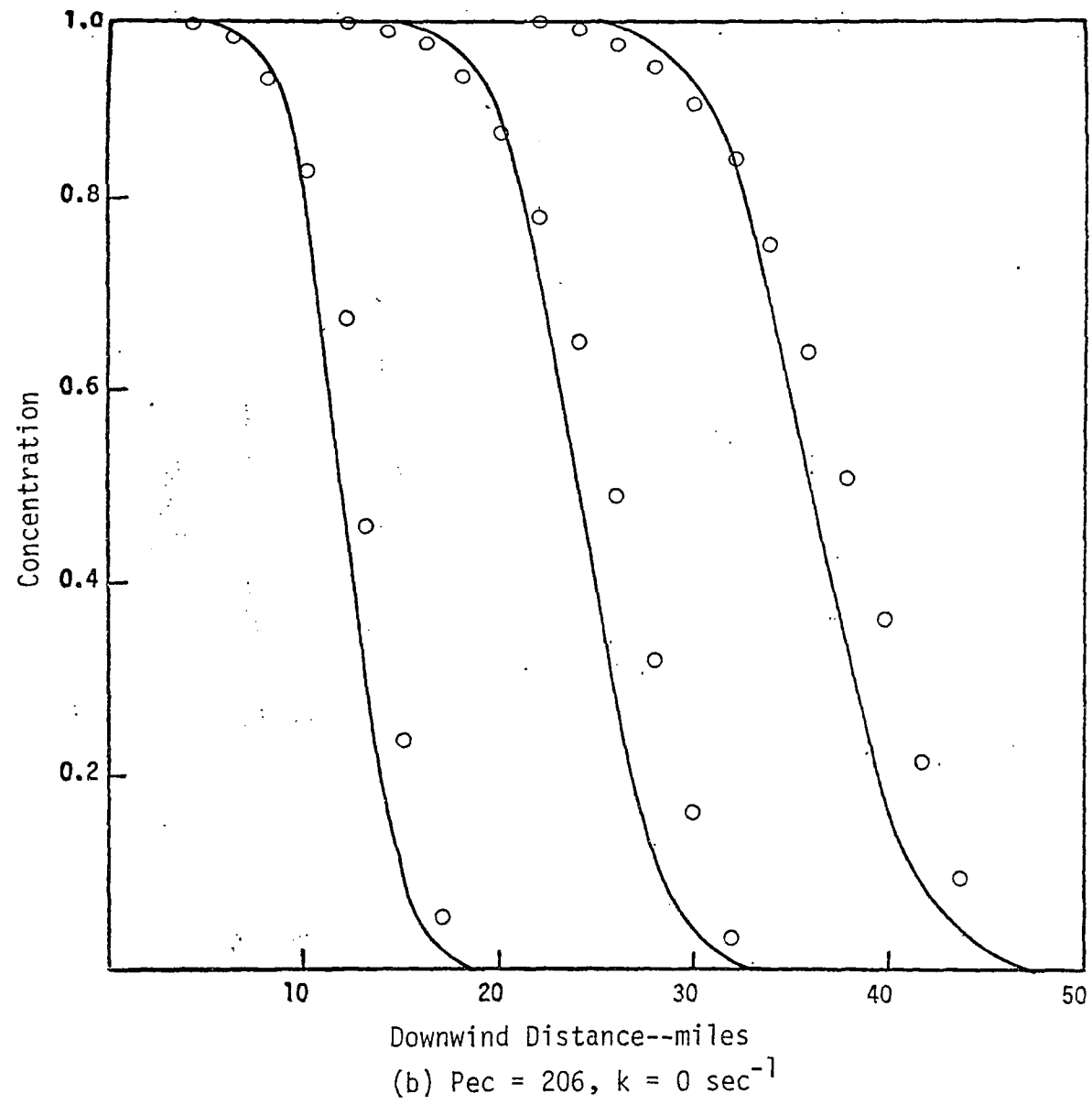


FIGURE 23. CONCENTRATION AS A FUNCTION OF DOWNWIND DISTANCE  
FOR THE IMPLICIT PRICE SCHEME (Continued)

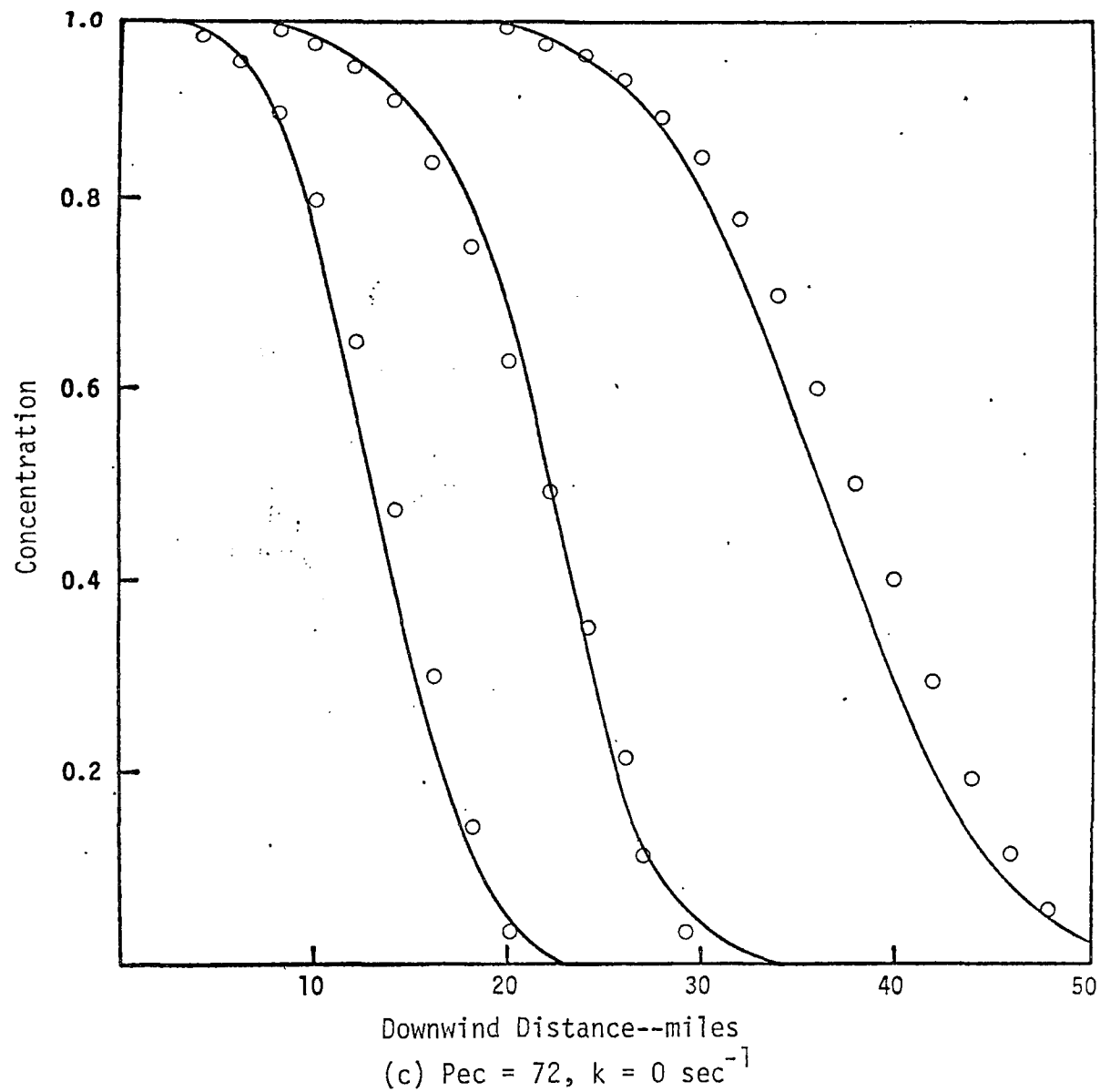


FIGURE 23. CONCENTRATION AS A FUNCTION OF DOWNWIND DISTANCE  
FOR THE IMPLICIT PRICE SCHEME (Continued)



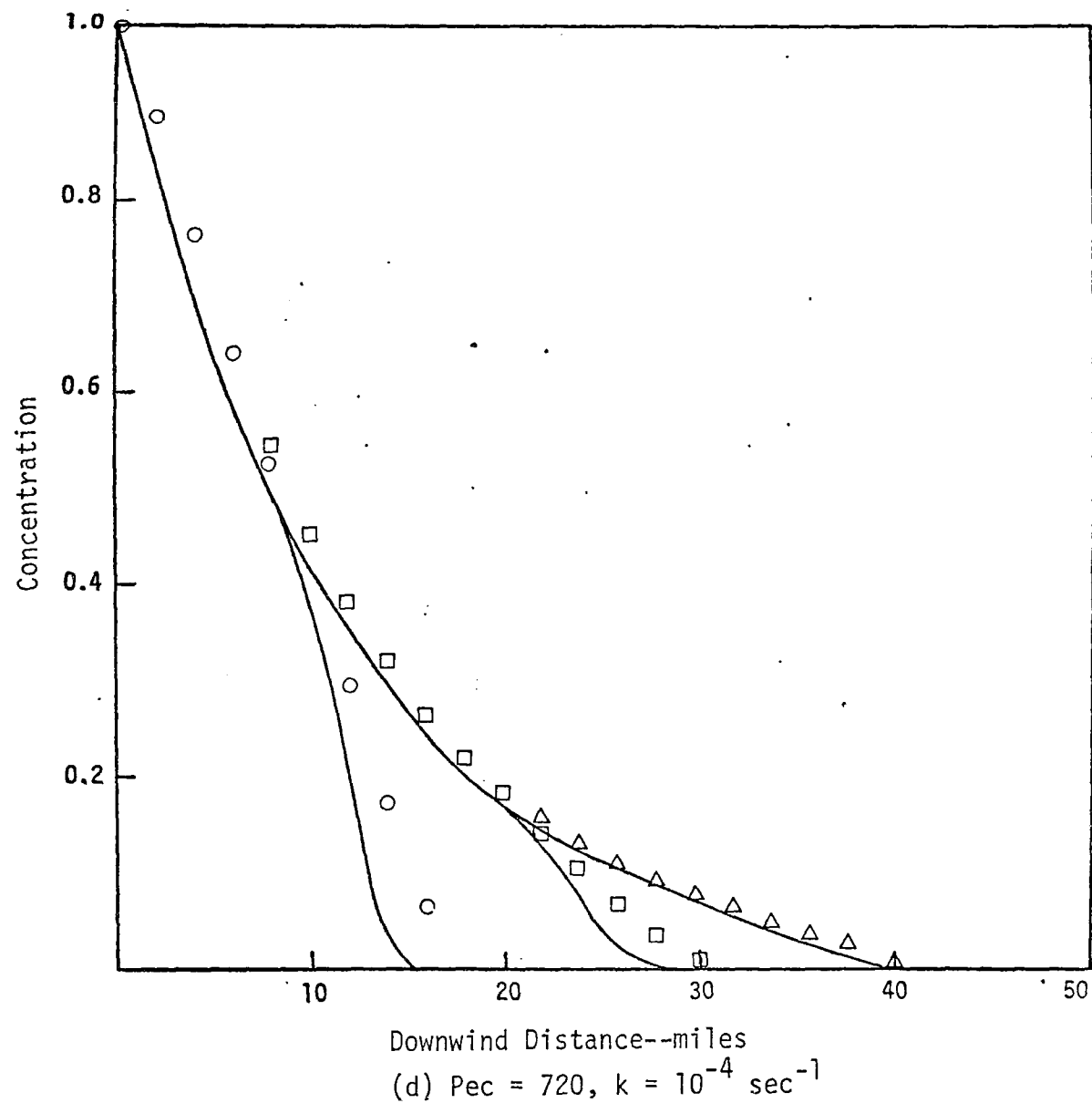


FIGURE 23. CONCENTRATION AS A FUNCTION OF DOWNWIND DISTANCE  
FOR THE IMPLICIT PRICE SCHEME (Continued)

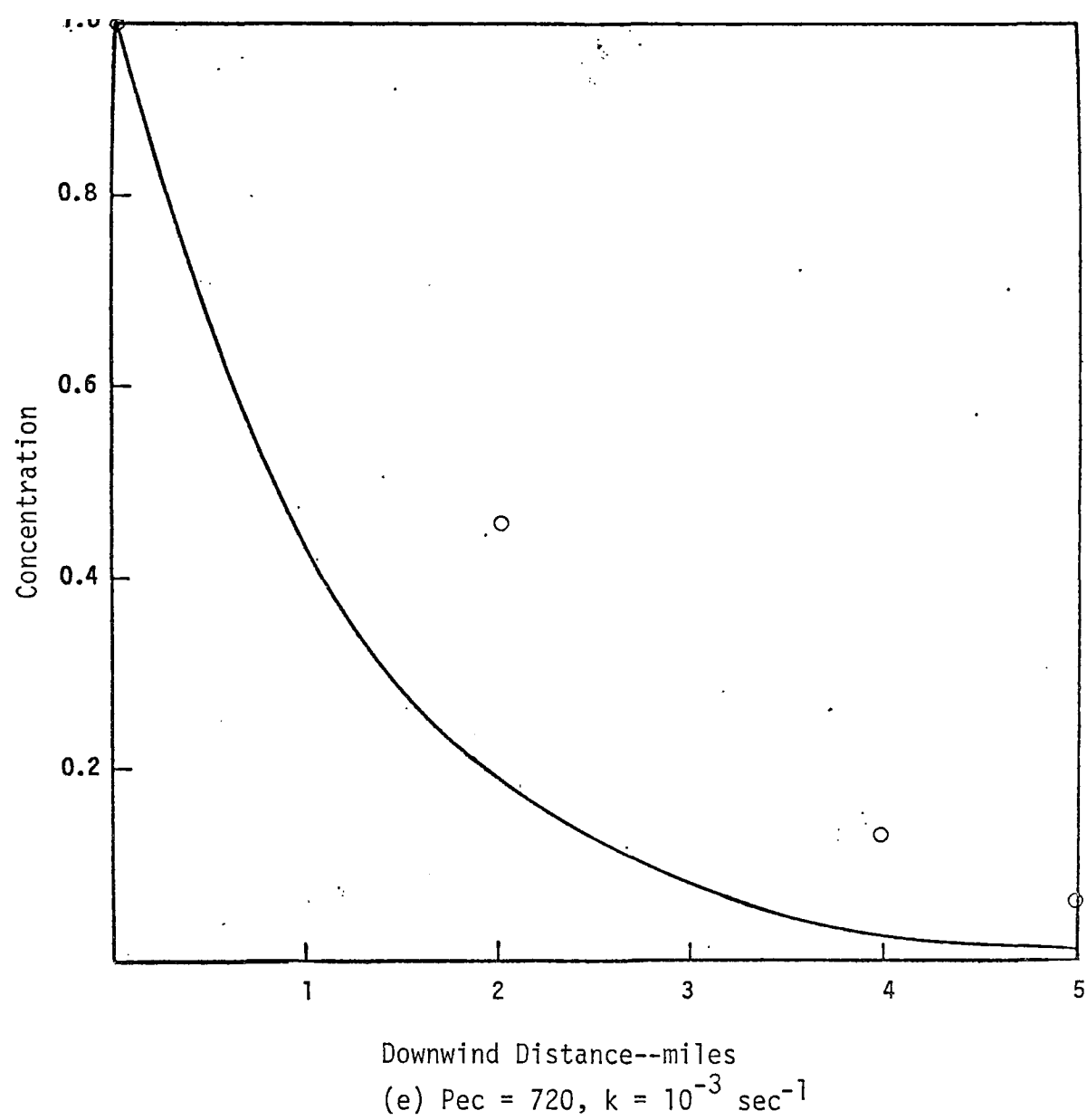


FIGURE 23. CONCENTRATION AS A FUNCTION OF DOWNWIND DISTANCE  
FOR THE IMPLICIT PRICE SCHEME (Concluded)

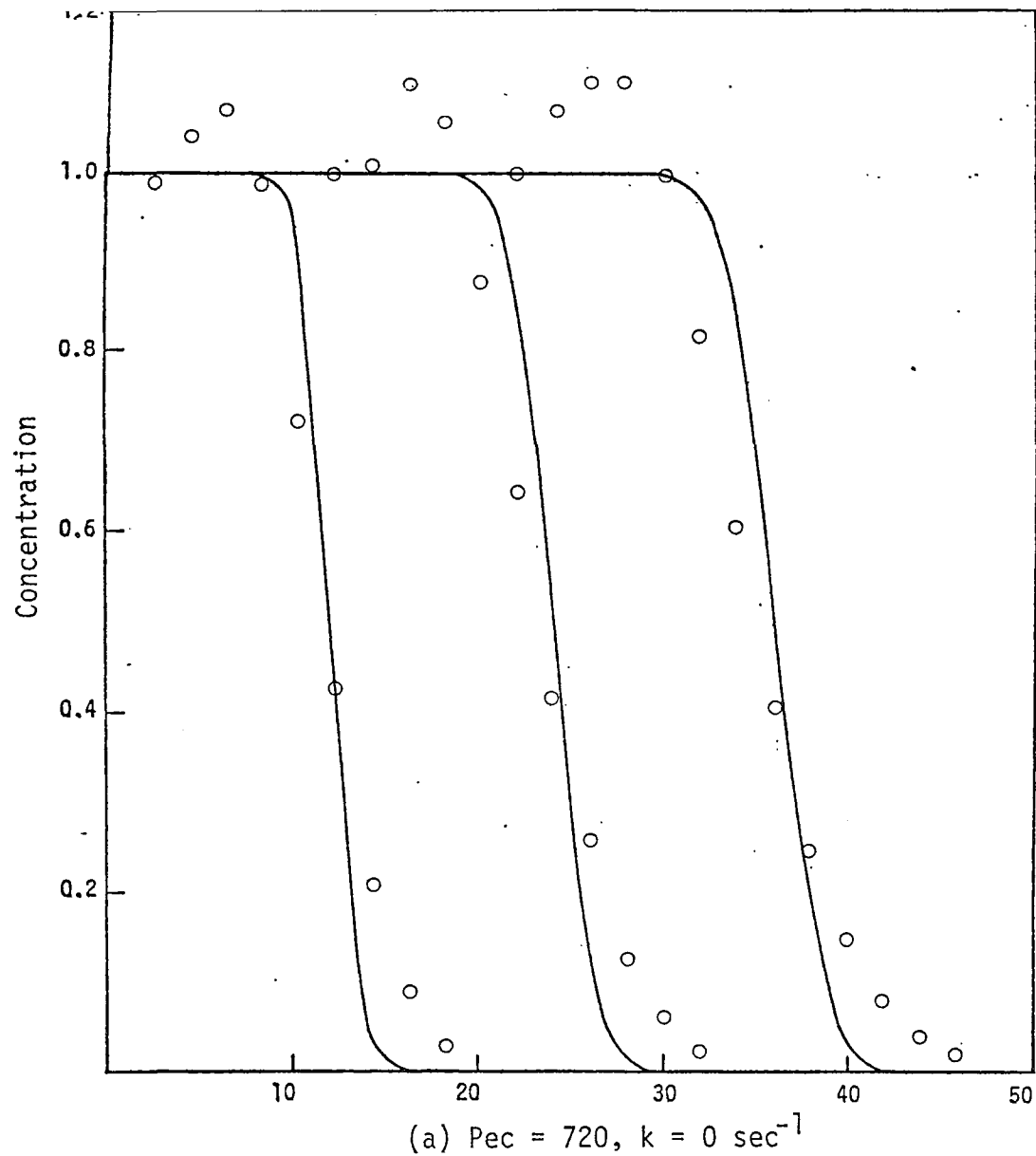


FIGURE 24. CONCENTRATION AS A FUNCTION OF DOWNWIND DISTANCE  
FOR THE CROWLEY SECOND-ORDER SCHEME

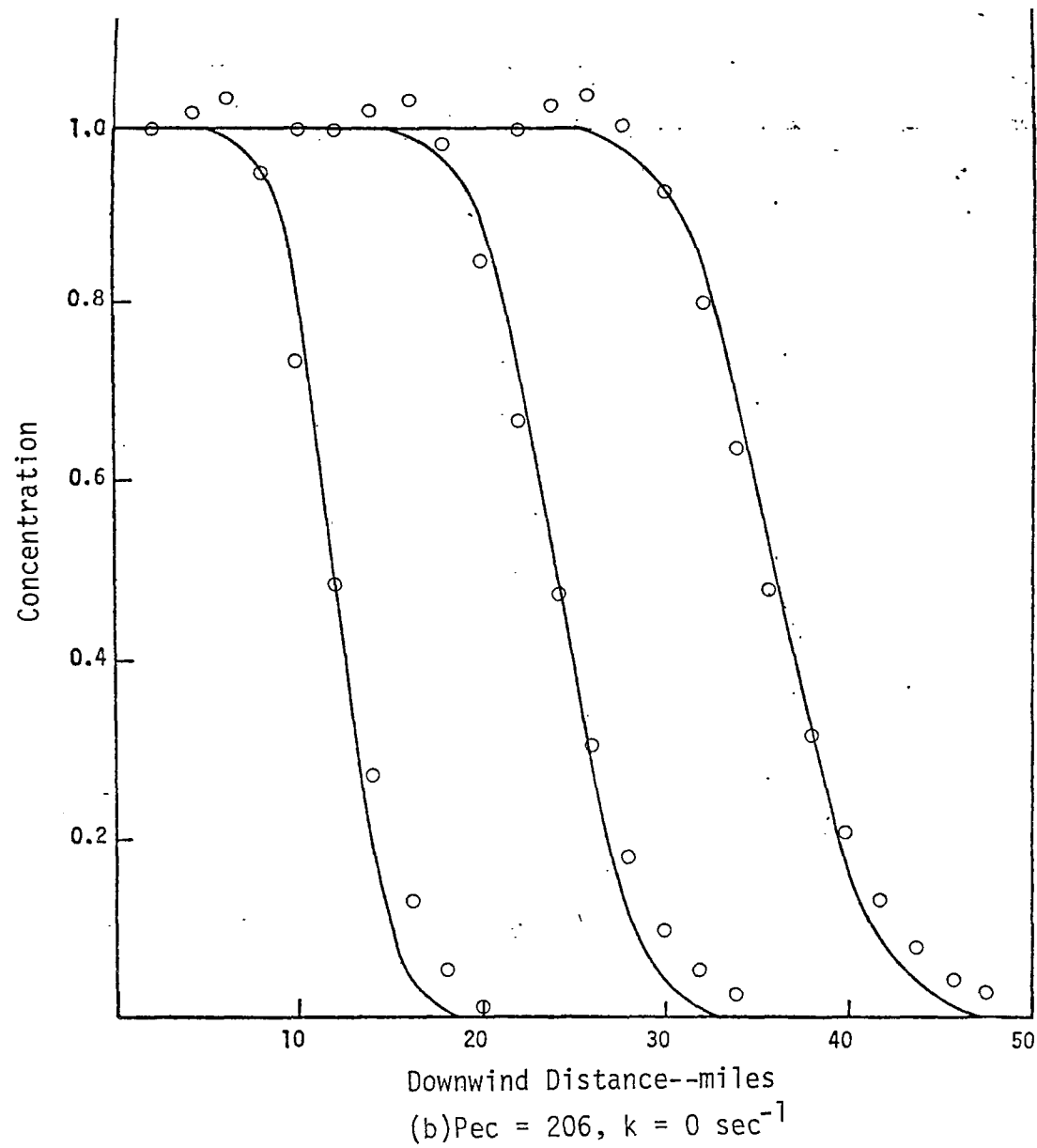


FIGURE 24. CONCENTRATION AS A FUNCTION OF DOWNWIND DISTANCE  
FOR THE CROWLEY SECOND-ORDER SCHEME (Continued)

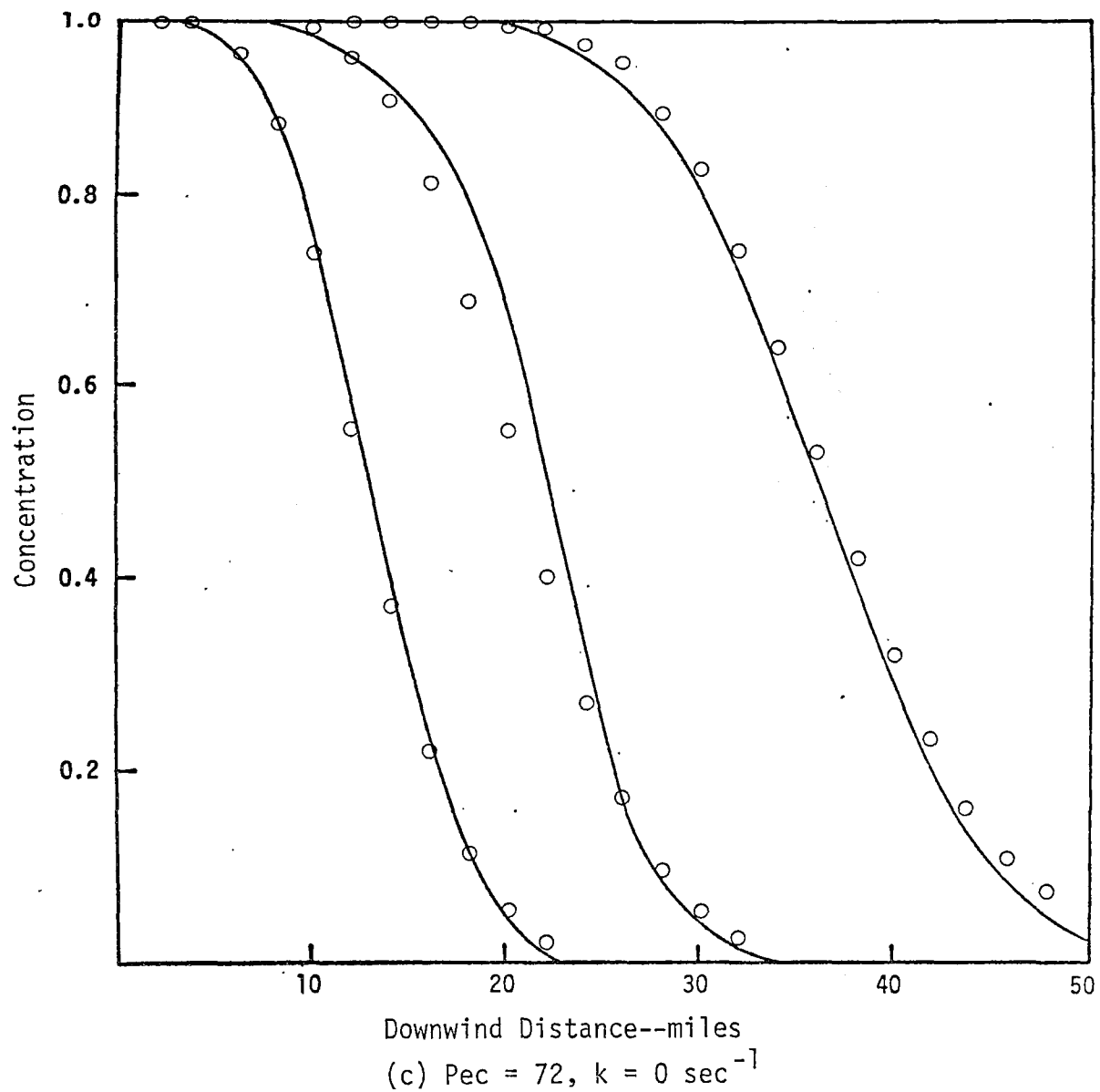


FIGURE 24. CONCENTRATION AS A FUNCTION OF DOWNWIND DISTANCE  
FOR THE CROWLEY SECOND-ORDER SCHEME (Continued)

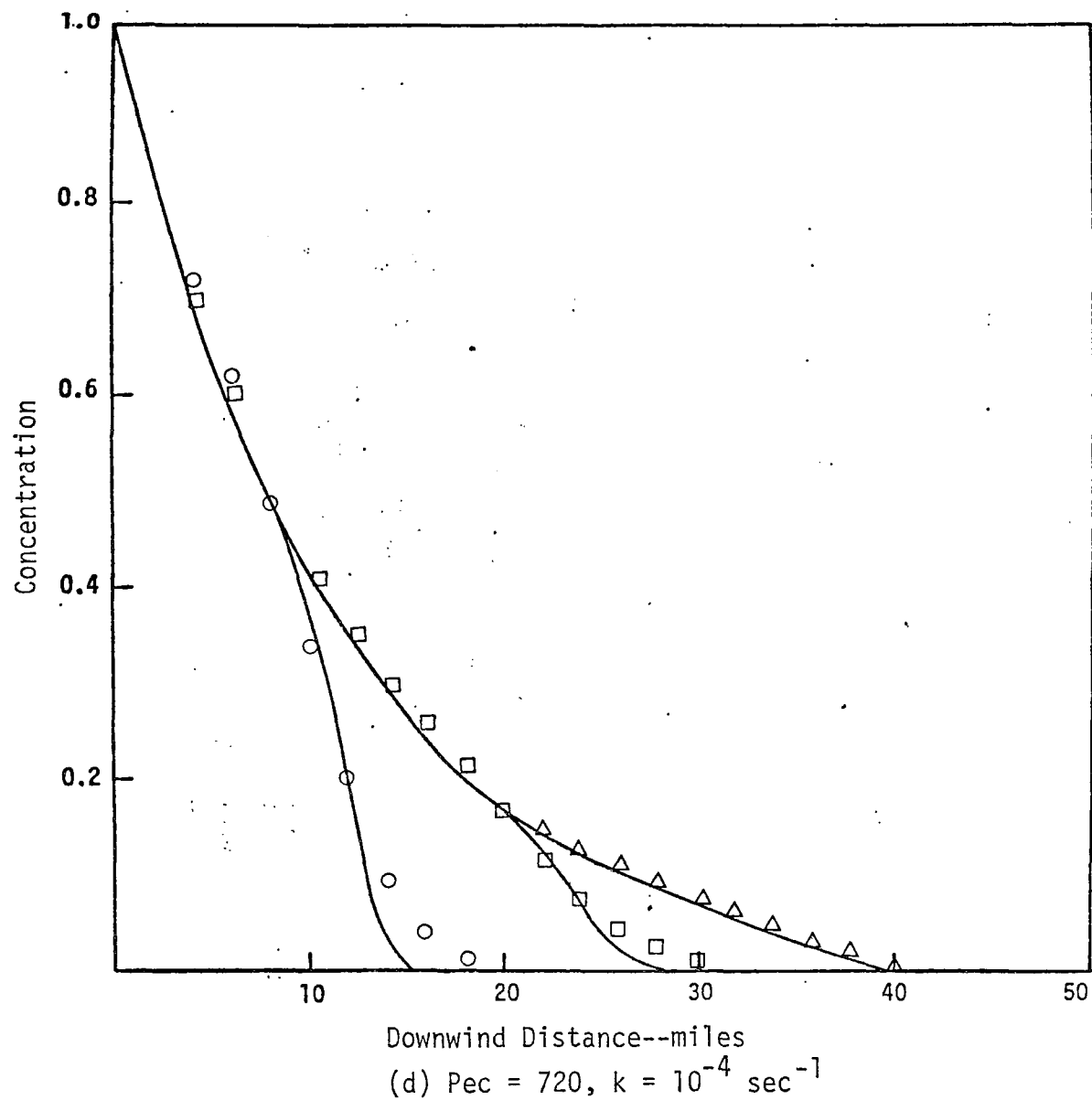


FIGURE 24. CONCENTRATION AS A FUNCTION OF DOWNWIND DISTANCE  
FOR THE CROWLEY SECOND-ORDER SCHEME (Continued)

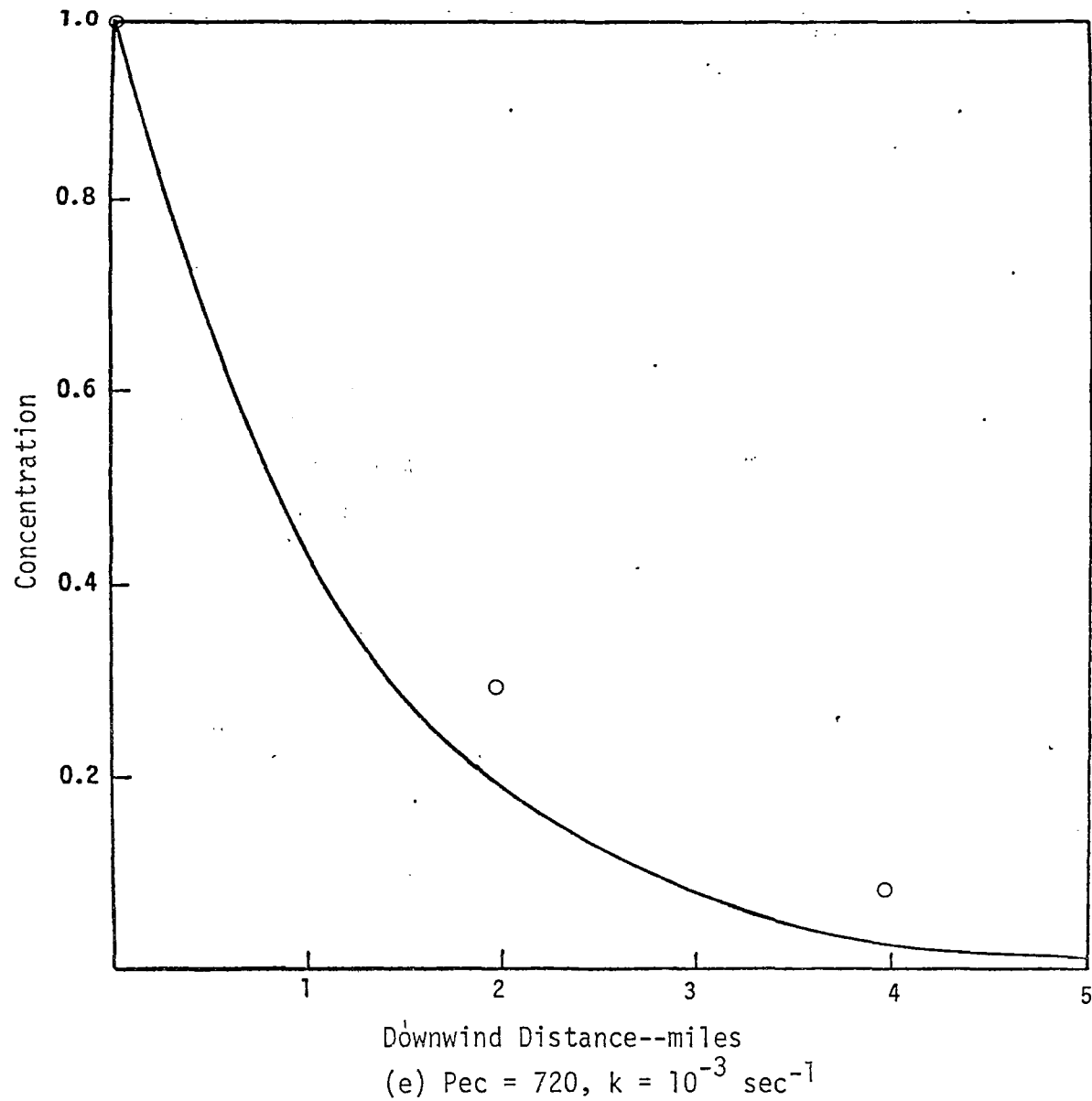


FIGURE 24. CONCENTRATION AS A FUNCTION OF DOWNWIND DISTANCE  
FOR THE CROWLEY SECOND-ORDER SCHEME (Concluded)

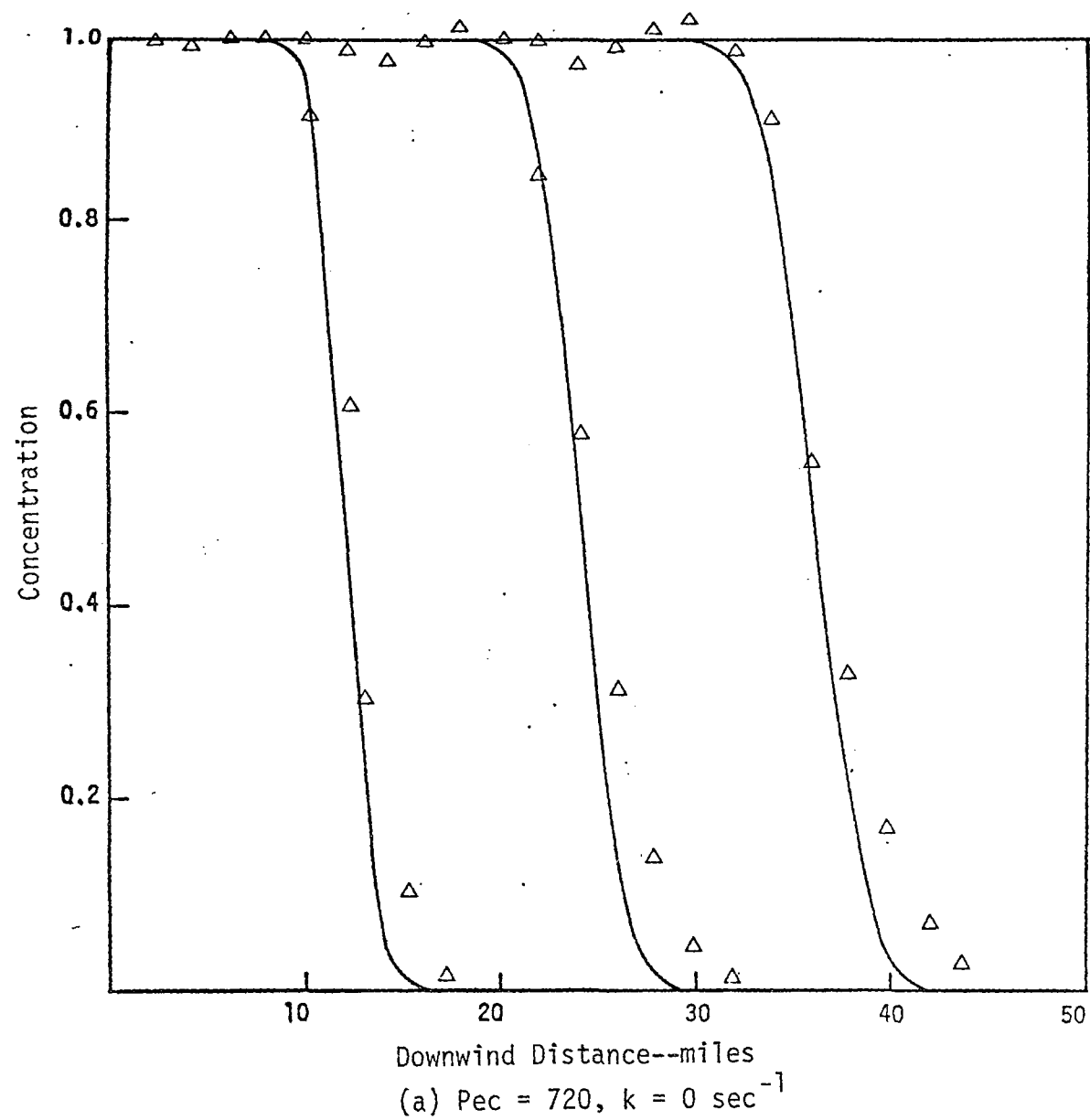


FIGURE 25. CONCENTRATION AS A FUNCTION OF DOWNWIND DISTANCE  
FOR THE CROWLEY FOURTH-ORDER SCHEME



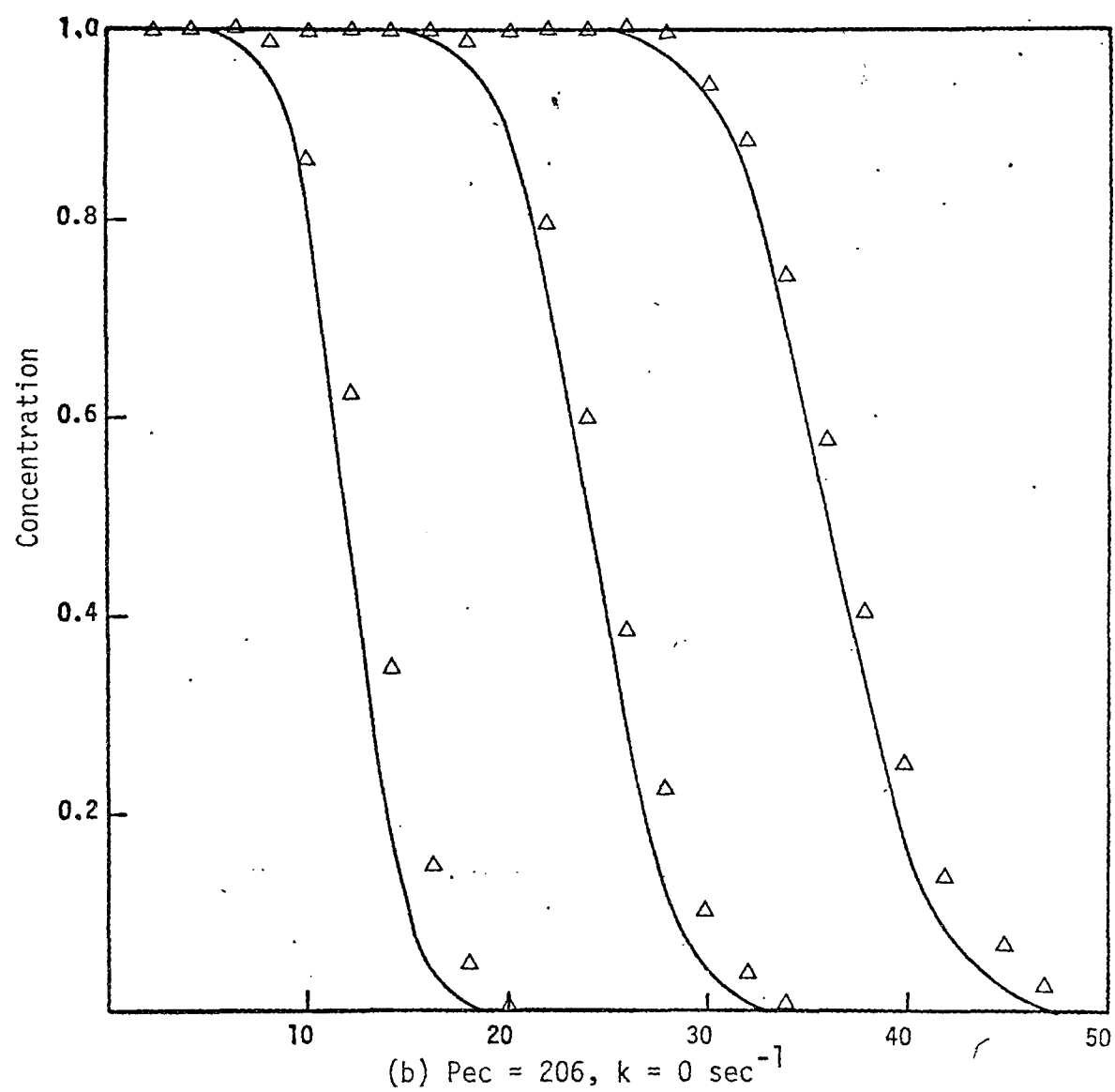


FIGURE 25. CONCENTRATION AS A FUNCTION OF DOWNWIND DISTANCE  
FOR THE CROWLEY FOURTH-ORDER SCHEME (Continued)

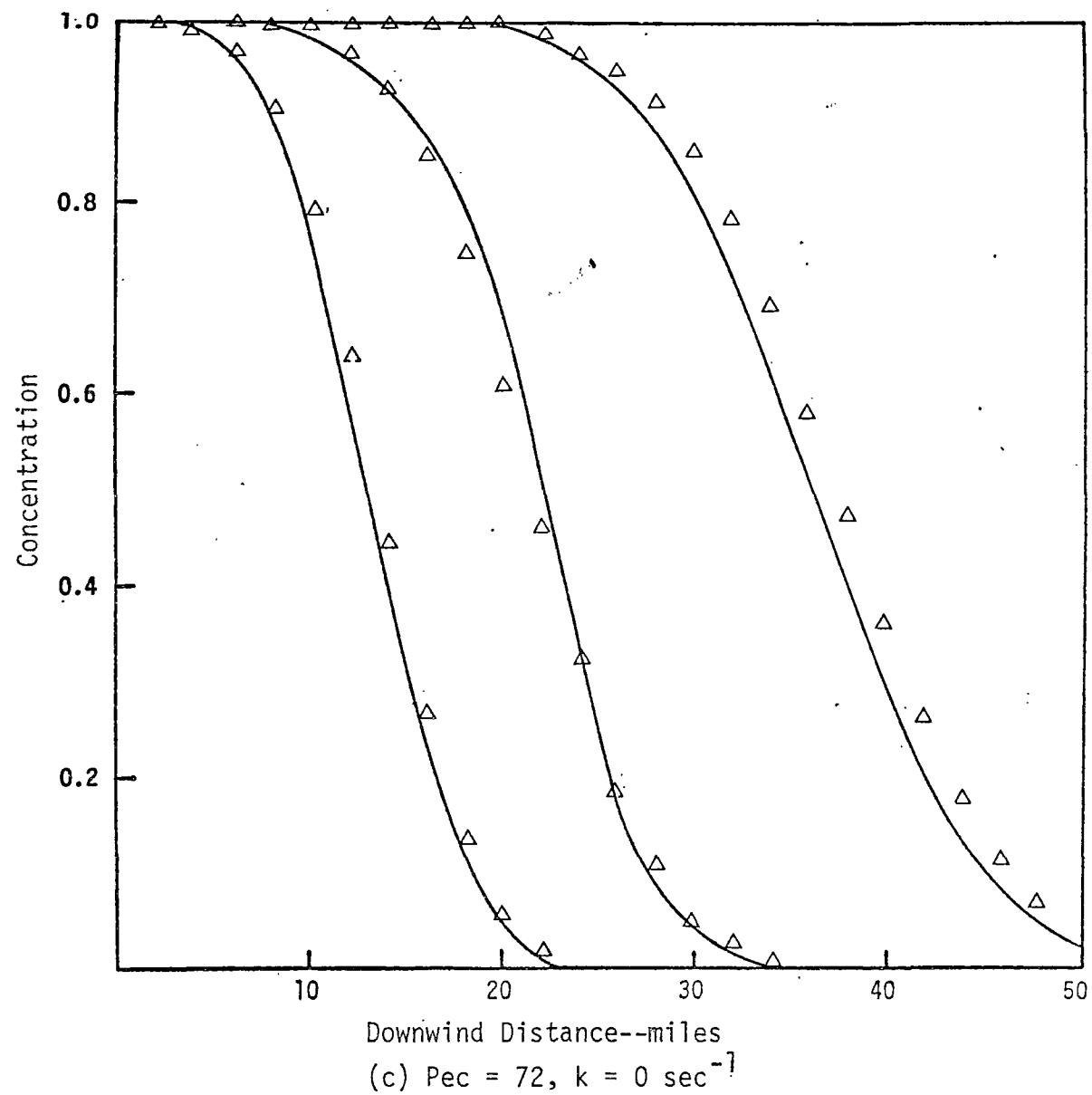


FIGURE 25. CONCENTRATION AS A FUNCTION OF DOWNWIND DISTANCE  
FOR THE CROWLEY FOURTH-ORDER SCHEME (Continued)

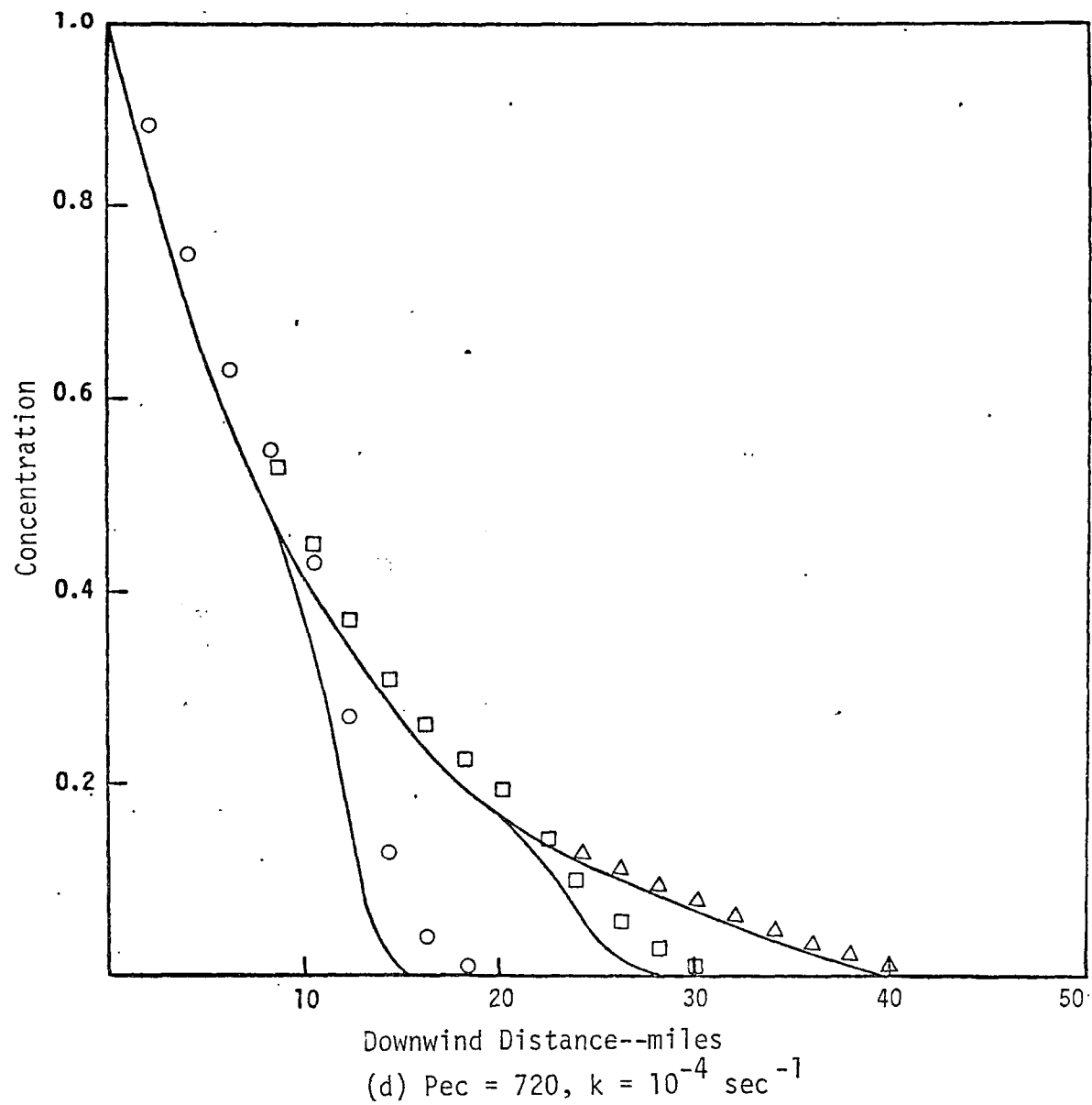
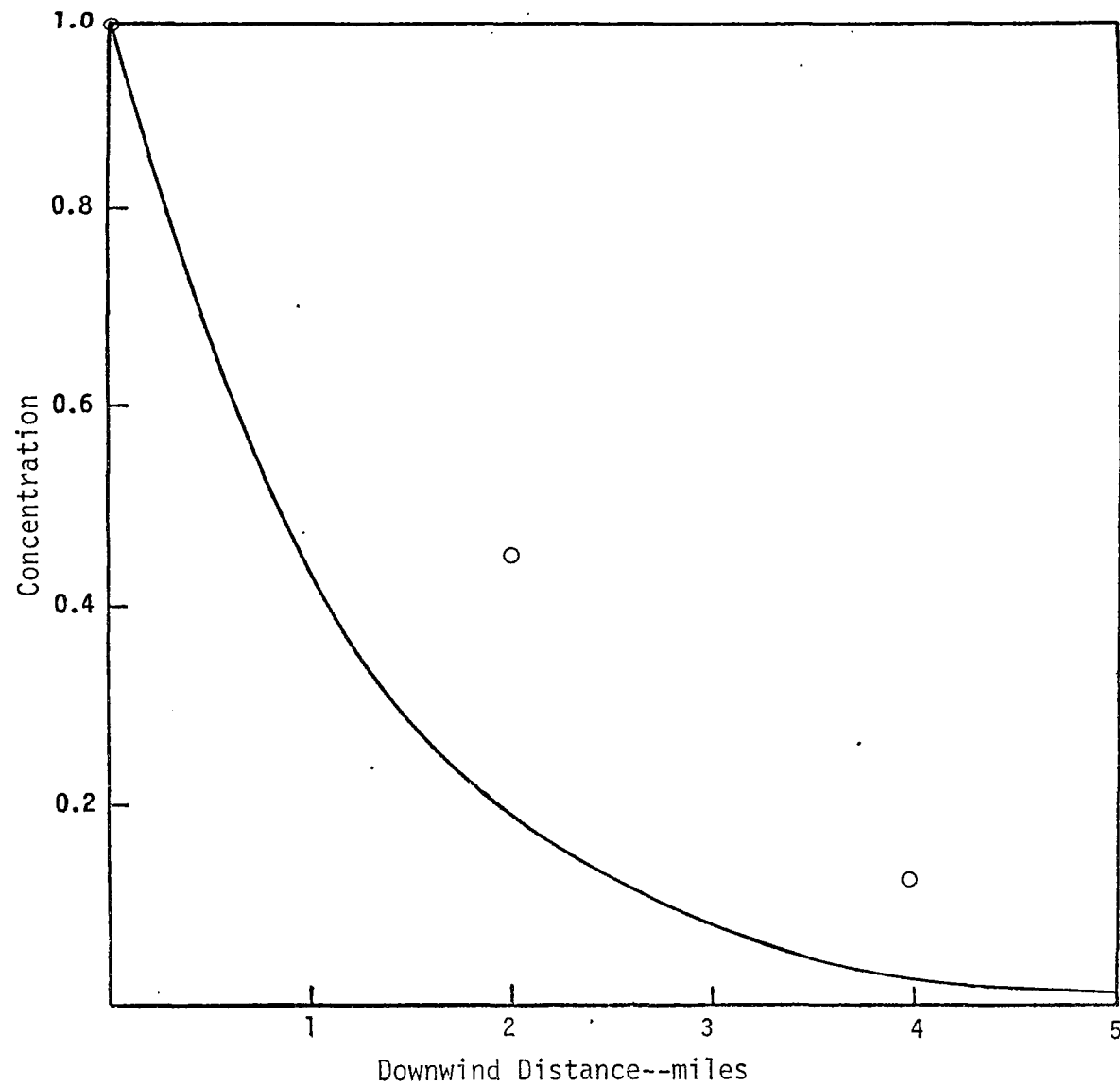


FIGURE 25. CONCENTRATION AS A FUNCTION OF DOWNWIND DISTANCE  
FOR THE CROWLEY FOURTH-ORDER SCHEME (Continued)



(e)  $Pec = 720$ ,  $k = 10^{-3} \text{ sec}^{-1}$ ,  $\delta t = 300 \text{ sec}$ ,  $\delta x = 2 \text{ miles}$

FIGURE 25. CONCENTRATION AS A FUNCTION OF DOWNWIND DISTANCE  
FOR THE CROWLEY FOURTH-ORDER SCHEME (Concluded)

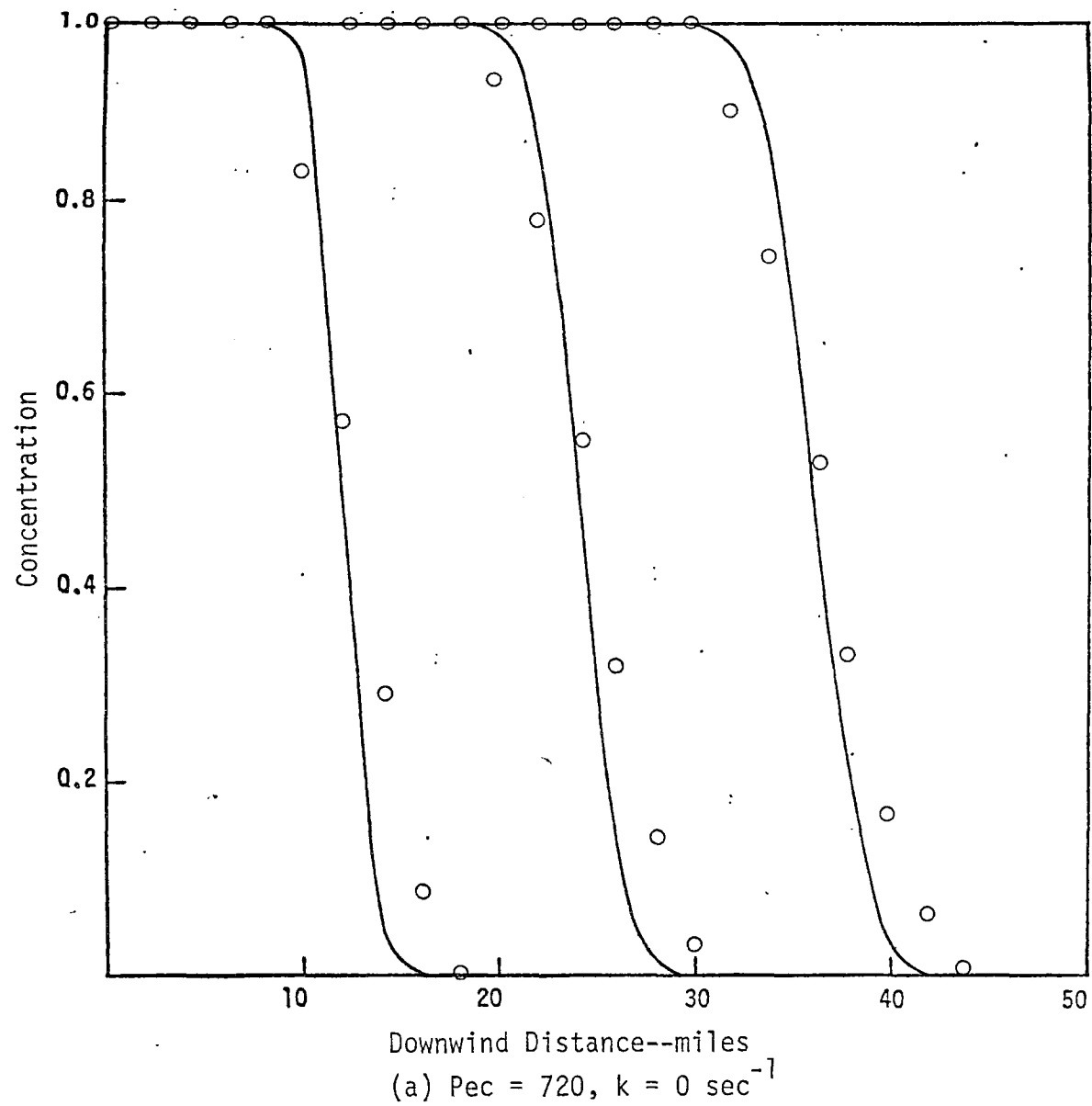


FIGURE 26. CONCENTRATION AS A FUNCTION OF DOWNWIND DISTANCE  
FOR THE SHASTA METHOD

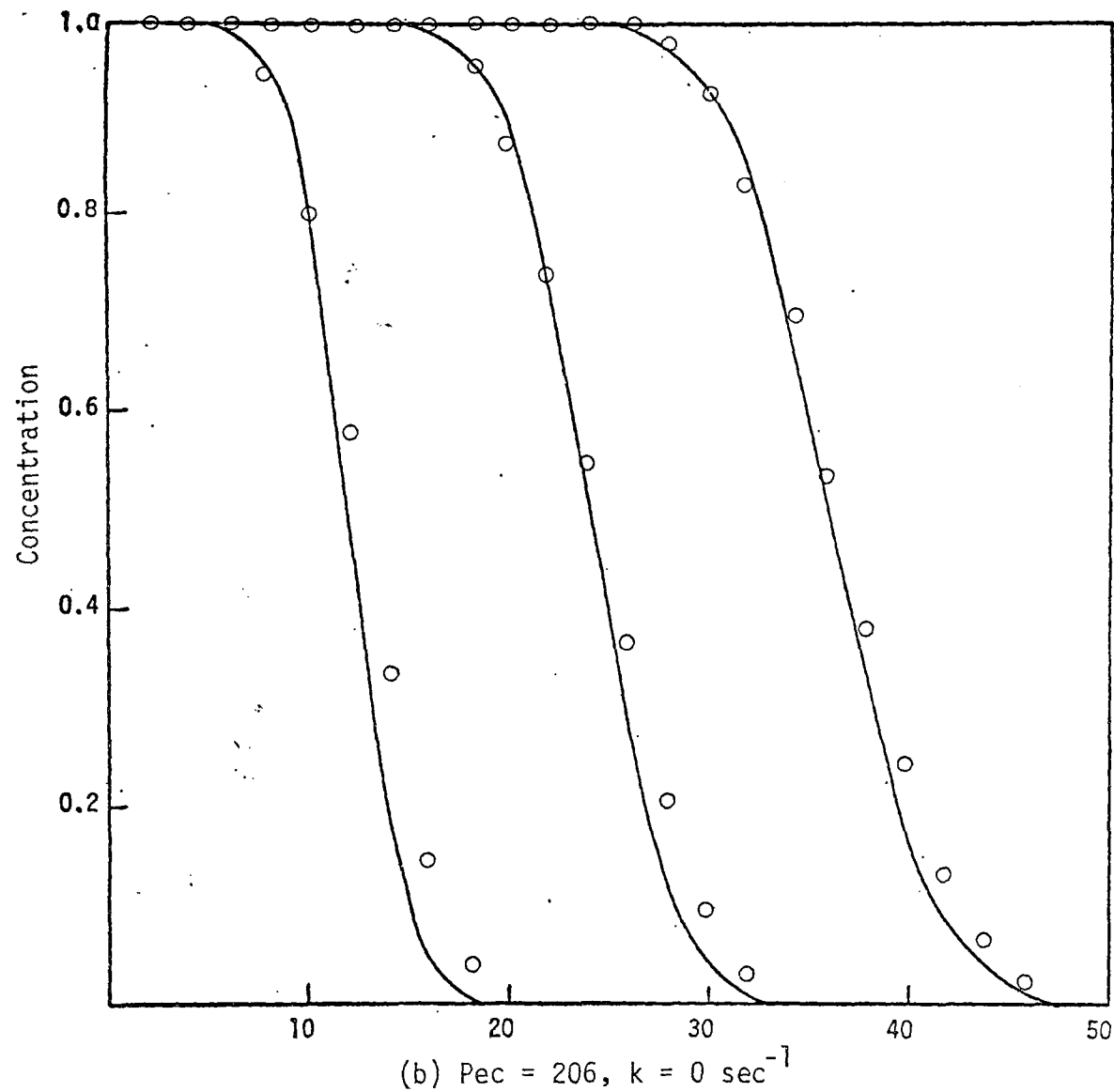


FIGURE 26. CONCENTRATION AS A FUNCTION OF DOWNWIND DISTANCE  
FOR THE SHASTA METHOD (Continued)

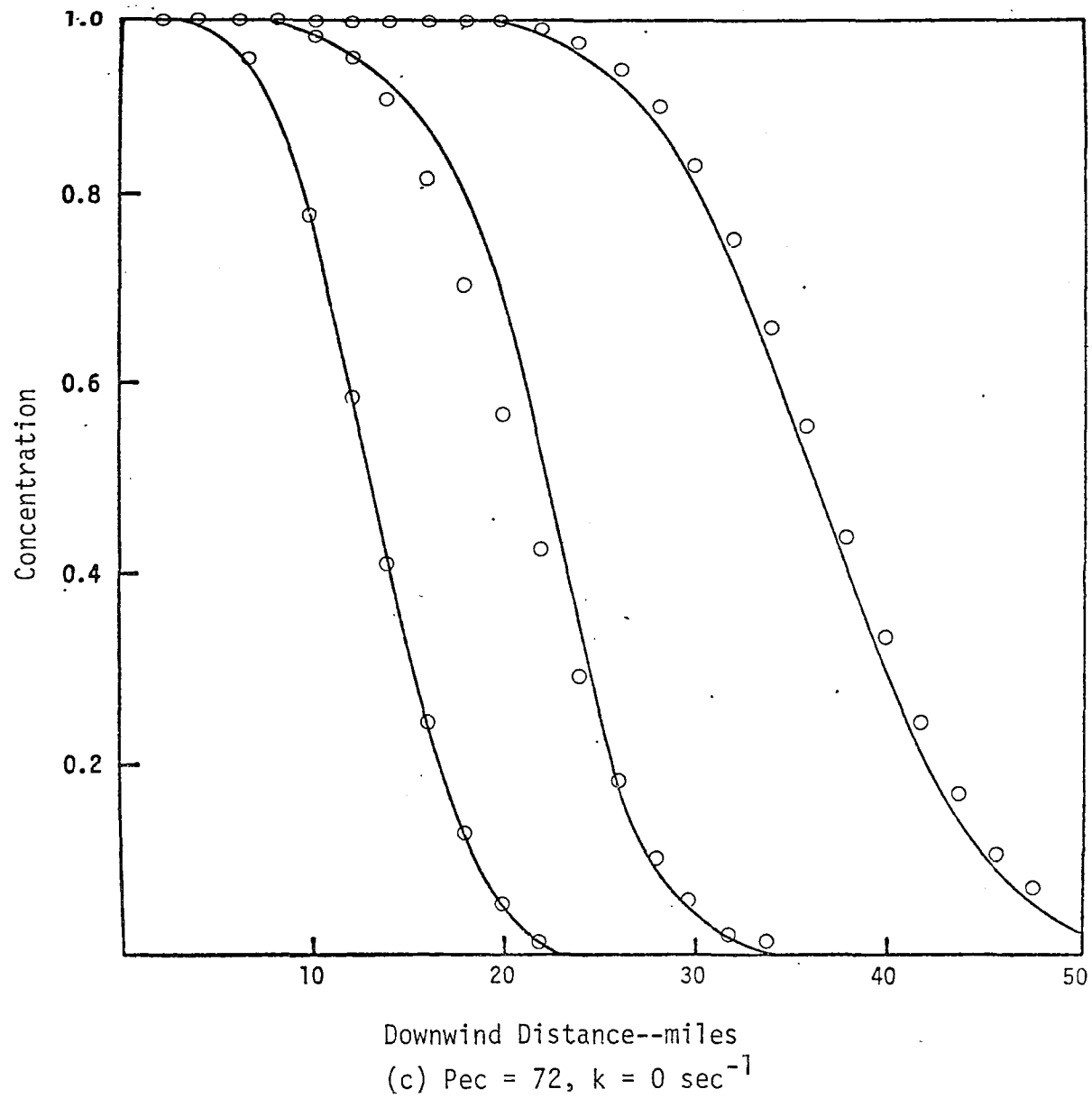


FIGURE 26. CONCENTRATION AS A FUNCTION OF DOWNWIND DISTANCE  
FOR THE SHASTA METHOD (Continued)

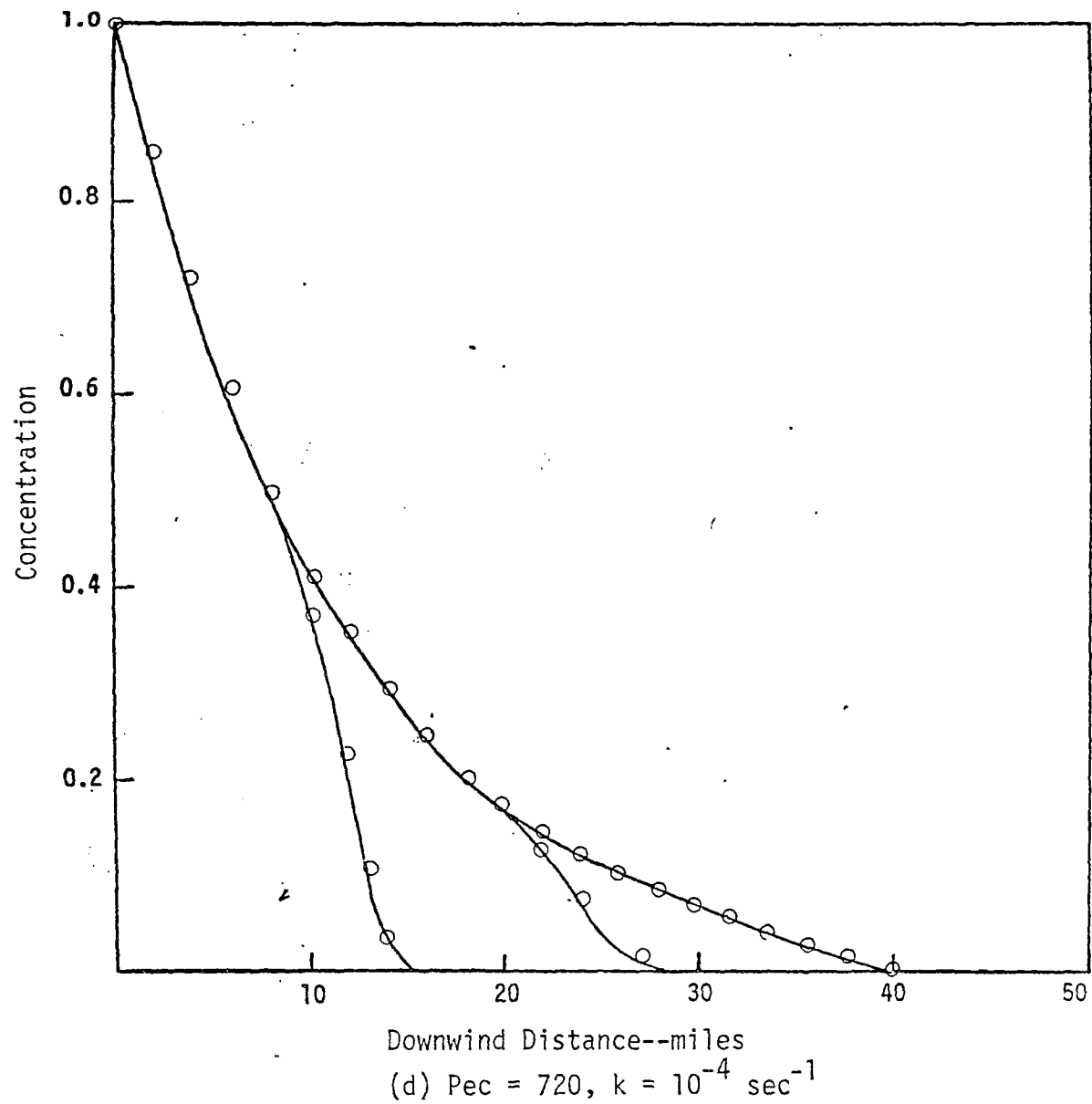
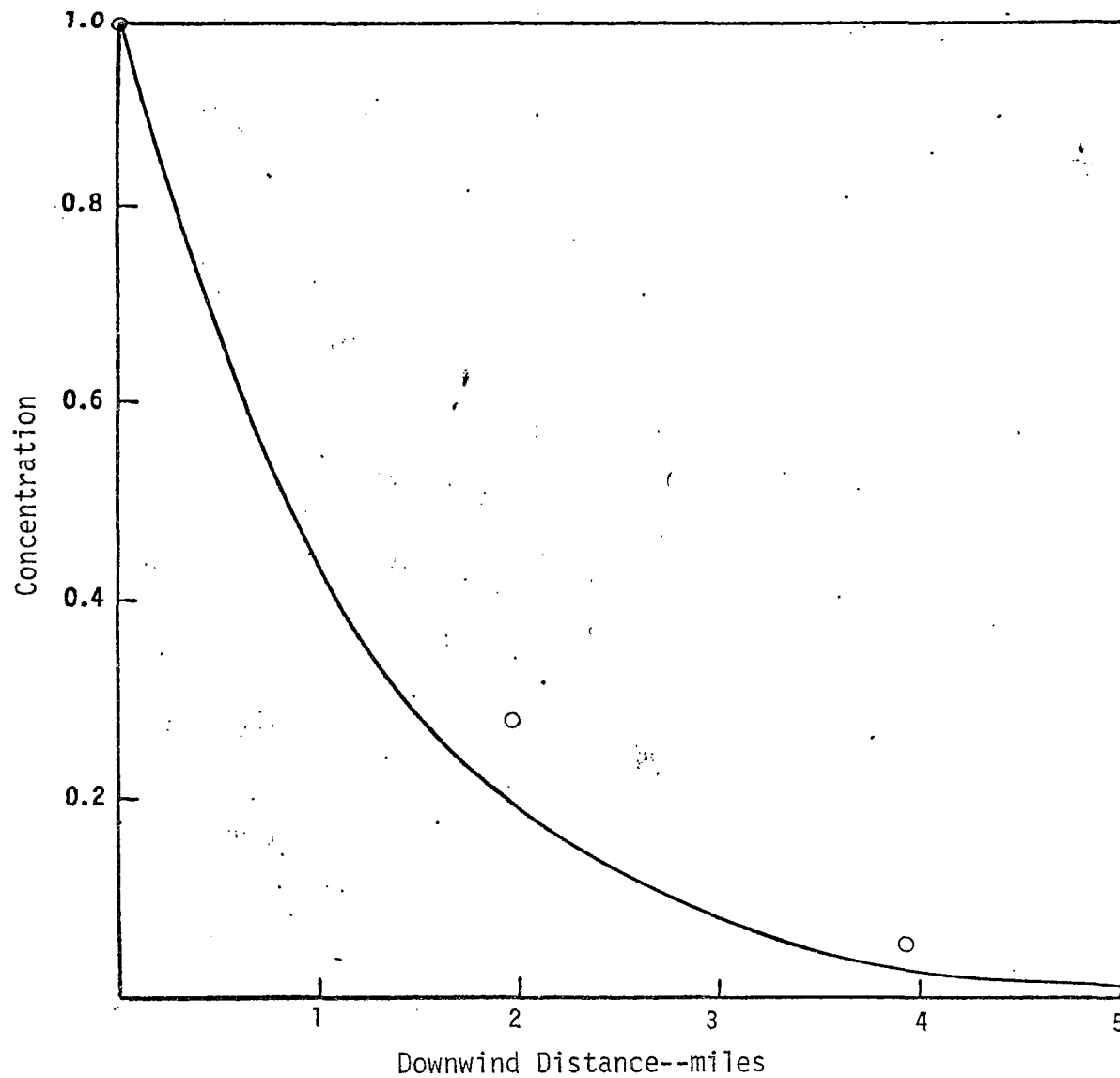


FIGURE 26. CONCENTRATION AS A FUNCTION OF DOWNWIND DISTANCE  
FOR THE SHASTA METHOD (Continued)





(e)  $Pec = 720$ ,  $k = 10^{-3} \text{ sec}^{-1}$ ,  $\delta t = 300 \text{ sec}$ ,  $\delta x = 2 \text{ miles}$

FIGURE 26. CONCENTRATION AS A FUNCTION OF DOWNWIND DISTANCE  
FOR THE SHASTA METHOD (Concluded)

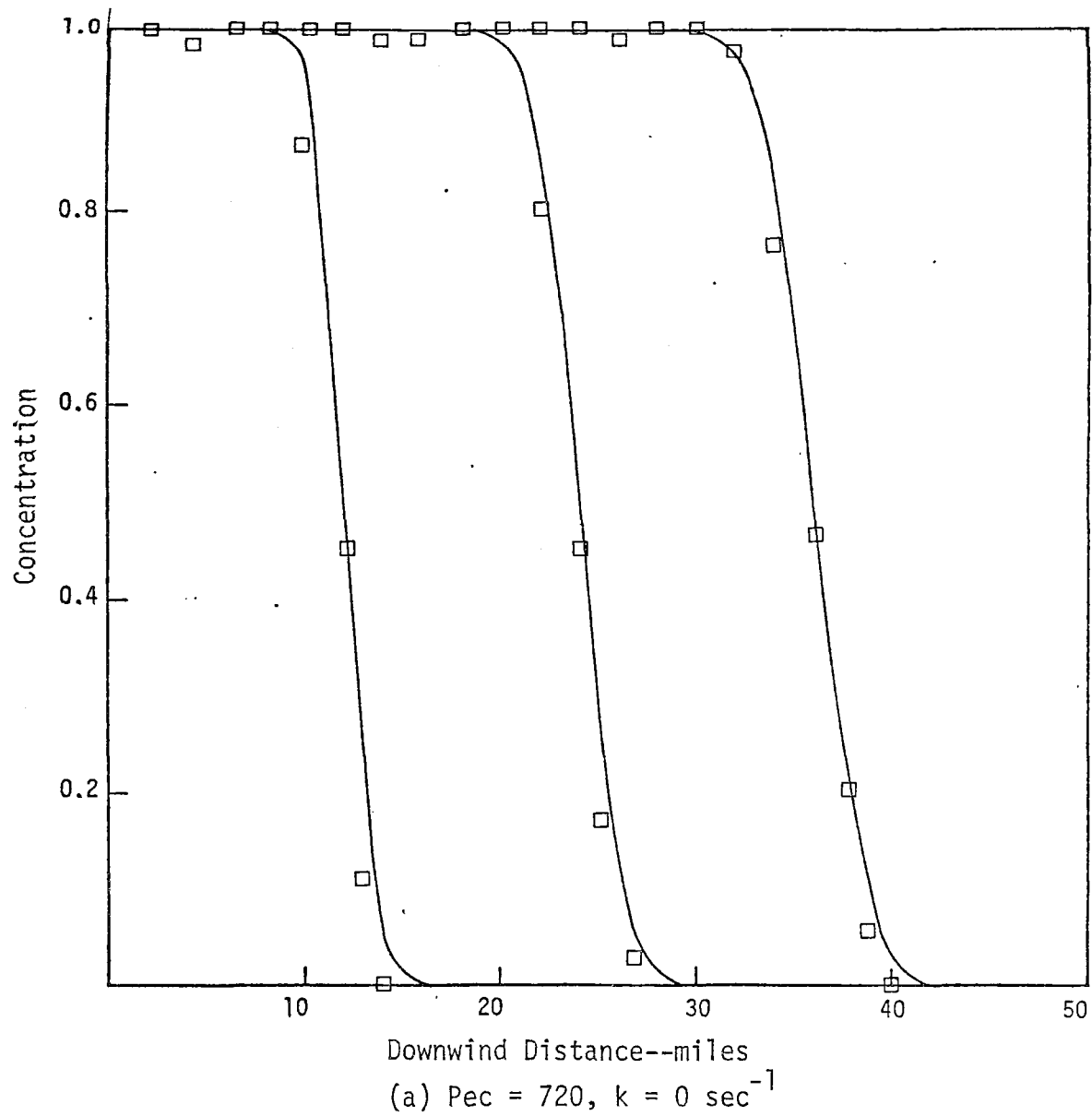


FIGURE 27. CONCENTRATION AS A FUNCTION OF DOWNWIND DISTANCE  
FOR THE GALERKIN METHOD

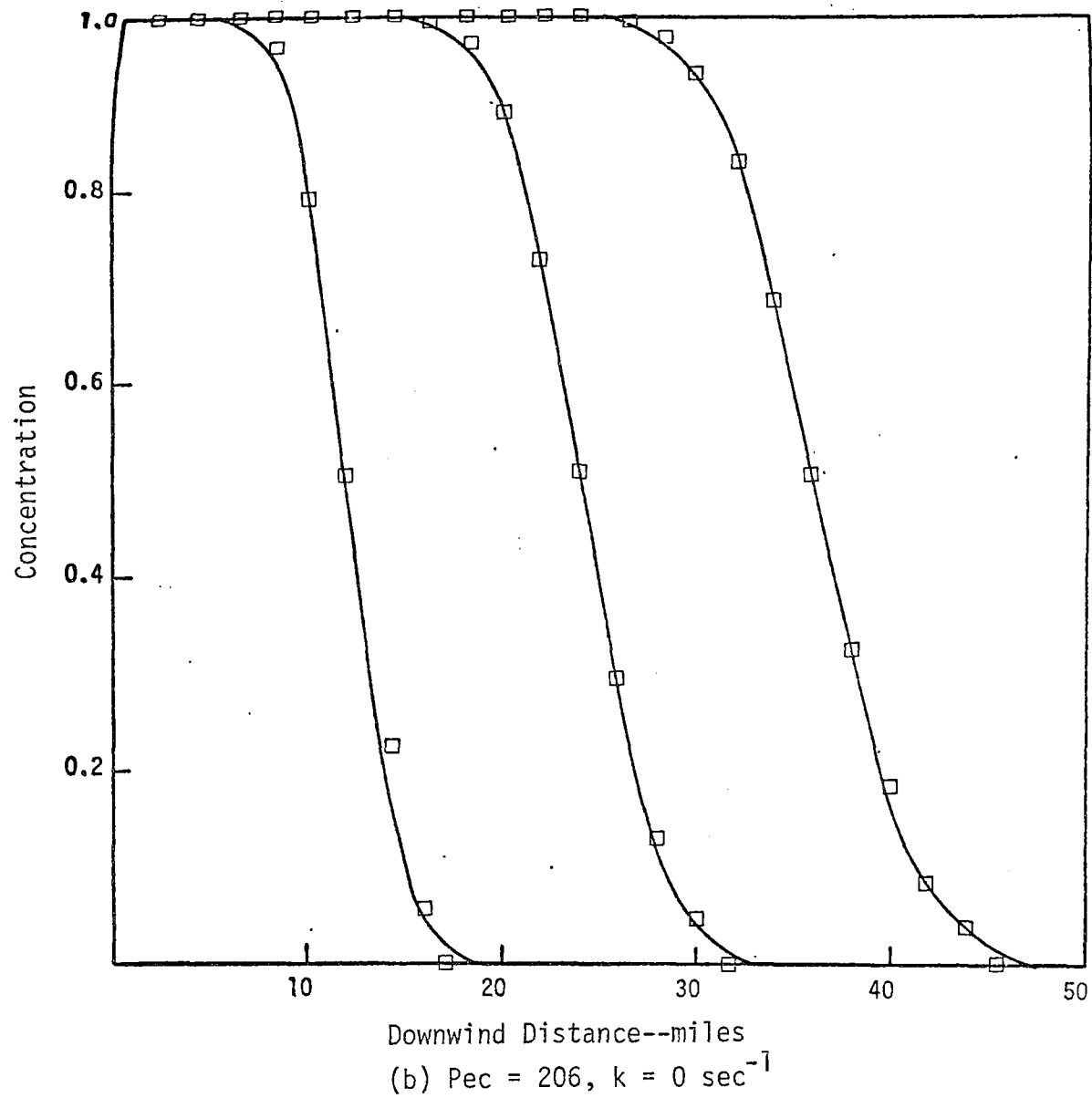


FIGURE 27. CONCENTRATION AS A FUNCTION OF DOWNWIND DISTANCE  
FOR THE GALERKIN METHOD (Continued)

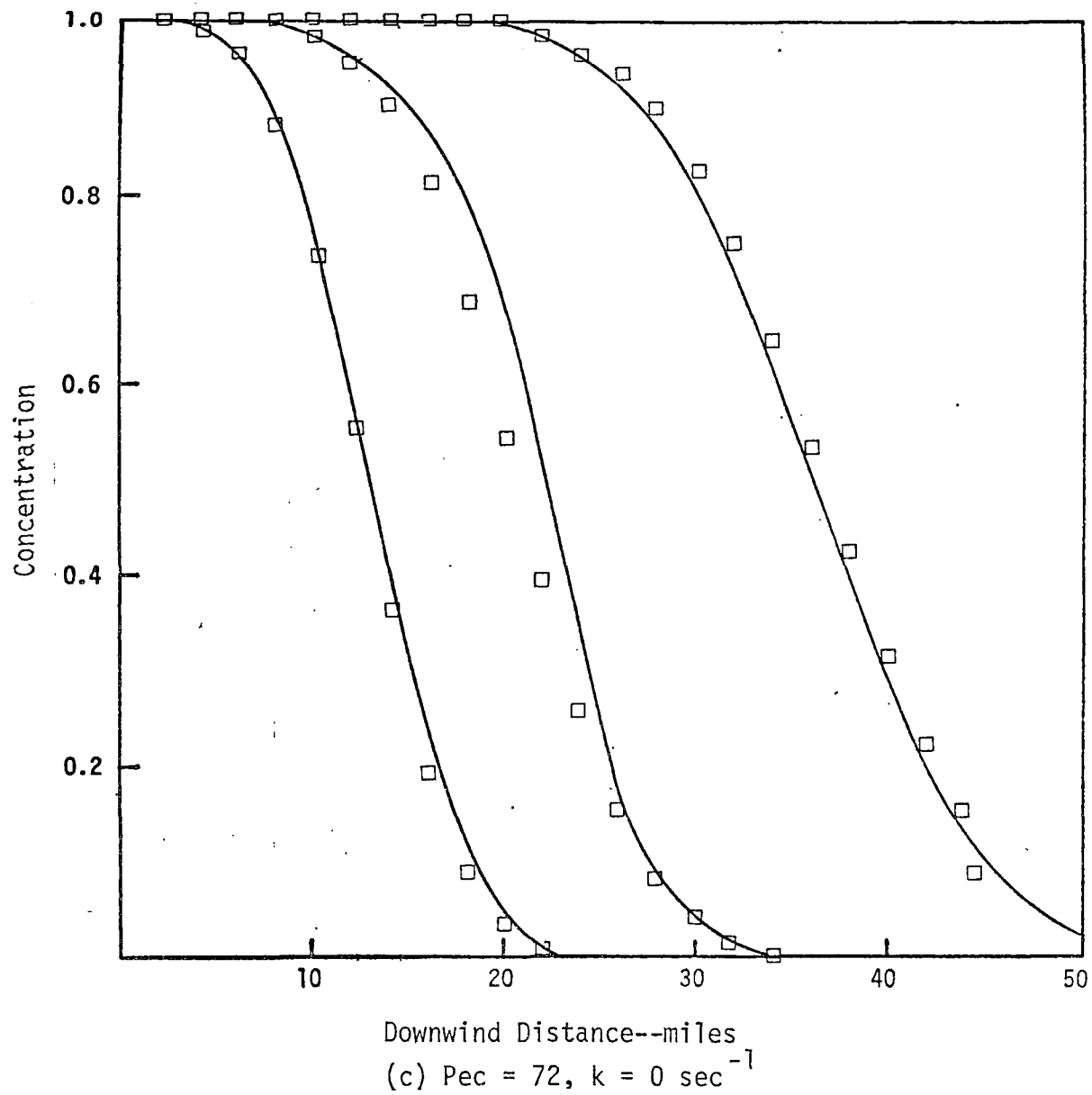


FIGURE 27. CONCENTRATION AS A FUNCTION OF DOWNWIND DISTANCE  
FOR THE GALERKIN METHOD (Continued)

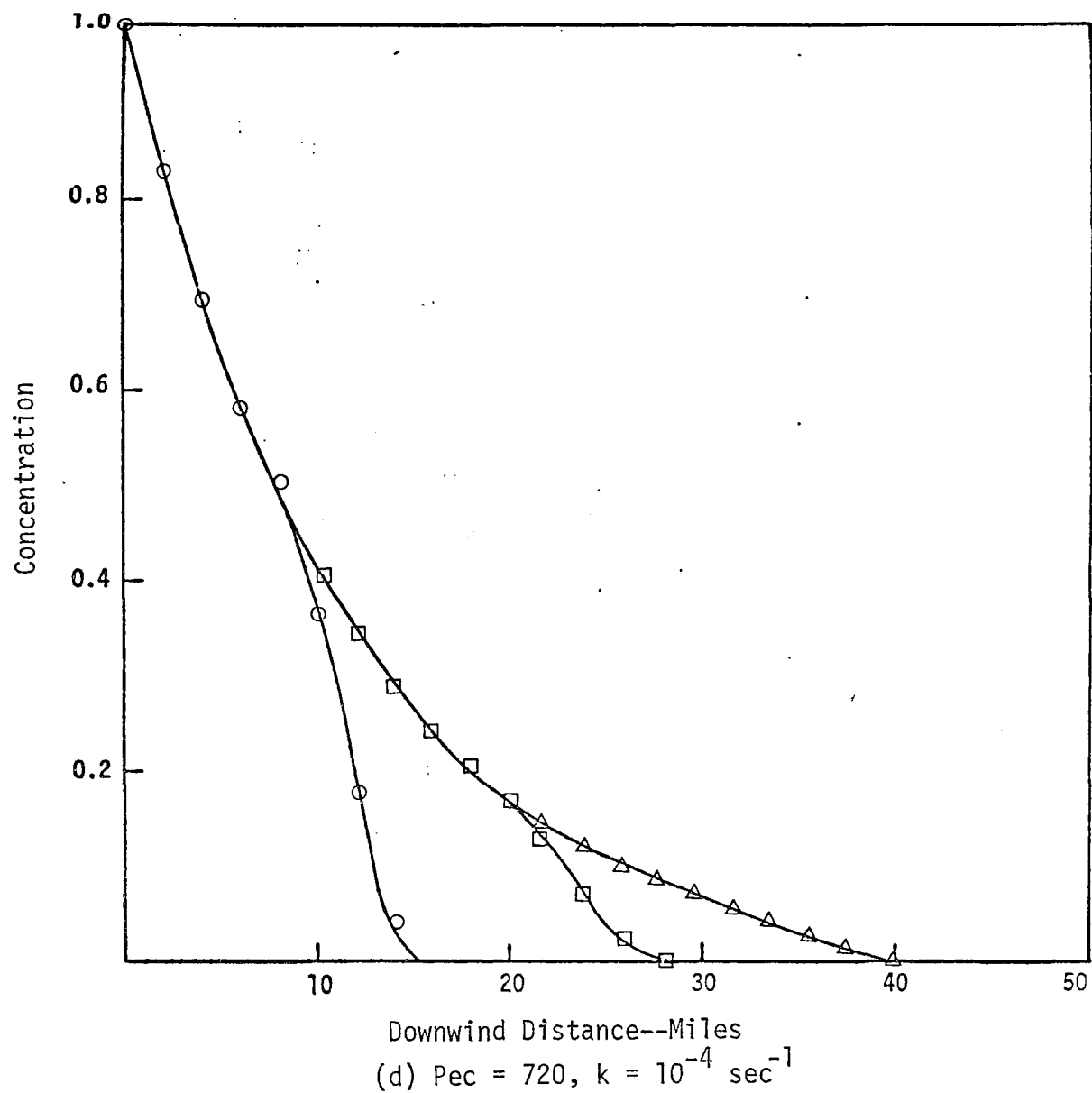


FIGURE 27. CONCENTRATION AS A FUNCTION OF DOWNWIND DISTANCE  
FOR THE GALERKIN METHOD (Continued)

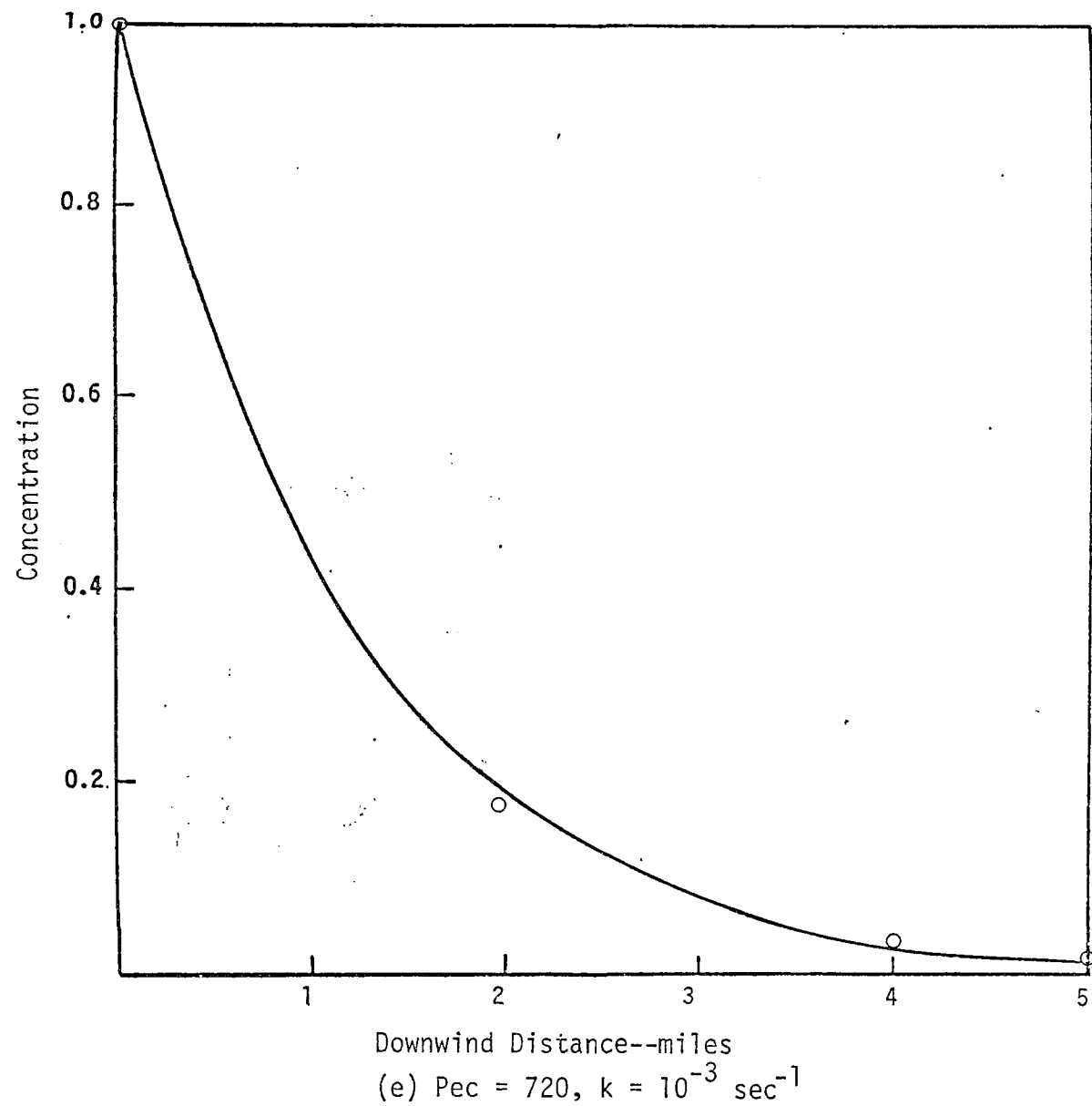


FIGURE 27. CONCENTRATION AS A FUNCTION OF DOWNWIND DISTANCE  
FOR THE GALERKIN METHOD (Continued)

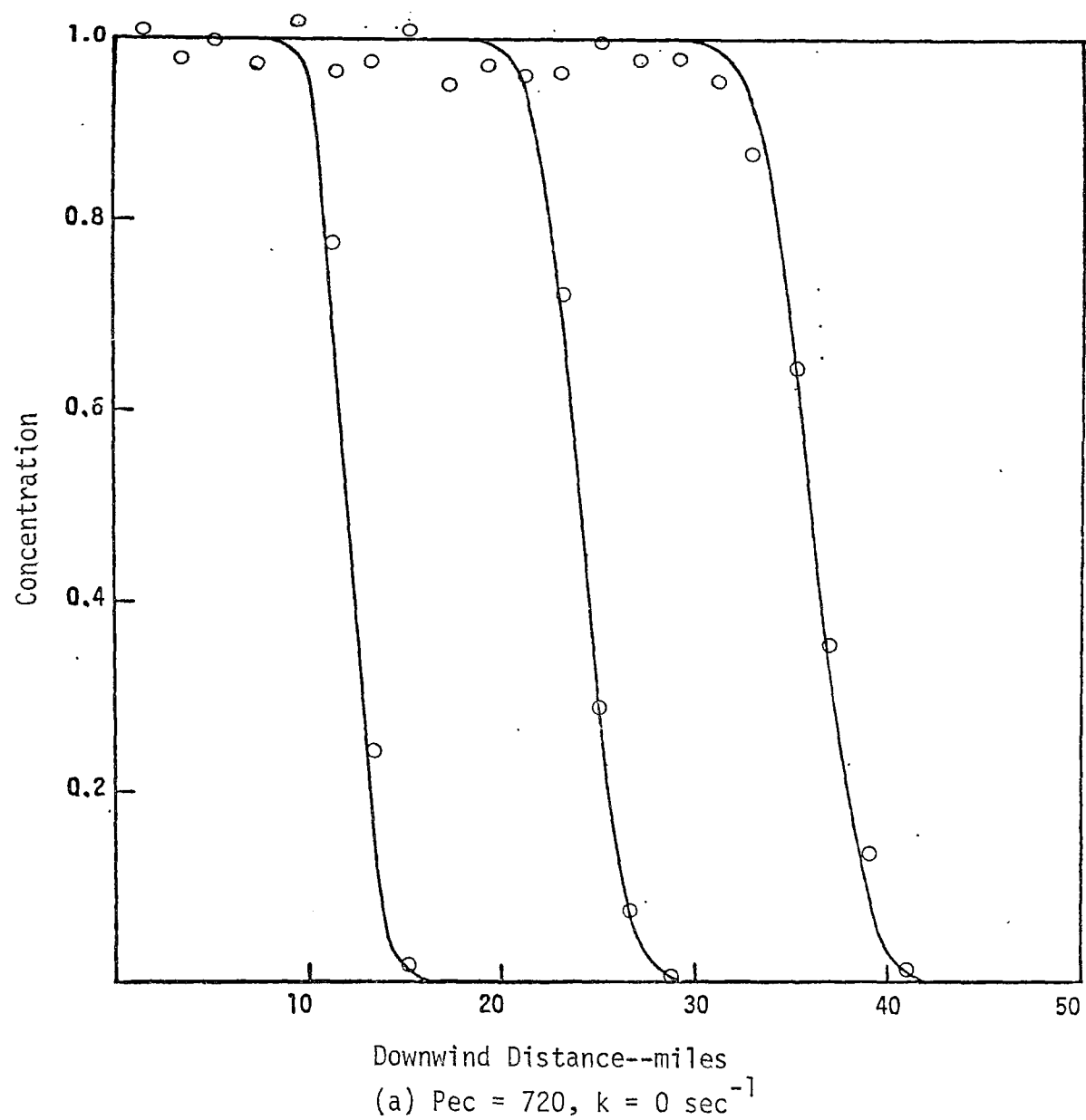


FIGURE 28. CONCENTRATION AS A FUNCTION OF DOWNWIND DISTANCE  
FOR THE PARTICLE-IN-CELL (SMOOTHED) METHODS

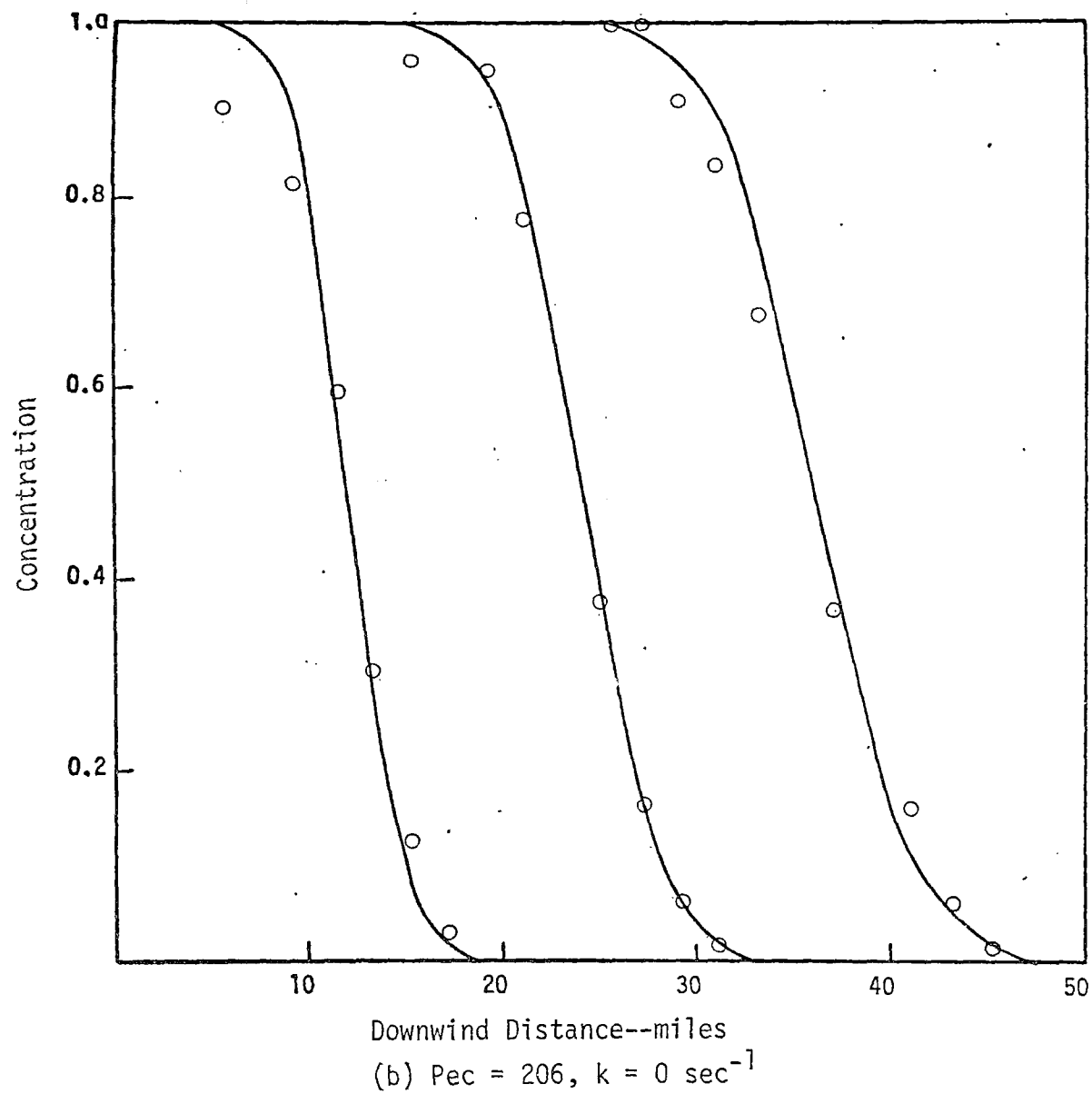


FIGURE 28. CONCENTRATION AS A FUNCTION OF DOWNWIND DISTANCE  
FOR THE PARTICLE-IN-CELL (SMOOTHED) METHODS (Continued)



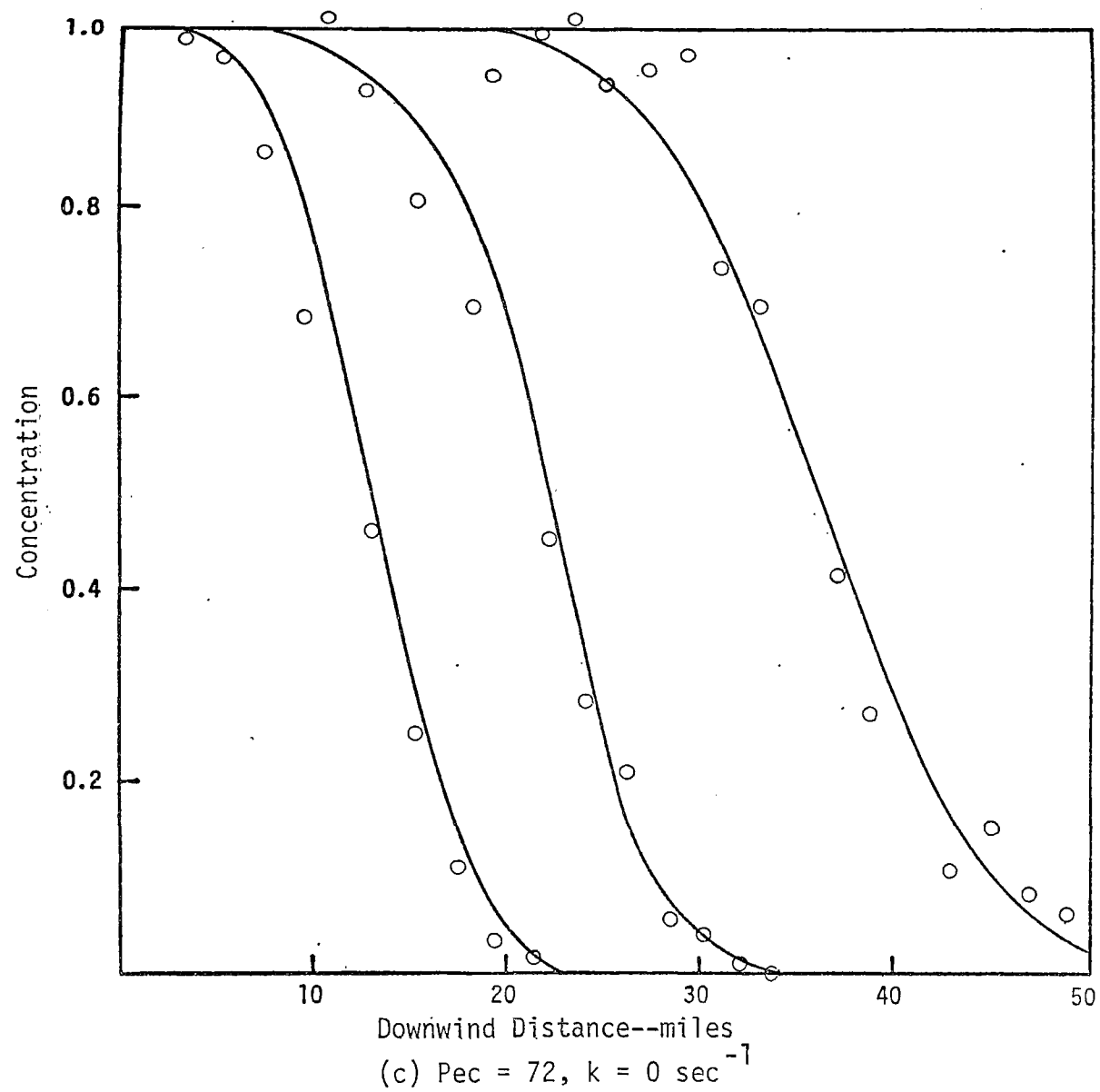


FIGURE 28. CONCENTRATION AS A FUNCTION OF DOWNWIND DISTANCE  
FOR THE PARTICLE-IN-CELL (SMOOTHED) METHODS (Continued)

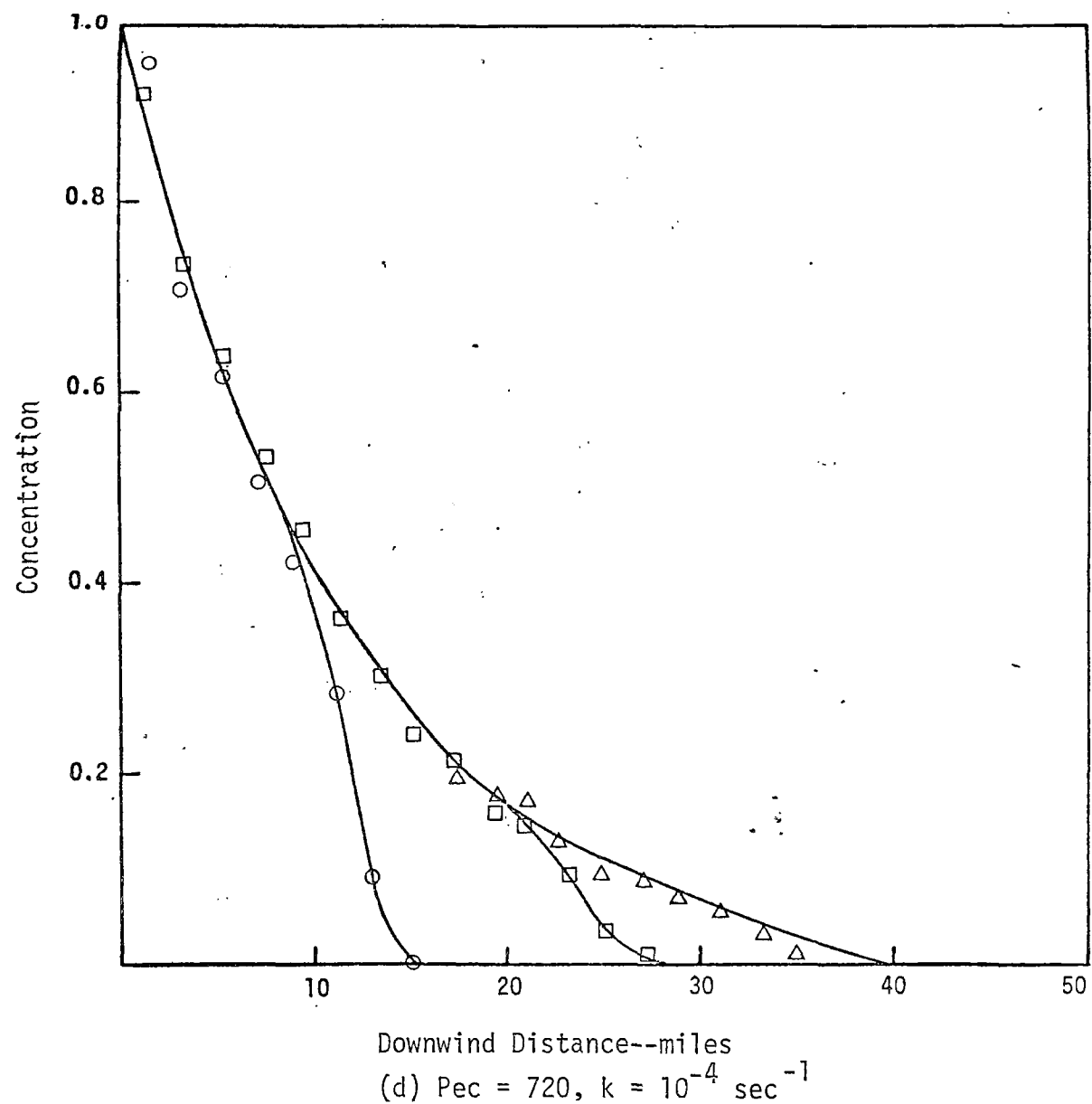


FIGURE 28. CONCENTRATION AS A FUNCTION OF DOWNWIND DISTANCE  
FOR THE PARTICLE-IN-CELL (SMOOTHED) METHODS (Continued)

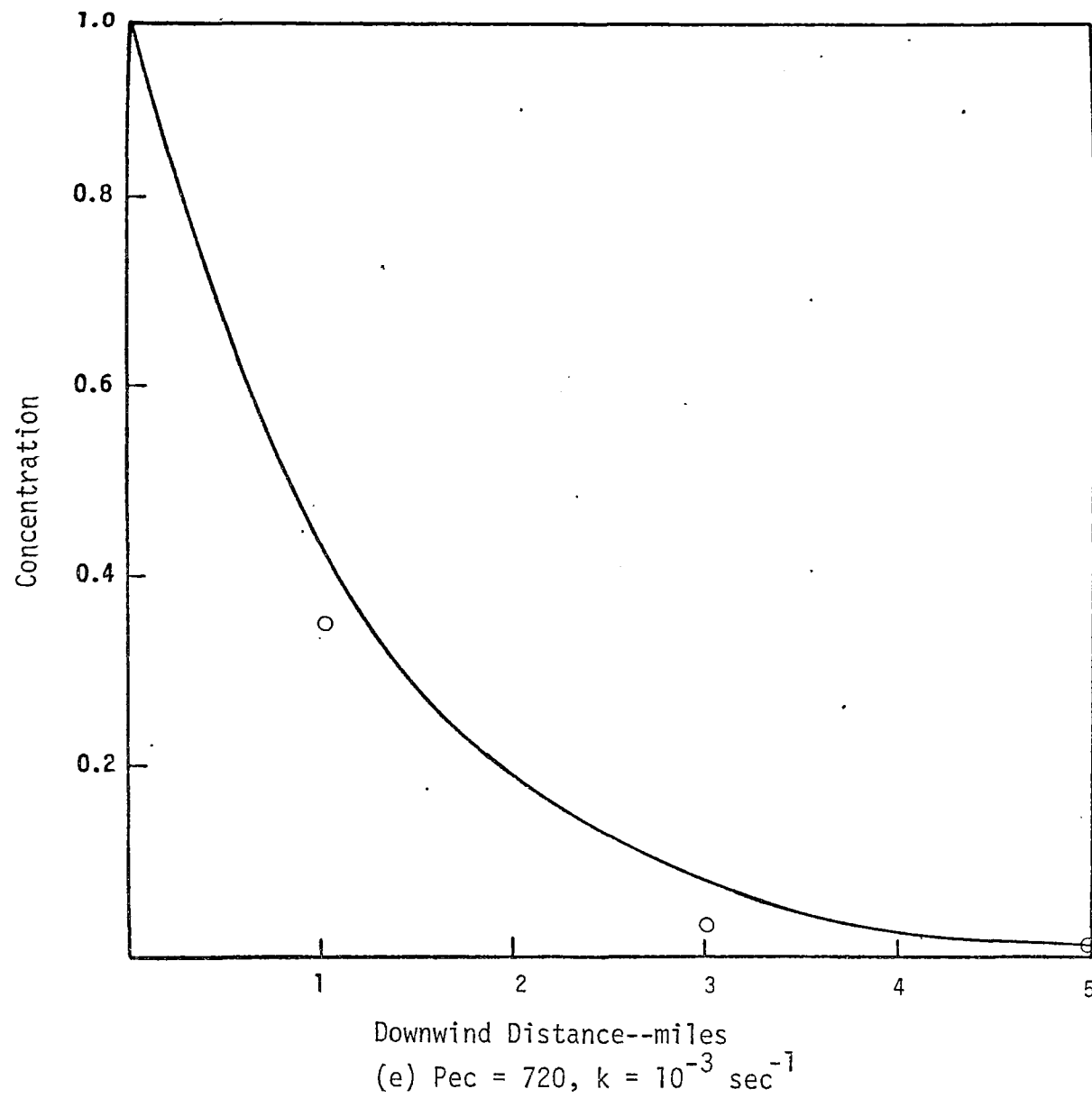


FIGURE 28. CONCENTRATION AS A FUNCTION OF DOWNWIND DISTANCE  
FOR THE PARTICLE-IN-CELL (SMOOTHED) METHODS (Concluded)

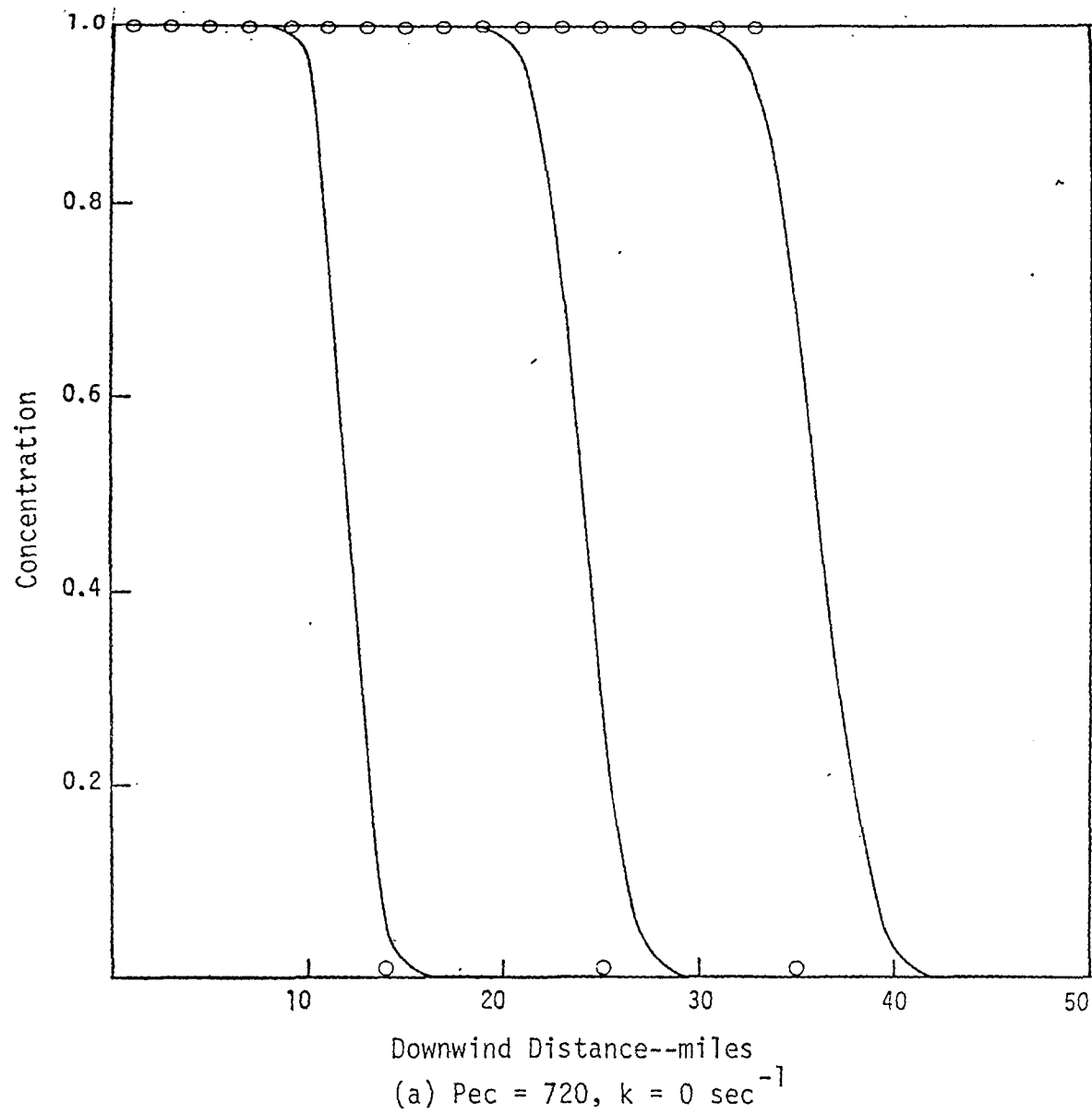


FIGURE 29. CONCENTRATION AS A FUNCTION OF DOWNWIND DISTANCE  
FOR THE EGAN AND MAHONEY METHOD

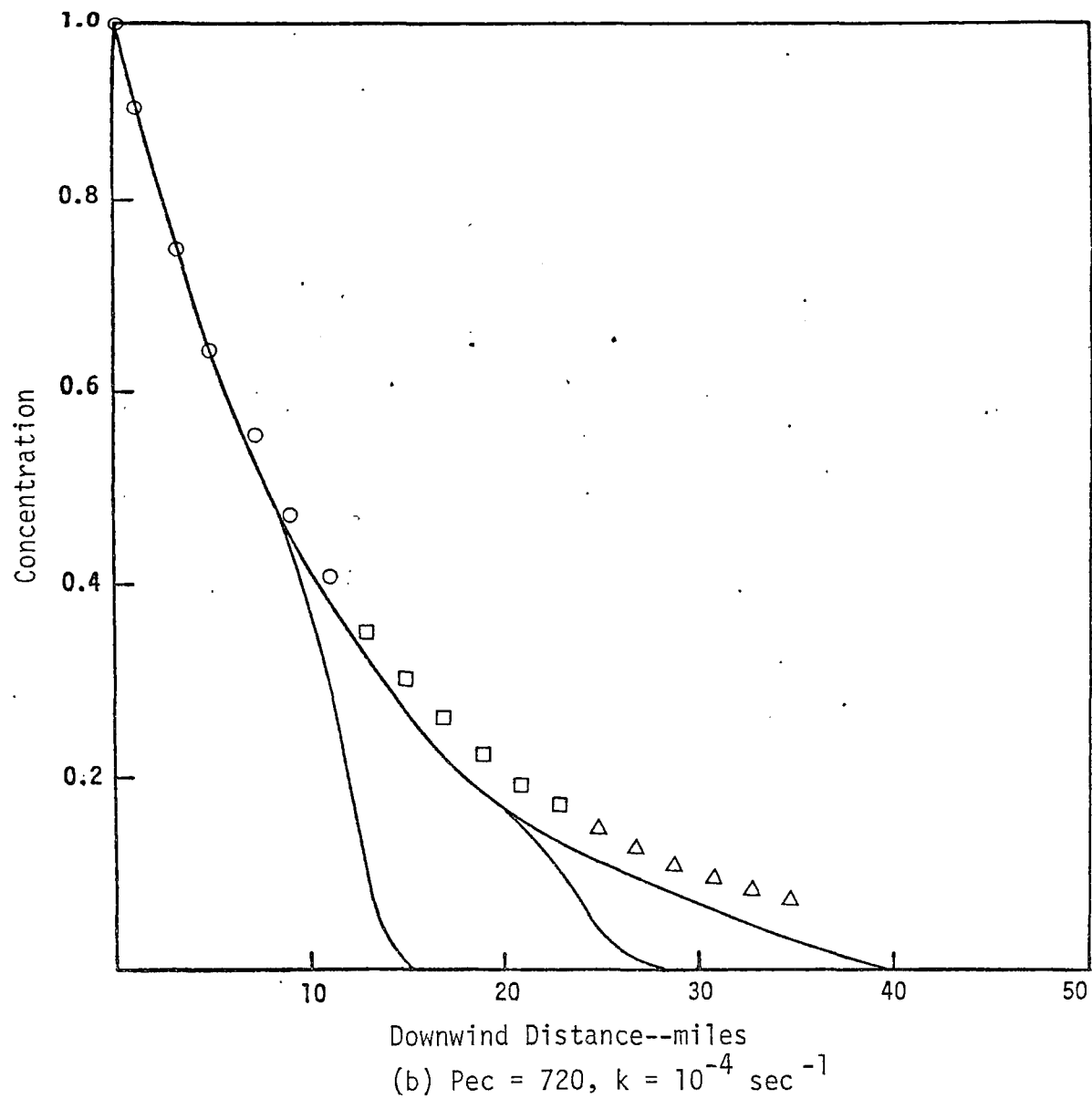


FIGURE 29. CONCENTRATION AS A FUNCTION OF DOWNWIND DISTANCE  
FOR THE EGAN AND MAHONEY METHOD (Continued)

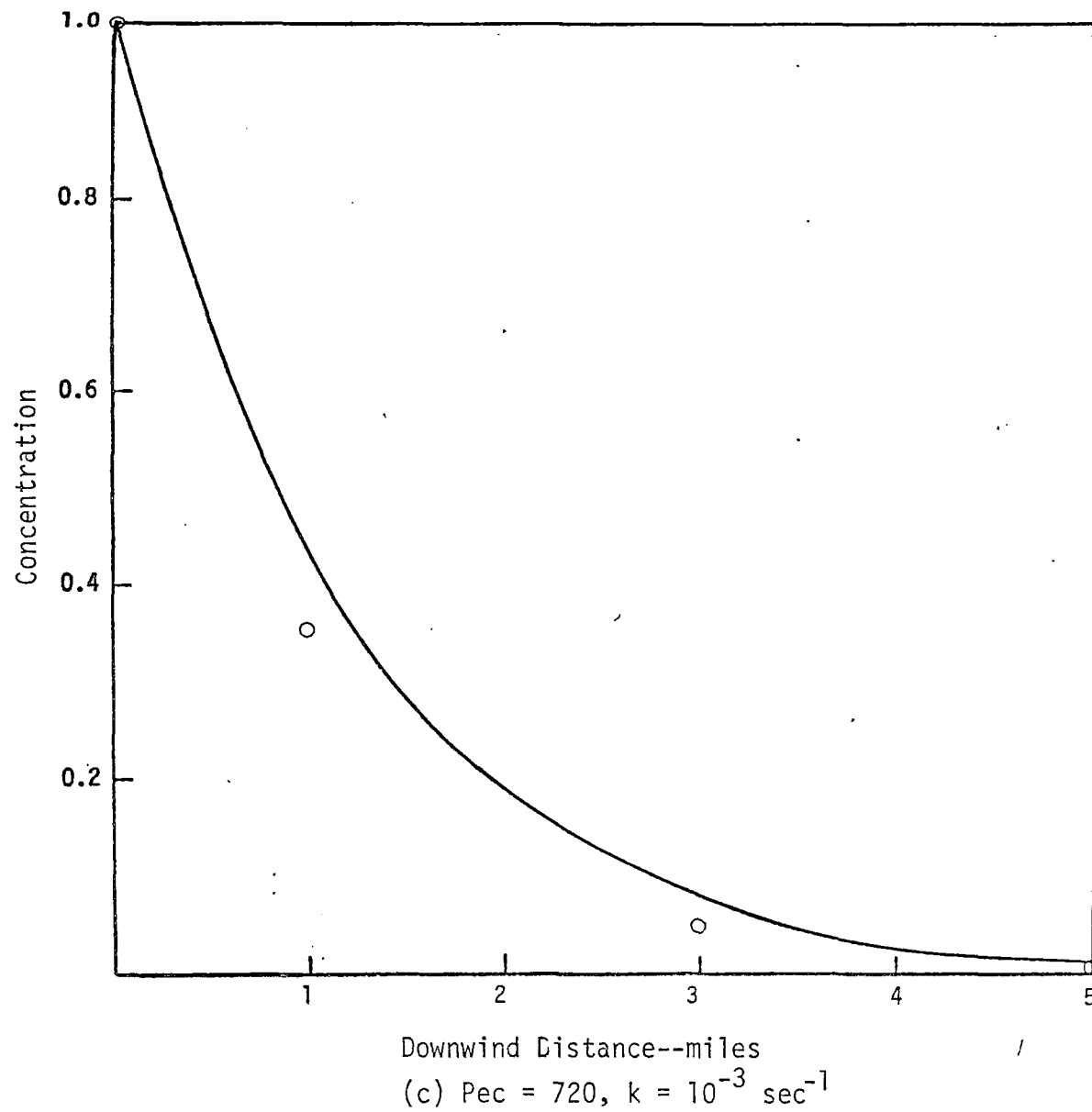


FIGURE 29. CONCENTRATION AS A FUNCTION OF DOWNWIND DISTANCE  
FOR THE EGAN AND MAHONEY METHOD (Concluded)

## 7. Computational Time

Concurrent with any appraisal of the accuracy associated with alternative solution techniques must be a comparison of the computing times required for these methods. Although a particular method may be extremely accurate, the computational time it requires may be so large that a less accurate, more efficient algorithm would be a better choice. Table 27 lists the computing times for the various methods surveyed in this study.

Table 27

### COMPUTING TIME REQUIRED FOR ALTERNATIVE SOLUTION METHODS

<u>Method</u>	<u>Computing Time (sec)</u>
Price--explicit	7.50
Price--implicit	11.10
Crowley--second order	7.40
Crowley--fourth order	7.40
SHASTA	7.95
Galerkin	13.2
Egan and Mahoney	1.10
Particle-in-cell	68.2

Note that all of the explicit finite difference methods use approximately the same amount of computing time (approximately 7.5 seconds). Of the implicit schemes, only a slight difference exists between the Galerkin and the Price methods. Obviously, the accuracy more than compensates for the larger computational time. Finally, the particle-in-cell methods are extremely costly in computing time and should be used only as a last resort.

## E. CONCLUSIONS

The selection of a solution algorithm for a set of partial differential equations should be based on considerations of both speed and accuracy. For the methods surveyed in this analysis, we drew the following conclusions:

- > For a rapid explicit scheme, the SHASTA technique should be chosen. Not only is the method accurate and efficient, but also it is guaranteed not to predict negative concentrations in areas having steep concentration gradients. This latter quality greatly enhances the appeal of the SHASTA method over competing schemes.
- > In those cases in which extremely high resolution is desirable, it is advisable to develop a Galerkin algorithm for the transport equation. The increase in accuracy, stability, and ease of modeling irregularly spaced regimes more than offsets the increased cost in computational time.
- > As more information becomes available in the open literature, the Egan and Mahoney method should be explored as a possible supplement or replacement for either the SHASTA or the Galerkin scheme.
- > Finite difference techniques introduce a considerable amount of numerical diffusion into the calculation, producing an over-prediction of pollutant concentrations downwind from the source. The effect is most pronounced using the Price scheme and is somewhat smaller using the Crowley second- and fourth-order systems. The Crowley fourth-order scheme tends to be more accurate than the corresponding second-order scheme in regions having a steep concentration gradient, though the fourth-order scheme frequently predicts negative concentrations in regions in which complex flow fields exist. Regardless of the technique used, finite difference methods are inaccurate for systems in which extremely fast reactions occur.



- > The particle-in-cell technique developed by Sklarew (1971) is accurate for both reactive and nonreactive systems, provided that a sufficient number of particles is used in the simulation. However, the time required for the simulation for a given accuracy can be prohibitively excessive and can thus invalidate the use of the technique.

In conclusion, we wish to caution the reader about interpreting the results obtained in this study: These results were developed for a simple one-dimensional, time-dependent problem in which a simple first-order reaction occurs. In a real situation, this idealized model can easily be invalidated by a complex flow field, a set of nonlinear reactions, or a complicated source emissions pattern. In essence, this analysis focused on one aspect of the complete problem: the identification and assessment of the errors associated with the solution of the one-dimensional advection-diffusion equation. The study did not treat problems that are associated with the method of fractional steps, nor did it consider systems in which nonlinearities occur (as they frequently do in the real world). Yet, since the numerical diffusion associated with finite difference techniques is considerable, the results of this study serve as a benchmark for identifying those schemes that are the most accurate in a one-dimensional sense. If one can assume that this accuracy is maintained throughout the entire solution, then the application of the most promising of these techniques to the current SAI model will most likely produce--but cannot guarantee--an improvement in the results.

## V AIRSHED MODEL MODIFICATION FOR MULTIDAY SIMULATION

Steven D. Reynolds  
Jody Ames

### A. INTRODUCTION

In the past, the application of the SAI airshed model has been limited to the simulation of one daytime period (usually 5 a.m. to 3 p.m.). During the present study, we adapted the model for multiday runs. The two most important benefits to be derived from multiday simulations are the following:

- > Treatment of multiday episodes. A primary objective of adapting models to perform multiday computations is to provide the basis for evaluating the effectiveness of air pollution control strategies. For example, difficulties in specifying initial conditions for some future year can be averted by performing a multiday run, since the predictions on the second and subsequent days are generally less sensitive to the choice of the initial concentration distribution input to the model. Also of interest is the short range prediction of the ground-level pollutant concentrations for strategies such as those that might be put into effect when meteorological conditions conducive to severe pollution episodes occur.
- > Identification of errors. Multiday simulations will be instrumental in establishing possible sources of error in the airshed model. Errors incurred in a short term simulation (say, less than 12 hours) would not accumulate to the extent that they would over a two- or three-day period. As an example, suppose that the predicted concentrations of total nitrogen oxides were much higher than measured values after a simulation of several days. This might suggest that either  $\text{NO}_x$  emissions are too high or sinks of  $\text{NO}_x$  have not been properly accounted for in the model.

One obvious difficulty that might preclude usage of the model for multiday runs is the accumulation of errors introduced by the numerical integration scheme. But as noted in the previous chapter, several promising numerical techniques are available that--if implemented in the model--should reduce numerical error propagation significantly.

In modifying the SAI model, we considered the following aspects of multiday usage:

- > Treatment of photochemistry at night.
- > Definition of the modeling region.
- > Use of a grid with variable resolution.
- > Generalization of the finite difference solution technique for use on a grid with variable vertical resolution.
- > Modification of the computer codes.

Furthermore, to obtain some experience in the performance of multiday runs, we prepared a set of emissions, meteorological, and air quality inputs applicable to the Los Angeles basin on 29 and 30 September 1969. These are two days that we studied under a previous EPA contract (68-02-0339). Using these days, we were able to compare results from the multiday simulation with those obtained from the corresponding 5 a.m. to 3 p.m. runs made previously. Of particular interest is the comparison of the two sets of predictions at 3 p.m. on 30 September to determine to what extent the two sets of predictions agree.

In the following sections, we summarize our efforts in each of the pursuits listed above.

## B. MODEL REFINEMENTS

### 1. Treatment of Photochemistry at Night

The primary objectives of this study were to examine the suitability of the kinetic mechanism employed in the airshed model for performing nighttime simulations and to determine whether chemical reaction effects can be ignored during a portion of the nighttime period to reduce computing costs. In addition, we wished to obtain some experience in running the model at night, since previous efforts were limited to the simulation of single daytime periods of 10 hours in duration. Because of the difficulties we experienced in incorporating the expanded 36-step mechanism in the airshed model, we decided to try to use the original version of the airshed model, which treats the kinetics using a 15-step mechanism.

To determine the applicability of the original 15-step kinetic mechanism employed in the airshed model (see Hecht, 1972) for use at night, we performed several "numerical" smog chamber simulations with photolysis rate constants set to only a small fraction of their nominal values. Since sunlight is one of the most important driving forces in the mechanism, we expected the photochemical processes to be slowed considerably after sunset. We set  $k_1$  (the  $\text{NO}_2$  photolysis rate constant) equal to  $0.01 \text{ min}^{-1}$  [the remaining rate constants and stoichiometric coefficients were assumed to be equal to those employed in the 29 September 1969 validation study (see Reynolds et al., 1973)] and employed the following initial conditions:

<u>Species</u>	<u>Initial Concentration (ppm)</u>
RHC	0.4
NO	0.5
$\text{NO}_2$	0.15
CO	15.0

The model predicted the following concentrations after eight hours:

<u>Species</u>	<u>Concentration (ppm)</u>
RHC	0.30
NO	0.32
NO <sub>2</sub>	0.32

These results clearly indicate that substantial chemical conversion is predicted in the absence of strong sunlight.

Since we expected the predicted concentrations to change only slightly from the initial conditions, we hypothesized that the HNO<sub>2</sub> steady-state assumption was responsible for the large change in concentrations. The RHC, NO, NO<sub>2</sub>, and O<sub>3</sub> concentrations predicted by the mechanism are independent of the value of  $k_7$  (the HNO<sub>2</sub> photolysis rate constant) used when HNO<sub>2</sub> is assumed to be in a pseudo-steady state. We then carried out a second simulation, which was similar in all respects to the first except that HNO<sub>2</sub> was not assumed to be in a steady state. The results of this simulation after eight hours were as follows:

<u>Species</u>	<u>Concentration (ppm)</u>
RHC	0.38
NO	0.45
NO <sub>2</sub>	0.17

These results indicate that considerably less chemical conversion is realized when it is assumed that  $d(\text{HNO}_2)/dt \neq 0$ .

As a final check on the old SAI mechanism employed above, we performed an eight-hour simulation using the new SAI mechanism currently being validated. The purpose of this test was to use the best available kinetic mechanism to obtain an estimate of how much chemical reaction takes place in the absence of intense sunlight. Assuming RHC to be entirely propylene,  $k_1$  to be equal to  $0.01 \text{ min}^{-1}$  (other photolysis rate constants were scaled accordingly), and initial conditions to be the same as those cited previously, the new mechanism predicted the following concentrations after eight hours:

<u>Species</u>	<u>Concentration (ppm)</u>
RHC	0.38
NO	0.45
NO <sub>2</sub>	0.18

These results reinforce our initial belief that the HNO<sub>2</sub> steady-state assumption is responsible for the observed conversion of NO to NO<sub>2</sub> in the 15-step mechanism.

It appears from the results of these tests that the 15-step kinetic mechanism previously employed in the airshed model with HNO<sub>2</sub> in a steady state will not be suitable for carrying out photochemical calculations at night. Since considerable effort would be required to remove the HNO<sub>2</sub> steady-state constraint from the old airshed model and, furthermore, since we are replacing the 15-step mechanism with the new expanded mechanism (in which HNO<sub>2</sub> is not assumed to be in a steady state), we decided to defer further study of the treatment of photochemistry at night. This effort should be resumed, however, when further experience is obtained in using the new mechanism in actual airshed simulations.

After reviewing the results of the smog chamber runs cited above, we found that we may be able to drop some, or perhaps all, of the reaction terms in the governing equations during a portion of the nighttime period. If this is possible, then computing requirements can be reduced significantly. And since we are concerned with multiday runs, it is especially important to find ways of reducing the costs of such simulations. To study further the possibility of modifying the treatment of chemistry at night, we need to perform appropriate nighttime simulations, both with and without chemistry in the model, to determine whether and when chemical reaction effects can be ignored. If the chemistry cannot be completely omitted from the model, perhaps the mechanism can be simplified.

## 2. Definition of the Modeling Region

To minimize errors resulting from the need to specify pollutant concentrations at points of transport into the modeling area, one should choose boundaries of the region such that either background levels or actual measurements can be

used to estimate the boundary conditions. In previous simulations of pollutants in the Los Angeles basin, we exercised particular care to account properly for pollutants transported into the region from areas over the ocean and aloft (i.e., contaminants originally residing in the inversion layer and subsequently injected into the mixed layer as the inversion was eroded by convective heating). Although significant amounts of pollutants are often carried out over the ocean at night, it is usually difficult to estimate the concentration levels in the returning off-shore air mass because of the absence of appropriate measurements. To employ background concentrations as the boundary conditions, one must model both the urban area of interest and a portion of the surrounding environs (suburban, rural, and ocean areas). In addition, the upper boundary of the modeling region should be defined at that elevation where background levels generally exist (1 to 2 kilometers should be sufficient). Thus, we modified our original treatment of the vertical extent of the model from the region between the ground and the inversion base to the region between the ground and a user-specified surface aloft. As an example, one could define the top of the region to correspond to the top of the inversion layer. The trapping effect of an elevated inversion layer within the model is treated through the z-dependence of the vertical diffusivity.

### 3. Use of a Grid with Variable Resolution

For efficient modeling of an urban area and a portion of its surroundings, a grid with variable resolution should be used. Choosing the appropriate degree of resolution in a particular area of the airshed depends primarily on the spatial characteristics of gradients in the concentration field. In areas where gradients are large, a relatively fine grid should be used; where gradients are small, a relatively coarse mesh spacing may be adequate. With respect to horizontal grid resolution, the mesh spacing in the outlying areas could be, say, two to four times that used over the urban center. Because many sources are located at "ground level," the vertical concentration gradient is often greatest near the surface. Thus, it may be advantageous to use fine vertical spacing near the ground and coarse spacing aloft. Since the numerical technique currently employed in the model is not readily adaptable for variable horizontal grid resolution, we developed only variable vertical grid resolution capabilities during this study.

However, inclusion of a variable horizontal mesh in the model, possibly using a nested grid approach, should be considered in future efforts to incorporate improved numerical solution techniques in the model.

#### 4. Modification of the Finite Difference Equations

Because the finite difference equations previously employed in the model were derived for an equally spaced grid, it was necessary to modify the difference expressions involving derivatives of the concentration field in the  $z$  (or  $\rho$ ) direction. [See Reynolds (1973) for a discussion of the numerical integration procedure.] In particular, changes were required in the advective and diffusive flux terms in Step III of the numerical integration technique. As an illustration of the nature of the changes made, Eqs. (44) through (54) in Reynolds (1973) become:

$$\begin{aligned} \ell C_{i,j,k}^{n+1} = & \ell C_{i,j,k}^{**} \frac{\Delta H_{i,j}^n}{\Delta H_{i,j}^{n+1}} + \frac{\Delta \tau}{2\Delta \rho_k \Delta H_{i,j}^{n+1}} \left( \ell F_{i,j,k-\frac{1}{2}}^{n+1} + \ell F_{i,j,k-\frac{1}{2}}^{**} \right. \\ & \left. - \ell F_{i,j,k+\frac{1}{2}}^{n+1} - \ell F_{i,j,k+\frac{1}{2}}^{**} \right) + \frac{\Delta \tau}{2\Delta H_{i,j}^{n+1}} \left( \ell R_{i,j,k}^{n+1} \Delta H_{i,j}^{n+1} \right. \\ & \left. + \ell R_{i,j,k}^{**} \Delta H_{i,j}^n \right) + \frac{\Delta \tau}{2\Delta H_{i,j}^{n+1}} \left( \ell S_{i,j,k}^{n+1} \Delta H_{i,j}^{n+1} + \ell S_{i,j,k}^n \Delta H_{i,j}^n \right) \quad , \quad (104) \end{aligned}$$

where

$$\begin{aligned} \ell F_{i,j,k-\frac{1}{2}}^{n+1} = & \frac{\phi_{i,j,k-\frac{1}{2}}^{n+1}}{2} \left( \lambda_k \ell C_{i,j,k-1}^{n+1} + (1 - \lambda_k) \ell C_{i,j,k}^{n+1} \right) \\ & + \mu_{i,j,k-\frac{1}{2}}^{n+1} \left( \ell C_{i,j,k-1}^{n+1} - \ell C_{i,j,k}^{n+1} \right) \quad , \quad k = 2, 3, \dots, K \quad . \quad (105) \end{aligned}$$



$$\begin{aligned} \ell F_{i,j,k-\frac{1}{2}}^{**} &= \frac{\phi_{i,j,k-\frac{1}{2}}^n}{2} \left( \lambda_k \ell C_{i,j,k-1}^{**} + (1 - \lambda_k) \ell C_{i,j,k}^{**} \right) \\ &+ \mu_{i,j,k-\frac{1}{2}}^n \left( \ell C_{i,j,k-1}^{**} - \ell C_{i,j,k}^{**} \right), \quad k = 2, 3, \dots, K \end{aligned} \quad (106)$$

$$\phi_{i,j,k-\frac{1}{2}}^n = W_{i,j,k-\frac{1}{2}}^n \quad (107)$$

$$\mu_{i,j,k-\frac{1}{2}}^n = \frac{V_{i,j,k-\frac{1}{2}}^{Kn}}{0.5 (\Delta \rho_{k-1} + \Delta \rho_k) \Delta H_{i,j}^n} \quad (108)$$

$$\lambda_k = \frac{\Delta \rho_k}{\Delta \rho_{k-1} + \Delta \rho_k} \quad .$$

In view of the discussion given in the previous section,  $\rho$  is now defined by the following relationship:

$$\rho = \frac{z - h(x,y)}{H(x,y,t) - h(x,y)}, \quad ,$$

where

$h(x,y)$  = terrain elevation,  
 $H(x,y,t)$  = elevation of the upper boundary of the modeling region,  
 $\Delta \rho_k$  = the dimensionless height of the  $k$ -th level grid cell.

The boundary conditions at the ground and aloft are the following:

$$(1) \quad \rho = 0$$

$$\ell F_{i,j,\frac{1}{2}}^{n+1} = \ell Q_{i,j}^{n+1}, \quad (109)$$

$$\ell F_{i,j,\frac{1}{2}}^{**} = \ell Q_{i,j}^n, \quad (110)$$

where  $k = 1/2$  is equivalent to  $\rho = 0$ .

$$(2) \quad \rho = 1$$

$$F_{i,j,K+\frac{1}{2}}^{n+1} = \phi_{i,j,K+\frac{1}{2}}^{n+1} \ell_{i,j,K+\frac{1}{2}}^{n+1} g_{i,j,K+\frac{1}{2}}^{n+1} \quad \text{if} \quad \phi_{i,j,K+\frac{1}{2}}^{n+1} \leq 0 \quad , , \quad (111)$$

$$\ell_{i,j,K+\frac{1}{2}}^{n+1} = \phi_{i,j,K+\frac{1}{2}}^{n+1} \ell_{i,j,K}^{n+1} C_{i,j,K}^{n+1} \quad \text{if} \quad \phi_{i,j,K+\frac{1}{2}}^{n+1} > 0 \quad , \quad (112)$$

$$\ell_{i,j,K+\frac{1}{2}}^{**} = \phi_{i,j,K+\frac{1}{2}}^n \ell_{i,j,K+\frac{1}{2}}^n g_{i,j,K+\frac{1}{2}}^n \quad \text{if} \quad \phi_{i,j,K+\frac{1}{2}}^n \leq 0 \quad , \quad (113)$$

$$\ell_{i,j,K+\frac{1}{2}}^{**} = \phi_{i,j,K+\frac{1}{2}}^n \ell_{i,j,K}^{**} C_{i,j,K}^{**} \quad \text{if} \quad \phi_{i,j,K+\frac{1}{2}}^n > 0 \quad , \quad (114)$$

where  $k = K + \frac{1}{2}$  is equivalent to  $\rho = 1$ .

Changes in the matrix expressions given in Eqs. (55) through (70) of Reynolds (1973) follow directly from the difference equations given above.

## 5. Modification of the Computer Codes

To carry out multiday simulations, we modified several portions of the computer programs. These changes essentially make the codes more general. Furthermore, the main code now allows the user to use a grid with variable vertical resolution, where the spacing interval is treated as a model input. As an example, in the Los Angeles simulation, which is discussed in the next section, we used a grid with 10 vertical levels and the following mesh spacing:

<u>Level</u>	<u>Grid Spacing (feet)</u>
10 (top)	1625
9	825
8	425
7	225
6	125
5	75
4	50
3	50
2	50
1 (ground level)	50

Thus, the modeling region is assumed to extend from the ground to an elevation of 3500 feet above the terrain. In addition, we implemented appropriate changes, corresponding to the discussion given in the previous section, in the coding of the finite difference equations.

In addition to the above-mentioned changes, we restructured the input data deck setup to operate in the following manner. First, all parameters global to the run--i.e., those parameters that would not be expected to vary from day to day--are input. Then, the remaining inputs are arranged in daily packets, one packet for each day to be simulated. When the simulation reaches midnight, the input packet for the next day is read from the input file. After the first day, some daily parameters can be omitted from the input packet, and the values used on the previous day can be used again.

We also included provisions that allow the user to establish multiple emission files for the input of emissions data to the program. For example, one might establish two sets of emissions, one applicable to weekdays and the other suitable for weekends. Once such a set of files is established for an urban area, multiday runs consisting of any pattern of weekdays and weekends can be simulated. Table 28 illustrates the deck setup and lists some of the main parameters included as part of the global and daily inputs.

## C. MULTIDAY SIMULATION OF THE LOS ANGELES BASIN

### 1. Preparation of Emissions and Meteorological Inputs

Since previous applications of the airshed model were limited to the simulation of a 10-hour daylight portion of each of six days in 1969, little consideration was given to the definition of emissions and meteorological inputs for use at night. Thus, to gain experience in the performance of multiday runs with the SAI model, we carried out a necessarily limited effort to estimate meteorological and emission inputs that would apply during the period from 3 p.m. on 29 September to 5 a.m. on 30 September 1969 (previous simulations were carried out for the 5 a.m. to 3 p.m. period on both 29 and 30 September 1969). In particular, we performed the following tasks:

Table 28

## ORGANIZATION OF MULTIDAY INPUT

## Global data

Run heading

Simulation options and grid definition

Start and stop times and dates

I/O units

Print options for maps

Region definition

Stations and landmarks

Integration parameters and stoichiometric coefficients

Activation energies

Initial Conditions

## Day 1 packet

Date, emissions type, input controls

Rate constants

Light intensity factors

Deposition velocities

Concentrations aloft

Point source emissions

Boundary conditions

## Day 2 packet

Date, emissions type, input controls

Rate constants\*

Light intensity factors\*

Deposition velocities\*

Concentrations aloft\*

Point source emissions\*

Boundary conditions\*

## Day 3 packet

•  
•  
•  
•

---

\* Can be omitted after Day 1.

- > We used the SAI automated wind field analysis package to generate hourly wind speed and direction maps spanning the period from 5 a.m. on 29 September to 3 p.m. on 30 September 1969.
- > We employed the SAI automated inversion analysis program to estimate hourly mixing depth maps, using actual observed mixing depths available for the daytime periods to the extent possible. We examined nighttime temperature profiles measured by Meteorological Research, Incorporated in the Los Angeles basin during the summer of 1973 and estimated that pollutants would typically be mixed throughout a depth of about 60 to 70 meters at night.
- > We prepared a set of fixed-source emission maps for hydrocarbons and  $\text{NO}_x$  that are applicable from 6 p.m. to 6 a.m. the following morning; the original SAI fixed-source maps were derived for the complementary 12-hour period. Using data presented in Appendix A of Roth et al. (1971), we estimated that about 25.5 tons of  $\text{NO}_x$  and 30 tons of low reactivity hydrocarbons are emitted in the modeling region between 6 p.m. and 6 a.m.
- > We specified boundary conditions at points of horizontal inflow into the model between 3 p.m. on 29 September and 5 a.m. on 30 September. Boundary conditions at other hours were available from the model validation studies reported in Reynolds et al. (1973).

At this point, it is appropriate to note that the paucity of meteorological and emissions data applicable specifically during the nighttime hours makes the estimation of mixing depths and emission rates highly uncertain. The primary objective of our present effort was simply to assemble a set of "reasonable" inputs that can be used in tests of the multiday version of the SAI airshed model. Further efforts should be made to refine the temporal distribution of surface street and freeway traffic activity and the spatial and temporal distributions of the HC and  $\text{NO}_x$  emissions from stationary sources at night [see Roberts et al., (1971)].

## 2. Discussion of the Multiday Simulation Results

To test the various modifications made in both the structure of the model and the computer codes, we performed a multiday simulation of pollutant concen-

trations in the Los Angeles basin. As noted in Section B-1, we decided that the 15-step chemical kinetic mechanism employed in the model is inappropriate for use at night. Thus, the simulation reported here was carried out for CO alone. When an appropriate set of emissions inputs suitable for usage with the new mechanism can be developed, multiday photochemical simulations should be undertaken.

Plots of predicted and measured CO concentrations at the downtown Los Angeles, Long Beach, West Los Angeles, Burbank, Reseda, Whittier, and Azusa stations are given in Figures 30 through 36, respectively. The simulation extends from 5 a.m. PST on 29 September to 3 p.m. PST on 30 September 1969. The results for the 5 a.m. to 3 p.m. period on 29 September are very similar to those obtained in the previously reported SAI validation effort. (Discrepancies in the two sets of predicted results are due to the manner in which the meteorological variables were specified--automatically in the former case and manually in the latter.) Of greater interest is an examination of the remaining results, which are best approached by considering the 5 p.m. to 5 a.m. nighttime period and the following 5 a.m. to 3 p.m. daytime period separately.

In general, the nighttime predictions are reasonably accurate considering the fact that neither vertical temperature measurements nor refined temporal distributions for motor vehicle activity were available to estimate the corresponding meteorological and emissions inputs. Results at the end of this period (5 a.m.) often fell within a few parts per million of the measured concentrations, as shown in Table 29. Two notable exceptions, however, are illustrated in the downtown Los Angeles and Burbank predictions (Figures 30 and 33, respectively). Upon further examination of the results for these two stations, we made the following observations:

- > Downtown Los Angeles. A rather substantial build-up in the CO concentration was observed to occur from 9 p.m. to midnight, but it was predicted to take place two hours earlier, from 7 p.m. to 10 p.m. Since the magnitudes of predicted and measured concentrations during the early morning hours of 30 September agree

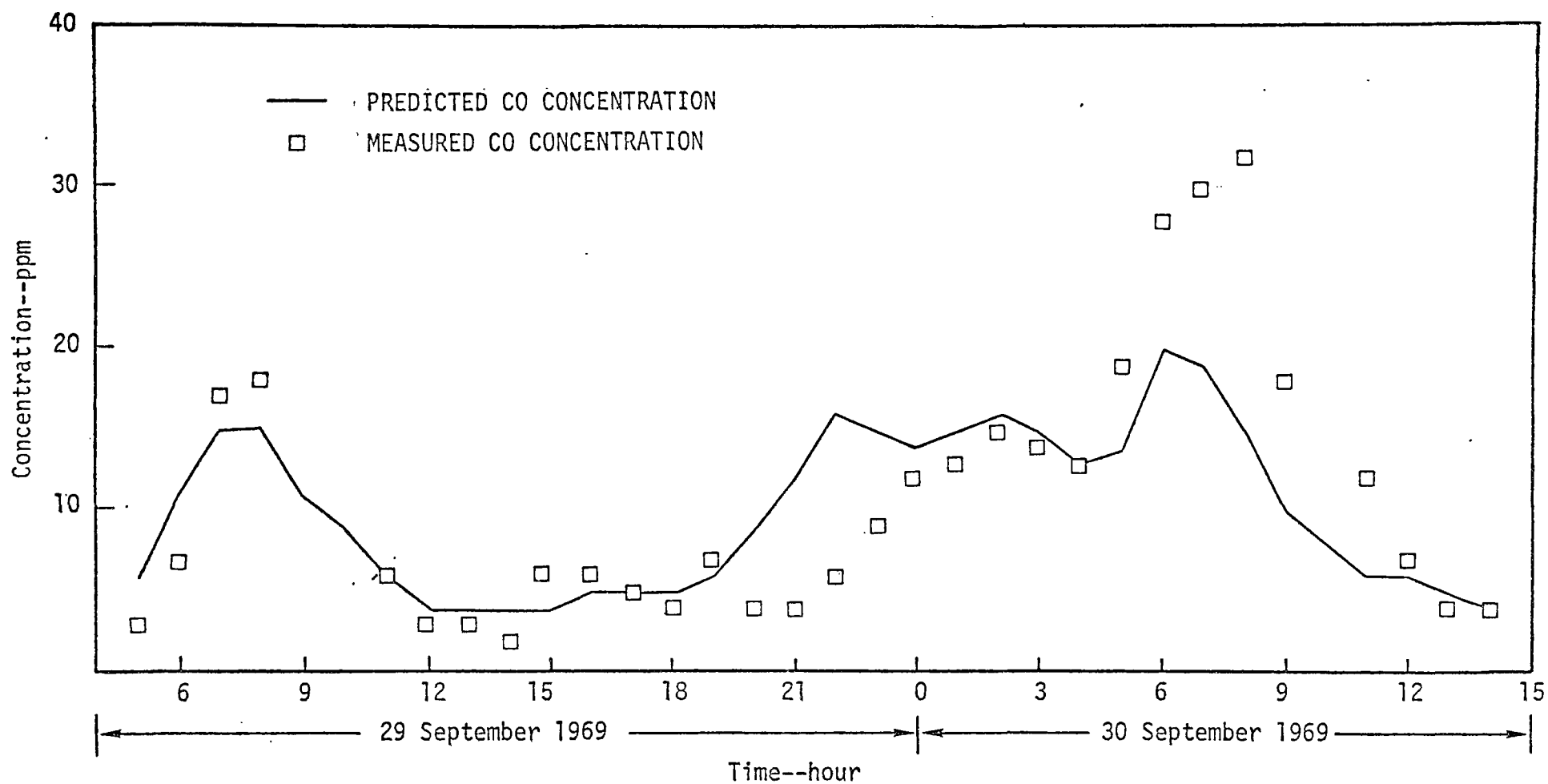


FIGURE 30. COMPARISON OF PREDICTED AND MEASURED HOURLY AVERAGED CO CONCENTRATIONS AT DOWNTOWN LOS ANGELES

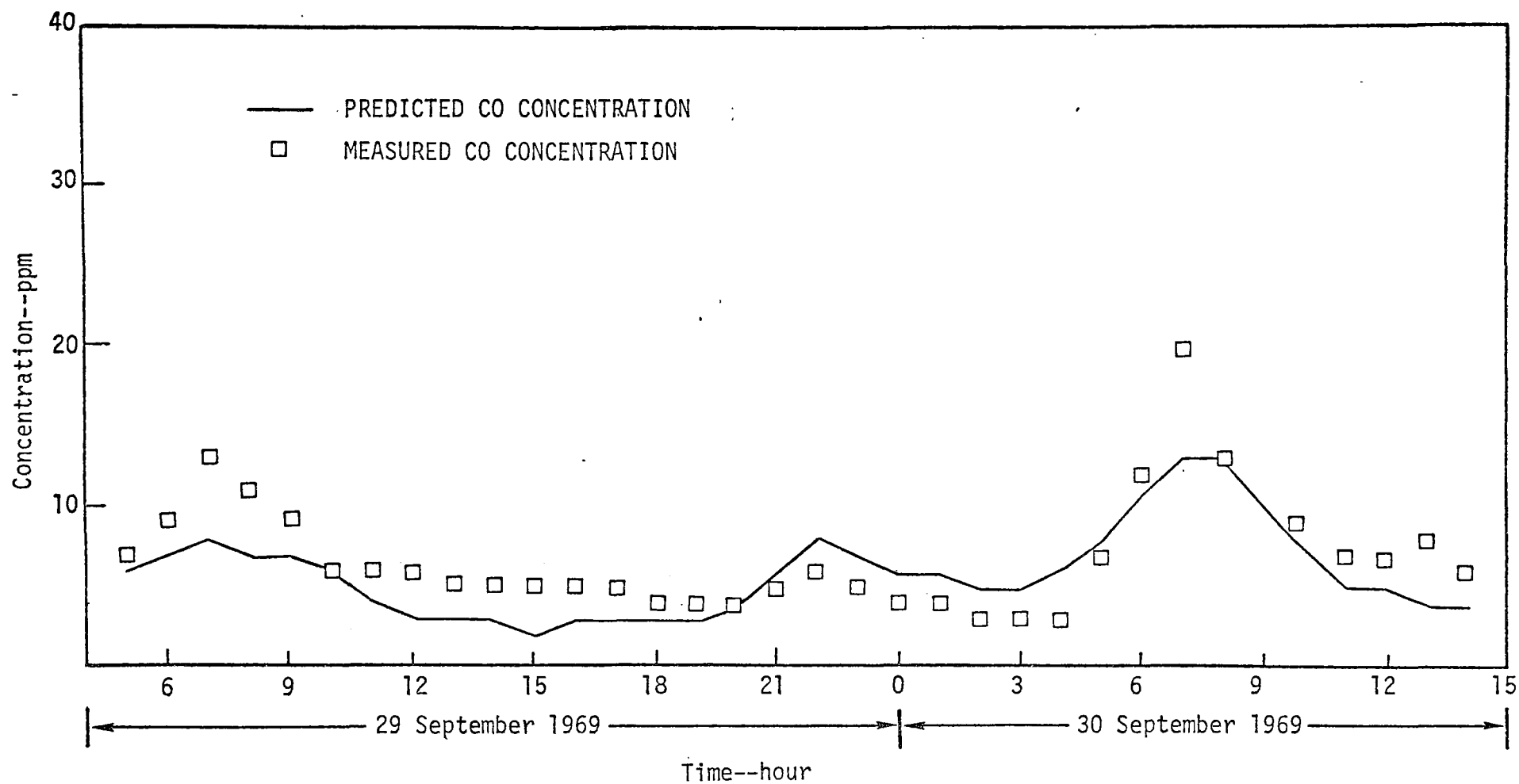


FIGURE 31. COMPARISON OF PREDICTED AND MEASURED HOURLY AVERAGED CO CONCENTRATIONS AT LONG BEACH



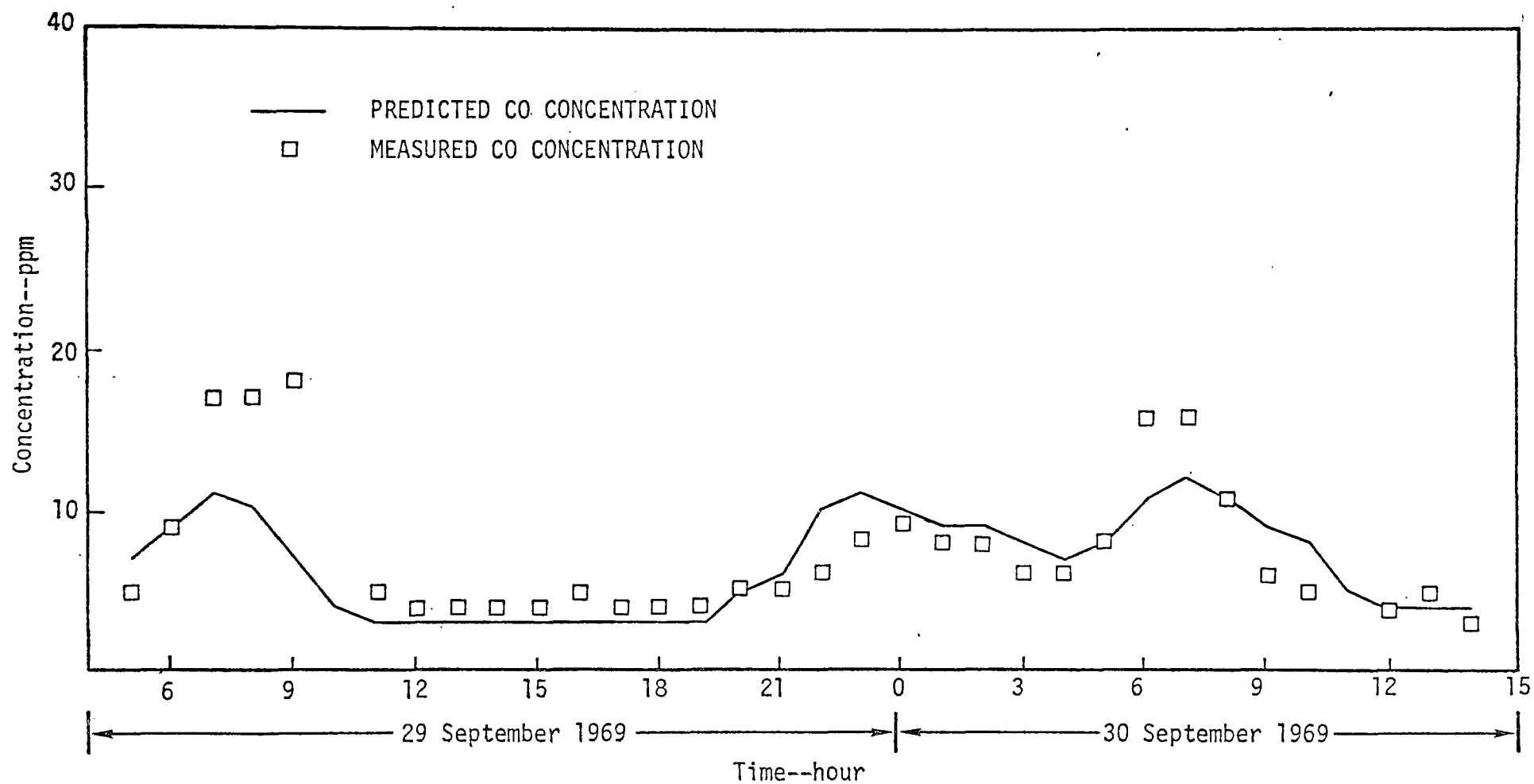


FIGURE 32. COMPARISON OF PREDICTED AND MEASURED HOURLY AVERAGED CO CONCENTRATIONS AT WEST LOS ANGELES

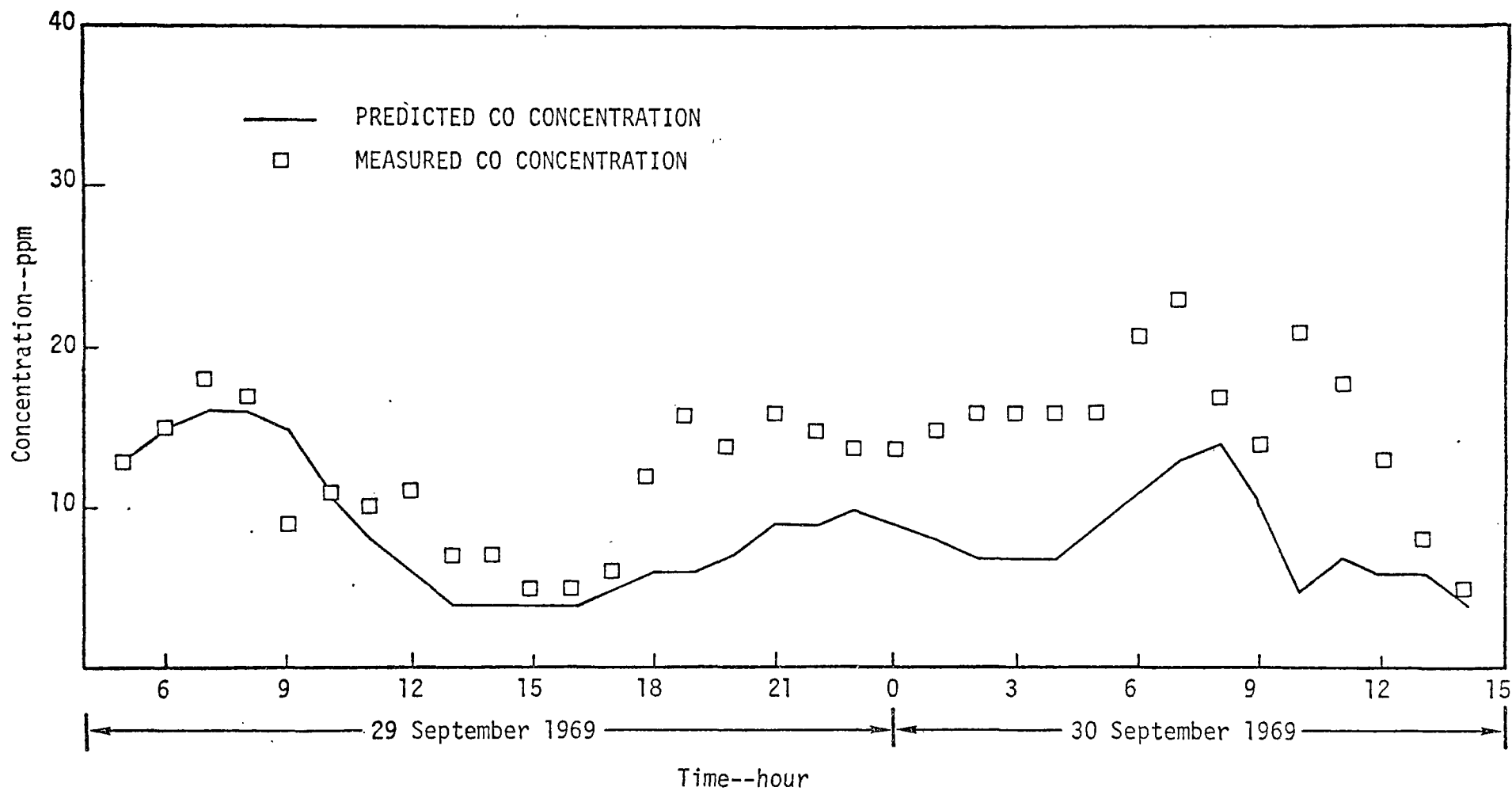


FIGURE 33. COMPARISON OF PREDICTED AND MEASURED HOURLY AVERAGED CO CONCENTRATIONS AT BURBANK

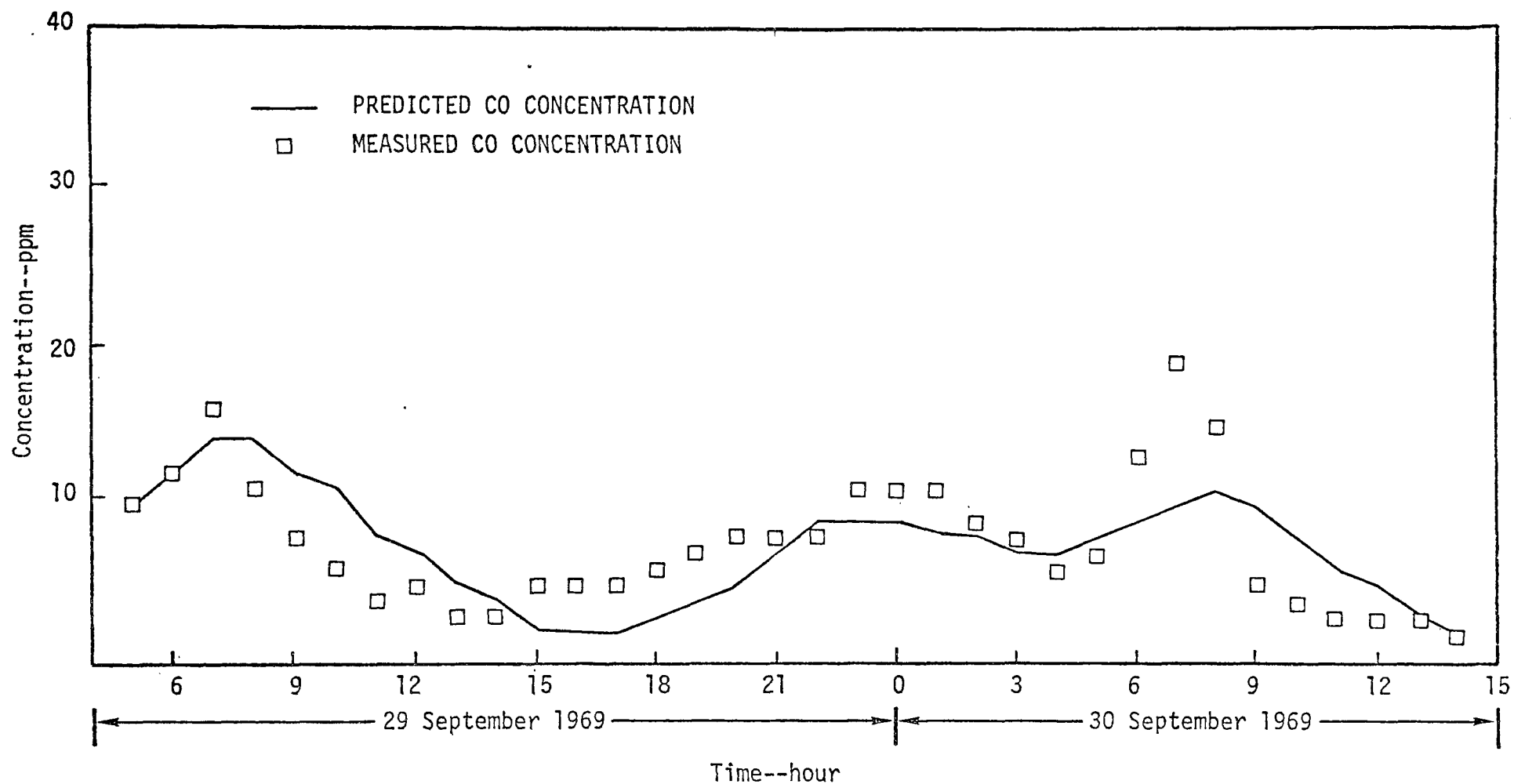


FIGURE 34. COMPARISON OF PREDICTED AND MEASURED HOURLY AVERAGED CO CONCENTRATIONS AT RESEDA

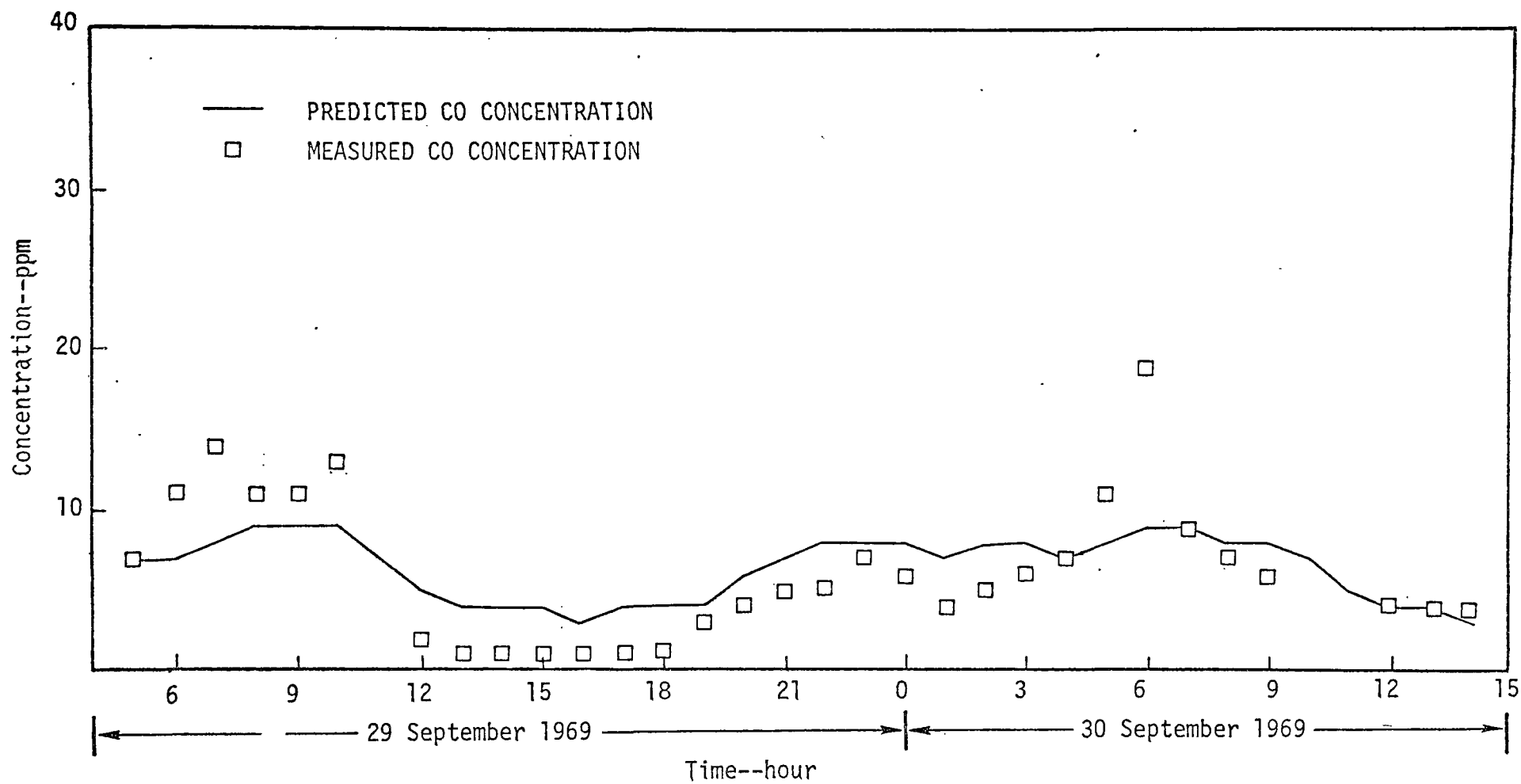


FIGURE 35. COMPARISON OF PREDICTED AND MEASURED HOURLY AVERAGED CO CONCENTRATIONS AT WHITTIER

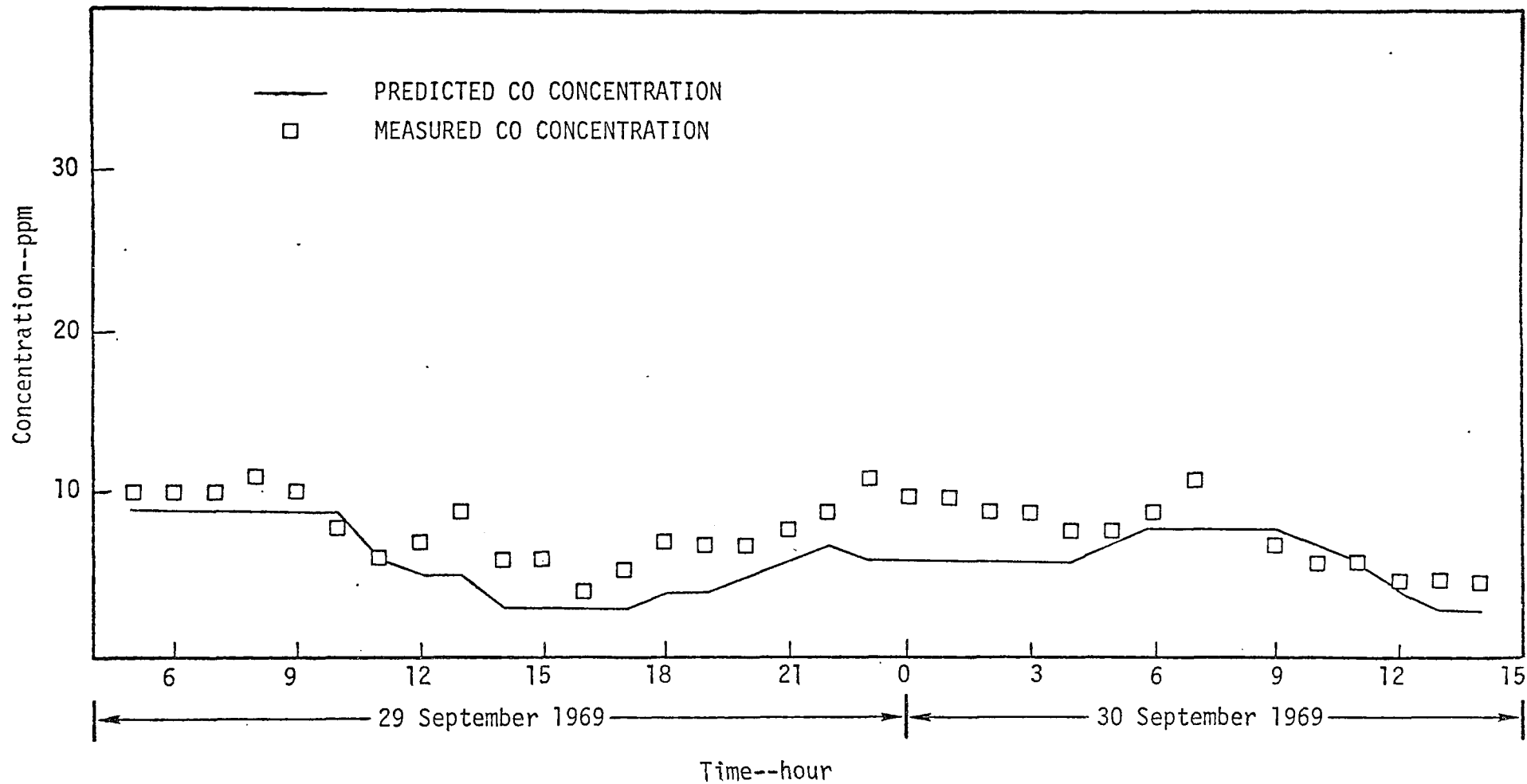


FIGURE 36. COMPARISON OF PREDICTED AND MEASURED HOURLY AVERAGED  
CO CONCENTRATIONS AT AZUSA

fairly well, the discrepancy in the time of occurrence of the build-up may well be the result of inaccuracies in the temporal distribution of motor vehicle emissions (the only source of CO in the model) during the period from 7 p.m. to midnight. Thus, the total loading seems correct, but the temporal distribution appears to be in error by about two hours. Traffic activity at 5 a.m. also seems to be greater than that predicted by the SAI emissions model.

- > Burbank. Of all the results presented in Figures 30 through 36, those calculated for the Burbank station are the poorest. Predicted concentrations after 5 p.m. on 29 September are consistently low by as much as 10 ppm. Upon examining the results for Reseda (also located in the San Fernando Valley), we noted that, although predictions are often low, the discrepancy in the predicted and measured concentrations is at most only 3 ppm. Meteorological data for Burbank indicate very light winds (1 mph) from the north. The high concentrations at this station may thus be the results of local emissions from the major interstate freeway situated to the north of the station. A shallow mixing layer coupled with near-calm conditions would certainly limit the extent to which local freeway emissions would be dispersed.

Basically, the nighttime predictions do not indicate any systematic errant behavior in the model. In fact, considering the absence of key meteorological and emissions data, the 5 p.m. to 5 a.m. results are about as good as might be expected under the circumstances.

Turning now to an examination of the daytime results for 30 September, we note that at many stations the multiday predictions are very similar to those previously reported in the single-day test of the model. Since the meteorological and emission inputs for these two runs were not significantly different, discrepancies in the two sets of predictions can be attributed primarily to differences between the multiday and single-day CO concentration distributions at 5 a.m. PST on 30 September 1969. In the single-day run, which began at 5 a.m., the initial CO concentration field, shown in

Table 29

PREDICTED AND MEASURED HOURLY AVERAGED CO CONCENTRATIONS  
AT THE END OF THE 29 TO 30 SEPTEMBER NIGHTTIME PERIOD\*

Station	Predicted Concentration (ppm)	Measured Concentration (ppm)
Downtown Los Angeles	13	13
Azusa	6	8
Burbank	7	16
West Los Angeles	7	6
Long Beach	6	3
Reseda	7	6
Pomona	3	3
Lennox	7	8
Whittier	7	7

\* The figures presented in this table were averaged from 4 a.m. to 5 a.m. PST on 30 September 1969.

Table 30, was estimated from the appropriate measurements reported by the Los Angeles and Orange County Air Pollution Control Districts. The concentration field on the grid at 5 a.m. in the multiday run is, of course, the result of a continuous simulation started at 5 a.m. on the previous morning. The ground-level concentration map for this case is illustrated in Table 31. Over much of the modeling region, the two sets of predictions agree within 2 or 3 ppm. However, the discrepancies are much higher in the Pasadena, downtown Los Angeles, and Burbank areas. The high CO levels in these areas given in Table 30 are the result of manual interpolation of the measured values reported at downtown Los Angeles and Burbank (the Pasadena station did not report CO levels on 30 September). In general, the single-day results for downtown Los Angeles and Burbank are better than the corresponding multi-day predictions. At other stations, the model predicted CO levels reasonably well, especially in view of the significant impact that local roadways may have on measured concentrations during the peak traffic hours in the morning.

It is also interesting to note the extent to which errors have accumulated throughout the multiday run. In Table 32, we give both the predicted and mea-

Table 30

MULTIDAY GROUND-LEVEL CO CONCENTRATION MAP  
AT 5 a.m. PST ON 30 SEPTEMBER 1969

CO GROUND LEVEL CONCENTRATIONS (PPM) AT 500.00 PST																									
1	2	3	4	5	6	7	8	9	10	11	12	13	14	15	16	17	18	19	20	21	22	23	24	25	
25	7.0	7.0	7.0	7.0	7.0	8.0	9.0	10.0	11.0	11.0	11.0														
24	7.0	7.0	7.0	7.0	8.0	9.0	10.0	12.0	13.0	13.0	13.0	12.0													
23	7.0	7.0	7.0	7.0	8.0	10.0	12.0	14.0	15.0	15.0	14.0	12.0	10.0												
22	7.0	7.0	7.0	7.0	8.0	10.0	12.0	14.0	16.0	16.0	16.0	14.0	12.0	11.0	10.0	9.0									
21	6.0	7.0	7.0	7.0	8.0	10.0	12.0	14.0	16.0	16.0	16.0	15.0	14.0	13.0	12.0	11.0	8.0	8.0	8.0	8.0	8.0	7.0	6.0	5.0	4.0
20	5.0	6.0	7.0	7.0	7.0	9.0	11.0	12.0	15.0	16.0	16.0	16.0	16.0	15.0	14.0	12.0	10.0	8.0	8.0	8.0	8.0	7.0	6.0	5.0	4.0
19	5.0	6.0	7.0	7.0	7.0	8.0	9.0	11.0	13.0	15.0	16.0	16.0	16.0	16.0	15.0	12.0	11.0	8.0	8.0	8.0	8.0	7.0	6.0	5.0	4.0
18	5.0	6.0	7.0	7.0	7.0	7.0	8.0	9.0	11.0	13.0	15.0	16.0	16.0	16.0	16.0	13.0	11.0	8.0	8.0	8.0	8.0	7.0	6.0	5.0	4.0
17	5.0	5.0	6.0	6.0	6.0	7.0	7.0	8.0	10.0	12.0	15.0	16.0	16.0	16.0	16.0	13.0	11.0	8.0	8.0	8.0	8.0	7.0	6.0	5.0	4.0
16			5.0	6.0	7.0	7.0	8.0	10.0	12.0	14.0	16.0	16.0	16.0	16.0	16.0	13.0	11.0	8.0	8.0	8.0	8.0	7.0	6.0	5.0	4.0
15				5.0	6.0	7.0	8.0	10.0	12.0	14.0	15.0	16.0	16.0	15.0	12.0	10.0	8.0	8.0	8.0	8.0	8.0	7.0	6.0	5.0	4.0
14					6.0	7.0	9.0	10.0	12.0	12.0	12.0	12.0	12.0	11.0	11.0	10.0	8.0	8.0	8.0	8.0	8.0	7.0	6.0	5.0	4.0
13					6.0	8.0	10.0	10.0	10.0	10.0	10.0	10.0	10.0	10.0	10.0	10.0	9.0	8.0	8.0	7.0	6.0	5.0	5.0	5.0	5.0
12						5.0	7.0	7.0	8.0	8.0	8.0	8.0	8.0	8.0	8.0	8.0	7.0	7.0	7.0	6.0	6.0	5.0	5.0	5.0	5.0
11							3.0	4.0	5.0	5.0	6.0	6.0	6.0	6.0	6.0	6.0	6.0	6.0	6.0	5.0	5.0	5.0	5.0	5.0	5.0
10								3.0	4.0	4.0	5.0	5.0	5.0	5.0	5.0	5.0	5.0	5.0	5.0	5.0	5.0	5.0	5.0	5.0	5.0
9									3.0	3.0	4.0	4.0	5.0	5.0	5.0	5.0	5.0	5.0	5.0	5.0	5.0	5.0	5.0	5.0	5.0
8										3.0	3.0	3.0	4.0	4.0	5.0	5.0	5.0	5.0	5.0	5.0	5.0	5.0	5.0	5.0	5.0
7											3.0	3.0	3.0	4.0	4.0	4.0	4.0	4.0	4.0	4.0	4.0	4.0	4.0	4.0	4.0
6												3.0	3.0	3.0	3.0	3.0	3.0	3.0	3.0	3.0	3.0	3.0	3.0	3.0	3.0
5																									
4																									
3																									
2																									
1																									



Table 31  
SINGLE-DAY GROUND-LEVEL CO CONCENTRATION MAP  
AT 5 a.m. PST ON 30 SEPTEMBER 1969

CO GROUND LEVEL CONCENTRATIONS (PPM) AT 509.00 ON 690930																								
1	2	3	4	5	6	7	8	9	10	11	12	13	14	15	16	17	18	19	20	21	22	23	24	25
25	5.2	4.9	4.8	5.2	6.1	6.7	7.1	7.6	7.9	7.9	8.0													
24	6.1	5.2	5.2	5.5	6.7	7.2	7.4	7.2	7.4	7.7	7.9													
23	5.4	5.8	5.9	6.5	8.4	8.5	8.6	8.0	7.2	7.0	7.4	8.0	8.1											
22	5.8	6.3	6.9	7.9	9.6	10.3	10.2	8.9	7.6	7.1	6.7	7.6	8.0	8.2	8.2	8.0								
21	6.0	6.5	7.0	6.7	8.1	9.7	10.8	10.8	8.8	7.7	6.8	7.3	7.7	8.4	8.7	8.5	8.5	9.2	9.0	8.1	6.6	5.1	4.1	3.5
20	4.5	4.7	4.6	4.0	4.6	5.5	7.9	9.9	8.4	7.4	7.5	6.8	7.5	8.3	9.0	9.1	9.1	9.5	8.9	7.1	6.2	5.5	4.5	3.6
19	3.7	3.6	3.3	3.0	3.8	4.0	5.9	8.7	10.2	8.8	8.4	7.7	7.6	8.2	8.8	9.1	9.3	9.2	8.0	6.6	6.5	6.2	4.8	3.6
18	2.8	2.8	2.8	3.0	3.9	4.5	5.9	8.4	10.0	10.6	10.7	10.0	9.0	8.9	9.4	10.0	10.4	10.1	8.8	8.1	8.3	7.6	6.7	4.1
17	2.1	2.6	3.1	3.7	4.7	6.5	6.3	8.5	10.7	12.5	14.0	12.5	11.8	11.0	10.0	9.8	10.7	10.6	9.1	8.1	7.8	7.3	5.9	4.2
16				4.7	6.2	6.9	7.6	7.8	10.0	12.6	15.4	14.2	14.0	13.6	11.1	10.5	11.0	10.5	9.1	7.9	7.2	7.2	6.2	4.4
15					5.8	6.6	7.5	7.8	9.1	11.6	14.1	13.0	12.3	13.4	12.7	11.0	10.9	9.4	7.9	6.5	6.3	6.9	5.9	4.3
14					5.7	6.8	7.9	8.0	9.3	11.2	10.4	10.7	12.3	12.1	11.4	9.7	8.5	6.5	5.0	4.9	5.8	6.6	4.3	3.3
13					4.3	6.0	7.1	6.9	7.2	8.3	8.1	9.0	10.5	11.0	11.2	8.8	7.4	5.8	4.8	4.6	5.4	5.3	4.2	3.3
12					4.4	5.8	5.8	6.0	6.3	6.5	7.6	8.5	9.5	10.3	9.1	7.2	5.7	4.9	5.0	5.5	5.4	4.3	3.3	
11					2.7	4.0	5.6	5.6	5.4	5.4	6.5	7.0	8.4	9.3	4.7	4.4	7.9	6.6	6.6	6.2	5.4	4.2	3.4	
10						1.7	3.0	3.9	4.5	5.4	4.9	5.9	6.4	7.7	8.6	8.2	8.6	9.3	9.7	9.2	7.8	6.1	4.7	3.4
9						1.4	2.2	2.9	3.7	4.5	5.2	6.5	6.7	7.8	7.8	7.5	8.1	9.3	10.1	10.1	8.3	6.3	4.7	3.3
8						1.4	1.7	2.3	3.2	4.1	4.8	6.2	6.7	7.6	8.5	7.8	7.9	9.0	9.9	10.4	10.0	7.6	5.5	3.4
7						1.4	1.4	1.7	2.4	3.1	3.8	4.9	5.8	6.7	6.9	6.5	7.2	8.2	9.4	10.0	4.4	8.5	5.6	3.5
6						1.2	1.1	1.4	2.0	2.2	2.6	3.4	4.2	4.7	4.8	4.9	5.8	7.1	7.4	7.6	7.2	6.1	4.9	3.7
5																	3.3	4.2	5.3	5.9	5.6	5.0	4.4	3.7
4																								
3																								
2																								
1																								

sured hourly averaged concentrations over the last hour of the simulation. Overall, the predicted results tend to be lower than the measurements by 1 to 2 ppm; in only one instance is the discrepancy greater than 2 ppm. Since we expect the model to predict concentrations somewhat lower than those measured at stations situated on heavily traveled streets, it is difficult to assess the cumulative effect of meteorological, emissions, and numerical errors in this simulation. Thus, it appears that we may have to carry out longer runs (three or four days) to observe the build-up of modeling errors clearly.

Table 32

PREDICTED AND MEASURED HOURLY AVERAGED CO CONCENTRATIONS  
FOR THE LAST HOUR OF THE MULTIDAY SIMULATION

<u>Station</u>	<u>Predicted Concentration (ppm)</u>	<u>Measured Concentration (ppm)</u>
Downtown Los Angeles	5	4
Azusa	3	5
Burbank	4	5
West Los Angeles	4	3
Long Beach	4	6
Reseda	2	3
Pomona	3	6
Lennox	3	5
Whittier	3	4

#### D. RECOMMENDATIONS FOR FUTURE WORK

During this study, we adapted the SAI airshed model for use in the prediction of inert pollutant concentrations over multiday periods. The prediction of photochemical contaminant concentrations should be undertaken when the program containing the new kinetic mechanism is fully operational and suitable hydrocarbon emission inputs are developed. To gain experience in multiday usage, we simulated pollutant concentrations in the Los Angeles basin for the

34-hour period extending from 5 a.m. on 29 September to 3 p.m. on 30 September 1969. In general, the results obtained from this run agree reasonably well with available measured pollutant concentration data.

We recommend that the following tasks be undertaken in the future:

- > Assembly of an accurate data base for both meteorological and emissions inputs for a multiple-day period.
- > Performance of photochemical simulations as soon as possible.
- > Performance of CO (and eventually photochemical) runs over several consecutive days (say, four or more) to obtain a better understanding of the cumulative effects of meteorological, emission, and numerical errors on our ability to exercise the model on a multiday basis.

Our present experience indicates that, given a suitable input data base, the model should be capable of producing reasonably good predictions of inert species concentrations for at least two consecutive days. However, further testing will be required to establish guidelines regarding the total number of days that can be simulated before errors accumulate to unacceptable levels.

APPENDIX  
A USER'S GUIDE TO MODKIN

David C. Whitney

## APPENDIX

### A USER'S GUIDE TO MODKIN

David C. Whitney

#### 1. INTRODUCTION

Quantitative description of the rates of chemical reaction of atmospheric contaminants is a vital ingredient in the formulation of a model capable of accurately predicting ground-level concentrations of gaseous pollutants. The formulation of a kinetic mechanism having general validity is, however, an endeavor beset by several inherent difficulties. First, many stable chemical species are present in the atmosphere. Most of these exist at very low concentrations, thereby creating major problems of detection and analysis. In fact, a number of atmospheric constituents remain unidentified. Second, the large variety of highly reactive, short-lived intermediate species and free radicals further complicates the picture. Finally, the enormous number of individual chemical reactions that these species undergo creates an even greater barrier to understanding. Nevertheless, despite our limited knowledge of atmospheric reaction processes, it is essential that we attempt to formulate quantitative descriptions of the processes that are suitable for inclusion in an overall simulation model.

The formulation and development of a kinetic mechanism that is to be incorporated in any airshed model is both delicate and exacting, an undertaking requiring a blend of science, craftsmanship, and art. On one hand, such a mechanism must not be overly complex because the computation times for integration of the continuity equations in which the mechanism is to be imbedded are likely to be excessive. On the other hand, too simplified a mechanism may omit important reaction steps and may thus be inadequate for describing atmospheric reaction processes. Therefore, one major issue is the requirement that the mechanism predict the chemical behavior of a complex mixture of many

hydrocarbons, and yet do so with a paucity of detail. Thus, in postulating a mechanism, the formulator must strike a careful balance between compactness of form and accuracy in prediction.

As an aid in the development of a kinetic mechanism for atmospheric photochemical reactions, we prepared a computer program that allows the user to present his proposed mechanism via data input cards in the same manner as he would formulate it on paper--i.e., as a series of chemical equations and their associated rate constants. Moreover, he can select the method of calculation for determining the concentration of each chemical species in the mechanism from among the following choices: the integration of coupled or uncoupled differential equations, the solution of algebraic equations for species in a steady-state, or the assumption of a constant concentration. Either static or dynamic smog chamber observations can be simulated, and plots of species concentration as a function of time are provided as part of the printed output. Reactions of similar species can be combined into a single "lumped" reaction. Changes in the reaction mechanism, rate constants, or species type designation can be effected by simple input card replacement; recoding or recompilation of the program is not necessary.

Since descriptions of the solution techniques and the development of the chemical mechanisms have appeared elsewhere (Seinfeld et al., 1971; Hecht, 1972), we do not repeat them here beyond the degree necessary for an understanding of the computer program. This appendix is designed to serve primarily as a user's guide to program operation and as a programmer's guide for such program maintenance and modification as may be needed in the future.

## 2. USE OF THE PROGRAM

The input to MODKIN consists of two control cards, a set of reaction cards, a set of species cards, a set of flow cards, and a set of plot cards. The card formats are described in Table A-1, and additional comments regarding program input are given below.

Table A-1

## INPUT CARD FORMAT FOR MODKIN

<u>Card No.</u>	<u>Column No.</u>	<u>Variable Name</u>	<u>Item Format</u>	<u>Units of Measure</u>	<u>Comments</u>
1	1-12	NTIT(J)	3A4	--	Twelve-character title for run heading
1	16-20	NRXN	15	--	Number of reactions in the mechanism (maximum 99)
1	21-25	NLMP	15	--	Number of reactions that contain species to be replaced, i.e., are lumped (maximum 10)
1	26-30	NDIF	15	--	Number of species to be solved in a coupled differential equation (maximum 40)
1	31-35	NSTS	15	--	Number of species to be solved in a steady-state approximation
1	36-40	NUNC	15	--	Number of species to be solved via uncoupled differential equations
1	41-45	NREP	15	--	Number of species that are replacements for lumped species
1	46-50	NINT	15	--	Number of inert (constant concentration) species (the total count of the above five species types cannot exceed 50)
1	51-55	NFLW	15	--	Number of species flowing into the reaction chamber
1	56-60	NRAT	15	--	If nonzero, reaction rates will be printed
2	1-10	TINCR	F10.0	min	Time increment for printing and plotting results
2	11-20	TEND	F10.0	min	Ending time for run
2	21-30	HSTART	F10.0	min	Initial time step size

Table A-1 (Continued)

Card No.	Column No.	Variable Name	Item Format	Units of Measure	Comments
2	31-40	HMINF	F10.0	min	Minimum time step size
2	41-50	HMAXF	F10.0	min	Maximum time step size
2	51-60	EPSF	F10.0	--	Fractional allowable error for iterative solutions
2	61-70	Q	F10.0	min <sup>-1</sup>	Dilution or flow rate (sampling and leakage compensation)
3	1-20	NMRC(J,K)	4(A4,1X)	--	Reactant names, up to four per reaction (if lumped reaction, species to be replaced must appear first)
3	21-50	COEFF(J,K)/ NMPD(J,K)	3(F6.0, A4)	--	Species coefficients and product names, up to three per reaction
3	51-60	RK(K)	F10.0	ppm <sup>1-n</sup> min <sup>-1</sup>	Rate constant; n is the number of reacting species
4	1-4	NTEST	A4	--	Name of species to be replaced in the lumped reaction
4	6-10	NLOC	I5	--	Number of reactions contributing to the lumped reaction (maximum 10)
5	1-20	NMRC(J,K)	4(A4,1X)	--	Reactant names, up to four per reaction (the first species name must be the replacement for the lumped species)
5	21-50	COEFF(J,K)/ NMPD(J,K)	3(F6.0, A4)	--	Species coefficient and product names, up to three per reaction
5	51-60	RK(K)	F10.0	ppm <sup>1-n</sup> min <sup>-1</sup>	Rate constant; n is the number of reacting species



Table A-1 (Continued)

<u>Card No.</u>	<u>Column No.</u>	<u>Variable Name</u>	<u>Item Format</u>	<u>Units of Measure</u>	<u>Comments</u>
6	1-4	NAME(L)	A4	--	Species name
6	11-20	YAX(L)	E10.0	ppm	Species initial concentration
7	1-4	NTEST	A4	--	Flowing species name
7	6-10	NTIM	I5	--	Number of flow points (maximum 10)
8	1-80	FTIME(J,L)/ FLOW(J,L)	4(2F10.0)	min ppm <sup>-1</sup>	Time of measurement and concentration of flowing species
9	1-4	NTEST	A4	--	Name of species to be plotted
9	6-7	NDAT	I2	--	Number of input data for the plot (maximum 80)
9	9	JSYMB	A1	--	Symbol to be used for the calculated data
9	11-14	JFACT	A4	--	Conversion factor for the label
9	16-40	JCONC(J)	5(A4,1X)	--	Concentration labels for the y-axis
9	41-50	CLOW	F10.0	ppm	Minimum concentration value to be considered for plotting
9	51-60	CHIGH	F10.0	ppm	Maximum concentration value to be considered for plotting
9	61-70	TLOW	F10.0	min	Minimum time value to be considered for plotting

Table A-1 (Concluded)

<u>Card No.</u>	<u>Column No.</u>	<u>Variable Time</u>	<u>Item Format</u>	<u>Units of Measure</u>	<u>Comments</u>
9	71-80	THIGH	F10.0	min	Maximum time value to be considered for plotting
10	1-80	TIME(J)/ DATA(J)	4(2F10.0)	min ppm <sup>-1</sup>	Time and concentration input data to be plotted
11	1-4	JBLANK	A4	--	Blank in Columns 1-4 stops plotting

The first control card contains title and parameter information for the run. The first field on this card is a 12-character title; the contents of this field will be printed following "MODULAR KINETICS RUN NO." on the first page of the printout. The number of reactions is given next; the program expects this number of reaction cards to follow the control card. The next entry specifies how many of these reactions represent lumped reactions and thus need to be recalculated from sets of contributing reactions. The following five entries are the counts of each of the different types of species: differential, steady state, uncoupled, replacement, and inert. Note that there are limits on both the number of differential species and the total number of species. The program expects to find one species card for every species named on the reaction cards; they must be ordered as shown above (i.e., all differential species first, then all steady-state species, and so forth). The next-to-last entry on the control card is the number of species that are flowing into the reaction chamber; there must be a set of flow cards for each of these species. The final entry is a request flag governing the printout of the reaction rates.

The first two entries on the second control card are printout parameters. The first one determines the time increments (e.g., every five minutes) for which the current concentration of all species are to be printed and plotted; the second specifies the time at which the kinetics run is to be terminated. The next four values are control parameters for the differential equation solution routine. In order, these parameters are the initial time step (normally on the order of  $10^{-4}$  min), the minimum allowable time step (normally about  $10^{-5}$  min), the maximum time step (about 1 to 10 min), and the fractional error acceptable for iterative solutions. The final entry on the second control card is the rate at which each species concentration would be reduced in the absence of reaction. This "dilution rate" primarily reflects the loss of material through sampling; if there is an inflow, it is presumed to occur at this same rate.

The set of reaction cards provides all the reactions and rate constants, one per card. Each card begins with a list of reactants, which must appear in consecutive fields, since a blank stops the scan. For a lumped reaction, the

name of the species to be replaced must appear first; otherwise, the order of reactant names is immaterial. Note, incidentally, that the reactants appear in the printed output in reverse order. If a species reacts with itself, it must appear twice in the list of reactants. The products, along with their coefficients, follow. Coefficients can be whole numbers or fractions; the printout is rounded to two decimal places. Again, products must appear consecutively, since a blank stops the scan, but their order is unimportant. The final entry on the card is the rate constant. The order of the reaction cards does not matter, except that lumped reactions must follow nonlumped reactions.

A set of contributing reactions consists of an identification card containing the name of the lumped reactant (the species being replaced) and the number of contributing reactions, followed by the list of contributing reactions. All of the comments offered above regarding reaction cards apply to these contributing reactions, except that these reactions cannot themselves be lumped ones. The contributing reaction must have its reactants and products in the same relative location on the card as they are on the lumped reaction card; i.e., the replacement species must appear first, and all products must be shown, even those that have zero coefficients. However, the order of the reactions within a set does not matter. The order of the sets of contributing reactions must be the same as the order of the lumped reactions in the set of reaction cards described above, and there must be one set of contributing reactions for each lumped reaction.

The set of species cards is used to identify the species by type and to initialize the species concentrations. Each card contains a species name and concentration. The following is the order of the species types: differential, steady state, uncoupled, replacement, and inert. Within a given type, no particular order is necessary; in fact, some orderings of steady-state species are clearly preferable to others in terms of elapsed computing time.

A set of flow cards consists of an identification card containing the species name and the number of input points, followed by cards specifying the data points themselves. The data are not interpolated; instead, the inflowing concentration is changed to a new value whenever the progression of time in the mechanism passes an input time. Note particularly that the concentration for the inflowing species is zero until its first input time is passed.

The plot cards control the pictorial representation of concentration as a function of time for each species. Instead of processing the output using a plotter, the plot cards map the concentration-time profile onto a page-size grid of the printout. The first card, which is the plot control card, contains the species name, the number of experimental data points to be read, the symbol to be used to represent the calculated data (an asterisk is used for experimental points), the conversion factor, the concentration labels, and the grid limits. These last three items require comment.

The grid has been divided into four vertical sections and eight horizontal sections. Aesthetically, therefore, the time (horizontal) limits should be chosen to give a span divisible evenly by eight (e.g., a limit of 0 to 400 will result in the printing of a label every 50 minutes). Similarly, the concentration (vertical) limits should be divisible evenly by four, and they should be the true rather than the scaled concentrations. The labels for the vertical axis are not calculated from the concentration span, but rather are read in from the control card. They can be any multiple of the true concentrations. The scale factor, which appears in the figure caption along with the run title and species values, indicates what multiplier was used. For example, if the data prints were expected to range between 0.08 and 0.16 ppm, a scale factor of "10+1"; concentration labels of "0.75", "1.00", "1.25", "1.50", and "1.75"; and concentration limits of "0.075" and "0.175" would give a plot containing all the points. Note that no check is made among the labels, scale factor, and limits to insure consistency. Also, the limit values themselves will not appear on the plot; plotted points must fall within the grid boundaries.

Experimental data cards, if any, come after the control card. If desired, sets of plot cards can be stacked. The end of the plot deck is denoted by a card with a blank species name; the program will then expect another MODKIN run control card.

### 3. PROGRAM DESCRIPTION

The modular kinetics program consists of a main routine labeled MODKIN, the subroutines LMPCAL, DIFSUB, and PLOT, which are called by MODKIN, and the subroutines DIFFUN, MATINV, and PEDERV, which are called by DIFSUB. Each routine is treated in detail below. Listings and samples of program inputs and outputs appear at the end of this appendix. Symbol glossaries are included within each routine that was written especially for this program.

#### a. MODKIN

The program begins by declaring a number of variables used by DIFSUB as being DOUBLE PRECISION. All arrays are identified in DIMENSION statements and variables needed by LMPCAL and DIFFUN are placed in COMMON. The DATA declarations include the input and output units, a blank word, and the maximum sizes of the various arrays used for holding user inputs.

The control cards are read (note that this is a return point for stacked data decks). An initial page is written listing all the control card parameters. The number of reactions is checked, and the set of reaction cards is read. The number of lumped reactions is checked, and the contributing sets are read. For each set, the number of contributing reactions and the lumped species name are checked, the reaction counter is incremented and checked, and the contributing reactions are read. The number of differential species is checked, the total number of species is calculated and checked, and the set of species cards is read. The number of flowing species is checked, the flow variables are cleared to zero, and the flow cards are checked and read.

The numerical identifiers for each species and the uncoupled species reaction rates are cleared to zero. The initial concentrations of the differential species are set to their input values, and the input errors and initial maxima are set. The numerical species identifiers for the reactants and products of each reaction are cleared to zero.

The counters for the lumped reactions are set. The reactions are analyzed, and each species is identified; if it does not match a species list name, a flag is set. Numerical identifiers are placed in the reaction and species matrices to allow reference by reaction and location within the reaction expression. If this is the first of a set of replacement reactions, a message is printed. The order of the reactants is reversed, and the list of chemical reactions and rate constants is printed. LMPCAL is called to adjust the lumped reactions and species concentrations, and the list of initial species concentrations, broken down by type, is printed. If the name flag is set, processing halts. A number of computation parameters are initialized. Initial concentrations are saved, and the incoming concentrations of any flowing species are initialized.

A call is made to the differential equation solution routine DIFSUB (which in turn calls DIFFUN for solution of the steady-state equations); note that this is a return point from the calculation loop. The time values are updated, and the concentration values are saved and checked for negative values. If a negative value is found, the time step is reset to one-tenth of its former value (note that this is done only once and that the time step must be greater than the user-specified minimum value), the concentrations from the previous time step are restored, and the call to DIFSUB is repeated.

The replacement species concentrations are calculated using the following algorithm:

$$Y_{i(n)} = Y_{i(o)} \exp \left[ -\Delta T \sum_{J=1}^J \left( RK_j \prod_{K=2}^K Y_k \right) \right] (1 - Q\Delta T) \quad ,$$

where

- $Y_{i(n)}$  = the new concentration of replacement species  $i$ ,
- $Y_{i(o)}$  = the old concentration of replacement species  $i$ ,
- $\Delta T$  = the change in time since the previous calculation,
- $RK_j$  = the rate constant of the  $j$ -th reaction of the set of  $J$  contributing reactions that have species  $i$  as the first reactant,
- $Y_k$  = the concentration of the  $K$ -th reactant species in the set of  $K$  reactants in contributing reaction  $j$ ,
- $Q$  = the dilution rate.

LMPCAL is then called to adjust the lumped reactions and species concentrations to reflect the changes in the replacement species concentrations.

The uncoupled species concentrations are calculated using the algorithm described below under DIFFUN. Note that the uncoupled species reaction rates are averaged with those derived during the previous time step. The current uncoupled species reaction rates are saved.

The time is checked against having passed the user-provided limit, in which case no plot points are saved. The incremental time since the last printout is checked against the user-specified value. If appropriate, the current concentration values are saved for plotting, unless the maximum number of plot points has been exceeded. The current concentrations are then printed, regardless of whether the plot points have been saved. If the user has indicated that the reaction rates are to be printed, they are sorted from largest to smallest and are listed five per line.

If the time limit has been passed, if a repeated negative concentration has been encountered, or if an error has occurred in DIFSUB, the error flag is printed and the PLOT routine is called. Control then passes back to the beginning of the program, where another set of input cards can be processed. Otherwise, the inflowing species are checked to determine whether any concentrations should be updated; if any updates are made, an appropriate message is printed. Finally, the current time and concentrations are saved (in case it is necessary to restart the calculation with a smaller time step), and control returns to the call of DIFSUB for calculation of the next time step.



b. LMPCAL

This subroutine is called by MODKIN to calculate the rate constants and product species coefficients for the lumped reactions. Two arguments are provided to this routine by MODKIN: the number of lumped reactions and the number of contributing reactions for each lumped reaction. COMMON is defined as in MODKIN, array sizes are set with DIMENSION statements, and parameters are defined via DATA statements.

The location and number of the current set of contributing reactions are established, and the corresponding lumped reaction is identified. The rate constants, product coefficients, and replacement species concentrations for each contributing reaction are transferred to local arrays, and the replacement species concentration is summed. The concentration of the lumped species is set to the sum of all the replacement concentrations, and the mole fraction of each replacement species is calculated. The rate constant of the lumped reaction is calculated as the sum of the rate constants for the contributing reactions multiplied by the replacement species mole fraction. The product species coefficients are calculated as the sum of the coefficients for the product species multiplied by the replacement species mole fraction for each contributing reaction, weighted by the ratio of the rate constant for the contributing reaction to that of the lumped reaction. Note that as a final step any product species coefficient below a minimum value is reset to zero to avoid underflow problems in later computations.

c. DIFSUB

This subroutine, which is called by MODKIN, is a copy of the program for the integration of coupled first-order ordinary differential equations that was presented in the Collected Algorithms of the Association for Computing Machinery (Gear, 1971). Since the algorithm and program are described in detail in the cited reference, they are not discussed further here. The only change likely to be needed is the alteration of the DIMENSION statement near the beginning.

d. DIFFUN

This subroutine is called by DIFSUB to calculate the rates of change of the differential species. It also includes, however, the algorithm for the steady-state calculations, since the reactions involving species in a steady state are presumed to be fast relative to the time steps in DIFSUB and must therefore be updated at every time trial. The three arguments provided to this subroutine by DIFSUB are the time, the differential species concentrations, and the rates of change of these concentrations; these are all DOUBLE PRECISION. The arguments are sized in a DIMENSION statement, COMMON is defined as in MODKIN, and several parameters are defined via DATA statements.

The concentrations are transferred to a local array, and the convergence loop is begun. The reaction rate for each reaction is calculated by using the following algorithm:

$$R_i = RK_i \prod_{j=1}^J Y_j \quad ,$$

where  $R_i$  is the reaction rate and  $RK_i$  is the rate constant of the  $i$ -th reaction, and  $Y_j$  is the concentration of the  $j$ -th reactant species in the set of  $J$  reactants in reaction  $i$ .

The steady-state concentrations are calculated by using the following dynamic mass-balance algorithm:

$$Y_j = \frac{\sum_{i=1}^I R_i C_{ij}}{Q + \sum_{m=1}^M RK_m \sum_{k=1}^K Y_k} \quad , \quad k \neq j \quad ,$$

where

$Y_j$  = the concentration of the  $j$ -th steady-state species,

$R_i$  and  $C_{ij}$  = the reaction rate of the  $i$ -th reaction and the coefficient of species  $j$  in the  $i$ -th reaction, respectively, of the set of  $I$  reactions in which species  $j$  is a product,

$Q$  = the dilution rate,

$RK_m$  = the rate constant for the  $m$ -th reaction in the set of  $M$  reactions in which species  $j$  is a reactant,

$Y_k$  = the concentration of the  $k$ -th reactant (except when  $k = j$ ) in the set of  $K$  reactants in reaction  $m$ .

Note that in the case of a species reacting with itself,  $Y_j$  may be the same as  $Y_k$  even though  $k \neq j$ ; this case has been explicitly programmed.

If the old and new steady-state values agree within the requisite tolerance, a convergence counter is incremented; in any event, the new value is saved. If the value registered on the convergence counter equals the number of steady-state species, the loop is completed; otherwise, another pass is made. If the steady-state concentrations do not converge, a warning message is written and processing continues.

As a final step, the differentials are calculated according to the following algorithm:

$$\Delta Y_j = \sum_{i=1}^I R_i C_{ij} - \sum_{m=1}^M R_m + Q(YF_j - Y_j) \quad ,$$

where

$\Delta Y_j$  = the change in concentration of the  $j$ -th species with time,

$R_i$  and  $C_{ij}$  = the reaction rate of the  $i$ -th reaction and the coefficient of species  $j$  in the  $i$ -th reaction, respectively, of the set of  $I$  reactions in which species  $j$  is a product,

$R_m$  = the reaction rate of the  $m$ -th reaction in the set of  $M$  reactions in which species  $j$  is a reactant,

$Q$            = the dilution rate,  
 $YF_j$         = the inflowing concentration of species  $j$ ,  
 $Y_j$           = the concentration of species  $j$ .

These differential values are returned to the calling program.

e. MATINV

This subroutine is called by DIFSUB to perform matrix inversions. Since it is a standard matrix inversion routine taken from the utility subroutine library at the California Institute of Technology, it is not described here. The only change likely to be needed is the alteration of the DIMENSION statement near the beginning.

f. PEDERV

This subroutine, which is called by DIFSUB, is used to provide a Jacobian matrix for the calculation of partial derivatives and is not necessary in this application. Nevertheless, to preserve the integrity of the Gear routine and to allow for possible future use of partial derivatives, we retained the routine in the program as a dummy subroutine. It does contain, however, a DIMENSION statement; thus, any alteration of array sizes in DIFSUB should also be made in PEDERV.

g. PLOT

This subroutine is called by MODKIN following completion of the time-concentration calculations. It maps the results, along with any user input data, onto a page-sized grid of concentration as a function of time cells for as many species as the user wishes.

The routine begins by providing DIMENSION statements for some of the arguments and the local arrays. The vertical axis and vertical label are established via DATA statements, as are the I/O units, some symbols, and the maximum array sizes.

The grid is cleared to blanks, and the control card is read. If the name is blank, control returns to MODKIN. If there are input data, the number is checked and the data are read. The normalization factors are calculated, and the numerical labels are placed on the axes. The species is identified; if it is misspelled, the plot is skipped.

The data points, if any, are scaled to the grid; the points are checked; and, if they are acceptable, the appropriate symbol is placed on the grid. The same procedure is used for the calculated points. A page is skipped, and the vertical labels and axis and the grid itself are printed. The horizontal axis and labels and the figure caption are printed, and the routine returns control to MODKIN.

#### 4. LISTINGS AND SAMPLE REPORT AND OUTPUT

The following pages contain a complete listing of the computer program, including the main routine MODKIN (Exhibit A-1) and the subroutines LMPCAL, DIFSUB, DIFFUN, MATINV, PEDERV, and PLOT (Exhibits A-2 through A-7). These routines are all written in ASA FORTRAN and should be acceptable without changes for any computer system that supports FORTRAN.

Following the program listings is an input deck describing a typical kinetics mechanism (Exhibit A-8) and selected printout from the computer run using this input deck (Exhibit A-9). We note that, except for the plot (which uses an entire 11 x 15 inch computer printout page), the output is contained on a standard 8½ x 11 inch page. With relatively minor changes in the PLOT routine, the plot can also be reduced to this size.

## EXHIBIT A-1. LISTING OF MAIN PROGRAM MODKIN

```

C MAIN PROGRAM ***** M O D K I N *****                                00000010
C                                                                                   00000020
C THIS PROGRAM READS AND ANALYZES INPUT FOR MODULAR KINETICS PROGRAM.          00000030
C SETS INITIAL VALUES, CONTROLS ITERATION PRINTOUT, AND CALLS THE              00000040
C DIFFERENTIAL EQUATION SOLVING AND PLOT ROUTINES.                             00000050
C                                                                                   00000060
C WRITTEN BY D. C. WHITNEY FOR SYSTEMS APPLICATIONS, INC.                      00000070
C ORIGINAL DATE 31 AUGUST 1973, LATEST MODIFICATION 25 OCTOBER 1973.           00000080
C THIS PROGRAM AND ALL SUBROUTINES (EXCEPT DIFSUB AND MATINV) ARE THE          00000090
C PROPERTY OF AND COPYRIGHT BY SYSTEMS APPLICATIONS, INC.                     00000100
C 950 NORTHGATE DRIVE, SAN RAFAEL, CALIFORNIA 94903.                          00000110
C                                                                                   00000120
C SYMBOL DESCRIPTIONS --                                                         00000130
C                                                                                   00000140
C COEFF      NUMBER OF PARTICLES, ONE PER PRODUCT SPECIES PER REACTION          00000150
C DELT       DIFFERENCE BETWEEN TWO CONSECUTIVE TIME STEPS                     00000160
C EPS        CONVERGENCE CRITERION, DOUBLE PRECISION, FOR DIFSUB               00000170
C EPSF       CONVERGENCE CRITERION                                             00000180
C ERROR      ESTIMATE OF ERROR IN CONCENTRATIONS, PPM, ONE PER SPECIES,         00000190
C            DOUBLE PRECISION, FOR DIFSUB                                       00000200
C ESUM       SUM OF THE EXPONENTIAL TERMS FOR THE REPLACEMENT SPECIES           00000210
C ETERM      TERM IN THE EXPONENTIAL CALCULATION OF THE REPLACEMENT SPEC.       00000220
C FLOW       SPECIES INFLOWS, PPM/MIN, 10 PER SPECIES                          00000230
C FTEST      TEMPORARY FLOW TIME OR CONCENTRATION FOR TESTING, MIN OR PPM       00000240
C FTIME      TIMES AT WHICH INFLOW IS MEASURED, MIN, 10 PER SPECIES            00000250
C H          NEXT STEP SIZE, MIN, DOUBLE PRECISION, FOR DIFSUB                 00000260
C HMAX       MAXIMUM TIME STEP, MIN, DOUBLE PRECISION, FOR DIFSUB              00000270
C HMAXF      MAXIMUM TIME STEP, MIN                                             00000280
C HMIN       MINIMUM TIME STEP, MIN, DOUBLE PRECISION, FOR DIFSUB              00000290
C HMIN       MINIMUM TIME STEP, MIN                                             00000300
C HSTART     INITIAL STEP SIZE FOR DIFSUB                                       00000310
C J          DO-LOOP INDICES OR LOCAL POINTERS                                00000320
C JBLANK     A HOLLERITH WORD OF FOUR BLANK CHARACTERS                        00000330
C JFLAG      INDICATES NEGATIVE SPECIES FOUND IN DIFFERENTIAL CALCULATION      00000340
C JSTART     INPUT FLAG, FOR DIFSUB                                             00000350
C K          DO-LOOP INDICES OR LOCAL POINTERS                                00000360
C KCOF       COEFFICIENT POINTERS, ONE PER REACTION PRODUCT PER SPECIES.       00000370
C KFLAG      PERFORMANCE FLAG FOR DIFSUB                                       00000380
C KLMP       NUMBER OF CONTRIBUTING REACTIONS TO EACH LUMPED REACTION           00000390
C KLOC       LOCAL POINTER TO CONTRIBUTING REACTION                           00000400
C KPRD       PRODUCT POINTERS, ONE PER PRODUCT SPECIES PER REACTION            00000410
C KRCT       REACTANT POINTERS, ONE PER REACTANT SPECIES PER REACTION          00000420
C KRXN       REACTION POINTERS, ONE PER REACTION PER SPECIES                  00000430
C L          DO-LOOP INDICES OR LOCAL POINTERS                                00000440
C LFLAG      INDICATES INCORRECT SPECIES NAME IN REACTION -- STOPS JOB         00000450
C LRXN       POINTER TO FIRST OF A SERIES OF REPLACEMENT REACTIONS             00000460
C M          DO-LOOP INDICES OR LOCAL POINTERS                                00000470
C MAXDER     MAXIMUM ORDER FOR DERIVATIVES, FOR DIFSUB                        00000480
C MAXDIF     MAXIMUM NUMBER OF DIFFERENTIAL SPECIES                           00000490
C MAXFLW     MAXIMUM NUMBER OF FLOW TIMES                                      00000500
C MAXLMP     MAXIMUM NUMBER OF LUMPED REACTIONS                               00000510
C MAXPNT     MAXIMUM NUMBER OF SAVED TIME AND CONCENTRATION POINTS             00000520
C MAXPRD     MAXIMUM NUMBER OF PRODUCTS                                        00000530
C MAXPRT     MAXIMUM NUMBER OF ENTRIES ON PRINT LINE FOR RATES                 00000540

```

## EXHIBIT A-1. LISTING OF MAIN PROGRAM MODKIN (Continued)

C MAXRCT	MAXIMUM NUMBER OF REACTANTS	00000550
C MAXREP	MAXIMUM NUMBER OF REPLACEMENT REACTIONS PER LUMPED REACTION	00000560
C MAXRXN	MAXIMUM NUMBER OF REACTIONS	00000570
C MAXSPC	MAXIMUM NUMBER OF SPECIES	00000580
C MF	METHOD INDICATOR, FOR DIFSUB	00000590
C MRXN	TOTAL NUMBER OF REACTIONS, INCLUDING REPLACEMENTS	00000600
C N	DO-LOOP INDICES OR LOCAL POINTERS	00000610
C NAME	SPECIES NAMES, ONE PER SPECIES	00000620
C NDIF	NUMBER OF DIFFERENTIAL SPECIES	00000630
C NFLW	NUMBER OF FLOWING SPECIES	00000640
C NIN	THE FORTRAN INPUT UNIT (NORMALLY 5)	00000650
C NINT	NUMBER OF INERT/CONSTANT SPECIES	00000660
C NLMP	NUMBER OF LUMPED REACTIONS	00000670
C NLOC	NUMBER OF CONTRIBUTING REACTIONS PERTAINING TO LUMPED REACTION	00000680
C NMPD	PRODUCT NAMES, ONE PER PRODUCT SPECIES PER REACTION	00000690
C NMRC	REACTANT NAMES, ONE PER REACTANT SPECIES PER REACTION	00000700
C NOUT	THE FORTRAN OUTPUT UNIT NUMBER (NORMALLY 6)	00000710
C NP	LOCAL POINTER TO REACTION RATE TO BE PRINTED	00000720
C NPNT	NUMBER OF SAVED TIMES AND CONCENTRATIONS	00000730
C NPRT	HOLDING AREA TO PRINT OUT A LINE OF NAMES OR NUMBERS	00000740
C NR	POINTER TO REPLACEMENT SPECIES	00000750
C NRAT	USER INPUT FLAG REQUESTING PRINT OF REACTION RATES	00000760
C NREP	NUMBER OF REPLACEMENT SPECIES	00000770
C NRESET	COUNTER FOR NUMBER OF TIMES STEP SIZE IS RESET SMALLER	00000780
C NRXN	NUMBER OF REACTIONS	00000790
C NS	POINTER TO REACTING SPECIES	00000800
C NSTS	NUMBER OF STEADY-STATE SPECIES	00000810
C NTEST	SPECIES NAME FOR TESTING	00000820
C NTIM	NUMBER OF TIMES AND FLOWS FOR A SPECIES	00000830
C NTIT	USER-INPUT TITLE FOR PRINTOUT, 3 FOUR-CHARACTER WORDS	00000840
C NTOT	TOTAL NUMBER OF SPECIES	00000850
C NU	LOCAL POINTER TO UNCOUPLED SPECIES	00000860
C NUNC	NUMBER OF UNCOUPLED SPECIES	00000870
C PSAVE	BLOCK STORAGE, NUMBER OF SPECIES SQUARED, FOR DIFSUB	00000880
C Q	DEGRADATION RATE, /MIN	00000890
C R	REACTION RATES, SEC, ONE PER REACTION	00000900
C RATE	LOCAL REPRESENTATION OF R, THE REACTION RATE	00000910
C RK	REACTION RATE CONSTANTS, PPM-MIN, ONE PER REACTION	00000920
C RPRT	HOLDING AREA TO PRINT OUT A LINE OF REACTION RATES	00000930
C SAVE	BLOCK STORAGE, 12 PER SPECIES, DOUBLE PRECISION, FOR DIFSUB	00000940
C SAVCON	SPECIES CONCENTRATIONS, PPM, ONE PER SPECIES AT 80 TIMES	00000950
C SAVTIM	TIMES THAT CONCENTRATIONS ARE SAVED, MIN, UP TO 80 VALUES	00000960
C T	CURRENT REACTION TIME, SEC, DOUBLE PRECISION,	00000970
C	FOR AND FROM DIFSUB	00000980
C TCOUNT	NEXT TIME FOR OUTPUT, MIN	00000990
C TEND	ENDING TIME, MIN	00001000
C TF	PREVIOUS TIME OF DIFSUB CALL, MIN	00001010
C TINCR	TIME INCREMENT FOR OUTPUT, MIN	00001020
C TOL	CONVERGENCE TOLERANCE ON STEADY-STATE ITERATION, PPM	00001030
C UNCOLD	PREVIOUS VALUES OF RATE OF CHANGE, PPM/MIN, ONE PER SPECIES	00001040
C TOLD	TIME OF PREVIOUS CALL TO DIFSUB	00001050
C Y	SPECIES CONCENTRATIONS, 8 PER SPECIES, DOUBLE PRECISION,	00001060
C	FOR AND FROM DIFSUB	00001070
C YAX	SPECIES CONCENTRATIONS, PPM, ONE PER SPECIES	00001080
C YCALC	LOCAL REPRESENTATION OF YDOT, THE RATE OF CHANGE	00001090
C YIN	SPECIES INFLOW RATES, PPM/MIN, ONE PER SPECIES	00001100

## EXHIBIT A-1. LISTING OF MAIN PROGRAM MODKIN (Continued)

```

C YMAX      CURRENT MAXIMUM CONCENTRATION VALUES, PPM, ONE-PER SPECIES, 00001110
C           DOUBLE PRECISION, FOR AND FROM DIFSUB 00001120
C YOLD      CONCENTRATIONS AT PREVIOUS CALL TO DIFSUB, ONE PER SPECIES 00001130
C YUNC      RATE OF CHANGE OF UNCOUPLED SPECIES, PPM/MIN 00001140
C           00001150
C BEGINNING OF PROGRAM. 00001160
C           00001170
C DECLARE VARIABLES FOR DIFSUB AS DOUBLE PRECISION 00001180
C           00001190
C           DOUBLE PRECISION HMIN, HMAX, EPS, YMAX, ERROR, H, SAVE, T, Y 00001200
C           00001210
C DEFINE VARIABLES AND DIMENSIONS OF COMMON STORAGE WITH DIFFUN 00001220
C           00001230
C           COMMON RK(99), R(99), YAX(50), YIN(50), COEFF(3,99) 00001240
C           COMMON KRCT(4,99), KPRD(3,99), KRXN(99,50), KCOF(99,50) 00001250
C           COMMON Q, TOL, NRXN, NDIF, NSTS 00001260
C           00001270
C DEFINE DIMENSIONS OF LOCAL ARRAYS 00001280
C           00001290
C           DIMENSION Y(8,40), YMAX(40), SAVE(12,40), ERROR(40), PSAVE(1600) 00001300
C           DIMENSION NMRC(4,99), NMPD(3,99), NTIT(3), NPRT(10), RPRT(10) 00001310
C           DIMENSION FTIME(10,50), FLOW(10,50), SAVCON(50,80), SAVTIM(80) 00001320
C           DIMENSION YOLD(50), NAME(50), UNCOLD(50), KLMP(10) 00001330
C           00001340
C SET MISCELLANEOUS DATA VALUES 00001350
C           00001360
C           DATA MAXRCT /4/, NIN /5/, NOUT /6/, MAXPRD /3/, JBLANK /4H / 00001370
C           DATA MAXRXN /99/, MAXDIF /40/, MAXFLW /10/, MAXPNT /80/ 00001380
C           DATA MAXSPC /50/, MAXLMP /10/, MAXREP /10/, MAXPRT /5/ 00001390
C           00001400
C READ CONTROL CARDS -- NOTE THIS IS RETURN POINT FROM PLOT CALL 00001410
C           00001420
10  READ (NIN,2,END=900) NTIT, NRXN, NLMP, NDIF, NSTS, NUNC, NREP, 00001430
   &  NINT, NFLW, NRAT 00001440
   READ (NIN,4) TINCR, TEND, HSTART, HMINF, HMAXF, EPSF, Q 00001450
C           00001460
C PRINT HEADING PAGE AND CONTROL CARD INPUTS 00001470
C           00001480
   WRITE (NOUT,1002) NTIT, NRXN, NLMP, NDIF, NSTS, NUNC, NREP, NINT, 00001490
   &  NFLW, NRAT, TINCR, TEND, HSTART, HMINF, HMAXF, EPSF, Q 00001500
C           00001510
C TEST REACTION COUNT 00001520
C           00001530
   IF (NRXN .GT. 0 .AND. NRXN .LE. MAXRXN) GO TO 12 00001540
   WRITE (NOUT,1001) MAXRXN 00001550
   GO TO 900 00001560
C           00001570
C SET SPECIES NAME FLAG AND OVERALL REACTION COUNT AND READ REACTIONS 00001580
C           00001590
12  LFLAG = 0 00001600
   MRXN = NRXN 00001610
   DO 15 K = 1,NRXN 00001620
   READ (NIN,1) (NMRC(J,K), J = 1,MAXRCT), 00001630
   &  (COEFF(J,K), NMPD(J,K), J = 1,MAXPRD), RK(K) 00001640
15  CONTINUE 00001650
C           00001660

```



## EXHIBIT A-1. LISTING OF MAIN PROGRAM MODKIN (Continued)

C TEST NUMBER OF LUMPED REACTIONS	00001670
C	00001680
IF (NLMP .LE. 0) GO TO 22	00001690
IF (NLMP .LE. MAXLMP) GO TO 16	00001700
WRITE (NOUT,1027) MAXLMP	00001710
GO TO 900	00001720
C	00001730
C READ AND TEST LUMPED SPECIES NAME AND NUMBER OF REPLACEMENT SPECIES	00001740
C	00001750
16 DO 21 L = 1,NLMP	00001760
READ (NIN,6) NTEST, NLOC	00001770
IF (NTEST .EQ. NMRC(1,NRXN - NLMP + L)) GO TO 17	00001780
WRITE (NOUT,1028) NTEST	00001790
LFLAG = 1	00001800
17 IF (NLOC .GT. 0 .AND. NLOC .LE. MAXREP) GO TO 18	00001810
WRITE (NOUT,1030) MAXREP	00001820
GO TO 900	00001830
C	00001840
C SAVE NUMBER OF REPLACEMENT REACTIONS AND UPDATE AND CHECK TOTAL	00001850
C	00001860
18 KLMP(L) = NLOC	00001870
MRXN = MRXN + NLOC	00001880
IF (MRXN .LE. MAXRXN) GO TO 19	00001890
WRITE (NOUT,1001) MAXRXN	00001900
GO TO 900	00001910
C	00001920
C READ REPLACEMENT REACTIONS	00001930
C	00001940
19 <del>DO 20 K = 1,NLOC</del>	00001950
KLOC = K + MRXN - NLOC	00001960
READ (NIN,1) (NMRC(J,KLOC), J = 1,MAXRCT), (COEFF(J,KLOC),	00001970
& NMPD(J,KLOC), J = 1,MAXPRD), RK(KLOC)	00001980
20 CONTINUE	00001990
21 CONTINUE	00002000
C	00002010
C TEST NUMBER OF DIFFERENTIAL SPECIES	00002020
C	00002030
22 IF (NDIF .LE. MAXDIF) GO TO 23	00002040
WRITE (NOUT,1012) MAXDIF	00002050
GO TO 900	00002060
C	00002070
C SET AND TEST TOTAL NUMBER OF SPECIES	00002080
C	00002090
23 NTOT = NDIF + NSTS + NUNC + NREP + NINT	00002100
IF (NTOT .LE. MAXSPC) GO TO 25	00002110
WRITE (NOUT,1011) MAXSPC	00002120
GO TO 900	00002130
IF (NFLW .LE. 0) GO TO 50	00002210
IF (NFLW .LE. NTOT) GO TO 30	00002220

## EXHIBIT A-1. LISTING OF MAIN PROGRAM MODKIN (Continued)

WRITE (NOUT, 1023) NTOT	00002230
GO TO 900	00002240
C	00002250
C SET FLOW RATES AND TIMES TO ZERO	00002260
IF (NFLW .LE. 0) GO TO 50	00002210
IF (NFLW .LE. NTOT) GO TO 30	00002220

## EXHIBIT A-1. LISTING OF MAIN PROGRAM MODKIN (Continued)

WRITE (NOUT, 1023) NTOT	00002230
GO TO 900	00002240
C	00002250
C SET FLOW RATES AND TIMES TO ZERO	00002260
C	00002270
30 DO 33 K = 1,NTOT	00002280
DO 32 J = 1,MAXFLW	00002290
FTIME(J,K) = 0.0	00002300
FLOW(J,K) = 0.0	00002310
32 CONTINUE	00002320
33 CONTINUE	00002330
C	00002340
C READ FLOW CONTROL CARD	00002350
C	00002360
DO 45 K = 1,NFLW	00002370
READ (NIN,6) NTEST, NTIM	00002380
C	00002390
C IDENTIFY SPECIES NAME -- EXIT IF NOT FOUND	00002400
C	00002410
DO 35 L = 1,NTOT	00002420
IF (NTEST .EQ. NAME(L)) GO TO 40	00002430
35 CONTINUE	00002440
WRITE (NOUT,1003) NTEST	00002450
GO TO 900	00002460
C	00002470
C CHECK NUMBER OF FLOW INPUTS	00002480
C	00002490
40 IF (NTIM .LE. MAXFLW) GO TO 42	00002500
WRITE (NOUT,1024) MAXFLW	00002510
GO TO 900	00002520
C	00002530
C READ FLOW INPUTS	00002540
C	00002550
42 READ (NIN,7) (FTIME(J,L), FLOW(J,L), J = 1,NTIM)	00002560
45 CONTINUE	00002570
C	00002580
C CLEAR REACTION POINTERS, FLOWS, AND UNCOUPLED RATES	00002590
C	00002600
50 DO 60 K = 1,NTOT	00002610
DO 55 J = 1,MRXN	00002620
KRXN(J,K) = 0	00002630
KCOF(J,K) = 0	00002640
55 CONTINUE	00002650
YIN(K) = 0.0	00002660
UNCOLD(K) = 0.0	00002670
60 CONTINUE	00002680
C	00002690
C MOVE INITIAL DIFFERENTIAL CONCENTRATIONS AND SET ERRORS AND MAXIMA	00002700
C	00002710
DO 65 J = 1,NDIF	00002720
Y(1,J) = YAX(J)	00002730
ERROR(J) = 0.0	00002740
YMAX(J) = 1.0	00002750
65 CONTINUE	00002760
C	00002770
C CLEAR SPECIES POINTERS	00002780

## EXHIBIT A-1. LISTING OF MAIN PROGRAM MODKIN (Continued)

```

C                                00002790
DO 90 K = 1,MRXN                00002800
DO 70 J = 1,MAXRCT              00002810
KRCT(J,K) = 0                  00002820
70  CONTINUE                    00002830
DO 80 J = 1,MAXPRD              00002840
KPRD(J,K) = 0                  00002850
80  CONTINUE                    00002860
90  CONTINUE                    00002870
C                                00002880
C SET LUMPED REACTION COUNTERS  00002890
C                                00002900
    LRXN = NRXN + 1             00002910
    KLOC = 1                    00002920
DO 190 M = 1,MRXN               00002930
DO 130 L = 1,MAXRCT             00002940
C                                00002950
C IDENTIFY REACTANT SPECIES -- FLAG IF MISSING 00002960
C                                00002970
    NTEST = NMRC(L,M)           00002980
    IF (NTEST .EQ. JBLANK) GO TO 140 00002990
DO 110 K = 1,NTOT               00003000
    IF (NTEST .EQ. NAME(K)) GO TO 115 00003010
110  CONTINUE                   00003020
    WRITE (NOUT,1003) NTEST       00003030
    LFLAG = 1                    00003040
    GO TO 130                    00003050
C                                00003060
C FILL IN REACTION AND SPECIES POINTERS AND COUNTERS 00003070
C                                00003080
115  KRCT(L,M) = K              00003090
DO 120 J = 1,MAXRXN             00003100
    IF (KRXN(J,K) .EQ. 0) GO TO 125 00003110
120  CONTINUE                   00003120
125  KRXN(J,K) = M              00003130
    KCOF(J,K) = -1              00003140
130  CONTINUE                   00003150
C                                00003160
C IDENTIFY PRODUCT SPECIES -- FLAG IF MISSING 00003170
C                                00003180
140  DO 170 L = 1,MAXPRD        00003190
    NTEST = NMPD(L,M)           00003200
    IF (NTEST .EQ. JBLANK) GO TO 180 00003210
DO 150 K = 1,NTOT               00003220
    IF (NTEST .EQ. NAME(K)) GO TO 155 00003230
150  CONTINUE                   00003240
    WRITE (NOUT,1003) NTEST       00003250
    LFLAG = 1                    00003260
    GO TO 170                    00003270
C                                00003280
C FILL IN REACTION AND SPECIES POINTERS AND COUNTERS 00003290
C                                00003300
155  KPRD(L,M) = K              00003310
DO 160 J = 1,MAXRXN             00003320
    IF (KRXN(J,K) .EQ. 0) GO TO 165 00003330
160  CONTINUE                   00003340

```

## EXHIBIT A-1. LISTING OF MAIN PROGRAM MODKIN (Continued)

```

165   KRXN(J,K) = M                                00003350
      KCOF(J,K) = L                                00003360
170   CONTINUE                                     00003370
C                                           00003380
C SAVE NUMBER OF PRODUCT SPECIES FOR THIS REACTION 00003390
C                                           00003400
      L = MAXPRD + 1                                00003410
180   NPRD = L - 1                                00003420
C                                           00003430
C IF REPLACEMENT FOR LUMPED REACTION, PRINT MESSAGE AND UPDATE POINTERS 00003440
C                                           00003450
      IF (M .NE. LRXN) GO TO 183                     00003460
      N = NRXN - NLMP + KLOC                         00003470
      WRITE (NOUT,1029) KLMP(KLOC), N                 00003480
      LRXN = LRXN + KLMP(KLOC)                       00003490
      KLOC = KLOC + 1                                00003500
C                                           00003510
C REVERSE ORDER OF REACTANTS FOR PRINTING           00003520
C                                           00003530
      183 DO 185 J = 1,MAXRCT                       00003540
          K = MAXRCT - J + 1                         00003550
          NPRT(J) = NMRC(K,M)                       00003560
185 / CONTINUE                                     00003570
C                                           00003580
C PRINT SET OF REACTIONS                         00003590
C                                           00003600
      WRITE (NOUT,1004) M, RK(M), (NPRT(J), J=1,MAXRCT),
&      (COEFF(J,M), NMPD(J,M), J = 1,NPRD)          00003610
190   CONTINUE                                     00003620
C                                           00003630
C GET INITIAL CONDITIONS FOR LUMPED REACTIONS AND SPECIES 00003640
C                                           00003650
      IF (NLMP .GT. 0) CALL LMPCAL(NLMP, KLMP)        00003660
C                                           00003670
C PRINT INITIAL SPECIES CONCENTRATIONS -- EXIT IF FLAG SET 00003680
C                                           00003690
      WRITE (NOUT,1013)                               00003700
      WRITE (NOUT,1005)                               00003710
      WRITE (NOUT,1006) (NAME(J), YAX(J), J=1,NDIF)   00003720
      IF (NSTS .GT. 0)                                00003730
&WRITE (NOUT,1025) (NAME(J+NDIF), YAX(J+NDIF), J=1,NSTS) 00003740
      IF (NUNC .GT. 0)                                00003750
&WRITE (NOUT,1007) (NAME(J+NDIF+NSTS),               00003760
&      YAX(J+NDIF+NSTS), J = 1,NUNC)                 00003770
      IF (NREP .GT. 0)                                00003780
&WRITE (NOUT,1031) (NAME(J+NDIF+NSTS+NUNC),           00003790
&      YAX(J+NDIF+NSTS+NUNC), J = 1,NREP)             00003800
      IF (NINT .GT. 0)                                00003810
&WRITE (NOUT,1008) (NAME(J+NDIF+NSTS+NUNC+NREP),      00003820
&      YAX(J+NDIF+NSTS+NUNC+NREP), J = 1,NINT)        00003830
      IF (LFLAG .EQ. 1) GO TO 900                   00003840
C                                           00003850
C SET INITIAL CONDITIONS                         00003860
C                                           00003870
      HMAX = HMAXF                                    00003880
      HMIN = HMINF                                    00003890

```

## EXHIBIT A-1. LISTING OF MAIN PROGRAM MODKIN (Continued)

```

TCOUNT = TINCR                                00003910
EPS = EPSF                                    00003920
TOL = EPSF                                    00003930
H = HSTART                                    00003940
MF = 2                                         00003950
JSTART = 0                                    00003960
NPNT = 0                                       00003970
TF = 0.0                                       00003980
T = 0.0                                        00003990
TOLD = 0.0                                    00004000
MAXDER = 6                                    00004010
JFLAG = 0                                     00004020
KFLAG = 1                                     00004030
NRESET = 0                                    00004040
C
C SAVE INITIAL CONCENTRATIONS AND FLOWS      00004050
C
DO 195 J = 1,NTOT                             00004070
YOLD(J) = YAX(J)                             00004080
IF (NFW .EQ. 0) GO TO 195                     00004090
IF (FTIME(1,J) .GT. 0.0) GO TO 195           00004100
YIN(J) = FLOW(1,J)                           00004110
195 CONTINUE                                  00004120
C
C CALL DIFFERENTIAL SPECIES SOLVER -- NOTE THIS IS A RETURN POINT 00004130
C
200 CALL DIFSUB(NDIF, T, Y, SAVE, H, HMIN, HMAX, EPS, MF, 00004140
& YMAX, ERROR, KFLAG, JSTART, MAXDER, PSAVE) 00004150
C
C UPDATE TIME AND SAVE CONCENTRATIONS, CHECKING FOR NEGATIVITY 00004160
C
TF = T                                         00004170
DELT = TF - TOLD                             00004180
DO 210 J = 1,NTOT                             00004190
IF (J .LE. NDIF) YAX(J) = Y(1,J)             00004200
IF (YAX(J) .LT. 0.0) JFLAG = 1               00004210
210 CONTINUE                                  00004220
IF (JFLAG .EQ. 0) GO TO 230                   00004230
JFLAG = 0                                     00004240
C
C NEGATIVE CONCENTRATION -- RESET AND TEST STEP SIZE 00004250
C
H = 0.1 * H                                   00004260
IF (H .LT. HMIN) KFLAG = 0                   00004270
C
C TEST RESET COUNTER FOR RE-ENTRY, THEN SET TO PREVENT SAME--TEST FLAG 00004280
C
IF (NRESET .GT. 0) KFLAG = 0                 00004290
NRESET = 1                                    00004300
IF (KFLAG .NE. 1) GO TO 330                  00004310
C
C RESTORE OLD CONCENTRATIONS AND RECALL DIFSUB WITH SMALLER STEP SIZE 00004320
C
DO 220 J = 1,NTOT                             00004330
YAX(J) = YOLD(J)                             00004340
220 CONTINUE                                  00004350

```

## EXHIBIT A-1. LISTING OF MAIN PROGRAM MODKIN (Continued)

```

JSTART = -1                                00004470
GO TO 200                                  00004480
C                                           00004490
C TEST FOR AND SET POINTERS TO REPLACEMENT SPECIES 00004500
C                                           00004510
230 IF (NREP .LE. 0) GO TO 265             00004520
    LRXN = NRXN + 1                        00004530
    DO 260 M = 1,NREP                      00004540
        NR = NDIF + NSTS + NUNC + M        00004550
        ESUM = 0.0                         00004560
C                                           00004570
C FIND REACTIONS CONTAINING REPLACEMENT SPECIES 00004580
C                                           00004590
    DO 250 L = LRXN, MRXN                  00004600
        IF (KRCT(1,L) .NE. NR) GO TO 250   00004610
C                                           00004620
C MULTIPLY TOGETHER ALL OTHER REACTANT CONCENTRATIONS 00004630
C                                           00004640
    ETERM = 1.0                            00004650
    DO 240 K = 2,MAXRCT                    00004660
        NS = KRCT(K,L)                    00004670
        IF (NS .EQ. 0) GO TO 245            00004680
        ETERM = ETERM * YAX(NS)             00004690
240 CONTINUE                               00004700
C                                           00004710
C MULTIPLY BY RATE CONSTANT AND ADD TO EXPONENTIAL SUM 00004720
C                                           00004730
245 ESUM = ESUM + RK(L) * ETERM             00004740
250 CONTINUE                               00004750
C                                           00004760
C CALCULATE NEW SPECIES CONCENTRATIONS        00004770
C                                           00004780
    YAX(NR) = YAX(NR) * EXP(-ESUM * DELT) * (1.0 - DELT * Q) 00004790
260 CONTINUE                               00004800
C                                           00004810
C UPDATE LUMPED REACTIONS AND SPECIES PARAMETERS 00004820
C                                           00004830
    CALL LMPCAL(NLMP, KLMP)                00004840
C                                           00004850
C TEST FOR AND SET POINTERS TO UNCOUPLED SPECIES 00004860
C                                           00004870
265 IF (NUNC .LE. 0) GO TO 300             00004880
    DO 290 M = 1,NUNC                      00004890
        NU = NDIF + NSTS + M              00004900
        YUNC = 0.0                        00004910
        DO 270 L = 1,NRXN                 00004920
            J = KCOF(L,NU)                 00004930
            K = KRXN(L,NU)                 00004940
C                                           00004950
C CALCULATE THE RATE OF CHANGE OF THE UNCOUPLED SPECIES 00004960
C                                           00004970
    IF (J) 267, 280, 268                   00004980
267 YUNC = YUNC - R(K)                     00004990
    GO TO 270                              00005000
268 YUNC = YUNC + R(K) * COEFF(J,K)        00005010
270 CONTINUE                               00005020

```

EXHIBIT A-7. LISTING OF MAIN PROGRAM MODKIN (Continued)

280	YUNC = YUNC + Q * (YIN(NU) - YAX(NU))	00005030
C		00005040
C	CALCULATE UNCOUPLED SPECIES CONCENTRATION AND UPDATE OLD RATE	00005050
C		00005060
	YAX(NU) = YAX(NU) + (YUNC + UNCOLD(NU)) * DELT * 0.5	00005070
	UNCOLD(NU) = YUNC	00005080
290	CONTINUE	00005090
C		00005100
C	CHECK TIME FOR END AND PRINTING AND SAVING OF PLOT POINTS	00005110
C		00005120
300	IF (TF .GT. TEND) GO TO 330	00005130
	IF (TF .LE. TCOUNT) GO TO 340	00005140
C		00005150
C	INCREMENT TIME AND PLOT POINT COUNTERS	00005160
C		00005170
	TCOUNT = TCOUNT + TINCR	00005180
	NPNT = NPNT + 1	00005190
C		00005200
C	CHECK PLOT POINT COUNTER FOR OVERFLOW	00005210
C		00005220
	IF (NPNT .LE. MAXPNT) GO TO 310	00005230
	WRITE (NOUT,1019) MAXPNT, TF	00005240
	NPNT = NPNT - 1	00005250
	GO TO 330	00005260
C		00005270
C	SAVE PLOT POINTS	00005280
C		00005290
310	SAVTIM(NPNT) = TF	00005300
	DO 320 J = 1,NTOT	00005310
	SAVCON(J,NPNT) = YAX(J)	00005320
320	CONTINUE	00005330
C		00005340
C	PRINT INTERMEDIATE RESULTS	00005350
C		00005360
330	WRITE (NOUT,1009) TF	00005370
	WRITE (NOUT,1005)	00005380
	WRITE (NOUT,1006) (NAME(J), YAX(J), J = 1,NDIF)	00005390
	IF (NSTS .GT. 0)	00005400
	&WRITE (NOUT,1025) (NAME(J+NDIF), YAX(J+NDIF), J=1,NSTS)	00005410
	IF (NUNC .GT. 0)	00005420
	&WRITE (NOUT,1007) (NAME(J+NDIF+NSTS),	00005430
	& YAX(J+NDIF+NSTS), J = 1,NUNC)	00005440
	IF (NREP .GT. 0)	00005450
	&WRITE (NOUT,1031) (NAME(J+NDIF+NSTS+NUNC),	00005460
	& YAX(J+NDIF+NSTS+NUNC), J = 1,NREP)	00005470
C		00005480
C	CHECK RATE PRINT FLAG, PRINT HEADER, AND SET SORT PARAMETERS	00005490
C		00005500
	IF (NRAT .EQ. 0) GO TO 339	00005510
	WRITE (NOUT,1032)	00005520
	N = 0	00005530
	RATE = -1.0	00005540
	NP = 0	00005550
	DO 338 M = 1,NRXN	00005560
C		00005570
C	FIND LARGEST RATE	00005580



## EXHIBIT A-1. LISTING OF MAIN PROGRAM MODKIN (Continued)

C		00005590
	DO 336 L = 1,NRXN	00005600
	IF (R(L) .LT. RATE) GO TO 336	00005610
	RATE = R(L)	00005620
	NP = L	00005630
	336 CONTINUE	00005640
C		00005650
C	SAVE AND FLAG THIS RATE AND RESET SORT PARAMETERS	00005660
C		00005670
	N = N + 1	00005680
	NPRT(N) = NP	00005690
	RPRT(N) = RATE	00005700
	R(NP) = -1.0	00005710
	RATE = -1.0	00005720
	NP = 0	00005730
C		00005740
C	CHECK PRINT COUNT AND PRINT IF FULL LINE OR END OF LOOP	00005750
C		00005760
	337 IF (N. LT. MAXPRT .AND. M .NE. NRXN) GO TO 338	00005770
	WRITE (NOUT,1033) (NPRT(K), RPRT(K), K = 1,N)	00005780
	N = 0	00005790
	338 CONTINUE	00005800
C		00005810
C	CHECK FOR ERROR OR FINAL TIME PASSED, IF SO PLOT AND GET NEXT SET	00005820
C		00005830
	339 IF (TF .LT. TEND .AND. KFLAG .EQ. 1) GO TO 340	00005840
	WRITE (NOUT,1010) KFLAG	00005850
	CALL PLOT(NTIT, NPNT, NTOT, NAME, SAVTIM, SAVCON)	00005860
	GO TO 10	00005870
C		00005880
C	CHECK FOR INFLOW UPDATES	00005890
C		00005900
	340 IF (INFLW .LE. 0) GO TO 380	00005910
	DO 370 K = 1,NTOT	00005920
	DO 350 J = 1,MAXFLW	00005930
	IF (J .EQ. MAXFLW) GO TO 360	00005940
	FTEST = FTIME(J+1,K)	00005950
	IF (FTEST .GT. TF) GO TO 360	00005960
	IF (FTEST .LE. 0.) GO TO 360	00005970
	350 CONTINUE	00005980
C		00005990
C	UPDATE INFLOWS AND WRITE MESSAGE	00006000
C		00006010
	360 FTEST = FLOW(J,K)	00006020
	IF (YIN(K) .EQ. FTEST) GO TO 370	00006030
	YIN(K) = FTEST	00006040
	WRITE (NOUT,1026) NAME(K), FTEST, TF	00006050
	370 CONTINUE	00006060
C		00006070
C	UPDATE TIME AND CONCENTRATION AND TAKE NEXT TIME STEP	00006080
C		00006090
	380 TOLD = TF	00006100
	NRESET = 0	00006110
	DO 390 J = 1,NTOT	00006120
	YOLD(J) = YAX(J)	00006130
	390 CONTINUE	00006140

## EXHIBIT A-1. LISTING OF MAIN PROGRAM MODKIN (Continued)

GO TO 200	00006150
C	00006160
C END OF PROGRAM	00006170
C	00006180
900 STOP	00006190
C	00006200
C LIST OF FORMAT STATEMENTS	00006210
C	00006220
1 FORMAT (4(A4, 1X), 3(F6.0, A4), F10.0)	00006230
2 FORMAT (3A4, 3X, 9I5)	00006240
3 FORMAT (A4, 6X, F10.0)	00006250
4 FORMAT (8F10.0)	00006260
6 FORMAT (A4, 1X, I5)	00006270
7 FORMAT (8F10.0)	00006280
1001 FORMAT (33H PROGRAM CANNOT HANDLE MORE THAN , I4,	00006290
& 26H REACTIONS -- JOB ABORTED.)	00006300
1002 FORMAT (1H1, 20X, 25HMODULAR KINFITICS RUN NO. , 3A4, ////,	00006310
& 29H TOTAL NUMBER OF REACTIONS = , I3, //,	00006320
& 30H NUMBER OF LUMPED REACTIONS = , I3, //,	00006330
& 34H NUMBER OF DIFFERENTIAL SPECIES = , I3, //,	00006340
& 34H NUMBER OF STEADY STATE SPECIES = , I3, //,	00006350
& 31H NUMBER OF UNCOUPLED SPECIES = , I3, //,	00006360
& 33H NUMBER OF REPLACEMENT SPECIES = , I3, //,	00006370
& 39H NUMBER OF INERT OR CONSTANT SPECIES = , I3, //,	00006380
& 29H NUMBER OF FLOWING SPECIES = , I3, //,	00006390
& 36H REACTION RATE PRINT REQUEST FLAG = , I3, //,	00006400
& 18H TIME INCREMENT = , 1PE12.3, 9H MINUTES , //,	00006410
& 15H ENDING TIME = , 1PE12.3, 9H MINUTES , //,	00006420
& 22H STARTING STEP SIZE = , 1PE12.3, 9H MINUTES , //,	00006430
& 21H MINIMUM STEP SIZE = , 1PE12.3, 9H MINUTES , //,	00006440
& 21H MAXIMUM STEP SIZE = , 1PE12.3, 9H MINUTES , //,	00006450
& 25H CONVERGENCE TOLERANCE = , 1PE12.3, //,	00006460
& 17H DILUTION RATE = , 1PE12.3, 12H MINUTES(-1), //,	00006470
& 1H1, 26X, 18H LIST OF REACTIONS, //,	00006480
& 14H R. CONST., 8X, 9HREACTANTS, 12X, 8HPRODUCTS, /)	00006490
1003 FORMAT (14H SPECIES NAME , A4, 21H NOT IN SPECIES LIST,	00006500
& 21H JOB WILL BE ABORTED.)	00006510
1004 FORMAT (I3, 1PE11.3, 4(1X, A4), 2H =,	00006520
& 3(OPF6.2, 1X, A4))	00006530
1005 FORMAT (/, 4(18H SPECIES VALUE ))	00006540
1006 FORMAT (/, 18H DIFFERENTIAL (PPM), //, (4(3X, A4, 1PE11.3)))	00006550
1007 FORMAT (/, 15H UNCOUPLED (PPM), //, (4(3X, A4, 1PE11.3)))	00006560
1008 FORMAT (/, 20H INERT/CONSTANT (PPM), //, (4(3X, A4, 1PE11.3)))	00006570
1009 FORMAT (//, 20X, 8H TIME = , 1PE12.3, 8H MINUTES, /)	00006580
1010 FORMAT (/, 33H THIS RUN TERMINATED WITH KFLAG = , I3)	00006590
1011 FORMAT (//, 33H PROGRAM CANNOT HANDLE MORE THAN , I4,	00006600
& 24H SPECIES -- JOB ABORTED.)	00006610
1012 FORMAT (//, 33H PROGRAM CANNOT HANDLE MORE THAN , I4,	00006620
& 30H DIFFERENTIALS -- JOB ABORTED.)	00006630
1013 FORMAT (/, 1H1, 20X, 30HINITIAL SPECIES CONCENTRATIONS, /)	00006640
1019 FORMAT (/, 31H MAXIMUM NUMBER OF PLOT POINTS , I3,	00006650
& 19H HAS BEEN EXCEEDED., /, 15H POINT AT TIME , F8.2,	00006660
& 21H WILL NOT BE PLOTTED.)	00006670
1023 FORMAT (//, 33H PROGRAM CANNOT HANDLE MORE THAN , I4,	00006680
& 22H FLOWS -- JOB ABORTED.)	00006690
1024 FORMAT (//, 33H PROGRAM CANNOT HANDLE MORE THAN , I4,	00006700

## EXHIBIT A-1. LISTING OF MAIN PROGRAM MODKIN (Concluded)

&	27H FLOW TIMES -- JOB ABORTED.)	00006710
1025	FORMAT (/ , 18H STEADY STATE (PPM), // , (4(3X, A4, 1PE11.3)))	00006720
1026	FORMAT (/ , 10H INCOMING , A4, 26H CONCENTRATION CHANGED TO ,	00006730
&	1PE11.3, 4H AT , 1PE11.3, 5H MIN.)	00006740
1027	FORMAT (// , 33H PROGRAM CANNOT HANDLE MORE THAN , I4,	00006750
&	33H LUMPED REACTIONS -- JOB ABORTED.)	00006760
1028	FORMAT (16H LUMPED SPECIES , A4, 24H IS NOT FIRST SPECIES IN,	00006770
&	54H CORRESPONDING LUMPED REACTION -- JOB WILL BE ABORTED.)	00006780
1029	FORMAT (/ , 21H THE FOLLOWING SET OF , I3,	00006790
&	42H REACTIONS CORRESPONDS TO REACTION NUMBER , I3, /)	00006800
1030	FORMAT (// , 33H PROGRAM CANNOT HANDLE MORE THAN , I4,	00006810
&	39H CONTRIBUTING REACTIONS -- JOB ABORTED.)	00006820
1031	FORMAT (/ , 17H REPLACEMENT (PPM), // , (4(3X, A4, 1PE11.3)))	00006830
1032	FORMAT (/ , 15X, 44H REACTION RATES (SORTED INTO DECREASING SIZE),	00006840
&	// , 5(15H NO. RATE ), /)	00006850
1033	FORMAT (5(I5, 1PE10.2))	00006860
	END	00006870

## EXHIBIT A-2. LISTING OF SUBROUTINE LMPCAL

```

C SUBROUTINE ***** L M P C A L ***** 00000010
C 00000020
C THIS SUBROUTINE CALCULATES THE CONCENTRATIONS OF LUMPED SPECIES AND 00000030
C THE COEFFICIENTS AND RATE CONSTANTS FOR THE CORRESPONDING REACTIONS 00000040
C 00000050
C SYMBOL DEFINITIONS -- 00000060
C 00000070
C ALPHA LOCAL VALUES OF COEFF, THE PRODUCT COEFFICIENTS 00000080
C COEFF NUMBER OF PARTICLES, ONE PER PRODUCT SPECIES PER REACTION 00000090
C COLOC LOCAL VALUE OF PRODUCT COEFFICIENT 00000100
C COMIN MINIMUM ALLOWABLE COEFFICIENT SIZE 00000110
C J DO-LOOP INDICES OR LOCAL POINTERS 00000120
C K DO-LOOP INDICES OR LOCAL POINTERS 00000130
C KCOF COEFFICIENT POINTERS, ONE PER REACTION PRODUCT PER SPECIES 00000140
C KLMP NUMBER OF CONTRIBUTING REACTIONS TO EACH LUMPED REACTION 00000150
C KPRD PRODUCT POINTERS, ONE PER PRODUCT SPECIES PER REACTION 00000160
C KRCT REACTANT POINTERS, ONE PER REACTANT SPECIES PER REACTION 00000170
C KRXN REACTION POINTERS, ONE PER REACTION PER SPECIES 00000180
C L DO-LOOP INDICES OR LOCAL POINTERS 00000190
C LRXN POINTER TO LUMPED REACTION 00000200
C M DO-LOOP INDICES OR LOCAL POINTERS 00000210
C MAXPRD MAXIMUM NUMBER OF PRODUCTS 00000220
C N DO-LOOP INDICES OR LOCAL POINTERS 00000230
C NDIF NUMBER OF DIFFERENTIAL SPECIES 00000240
C NLMP NUMBER OF LUMPED REACTIONS 00000250
C NLOC NUMBER OF REPLACEMENT REACTIONS FOR THIS LUMPED REACTION 00000260
C NOUT THE FORTRAN OUTPUT UNIT NUMBER (NORMALLY 6) 00000270
C NR POINTER TO REPLACEMENT REACTION 00000280
C NRXN NUMBER OF REACTIONS 00000290
C NS POINTER TO REACTANT SPECIES 00000300
C NSTS NUMBER OF STEADY-STATE SPECIES 00000310
C Q DEGRADATION RATE, /MIN 00000320
C R REACTION RATES, SEC, ONE PER REACTION 00000330
C RK REACTION RATE CONSTANTS, PPM-MIN, ONE PER REACTION 00000340
C RKLMP LOCAL VALUE OF LUMPED RATE CONSTANT 00000350
C RKLOC LOCAL VALUES OF RK, THE REACTION RATE CONSTANTS 00000360
C SUM SUM OF CONCENTRATIONS OF ALL THE REPLACEMENT SPECIES 00000370
C TOL CONVERGENCE TOLERANCE ON STEADY-STATE ITERATION, PPM 00000380
C YAX SPECIES CONCENTRATIONS, PPM, ONE PER SPECIES 00000390
C YF THE MOLE FRACTIONS OF THE REPLACEMENT SPECIES 00000400
C YIN SPECIES INFLOW RATES, PPM/MIN, ONE PER SPECIES 00000410
C YLOC LOCAL VALUES OF YAX, THE SPECIES CONCENTRATIONS 00000420
C 00000430
C SUBROUTINE ENTRY POINT 00000440
C 00000450
C SUBROUTINE LMPCAL(NLMP, KLMP) 00000460
C 00000470
C DECLARE COMMON STORAGE 00000480
C 00000490
C COMMON RK(99), R(99), YAX(50), YIN(50), COEFF(3,99) 00000500
C COMMON KRCT(4,99), KPRD(3,99), KRXN(99,50), KCOF(99,50) 00000510
C COMMON Q, TOL, NRXN, NDIF, NSTS 00000520
C 00000530
C SET DIMENSIONS 00000540

```

## EXHIBIT A-2. LISTING OF SUBROUTINE LMPICAL (Continued)

```

C          DIMENSION YLOC(10), RKLOC(10), ALPHA(3,10), YF(10), KLMP(NLMP)      00000550
C          00000560
C          SET DATA STATEMENT PARAMETERS      00000570
C          00000580
C          DATA MAXPRD /3/, COMIN /0.0001/      00000590
C          00000600
C          SET CONTRIBUTING REACTION POINTER AND NUMBER OF CONTRIBUTING REACTIONS 00000610
C          00000620
C          NR = NRXN + 1      00000630
C          DO 70 N = 1,NLMP      00000640
C          NLOC = KLMP(N)      00000650
C          LRXN = NRXN - NLMP + N      00000660
C          00000670
C          00000680
C          SAVE RATE CONSTANT AND SAVE AND SUM SPECIES CONCENTRATIONS      00000690
C          00000700
C          SUM = 0.0      00000710
C          DO 20 K = 1,NLOC      00000720
C          NS = KRCT(1,NR)      00000730
C          RKLOC(K) = RK(NR)      00000740
C          YLOC(K) = YAX(NS)      00000750
C          SUM = SUM + YLOC(K)      00000760
C          00000770
C          SAVE PRODUCT COEFFICIENTS      00000780
C          00000790
C          DO 10 J = 1,MAXPRD      00000800
C          ALPHA(J,K) = COEFF(J,NR)      00000810
C          10 CONTINUE      00000820
C          00000830
C          ADVANCE REACTION POINTER AND SAVE OVERALL SUM      00000840
C          00000850
C          NR = NR + 1      00000860
C          20 CONTINUE      00000870
C          NS = KRCT(1,LRXN)      00000880
C          YAX(NS) = SUM      00000890
C          00000900
C          CALCULATE THE MOLE FRACTIONS      00000910
C          00000920
C          DO 30 K = 1,NLOC      00000930
C          YF(K) = YLOC(K) / SUM      00000940
C          30 CONTINUE      00000950
C          00000960
C          CALCULATE LUMPED RATE CONSTANT      00000970
C          00000980
C          RKLMP = 0.0      00000990
C          DO 40 K = 1,NLOC      00001000
C          RKLMP = RKLMP + YF(K) * RKLOC(K)      00001010
C          40 CONTINUE      00001020
C          RK(LRXN) = RKLMP      00001030
C          00001040
C          CALCULATE SPECIES COEFFICIENTS      00001050
C          00001060
C          DO 60 J = 1,MAXPRD      00001070
C          COLOC = 0.0      00001080
C          DO 50 K = 1,NLOC      00001090
C          COLOC = COLOC + ALPHA(J,K) * RKLOC(K) * YF(K)      00001100

```

## EXHIBIT A-2. LISTING OF SUBROUTINE LMPCAL (Concluded)

50 CONTINUE	00001110
C	00001120
C NORMALIZE COEFFICIENT AND CHECK FOR UNDERFLOW	00001130
C	00001140
COLOC = COLOC / RKLMP	00001150
IF (COLOC .LT. COMIN) COLOC = 0.0	00001160
COEFF(J,LRXN) = COLOC	00001170
60 CONTINUE	00001180
70 CONTINUE	00001190
C	00001200
C END OF PROGRAM -- RETURN TO CALLER	00001210
C	00001220
RETURN	00001230
END	00001240

## EXHIBIT A-3. LISTING OF SUBROUTINE DIFSUB

```

*****00000010
C* THE PARAMETERS TO THE SUBROUTINE DIFSUB HAVE 00000020
C* THE FOLLOWING MEANINGS: 00000030
C* 00000040
C* N THE NUMBER OF FIRST ORDER DIFFERENTIAL EQUATIONS. N 00000050
C* MAY BE DECREASED ON LATER CALLS IF THE NUMBER OF 00000060
C* ACTIVE EQUATIONS REDUCES. BUT IT MUST NOT BE 00000070
C* INCREASED WITHOUT CALLING WITH JSTART = 0 00000080
C* T THE INDEPENDENT VARIABLE. 00000090
C* Y AN 8 BY N ARRAY CONTAINING THE DEPENDENT VARIABLES AND 00000100
C* THEIR SCALED DERIVATIVES. Y(J+1,I) CONTAINS 00000110
C* THE J-TH DERIVATIVE OF Y(I) SCALED BY 00000120
C* H**J/FACTORIAL(J) WHERE H IS THE CURRENT 00000130
C* STEP SIZE. ONLY Y(1,I) NEED BE PROVIDED BY 00000140
C* THE CALLING PROGRAM ON THE FIRST ENTRY. 00000150
C* IF IT IS DESIRED TO INTERPOLATE TO NON MESH POINTS 00000160
C* THESE VALUES CAN BE USED. IF THE CURRENT STEP SIZE 00000170
C* IS H AND THE VALUE AT T + E IS NEEDED, FORM 00000180
C*  $S = E/H$ , AND THEN COMPUTE 00000190
C* NQ 00000200
C*  $Y(I)(T+E) = \sum_{J=0} Y(J+1,I)*S**J$  00000210
C* 00000220
C* SAVE A BLOCK OF AT LEAST 12*N FLOATING POINT LOCATIONS 00000230
C* USED BY THE SUBROUTINES. 00000240
C* H THE STEP SIZE TO BE ATTEMPTED ON THE NEXT STEP. 00000250
C* H MAY BE ADJUSTED UP OR DOWN BY THE PROGRAM 00000260
C* IN ORDER TO ACHIEVE AN ECONOMICAL INTEGRATION. 00000270
C* HOWEVER, IF THE H PROVIDED BY THE USER DOES 00000280
C* NOT CAUSE A LARGER ERROR THAN REQUESTED, IT 00000290
C* WILL BE USED. TO SAVE COMPUTER TIME, THE USER IS 00000300
C* ADVISED TO USE A FAIRLY SMALL STEP FOR THE FIRST 00000310
C* CALL. IT WILL BE AUTOMATICALLY INCREASED LATER. 00000320
C* HMIN THE MINIMUM STEP SIZE THAT WILL BE USED FOR THE 00000330
C* INTEGRATION. NOTE THAT ON STARTING THIS MUST 00000340
C* BE MUCH SMALLER THAN THE AVERAGE H EXPECTED SINCE 00000350
C* A FIRST ORDER METHOD IS USED INITIALLY. 00000360
C* EPS THE ERROR TEST CONSTANT. SINGLE STEP ERROR ESTIMATES 00000370
C* DIVIDED BY YMAX(I) MUST BE LESS THAN THIS 00000380
C* IN THE EUCLIDEAN NORM. THE STEP AND/OR ORDER IS 00000390
C* ADJUSTED TO ACHIEVE THIS. 00000400
C* MF THE METHOD INDICATOR. THE FOLLOWING ARE ALLOWED: 00000410
C* 0 AN ADAMS PREDICTOR CORRECTOR IS USED. 00000420
C* 1 A MULTI-STEP METHOD SUITABLE FOR STIFF 00000430
C* SYSTEMS IS USED. IT WILL ALSO WORK FOR 00000440
C* NON-STIFF SYSTEMS. HOWEVER THE USER 00000450
C* MUST PROVIDE A SUBROUTINE PEDERV WHICH 00000460
C* EVALUATES THE PARTIAL DERIVATIVES OF 00000470
C* THE DIFFERENTIAL EQUATIONS WITH RESPECT 00000480
C* Y'S. THIS IS DONE BY CALLING 00000490
C* PEDERV(T,Y,PW,M). PW IS AN N BY N ARRAY 00000500
C* WHICH MUST BE SET TO THE PARTIAL OF 00000510
C* THE I-TH EQUATION WITH RESPECT 00000520
C* TO THE J DEPENDENT VARIABLE IN PW(I,J). 00000530
C* PW IS ACTUALLY STORED IN AN M BY M 00000540

```

## EXHIBIT A-3. LISTING OF SUBROUTINE DIFSUB (Continued)

```

C*          ARRAY WHERE M IS THE VALUE OF N USED ON          00000550
C*          THE FIRST CALL TO THIS PROGRAM.                  00000560
C*          2 THE SAME AS CASE 1, EXCEPT THAT THIS          00000570
C*          SUBROUTINE COMPUTES THE PARTIAL                   00000580
C*          DERIVATIVES BY NUMERICAL DIFFERENCING             00000590
C*          OF THE DERIVATIVES. HENCE PEDERV IS               00000600
C*          NOT CALLED.                                       00000610
C* YMAX AN ARRAY OF N LOCATIONS WHICH CONTAINS THE MAXIMUM    00000620
C*       OF EACH Y SEEN SO FAR. IT SHOULD NORMALLY BE SET TO  00000630
C*       1 IN EACH COMPONENT BEFORE THE FIRST ENTRY. (SEE THE  00000640
C*       DESCRIPTION OF EPS.)                                00000650
C* ERROR AN ARRAY OF N ELEMENTS WHICH CONTAINS THE ESTIMATED  00000660
C*       ONE STEP ERROR IN EACH COMPONENT.                   00000670
C* KFLAG A COMPLETION CODE WITH THE FOLLOWING MEANINGS:       00000680
C*       +1 THE STEP WAS SUCCESSFUL.                          00000690
C*       -1 THE STEP WAS TAKEN WITH H = HMIN, BUT THE         00000700
C*           REQUESTED ERROR WAS NOT ACHIEVED.                00000710
C*       -2 THE MAXIMUM ORDER SPECIFIED WAS FOUND TO         00000720
C*           BE TOO LARGE.                                    00000730
C*       -3 CORRECTOR CONVERGENCE COULD NOT BE               00000740
C*           ACHIEVED FOR H .GT. HMIN.                       00000750
C*       -4 THE REQUESTED ERROR IS SMALLER THAN CAN          00000760
C*           BE HANDLED FOR THIS PROBLEM.                    00000770
C* JSTART AN INPUT INDICATOR WITH THE FOLLOWING MEANINGS:     00000780
C*       -1 REPEAT THE LAST STEP WITH A NEW H               00000790
C*       0 PERFORM THE FIRST STEP. THE FIRST STEP           00000800
C*         MUST BE DONE WITH THIS VALUE OF JSTART            00000810
C*         SO THAT THE SUBROUTINE CAN INITIALIZE             00000820
C*         ITSELF.                                           00000830
C*       +1 TAKE A NEW STEP CONTINUING FROM THE LAST.        00000840
C* JSTART IS SET TO NQ, THE CURRENT ORDER OF THE METHOD       00000850
C* DERIVATIVE USED, THIS RESTRICTS THE ORDER. IT MUST      00000900
C* BE LESS THAN 8 FOR ADAMS AND 7 FOR STIFF METHODS.        00000910
C* PSAVE A BLOCK OF AT LEAST N**2 FLOATING POINT LOCATIONS.  00000920
C*****00000930
C* DERIVATIVE USED, THIS RESTRICTS THE ORDER. IT MUST      00000900
C* BE LESS THAN 8 FOR ADAMS AND 7 FOR STIFF METHODS.        00000910
C* PSAVE A BLOCK OF AT LEAST N**2 FLOATING POINT LOCATIONS.  00000920
C*****00000930
SUBROUTINE DIFSUB(N,T,Y,SAVE,H,HMIN,HMAX,EPS,MF,YMAX,ERROR,KFLAG, 00000940
1 JSTART,MAXDER,PSAVE) 00000950
DOUBLE PRECISION A,D,E,H,R,T,Y,R1,R2,RND,EPS,EUP,EDWN,ENQ1 00000960
1 ,ENQ2,ENQ3,HMAX,HMIN,HNEW,HOLD,SAVE,TOLD,YMAX,ERROR,RACUM 00000970
2,SDOT1,SDOT2 00000980
DIMENSION Y(8,40), YMAX(40), SAVE(12,40), ERROR(40), PSAVE(1600) 00000990
DIMENSION A(8), PERTST(7,2,3), SDOT1(40), SDOT2(40) 00001000
C*****00001010
C* THE COEFFICIENTS IN PERTST ARE USED IN SELECTING THE STEP AND 00001020
C* ORDER. THEREFORE ONLY ABOUT ONE PERCENT ACCURACY IS NEEDED. 00001030
C*****00001040
DATA PERTST /2.0,4.5,7.333,10.42,13.7,17.15,1.0, 00001050
1 2.0,12.0,24.0,37.89,53.33,70.08,87.97, 00001060
1 3.0,6.0,9.167,12.5,15.98,1.0,1.0, 00001070
1 12.0,24.0,37.89,53.33,70.08,87.97,1.0, 00001080
1 1.,1.,0.5,0.1667,0.04133,0.008267,1.0, 00001090
1 1.0,1.0,2.0,1.0,.3157,.07407,.0139/ 00001100

```



## EXHIBIT A-3. LISTING OF SUBROUTINE DIFSUB (Continued)

```

      A(2)=-1.                                00001110
      IRET = 1                                00001120
      KFLAG = 1                               00001130
      IF(JSTART.LE.0) GO TO 140                00001140
C*****00001150
C* BEGIN BY SAVING INFORMATION FOR POSSIBLE RESTARTS AND CHANGING
C* H BY THE FACTOR R IF THE CALLER HAS CHANGED H. ALL VARIABLES
C* DEPENDENT ON H MUST ALSO BE CHANGED.        00001160
C* E IS A COMPARISON FOR ERRORS OF THE CURRENT ORDER NQ. EUP IS
C* TO TEST FOR INCREASING THE ORDER, EDWN. FOR DECREASING THE ORDER. 00001170
C* HNEW IS THE STEP SIZE THAT WAS USED ON THE LAST CALL. 00001180
C*****00001190
100 DO 110 I = 1,N                            00001200
      DO 110 J = 1,K                            00001210
110 SAVE(J,I) = Y(J,I)                        00001220
      HOLD = HNEW                               00001230
      IF (H.EQ.HOLD) GO TO 130                  00001240
120 RACUM = H/HOLD                             00001250
      IRET1 = 1                                00001260
      GO TO 750                                00001270
130 NQOLD = NQ                                00001280
      TOLD = T                                 00001290
      RACUM = 1.0                             00001300
      IF (JSTART.GT.0) GO TO 250                00001310
      GO TO 170                                00001320
140 IF (JSTART.EQ.-1) GO TO 160                00001330
C*****00001340
C* ON THE FIRST CALL, THE ORDER IS SET TO 1 AND THE INITIAL
C* DERIVATIVES ARE CALCULATED.                 00001350
C*****00001360
      NQ = 1                                   00001370
      N3 = N                                   00001380
      N1 = N*10                                00001390
      N2 = N1 + 1                              00001400
      N4 = N**2                                00001410
      N5 = N1 + N                              00001420
      N6 = N5 + 1                              00001430
      CALL DIFFUN(T,Y,SDOT1)                   00001440
      DO 150 I = 1,N                           00001450
150 Y(2,I) = SDOT1(I)*H                       00001460
      HNEW = H                                 00001470
      K = 2                                    00001480
      GO TO 100                                00001490
C*****00001500
C* REPEAT LAST STEP BY RESTORING SAVED INFORMATION. 00001510
C*****00001520
160 IF (NQ.EQ.NQOLD) JSTART = 1                00001530
      IF(KFLAG.GE.-1) T = T - HOLD              00001540
      NQ = NQOLD                               00001550
      K = NQ + 1                              00001560
      GO TO 120                                00001570
C*****00001580
C* SET THE COEFFICIENTS THAT DETERMINE THE ORDER AND THE METHOD
C* TYPE. CHECK FOR EXCESSIVE ORDER. THE LAST TWO STATEMENTS OF
C* THIS SECTION SET IWEVAL.GT.0 IF PW IS TO BE RE-EVALUATED
C* BECAUSE OF THE ORDER CHANGE, AND THEN REPEAT THE INTEGRATION 00001590
C*****00001600

```

## EXHIBIT A-3. LISTING OF SUBROUTINE DIFSUB (Continued)

```

C* STEP IF IT HAS NOT YET BEEN DONE (IRET = 1) OR SKIP TO A FINAL      00001670
C* SCALING BEFORE EXIT IF IT HAS BEEN COMPLETED (IRET = 2).          00001680
C*****00001690
170 IF(MF.EQ.0) GO TO 180      00001700
    IF (NQ.GT.6) GO TO 190      00001710
    GO TO (221,222,223,224,225,226),NQ      00001720
180 IF(NQ.GT.7) GO TO 190      00001730
    GO TO (211,212,213,214,215,216,217),NQ      00001740
190 KFLAG = -2      00001750
    RETURN      00001760
C*****00001770
C* THE FOLLOWING COEFFICIENTS SHOULD BE DEFINED TO THE MAXIMUM      00001780
C* ACCURACY PERMITTED BY THE MACHINE. THEY ARE IN THE ORDER USED:    00001790
C*      00001800
C* -1      00001810
C* -1/2,-1/2      00001820
C* -5/12,-3/4,-1/6      00001830
C* -3/8,-11/12,-1/3,-1/24      00001840
C* -251/720,-25/24,-35/72,-5/48,-1/120      00001850
C* -95/288,-137/120,-5/8,-17/96,-1/40,-1/720      00001860
C* -19087/60480,-49/40,-203/270,-49/192,-7/144,-7/1440,-1/5040      00001870
C*      00001880
C* -1      00001890
C* -2/3,-1/3      00001900
C* -6/11,-6/11,-1/11      00001910
C* -12/25,-7/10,-1/5,-1/50      00001920
C* -120/274,-225/274,-85/274,-15/274,-1/274      00001930
C* -180/441,-58/63,-15/36,-25/252,-3/252,-1/1764      00001940
C*****00001950
211 A(1) = -1.0      00001960
    GO TO 230      00001970
212 A(1) = -0.500000000      00001980
    A(3) = -0.500000000      00001990
    GO TO 230      00002000
213 A(1) = -0.4166666666666667      00002010
    A(3) = -0.750000000      00002020
    A(4) = -0.1666666666666667      00002030
    GO TO 230      00002040
214 A(1) = -0.375000000      00002050
    A(3) = -0.9166666666666667      00002060
    A(4) = -0.3333333333333333      00002070
    A(5) = -0.0416666666666667      00002080
    GO TO 230      00002090
215 A(1) = -0.3486111111111111      00002100
    A(3) = -1.041666666666667      00002110
    A(4) = -0.4861111111111111      00002120
    A(5) = -0.1041666666666667      00002130
    A(6) = -0.008333333333333333      00002140
    GO TO 230      00002150
216 A(1) = -0.3298611111111111      00002160
    A(3) = -1.1416666666666667      00002170
    A(4) = -0.625000000      00002180
    A(5) = -0.17708333333333333333      00002190
    A(6) = -0.02500000000      00002200
    A(7) = -0.001388888888888889      00002210
    GO TO 230      00002220

```

## EXHIBIT A-3. LISTING OF SUBROUTINE DIFSUB (Continued)

```

217  A(1) = -0.3155919312169312      00002230
      A(3) = -1.2350000000            00002240
      A(4) = -0.7518518518518519      00002250
      A(5) = -0.2552083333333333      00002260
      A(6) = -0.0486111111111111      00002270
      A(7) = -0.0048611111111111      00002280
      A(8) = -0.0001984126984126984   00002290
      GO TO 230                        00002300
221  A(1) = -1.0000000000            00002310
      GO TO 230                        00002320
222  A(1) = -0.6666666666666667      00002330
      A(3) = -0.3333333333333333      00002340
      GO TO 230                        00002350
223  A(1) = -0.5454545454545455      00002360
      A(3) = A(1)                     00002370
      A(4) = -0.09090909090909091     00002380
      GO TO 230                        00002390
224  A(1) = -0.4800000000            00002400
      A(3) = -0.7000000000            00002410
      A(4) = -0.2000000000            00002420
      A(5) = -0.0200000000            00002430
      GO TO 230                        00002440
225  A(1) = -0.437956204379562      00002450
      A(3) = -0.8211678832116788      00002460
      A(4) = -0.3102189781021898      00002470
      A(5) = -0.05474452554744526     00002480
      A(6) = -0.0036496350364963504   00002490
      GO TO 230                        00002500
226  A(1) = -0.4081632653061225      00002510
      A(3) = -0.9206349206349206      00002520
      A(4) = -0.4166666666666667      00002530
      A(5) = -0.0992063492063492      00002540
      A(6) = -0.0119047619047619      00002550
      A(7) = -0.000566893424036282     00002560
230  K = NQ+1                         00002570
      IDOUB = K                       00002580
      MTYP = (4 -MF)/2                00002590
      ENQ2 = .5/FLOAT(NQ + 1)          00002600
      ENQ3 = .5/FLOAT(NQ + 2)          00002610
      ENQ1 = .5/FLOAT(NQ)              00002620
      PEP SH = EPS                     00002630
      EUP = (PERTST(NQ,MTYP,2)*PEPSH)**2 00002640
      E = (PERTST(NQ,MTYP,1)*PEPSH)**2 00002650
      EDWN = (PERTST(NQ,MTYP,3)*PEPSH)**2 00002660
      IF (EDWN.EQ.0) GO TO 780          00002670
      BND = EPS*ENQ3/FLOAT(N)          00002680
240  IWEVAL = MF                      00002690
      GO TO (250 ,680 ),IRET           00002700
C*****00002710
C* THIS SECTION COMPUTES THE PREDICTED VALUES BY EFFECTIVELY
C* MULTIPLYING THE SAVED INFORMATION BY THE PASCAL TRIANGLE
C* MATRIX.                            00002740
C*****00002750
250  T = T + H                        00002760
      DO 260 J = 2,K                  00002770
      DO 260 J1 = J,K                 00002780

```

## EXHIBIT A-3. LISTING OF SUBROUTINE DIFSUB (Continued)

```

      J2 = K-J1 + J - 1                                00002790
      DO 260 I = 1,N                                    00002800
260   Y(J2,I) = Y(J2,I) + Y(J2+1,I)                    00002810
C*****00002820
C* UP TO 3 CORRECTOR ITERATIONS ARE TAKEN. CONVERGENCE IS TESTED 00002830
C* BY REQUIRING CHANGES TO BE LESS THAN BND WHICH IS DEPENDENT ON 00002840
C* THE ERROR TEST CONSTANT.                                00002850
C* THE SUM OF THE CORRECTIONS IS ACCUMULATED IN THE ARRAY      00002860
C* ERROR(I). IT IS EQUAL TO THE I-TH DERIVATIVE OF Y MULTIPLIED 00002870
C* BY H**K/(FACTORIAL(K-1)*A(K)), AND IS THEREFORE PROPORTIONAL 00002880
C* TO THE ACTUAL ERRORS TO THE LOWEST POWER OF H PRESENT. (H**K) 00002890
C*****00002900
      DO 270 I = 1,N                                    00002910
270   ERROR(I) = 0.0                                    00002920
      DO 430 L = 1,3                                    00002930
      CALL DIFFUN(T,Y,SDOT1)                            00002940
C*****00002950
C* IF THERE HAS BEEN A CHANGE OF ORDER OR THERE HAS BEEN TROUBLE 00002960
C* WITH CONVERGENCE, PW IS RE-EVALUATED PRIOR TO STARTING THE    00002970
C* CORRECTOR ITERATION IN THE CASE OF STIFF METHODS. IWEVAL IS   00002980
C* THEN SET TO -1 AS AN INDICATOR THAT IT HAS BEEN DONE.        00002990
C*****00003000
      IF (IWEVAL.LT.1) GO TO 350                        00003010
      IF (MF.EQ.2) GO TO 310                             00003020
      CALL PEDERV(T,Y,PSAVE,N3)                          00003030
      R = A(1)*H                                          00003040
      DO 280 I = 1,N4                                    00003050
280   PSAVE(I) = PSAVE(I)*R                              00003060
290   DO 300 I = 1,N                                    00003070
300   PSAVE(I*(N3+1)-N3) = 1.0 + PSAVE(I*(N3+1)-N3)      00003080
      IWEVAL = -1                                         00003090
      CALL MATINV(PSAVE,N3,N3,J1)                        00003100
      IF (J1.GT.0) GO TO 350                             00003110
      GO TO 440                                           00003120
310   DO 320 I = 1,N                                    00003130
320   SAVE(9,I) = Y(1,I)                                00003140
      DO 340 J = 1,N                                    00003150
      R = EPS*DMAX1(EPS,DABS(SAVE(9,J)))                 00003160
      Y(1,J) = Y(1,J) + R                               00003170
      D = A(1)*H/R                                       00003180
      CALL DIFFUN(T,Y,SDOT2)                             00003190
      DO 330 I = 1,N                                    00003200
330   PSAVE(I+(J-1)*N3) = (SDOT2(I)-SDOT1(I))*D          00003210
340   Y(1,J) = SAVE(9,J)                                00003220
      GO TO 290                                           00003230
350   IF (MF.NE.0) GO TO 370                             00003240
      DO 360 I = 1,N                                    00003250
360   SAVE(9,I) = Y(2,I)-SDOT1(I)*H                     00003260
      GO TO 410                                           00003270
370   DO 380 I = 1,N                                    00003280
380   SDOT2(I) = Y(2,I)-SDOT1(I)*H                      00003290
      DO 400 I = 1,N                                    00003300
      D = 0.0                                             00003310
      DO 390 J = 1,N                                    00003320
390   D = D + PSAVE(I+(J-1)*N3)*SDOT2(J)                00003330
400   SAVE(9,I) = D                                      00003340

```

## EXHIBIT A-3. LISTING OF SUBROUTINE DIFSUB (Continued)

```

410 NT = N
DO 420 I = 1,N
Y(1,I) = Y(1,I) + A(1)*SAVE(9,I)
Y(2,I) = Y(2,I) - SAVE(9,I)
ERROR(I) = ERROR(I) + SAVE(9,I)
IF (DABS(SAVE(9,I)).LE.(BND*YMAX(I))) NT = NT - 1
420 CONTINUE
IF (NT.LE.0) GO TO 490
430 CONTINUE
C*****
C* THE CORRECTOR ITERATION FAILED TO CONVERGE IN 3 TRIES. VARIOUS
C* POSSIBILITIES ARE CHECKED FOR. IF H IS ALREADY HMIN AND
C* THIS IS EITHER ADAMS METHOD OR THE STIFF METHOD IN WHICH THE
C* MATRIX PW HAS ALREADY BEEN RE-EVALUATED, A NO CONVERGENCE EXIT
C* IS TAKEN. OTHERWISE THE MATRIX PW IS RE-EVALUATED AND/OR THE
C* STEP IS REDUCED TO TRY AND GET CONVERGENCE.
C*****
440 IF ((H.LE.(HMIN*1.00001)).AND.((IWEVAL - MTPY).LT.-1)) GO TO 460
IF ((MF.EQ.0).OR.(IWEVAL.NE.0)) RACUM = RACUM**2*.5
IWEVAL = MF
T = T - H
IRET1 = 2
GO TO 750
460 KFLAG = -3
470 DO 480 I = 1,N
DO 480 J = 1,K
480 Y(J,I) = SAVE(J,I)
H = HOLD
NQ = NQOLD
JSTART = NQ
RETURN
C*****
C* THE CORRECTOR CONVERGED AND CONTROL IS PASSED TO STATEMENT 520
C* IF THE ERROR TEST IS O.K., AND TO 540 OTHERWISE.
C* IF THE STEP IS O.K. IT IS ACCEPTED. IF IDOUB HAS BEEN REDUCED
C* TO ONE, A TEST IS MADE TO SEE IF THE STEP CAN BE INCREASED
C* AT THE CURRENT ORDER OR BY GOING TO ONE HIGHER OR ONE LOWER.
C* SUCH A CHANGE IS ONLY MADE IF THE STEP CAN BE INCREASED BY AT
C* LEAST 1.1. IF NO CHANGE IS POSSIBLE IDOUB IS SET TO 10 TO
C* PREVENT FURTHER TESTING FOR 10 STEPS
C* IF A CHANGE IS POSSIBLE, IT IS MADE AND IDOUB IS SET TO
C* NQ + 1 TO PREVENT FURTHER TESTING FOR THAT NUMBER OF STEPS.
C* IF THE ERROR WAS TOO LARGE, THE OPTIMUM STEP SIZE FOR THIS OR
C* LOWER ORDER IS COMPUTED, AND THE STEP RETRIED. IF IT SHOULD
C* FAIL TWICE MORE IT IS AN INDICATION THAT THE DERIVATIVES THAT
C* HAVE ACCUMULATED IN THE Y ARRAY HAVE ERRORS OF THE WRONG ORDER
C* SO THE FIRST DERIVATIVES ARE RECOMPUTED AND THE ORDER IS SET
C* TO 1.
C*****
490 D = 0.0
DO 500 I = 1,N
500 D = D + (ERROR(I)/YMAX(I))**2
IWEVAL = 0
IF (D.GT.E) GO TO 540
IF (K.LT.3) GO TO 520
DO 510 J = 3,K

```

## EXHIBIT A-3. LISTING OF SUBROUTINE DIFSUB (Continued)

```

DO 510 I = 1,N                                00003910
510 Y(J,I) = Y(J,I) + A(J)*ERROR(I)           00003920
520 KFLAG = +1                                00003930
HNEW = H                                       00003940
IF (IDOUR.LE.1) GO TO 550                     00003950
IDOUR = IDOUR - 1                             00003960
IF (IDOUR.GT.1) GO TO 700                     00003970
DO 530 I = 1,N                                00003980
530 SAVE(10,I) = ERROR(I)                     00003990
GO TO 700                                     00004000
540 KFLAG = KFLAG - 2                         00004010
T = TOLD                                       00004020
IF (H.LE.(HMIN*1.00001)) GO TO 740           00004030
IF (KFLAG.LE.-5) GO TO 720                    00004040
550 PR2 = (D/E)**ENQ2*1.2                     00004050
PR3 = 1.E+20                                  00004060
IF ((NQ.GE.MAXDER).OR.(KFLAG.LE.-1)) GO TO 570 00004070
D = 0.0                                        00004080
DO 560 I = 1,N                                00004090
560 D = D + ((ERROR(I) - SAVE(10,I))/YMAX(I))**2 00004100
PR3 = (D/EUP)**ENQ3*1.4                      00004110
570 PR1 = 1.E+20                              00004120
IF (NQ.LE.1) GO TO 590                       00004130
D = 0.0                                        00004140
DO 580 I = 1,N                                00004150
580 D = D + (Y(K,I)/YMAX(I))**2              00004160
PR1 = (D/EDWN)**ENQ1*1.3                     00004170
590 CONTINUE                                  00004180
IF (PR2.LE.PR3) GO TO 650                     00004190
IF (PR3.LT.PR1) GO TO 660                     00004200
600 R = 1.0/AMAX1(PR1,1.E-4)                  00004210
NEWQ = NQ - 1                                00004220
610 IDOUR = 10                                00004230
IF ((KFLAG.EQ.1).AND.(R.LT.(1.1))) GO TO 700 00004240
IF (NEWQ.LE.NQ) GO TO 630                     00004250
DO 620 I = 1,N                                00004260
620 Y(NEWQ+1,I) = ERROR(I)*A(K)/FLOAT(K)     00004270
630 K = NEWQ + 1                              00004280
IF (KFLAG.EQ.1) GO TO 670                     00004290
RACUM = RACUM*R                              00004300
IRET1 = 3                                     00004310
GO TO 750                                     00004320
640 IDOUR = K                                 00004330
IF (NEWQ.EQ.NQ) GO TO 250                     00004340
NQ = NEWQ                                     00004350
GO TO 170                                     00004360
650 IF (PR2.GT.PR1) GO TO 600                 00004370
NEWQ = NQ                                     00004380
R = 1.0/AMAX1(PR2,1.E-4)                     00004390
GO TO 610                                     00004400
660 R = 1.0/AMAX1(PR3,1.E-4)                 00004410
NEWQ = NQ + 1                                00004420
GO TO 610                                     00004430
670 IRET = 2                                  00004440
R = DMIN1(R,HMAX/DABS(H))                     00004450
H=H*R                                         00004460

```

## EXHIBIT A-3. LISTING OF SUBROUTINE DIFSUB (Concluded)

```

      HNEW = H                                00004470
      IF (NQ.EQ.NEWQ) GO TO 680                00004480
      NQ = NEWQ                                00004490
      GO TO 170                                00004500
680   R1 = 1.0                                00004510
      DO 690 J = 2,K                           00004520
      R1 = R1*R                                00004530
      DO 690 I = 1,N                           00004540
690   Y(J,I) = Y(J,I)*R1                      00004550
      IDOUB = K                                00004560
700   DO 710 I = 1,N                           00004570
710   YMAX(I) = DMAX1(YMAX(I),DABS(Y(1,I)))    00004580
      JSTART = NQ                             00004590
      RETURN                                   00004600
720   IF (NQ.EQ.1) GO TO 780                  00004610
      CALL DIFFUN(T,Y,SDOT1)                  00004620
      R = H/HOLD                               00004630
      DO 730 I = 1,N                           00004640
      Y(1,I) = SAVE(1,I)                      00004650
      SAVE(2,I) = HOLD*SDOT1(I)               00004660
730   Y(2,I) = SAVE(2,I)*R                   00004670
      NQ = 1                                   00004680
      KFLAG = 1                               00004690
      GO TO 170                                00004700
740   KFLAG = -1                             00004710
      HNEW = H                                00004720
      JSTART = NQ                             00004730
      RETURN                                   00004740
C*****00004750
C* THIS SECTION SCALES ALL VARIABLES CONNECTED WITH H AND RETURNS 00004760
C* TO THE ENTERING SECTION. 00004770
C*****00004780
750   RACUM = DMAX1(DABS(HMIN/HOLD),RACUM)    00004790
      RACUM = DMIN1(RACUM,DABS(HMAX/HOLD))    00004800
      R1 = 1.0                                00004810
      DO 760 J = 2,K                           00004820
      R1 = R1*RACUM                            00004830
      DO 760 I = 1,N                           00004840
760   Y(J,I) = SAVE(J,I)*R1                  00004850
      H = HOLD*RACUM                          00004860
      DO 770 I = 1,N                           00004870
770   Y(1,I) = SAVE(1,I)                     00004880
      GO TO (130,250,640),IRET1              00004890
780   KFLAG = -4                             00004900
      GO TO 470                               00004910
      END                                     00004920

```

## EXHIBIT A-4. LISTING OF SUBROUTINE DIFFUN

```

C SUBROUTINE ***** D I F F U N *****                                0000001
C                                                                            0000002
C THIS SUBROUTINE CALCULATES THE RATE OF CHANGE OF DIFFERENTIAL AND      0000003
C STEADY-STATE SPECIES CONCENTRATIONS -- CALLED BY DIFSUB.                0000004
C                                                                            0000005
C                                                                            0000006
C SYMBOL DESCRIPTIONS --                                                  0000007
C                                                                            0000008
C COEFF      NUMBER OF PARTICLES, ONE PER PRODUCT SPECIES PER REACTION    0000009
C J          DO-LOOP INDICES OR LOCAL POINTERS                           0000010
C JFLAG      INDICATES SPECIES HAS BEEN SEPARATED FROM SDEN CALCULATION    0000011
C K          DO-LOOP INDICES OR LOCAL POINTERS                           0000012
C KCOF       COEFFICIENT POINTERS, ONE PER REACTION PRODUCT PER SPECIES   0000013
C KPRD       PRODUCT POINTERS, ONE PER PRODUCT SPECIES PER REACTION        0000014
C KRCT       REACTANT POINTERS, ONE PER REACTANT SPECIES PER REACTION      0000015
C KRXN       REACTION POINTERS, ONE PER REACTION PER SPECIES              0000016
C L          DO-LOOP INDICES OR LOCAL POINTERS                           0000017
C M          DO-LOOP INDICES OR LOCAL POINTERS                           0000018
C MAXPRD     MAXIMUM NUMBER OF PRODUCTS                                  0000019
C MAXRCT     MAXIMUM NUMBER OF REACTANTS                                  0000020
C N          DO-LOOP INDICES OR LOCAL POINTERS                           0000021
C NCNV       NUMBER OF CONVERGED STEADY-STATES                            0000022
C NDIF       NUMBER OF DIFFERENTIAL SPECIES                              0000023
C NOUT       THE FORTRAN OUTPUT UNIT NUMBER (NORMALLY 6)                  0000024
C NRXN       NUMBER OF REACTIONS                                           0000025
C NS         LOCAL POINTER TO STEADY-STATE SPECIES                        0000026
C NSTS       NUMBER OF STEADY-STATE SPECIES                               0000027
C NTRY       NUMBER OF ITERATION ATTEMPTS FOR STEADY-STATE CONVERGENCE     0000028
C Q          DEGRADATION RATE, /MIN                                       0000029
C R          REACTION RATES, SEC, ONE PER REACTION                       0000030
C RATE       LOCAL REPRESENTATION OF R, THE REACTION RATE                 0000031
C RK         REACTION RATE CONSTANTS, PPM-MIN, ONE PER REACTION           0000032
C SDEN       DENOMINATOR IN STEADY-STATE CALCULATION, /MIN                0000033
C SNUM       NUMERATOR IN STEADY-STATE CALCULATION, PPM/MIN               0000034
C STEST      TEST VALUE FOR STEADY-STATE CONVERGENCE, PPM                 0000035
C T          CURRENT REACTION TIME, SEC, DOUBLE PRECISION,                0000036
C           FOR AND FROM DIFSUB                                           0000037
C TOL        CONVERGENCE TOLERANCE ON STEADY-STATE ITERATION, PPM         0000038
C Y          SPECIES CONCENTRATIONS, 8 PER SPECIES, DOUBLE PRECISION,     0000039
C           FOR AND FROM DIFSUB                                           0000040
C YAX        SPECIES CONCENTRATIONS, PPM, ONE PER SPECIES                 0000041
C YCALC      LOCAL REPRESENTATION OF YDOT, THE RATE OF CHANGE             0000042
C YDOT       RATES OF CHANGE OF SPECIES CONCENTRATION, PPM/MIN, ONE PER   0000043
C           DIFFERENTIAL SPECIES, DOUBLE PRECISION, FOR DIFSUB           0000044
C YIN        SPECIES INFLOW RATES, PPM/MIN, ONE PER SPECIES               0000045
C           0000046
C BEGINNING OF PROGRAM.                                                  0000047
C           0000048
C ENTRY POINT                                                            0000049
C           0000050
C           SUBROUTINE DIFFUN(T, Y, YDOT)                                0000051
C           0000052
C DECLARE INPUTS FROM DIFSUB TO BE DOUBLE PRECISION WITH DIMENSIONS      0000053
C           0000054

```



## EXHIBIT A-4. LISTING OF SUBROUTINE DIFFUN (Continued)

```

DOURLE PRECISION T, Y, YDOT
DIMENSION Y(8,40), YDOT(40)
C
C DEFINE VARIABLES AND DIMENSIONS OF COMMON STORAGE WITH MODKIN
C
COMMON RK(99), R(99), YAX(50), YIN(50), COEFF(3,99)
COMMON KRCT(4,99), KPRD(3,99), KRXN(99,50), KCOF(99,50)
COMMON Q, TOL, NRXN, NDIF, NSTS
C
C DEFINE MISCELLANEOUS DATA VALUES
C
DATA NTRY /25/, MAXRCT /4/, MAXPRD /3/, NOUT /6/, NWARN /0/
C
C MOVE DIFFERENTIAL CONCENTRATIONS TO LOCAL ARRAY
C
DO 110 J = 1,NDIF
YAX(J) = Y(1,J)
110 CONTINUE
C
C SET ITERATION LOOP AND CALCULATE REACTION RATES
C
DO 260 N = 1,NTRY
DO 140 L = 1,NRXN
RATE = RK(L)
DO 120 K = 1,MAXRCT
J = KRCT(K,L)
IF (J .EQ. 0) GO TO 130
RATE = RATE * YAX(J)
120 CONTINUE
130 R(L) = RATE
140 CONTINUE
C
C SET CONVERGENCE COUNTER AND BEGIN STEADY-STATE CALCULATION LOOP
C
NCNV = 0
IF (NSTS .LE. 0) GO TO 255
DO 250 M = 1,NSTS
SDEN = 0
SNUM = 0.0
NS = NDIF + M
STEST = YAX(NS)
C
C IDENTIFY STEADY STATE SPECIES IN REACTION
C
DO 230 L = 1,NRXN
J = KCOF(L,NS)
K = KRXN(L,NS)
C
C SKIP OVER LUMPED MECHANISM REPLACEMENT SPECIES
C
IF (K .GT. NRXN) GO TO 230
IF (J) 205, 235, 203
C
C CALCULATE NUMERATOR OF STEADY STATE EQUATION
C
203 SNUM = SNUM + R(K) * COEFF(J,K)

```

## EXHIBIT A-4. LISTING OF SUBROUTINE DIFFUN (Continued)

```

      GO TO 230                                0000111
C                                             0000112
C START REACTION RATE CALCULATION AND SET SPECIES FLAG 0000113
C                                             0000114
205  RATE = RK(K)                             0000115
      JFLAG = 0                               0000116
      DO 210 NR = 1,MAXRCT                     0000117
      J = KRCT(NR,K)                           0000118
      IF (J .EQ. 0) GO TO 220                   0000119
      IF (J .NE. NS) GO TO 208                  0000120
C                                             0000121
C CALCULATE RATE, SKIPPING FIRST OCCURRENCE OF SPECIES IN REACTION 0000122
C                                             0000123
      IF (JFLAG .EQ. 1) GO TO 208              0000124
      JFLAG = 1                               0000125
      GO TO 210                                0000126
208  RATE = RATE * YAX(J)                     0000127
210  CONTINUE                                0000128
C                                             0000129
C CALCULATE DENOMINATOR OF STEADY STATE EQUATION 0000130
C                                             0000131
220  SDEN = SDEN + RATE                       0000132
230  CONTINUE                                0000133
C                                             0000134
C TEST VALUES FOR ZERO -- SKIP CONVERGENCE TEST IF SO 0000135
C                                             0000136
235  IF (SDEN .LE. 0.0) GO TO 240              0000137
      IF (SNUM .LE. 0.0) GO TO 240            0000138
C                                             0000139
C CALCULATE STEADY-STATE CONCENTRATION AND CHECK FOR CONVERGENCE 0000140
C                                             0000141
      STEST = SNUM / SDEN                     0000142
      IF (ABS((STEST - YAX(NS)) / STEST) .GT. TOL) GO TO 245 0000143
C                                             0000144
C UPDATE CONVERGENCE COUNTER AND SPECIES CONCENTRATION 0000145
C                                             0000146
240  NCNV = NCNV + 1                          0000147
245  YAX(NS) = STEST                          0000148
250  CONTINUE                                0000149
C                                             0000150
C TEST FOR CONVERGENCE OF ALL STEADY-STATES -- WRITE MESSAGE IF FAILED 0000151
C                                             0000152
255  IF (NCNV .EQ. NSTS) GO TO 300            0000153
260  CONTINUE                                0000154
      WRITE (NOUT,1031) NTRY                   0000155
1031 FORMAT (' STEADY STATE FAILED TO CONVERGE IN ', I3, 0000156
&          ' ITERATIONS.')                   0000157
C                                             0000158
C INCREMENT WARNING COUNTER AND STOP IF TOO MANY 0000159
C                                             0000160
      NWARN = NWARN + 1                       0000161
      IF (NWARN .GT. NTRY) STOP                0000162
C                                             0000163
C CALCULATE RATE OF CHANGE OF CONCENTRATION FOR DIFFERENTIAL SPECIES 0000164
C                                             0000165
300  DO 330 M = 1,NDIF                       0000166

```

## EXHIBIT A-4. LISTING OF SUBROUTINE DIFFUN (concluded)

YCALC = 0.0	0000167
DO 310 L = 1,NRXN	0000168
J = KCOF(L,M)	0000169
K = KRXN(L,M)	0000170
C	0000171
C SKIP OVER LUMPED MECHANISM REPLACEMENT SPECIES	0000172
C	0000173
IF (K .GT. NRXN) GO TO 310	0000174
IF (J) 305, 320, 307	0000175
305 YCALC = YCALC - R(K)	0000176
GO TO 310	0000177
307 YCALC = YCALC + R(K) * COEFF(J,K)	0000178
310 CONTINUE	0000179
320 YDOT(M) = YCALC + Q * (YIN(M) - YAX(M))	0000180
330 CONTINUE	0000181
C	0000182
C END OF ROUTINE -- RETURN TO CALLER	0000183
C	0000184
RETURN	0000185
END	0000186

## EXHIBIT A-5. LISTING OF SUBROUTINE MATINV

```

SUBROUTINE MATINV(PSAVE,N,MM,J1)                                00000010
DIMENSION A(40,40), INDEX(40,2), PIVOT(40), IPIVOT(40)        00000020
DIMENSION PSAVF(1600)                                          00000030
EQUIVALENCE (IROW,JROW), (ICOLUM,JCOLUM), (AMAX, T, SWAP)     00000040
KK = 0                                                         00000050
DO 67 I = 1,N                                                  00000060
DO 67 J = 1,N                                                  00000070
KK = KK + 1                                                    00000080
67  A(J,I) = PSAVE(KK)                                         00000090
10  DETERM=1.0                                                 00000100
15  DO 20 J=1,N                                                00000110
20  IPIVOT(J)=0                                                00000120
30  DO 550 I=1,N                                               00000130
40  AMAX=0.0                                                    00000140
45  DO 105 J=1,N                                               00000150
50  IF (IPIVOT(J)-1) 60, 105, 60                               00000160
60  DO 100 K=1,N                                               00000170
70  IF (IPIVOT(K)-1) 80, 100, 740                             00000180
80  IF (ABS (AMAX)-ABS (A(J,K))) 85, 100, 100                 00000190
85  IROW=J                                                      00000200
90  ICOLUM=K                                                    00000210
95  AMAX=A(J,K)                                                 00000220
100 CONTINUE                                                    00000230
105 CONTINUE                                                    00000240
    IF(AMAX .EQ. 0.) GO TO 760                                  00000250
110 IPIVOT(ICOLUM)=IPIVOT(ICOLUM)+1                            00000260
130 IF (IROW-ICOLUM) 140, 260, 140                             00000270
140 DETERM=-DETERM                                              00000280
150 DO 200 L=1,N                                               00000290
160 SWAP=A(IROW,L)                                              00000300
170 A(IROW,L)=A(ICOLUM,L)                                       00000310
200 A(ICOLUM,L)=SWAP                                           00000320
260 INDEX(I,1)=IROW                                             00000330
270 INDEX(I,2)=ICOLUM                                           00000340
310 PIVOT(I)=A(ICOLUM,ICOLUM)                                   00000350
320 DETERM=DETERM*PIVOT(I)                                     00000360
330 A(ICOLUM,ICOLUM)=1.0                                        00000370
340 DO 350 L= 1,N                                              00000380
350 A(ICOLUM,L)=A(ICOLUM,L)/PIVOT(I)                           00000390
380 DO 550 L1=1,N                                              00000400
390 IF(L1-ICOLUM) 400, 550, 400                                00000410
400 T=A(L1,ICOLUM)                                              00000420
420 A(L1,ICOLUM)=0.0                                            00000430
430 DO 450 L=1,N                                                00000440
450 A(L1,L)=A(L1,L)-A(ICOLUM,L)*T                              00000450
550 CONTINUE                                                    00000460
600 DO 710 I=1,N                                               00000470
610 L=N+1-I                                                    00000480
620 IF (INDEX(L,1)-INDEX(L,2)) 630, 710, 630                 00000490
630 JROW=INDEX(L,1)                                             00000500
640 JCOLUM=INDEX(L,2)                                           00000510
650 DO 705 K=1,N                                               00000520
660 SWAP=A(K,JROW)                                              00000530
670 A(K,JROW)=A(K,JCOLUM)                                      00000540

```

## EXHIBIT A-5. LISTING OF SUBROUTINE MATINV (Concluded)

700 A(K,JCOLUM)=SWAP	00000550
705 CONTINUE	00000560
J1 = 1	00000570
710 CONTINUE	00000580
740 GO TO 780	00000590
760 DETERM = 0.	00000600
J1 = -1	00000610
780 KK = 0	00000620
DO 68 I = 1,N	00000630
DO 68 J = 1,N	00000640
KK = KK + 1	00000650
68 PSAVE(KK). = A(J,I)	00000660
RETURN	00000670
END	00000680

## EXHIBIT A-6. LISTING OF SUBROUTINE PEDERV

SUBROUTINE PEDERV(T,Y,PSAVE,N)	00000010
DOUBLE PRECISION T, Y	00000020
DIMENSION Y(8,40), PSAVE(1600)	00000030
RETURN	00000040
END	00000050

## EXHIBIT A-7. LISTING OF SUBROUTINE PLOT

```

C SUBROUTINE ***** P L O T *****                                00000010
C                                                                    00000020
C THIS SUBROUTINE READS THE PLOT CARDS AND PLOTS THE RESULTS AS PART 00000030
C OF THE PRINTED OUTPUT -- IT DOES NOT DRIVE A PLOTTER.              00000040
C                                                                    00000050
C SYMBOL DESCRIPTIONS --                                           00000060
C                                                                    00000070
C CGRID      THE LENGTH OF THE VERTICAL AXIS, PPM                   00000080
C CHIGH      HIGHEST CONCENTRATION VALUE, PPM                       00000090
C CLOW       LOWEST CONCENTRATION VALUE, PPM                         00000100
C CSPAN      CONCENTRATION NORMALIZATION FACTOR                     00000110
C DATA      CONCENTRATION DATA POINTS, PPM, UP TO 80              00000120
C J          DO-LOOP INDICES OR LOCAL POINTERS                       00000130
C JBLANK     A HOLLERITH WORD OF FOUR BLANK CHARACTERS              00000140
C JCONC      CONCENTRATION LABELS                                    00000150
C JFACT      CONVERSION FACTOR FOR LABEL                             00000160
C JGRID      THE PLOTTING GRID                                       00000170
C JSTAR      THE CHARACTER '*'                                       00000180
C JSYMB      SYMBOL TO BE USED FOR PLOTTING SAVED POINTS           00000190
C JVERT      VERTICAL LEGEND                                         00000200
C K          DO-LOOP INDICES OR LOCAL POINTERS                       00000210
C KCON       CONCENTRATION COORDINATE ON GRID                       00000220
C KTIM       TIME COORDINATE ON GRID                                 00000230
C L          DO-LOOP INDICES OR LOCAL POINTERS                       00000240
C M          DO-LOOP INDICES OR LOCAL POINTERS                       00000250
C MAXCON     LIMIT ON NUMBER OF VERTICAL POINTS                     00000260
C MAXPNT     MAXIMUM NUMBER OF SAVED TIME AND CONCENTRATION POINTS 00000270
C MAXTIM     LIMIT ON NUMBER OF HORIZONTAL POINTS                   00000280
C N          DO-LOOP INDICES OR LOCAL POINTERS                       00000290
C NAME       SPECIES NAMES, ONE PER SPECIES                         00000300
C NDAT       NUMBER OF CONCENTRATION DATA POINTS                   00000310
C NIN        THE FORTRAN INPUT UNIT (NORMALLY 5)                    00000320
C NOUT       THE FORTRAN OUTPUT UNIT NUMBER (NORMALLY 6)            00000330
C NPNT       NUMBER OF SAVED TIMES AND CONCENTRATIONS               00000340
C NTEST      SPECIES NAME FOR TESTING                                00000350
C NTIT       USER-INPUT TITLE FOR PRINTOUT, 3 FOUR-CHARACTER WORDS 00000360
C NTOT       TOTAL NUMBER OF SPECIES                                 00000370
C SAVCON     SPECIES CONCENTRATIONS, PPM, ONE PER SPECIES AT 80 TIMFS 00000380
C SAVTIM     TIMES THAT CONCENTRATIONS ARE SAVED, MIN, UP TO 80 VALUES 00000390
C TGRID      THE LENGTH OF THE HORIZONTAL AXIS, MIN                 00000400
C THIGH      HIGHEST TIME VALUE, MIN                                 00000410
C TIME       TIMES AT WHICH CONCENTRATIONS ARE INPUT, MIN, UP TO 80 00000420
C TLOW       LOWEST TIME VALUE, MIN                                  00000430
C TPRINT     TIMES FOR PRINTOUT ON HORIZONTAL AXIS, MIN              00000440
C TSPAN      TIME NORMALIZATION FACTOR                               00000450
C                                                                    00000460
C BEGINNING OF PROGRAM.                                           00000470
C                                                                    00000480
C ENTRY POINT                                                       00000490
C   SUBROUTINE PLOT(NTIT, NPNT, NTOT, NAME, SAVTIM, SAVCON)          00000500
C                                                                    00000510
C SET DIMENSIONS OF INCOMING ARRAYS                                00000520
C                                                                    00000530
C   DIMENSION SAVCON(50,80), SAVTIM(80), NTIT(3), NAME(50)          00000540

```

## EXHIBIT A-7. LISTING OF SUBROUTINE PLOT (Continued)

[illegible]



## EXHIBIT A-7. LISTING OF SUBROUTINE PLOT (Continued)

```

      IF (NTEST .EQ. JBLANK) GO TO 800
C
C TEST NUMBER OF DATA POINTS AND READ DATA
C
      IF (NDAT .LE. 0) GO TO 308
      IF (NDAT .LE. MAXPNT) GO TO 305
      WRITE (NOUT,1020) MAXPNT
      GO TO 900
C
C READ DATA POINTS
C
305  READ (NIN,5) (TIME(J), DATA(J), J = 1,NDAT)
C
C SET NORMALIZATION FACTORS AND VERTICAL CONCENTRATION LABELS
C
308  CSPAN = CGRID / (CHIGH - CLOW)
      TSPAN = TGRID / (THIGH - TLOW)
      JVERT(1,2) = JCONC(5)
      JVERT(14,2) = JCONC(4)
      JVERT(27,2) = JCONC(3)
      JVERT(40,2) = JCONC(2)
C
C SET HORIZONTAL TIME LABELS
C
      DO 310 J = 1,9
      TPRINT(J) = FLOAT(J - 1) / 8. * (THIGH - TLOW) + TLOW
310  CONTINUE
C
C TEST FOR CORRECT SPECIES NAME
C
      DO 320 L = 1,NTOT
      IF (NTEST .EQ. NAME(L)) GO TO 325
320  CONTINUE
      WRITE (NOUT,1021) NTEST
      GO TO 360
C
C IF THERE ARE DATA POINTS, GET THEIR COORDINATES
C
325  IF (NDAT .LE. 0) GO TO 335
      DO 330 J = 1,NDAT
      KTIM = IFIX((TIME(J) - TLOW) * TSPAN + 1.5)
      KCON = IFIX((DATA(J) - CLOW) * CSPAN - 1.5)
      KCON = MAXCON - KCON
C
C CHECK FOR BEING WITHIN GRID, THEN PLACE ON GRID
C
      IF (KTIM .LT. 2) GO TO 330
      IF (KCON .LT. 1) GO TO 330
      IF (KTIM .GT. MAXTIM) GO TO 330
      IF (KCON .GT. MAXCON) GO TO 330
      JGRID(KTIM,KCON) = JSTAR
330  CONTINUE
C
C IF THERE ARE CALCULATED POINTS, GET THEIR COORDINATES
C
335  IF (NPNT .LE. 0) GO TO 345

```

## EXHIBIT A-7. LISTING OF SUBROUTINE PLOT (Concluded)

```

DO 340 J = 1, NPNT
KTIM = IFIX((SAVTIM(J) - TLOW) * TSPAN + 1.5)
KCON = IFIX((SAVCON(L,J) - CLOW) * CSPAN - 1.5)
KCON = MAXCON - KCON
C
C CHECK FOR BEING WITHIN GRID, THEN PLACE ON GRID
C
IF (KTIM .LT. 2) GO TO 340
IF (KCON .LT. 1) GO TO 340
IF (KTIM .GT. MAXTIM) GO TO 340
IF (KCON .GT. MAXCON) GO TO 340
JGRID(KTIM,KCON) = JSYMB
340 CONTINUE
C
C SKIP A PAGE, THEN PRINT THE VERTICAL AXIS AND GRID
C
345 WRITE (NOUT,1014)
DO 350 K = 1, MAXCON
WRITE (NOUT,1015) JVERT(K,1), JVERT(K,2),
& (JGRID(J,K), J = 1, MAXTIM)
350 CONTINUE
C
C PRINT THE HORIZONTAL AXIS AND LABELS
C
WRITE (NOUT, 1016) JCONC(1)
WRITE (NOUT,1017) TPRINT
WRITE (NOUT,1018) NTIT, NAME(L), JFACT
360 CONTINUE
C
C END OF SUBROUTINE -- RETURN TO CALLER
C
800 RETURN
900 STOP
C
C LIST OF FORMAT STATEMENTS
C
4 FORMAT (A4, 1X, I2, 1X, A1, 1X, 6(A4, 1X), 4F10.0)
5 FORMAT (8F10.0)
1014 FORMAT (1H1)
1015 FORMAT(1X, 2A4, 121A1)
1016 FORMAT (5X, A4, 1H+, 8(15H-----1))
1017 FORMAT (F12.2, 8F15.2, /, 62X, 14H TIME (MINUTES), /)
1018 FORMAT (27X, 11H FIGURE . , 3A4, 12H. SPECIES: , A4,
& 5X, 28H CONCENTRATION SCALE FACTOR: , A4)
1020 FORMAT (33H PROGRAM CANNOT HANDLE MORE THAN , I4,
& 28H PLOT POINTS -- JOB ABORTED.)
1021 FORMAT (14H1 SPECIES NAME , A4, 21H NOT IN SPECIES LIST.,
& 23H SKIPPING TO NEXT PLOT.)
END

```

EXHIBIT A-8. SAMPLE MODKIN INPUT

SAMPLE DECK			38	3	13	4	4	2	4	5	1
5.0			375.0	0.0001	0.00001	5.0			0.001		0.00835
N02				1N0		10				2.66E-1	
0	02	M		103		1M				2.00E-5	
03	N0			1N02		102				2.08E+1	
03	N02			1N03		102				4.65E-2	
N03	N0			2N02						1.50E+4	
N03	N02			1N205						4.50E+3	
N205				1N02		1N03				2.70E+1	
N205	H20			2HN03						1.00E-5	
N0	N02	H20		2HN02						2.10E-6	
HN02	HN02			1N0		1N02		1H20		4.50E00	
HN02				10H		1N0				1.30E-2	
0H	N02			1HN03						1.50E+4	
H02	N0			10H		1N02				7.00E+2	
H02	H02			1H202		102				5.30E+3	
H202				20H						1.06E-3	
ALD				0.63R02		1.37H02				2.50E-3	
ALD	0H			0.63RC03		0.37H02		1H20		2.30E+4	
R02	N0			1R0		1N02				9.10E+2	
0H	N0			1HN02						1.20E+4	
RC03	N0			1R02		1N02		1C02		9.10E+2	
RC03	N02			1PAN						1.00E+2	
R0	02			1H02		1ALD				2.40E-2	
R0	N0			1RN02						2.50E+2	
R0	N02			1RN03						4.90E+2	
R02	R02			2R0							
R02	H02			1R0		10H					
0	N0			1N02							
0	N02			1N0		102				1.38E+4	
0	N02			1N03							
N0	HN03			1HN02		1N02					
HN02	HN03			1H20		2N02					
H02	S02			1S03		10H				4.5000E-1	
R02	S02			1S03		1R0				6.0000E-1	
N03	S02			1S03		1N02				1.5000E+4	
N205	S02			1S03		2N02				4.0000E-1	
OLEF	0			1R02		0.5RC03		0.5H02		1.9776E+3	
OLEF	03			1RC03		1R0		1ALD		0.64E-2	
OLEF	0H			1R02		1ALD				0.70E+4	
OLEF		2									
PROP	0			1R02		0.5RC03		0.5H02		6.80E+3	
ETHY	0			1R02		0RC03		1H02		7.72E+2	
OLEF		2									
PROP	03			1RC03		1R0		1ALD		1.60E-2	
ETHY	03			1RC03		1R0		1ALD		4.00E-3	
OLEF											

## EXHIBIT A-8. SAMPLE MODKIN INPUT (Concluded)

H2O2									
ALD	0.10								
S02	0.334								
OLEF	1.90								
HN03									
O	1.0E-9								
N03	1.0E-10								
OH	5.0E-10								
RO	0.0								
PAN									
RN02									
RN03									
S03									
ETHY	0.19								
PROP	1.71								
M	1000000.0								
O2	210000.0								
H2O	20000.0								
CO2	10000.0								
S02	5								
	0	0.291	49	0.241	108	0.396	173	0.409	
	231	0.328							
N02	7								
	0	0.035	29	0.039	64	0.040	117	0.048	
	157	0.040	187	0.043	297	0.034			
NO	7								
	0	0.35	29	0.36	64	0.36	117	0.43	
	157	0.36	187	0.39	297	0.31			
ETHY	7								
	0	0.184	35	0.193	91	0.201	121	0.202	
	177	0.197	271	0.200	330	0.204			
PROP	7								
	0	1.656	35	1.737	91	1.809	121	1.818	
	177	1.773	271	1.800	330	1.836			
N02	9 0 10+0	0.00 0.15 0.30 0.45	0.60	0.0	0.6	0.0	400.0		
	8	0.09	29	0.27	44	0.40	64	0.33	
	117	0.26	157	0.12	187	0.14	228	0.12	
	297	0.090							
NO	7 0 10+0	0.00 0.15 0.30 0.45	0.60	0.0	0.60	0.0	400.0		
	8	0.26	29	0.16	44	0.05	64	0.00	
	117	0.00	157	0.010	187	0.00			
O3	10 0 10+0	0.00 0.15 0.30 0.45	0.60	0.0	0.6	0.0	400.0		
	11	0.025	32	0.036	47	0.314	67	0.496	
	118	0.54	158	0.46	188	0.41	229	0.41	
	298	0.45	298	0.43					
S02	10 0 10+0	0.00 0.15 0.30 0.45	0.60	0.0	0.6	0.0	400.0		
	11	0.353	11	0.384	47	0.285	108	0.186	
	108	0.136	173	0.291	231	0.173	231	0.080	
	305	0.241	305	0.415					
PAN	7 0 10+0	0.00 0.15 0.30 0.45	0.60	0.0	0.6	0.0	400.0		
	30	0.000	101	0.054	162	0.109	185	0.197	
	225	0.211	266	0.220	311	0.213			
OLEF	16 0 10+0	0.00 0.50 1.00 1.50	2.00	0.0	2.0	0.0	400.0		
	16	1.85	31	1.78	42	1.63	51	1.56	
	66	1.16	71	1.09	86	0.88	102	0.72	
	116	0.71	132	0.69	151	0.70	191	0.69	
	237	0.69	261	0.70	301	0.68	323	0.65	

## EXHIBIT A-9. SAMPLE MODKIN OUTPUT--SELECTED PAGES

## MODULAR KINETICS RUN NO. SAMPLE DECK

TOTAL NUMBER OF REACTIONS = 38  
NUMBER OF LUMPED REACTIONS = 3  
NUMBER OF DIFFERENTIAL SPECIES = 13  
NUMBER OF STEADY STATE SPECIES = 4  
NUMBER OF UNCOUPLED SPECIES = 4  
NUMBER OF REPLACEMENT SPECIES = 2  
NUMBER OF INERT OR CONSTANT SPECIES = 4  
NUMBER OF FLOWING SPECIES = 5  
REACTION RATE PRINT REQUEST FLAG = 1  
TIME INCREMENT = 5.000E 00 MINUTES  
ENDING TIME = 3.750E 02 MINUTES  
STARTING STEP SIZE = 1.000E-04 MINUTES  
MINIMUM STEP SIZE = 1.000E-05 MINUTES  
MAXIMUM STEP SIZE = 5.000E 00 MINUTES  
CONVERGENCE TOLERANCE = 1.000E-03  
DILUTION RATE = 8.350E-03 MINUTES(-1)

## EXHIBIT A-9. SAMPLE MODKIN OUTPUT--SELECTED PAGES (Continued)

## LIST OF REACTIONS

R. CONST.	REACTANTS		PRODUCTS			
1 2.660E-01		N02	=	1.00	N0	1.00 0
2 2.000E-05	M	O2	=	1.00	O3	1.00 M
3 2.080E 01		N0	=	1.00	N02	1.00 O2
4 4.650E-02		N02	=	1.00	N03	1.00 O2
5 1.500E 04		N0	=	2.00	N02	
6 4.500E 03		N02	=	1.00	N2O5	
7 2.700E 01		N2O5	=	1.00	N02	1.00 N03
8 1.000E-05		H2O	=	2.00	HN03	
9 2.100E-06	H2O	N02	=	2.00	HN02	
10 4.500E 00		HN02	=	1.00	N0	1.00 N02 1.00 H2O
11 1.300E-02		HN02	=	1.00	OH	1.00 N0
12 1.500E 04		N02	=	1.00	HN03	
13 7.000E 02		N0	=	1.00	OH	1.00 N02
14 5.300E 03		H02	=	1.00	H2O2	1.00 O2
15 1.060E-03		H2O2	=	2.00	OH	
16 2.500E-03		ALD	=	0.63	R02	1.37 H02
17 2.300E 04		OH	=	0.63	RC03	0.37 H02 1.00 H2O
18 9.100E 02		N0	=	1.00	R0	1.00 N02
19 1.200E 04		N0	=	1.00	HN02	
20 9.100E 02		N0	=	1.00	R02	1.00 N02 1.00 CO2
21 1.000E 02		N02	=	1.00	PAN	
22 2.400E-02		O2	=	1.00	H02	1.00 ALD
23 2.500E 02		N0	=	1.00	RN02	
24 4.900E 02		N02	=	1.00	RN03	
25 0.0		R02	=	2.00	R0	
26 0.0		H02	=	1.00	R0	1.00 OH
27 0.0		N0	=	1.00	N02	
28 1.380E 04		N02	=	1.00	N0	1.00 O2
29 0.0		N02	=	1.00	N03	
30 0.0		HN03	=	1.00	HN02	1.00 N02
31 0.0		HN03	=	1.00	H2O	2.00 N02
32 4.500E-01		S02	=	1.00	S03	1.00 OH
33 6.000E-01		S02	=	1.00	S03	1.00 R0
34 1.500E 04		S02	=	1.00	S03	1.00 N02
35 4.000E-01		S02	=	1.00	S03	2.00 N02
36 1.978E 03		O	=	1.00	R02	0.50 RC03 0.50 H02
37 6.400E-03		O3	=	1.00	RC03	1.00 R0 1.00 ALD
38 7.000E 03		OH	=	1.00	R02	1.00 ALD

THE FOLLOWING SET OF 2 REACTIONS CORRESPONDS TO REACTION NUMBER 36

39 6.800E 03	0	PROP	=	1.00	R02	0.50	RC03	0.50	H02
40 7.720E 02	0	ETHY	=	1.00	R02	0.0	RC03	1.00	H02

THE FOLLOWING SET OF 2 REACTIONS CORRESPONDS TO REACTION NUMBER 37

41 1.600E-02	03	PROP	=	1.00	RC03	1.00	R0	1.00	ALD
42 4.000E-03	03	ETHY	=	1.00	RC03	1.00	R0	1.00	ALD

THE FOLLOWING SET OF 2 REACTIONS CORRESPONDS TO REACTION NUMBER 38

43 2.500E 04	OH	PROP	=	1.00	R02	1.00	ALD	
44 2.500E 03	OH	ETHY	=	1.00	R02	1.00	ALD	

## EXHIBIT A-9. SAMPLE MODKIN OUTPUT--SELECTED PAGES (Continued)

## INITIAL SPECIES CONCENTRATIONS

SPECIES	VALUE	SPECIES	VALUE	SPECIES	VALUE	SPECIES	VALUE
DIFFERENTIAL (PPM)							
N02	8.000E-02	N0	2.700E-01	O3	2.200E-02	N205	0.0
H02	0.0	R02	0.0	RC03	0.0	HN02	0.0
H202	0.0	ALD	1.000E-01	S02	3.340E-01	OLEF	1.900E 00
HN03	0.0						

## STEADY STATE (PPM)

O	1.000E-09	N03	1.000E-10	OH	5.000E-10	R0	0.0
---	-----------	-----	-----------	----	-----------	----	-----

## UNCOUPLED (PPM)

PAN	0.0	RN02	0.0	RN03	0.0	S03	0.0
-----	-----	------	-----	------	-----	-----	-----

## REPLACEMENT (PPM)

ETHY	1.900E-01	PROP	1.710E 00
------	-----------	------	-----------

## INERT/CONSTANT (PPM)

M	1.000E 06	O2	2.100E 05	H2O	2.000E 04	CO2	1.000E 04
---	-----------	----	-----------	-----	-----------	-----	-----------

TIME = 5.021E 00 MINUTES

SPECIES	VALUE	SPECIES	VALUE	SPECIES	VALUE	SPECIES	VALUE
DIFFERENTIAL (PPM)							
N02	1.856E-01	N0	1.505E-01	O3	1.436E-02	N205	5.113E-07
H02	1.367E-04	R02	9.789E-05	RC03	8.061E-06	HN02	1.142E-02
H202	1.937E-04	ALD	1.904E-01	S02	3.319E-01	OLEF	1.773E 00
HN03	2.405E-03						

## STEADY STATE (PPM)

O	1.172E-08	N03	1.706E-08	OH	2.960E-07	R0	2.670E-06
---	-----------	-----	-----------	----	-----------	----	-----------

## UNCOUPLED (PPM)

PAN	2.988E-04	RN02	5.147E-04	RN03	7.154E-04	S03	3.069E-04
-----	-----------	------	-----------	------	-----------	-----	-----------

## REPLACEMENT (PPM)

ETHY	1.816E-01	PROP	1.591E 00
------	-----------	------	-----------

## EXHIBIT A-9. SAMPLE MODKIN OUTPUT--SELECTED PAGES (Continued)

## REACTION RATES (SORTED INTO DECREASING SIZE)

NO.	RATE	NO.	RATE	NO.	RATE	NO.	RATE	NO.	RATE
1	4.94E-02	2	4.92E-02	3	4.49E-02	13	1.44E-02	22	1.35E-02
18	1.34E-02	38	1.19E-02	17	1.30E-03	9	1.17E-03	20	1.10E-03
12	8.24E-04	10	5.87E-04	19	5.34E-04	16	4.76E-04	37	3.76E-04
24	2.43E-04	21	1.50E-04	11	1.48E-04	36	1.28E-04	4	1.24E-04
23	1.00E-04	14	9.91E-05	34	8.50E-05	5	3.85E-05	28	3.00E-05
32	2.04E-05	33	1.95E-05	6	1.43E-05	7	1.38E-05	15	2.05E-07
8	1.02E-07	35	6.79E-08	31	0.0	30	0.0	29	0.0
27	0.0	26	0.0	25	0.0				

TIME = 1.007E 01 MINUTES

SPECIES	VALUE	SPECIES	VALUE	SPECIES	VALUE	SPECIES	VALUE
---------	-------	---------	-------	---------	-------	---------	-------

## DIFFERENTIAL (PPM)

N02	2.753E-01	N0	5.053E-02	03	5.492E-02	N205	5.508E-06
H02	4.046E-04	R02	2.890E-04	RC03	3.710E-05	HN02	1.311E-02
H202	2.104E-03	ALD	3.073E-01	S02	3.285E-01	OLEF	1.634E 00
HN03	7.896E-03						

## STEADY STATE (PPM)

0	1.738E-08	N03	1.230E-07	OH	2.982E-07	R0	2.827E-06
---	-----------	-----	-----------	----	-----------	----	-----------

## UNCOUPLED (PPM)

PAN	2.737E-03	RN02	8.319E-04	RN03	2.355E-03	S03	2.064E-03
-----	-----------	------	-----------	------	-----------	-----	-----------

## REPLACEMENT (PPM)

ETHY	1.733E-01	PROP	1.461E 00
------	-----------	------	-----------

## REACTION RATES (SORTED INTO DECREASING SIZE)

NO.	RATE	NO.	RATE	NO.	RATE	NO.	RATE	NO.	RATE
1	7.32E-02	2	7.30E-02	3	5.77E-02	13	1.43E-02	22	1.43E-02
18	1.33E-02	38	1.10E-02	17	2.11E-03	20	1.71E-03	37	1.32E-03
12	1.23E-03	21	1.02E-03	14	8.68E-04	10	7.74E-04	16	7.68E-04
4	7.03E-04	34	6.06E-04	9	5.84E-04	24	3.81E-04	19	1.81E-04
36	1.75E-04	11	1.70E-04	6	1.52E-04	7	1.49E-04	5	9.32E-05
28	6.60E-05	32	5.98E-05	33	5.70E-05	23	3.57E-05	15	2.23E-06
8	1.10E-06	35	7.24E-07	31	0.0	30	0.0	29	0.0
27	0.0	26	0.0	25	0.0				



## EXHIBIT A-9. SAMPLE MODKIN OUTPUT--SELECTED PAGES (Continued)

INCOMING SO2 CONCENTRATION CHANGED TO 3.960E-01 AT 1.103E 02 MIN.

TIME = 1.160E 02 MINUTES

SPECIES VALUE SPECIES VALUE SPECIES VALUE SPECIES VALUE

## DIFFERENTIAL (PPM)

N02	1.451E-01	N0	7.451E-03	O3	2.239E-01	N205	1.497E-05
H02	5.998E-04	R02	4.193E-04	RC03	1.155E-04	HN02	2.416E-03
H202	1.795E-01	ALD	6.646E-01	S02	1.532E-01	OLEF	3.383E-01
HN03	3.199E-02						

## STEADY STATE (PPM)

O	9.179E-09	N03	6.252E-07	OH	1.454E-07	R0	7.696E-07
---	-----------	-----	-----------	----	-----------	----	-----------

## UNCOUPLED (PPM)

PAN	1.826E-01	RN02	6.014E-04	RN03	1.037E-02	S03	1.405E-01
-----	-----------	------	-----------	------	-----------	-----	-----------

## REPLACEMENT (PPM)

ETHY	6.209E-02	PROP	2.762E-01
------	-----------	------	-----------

## REACTION RATES (SORTED INTO DECREASING SIZE)

NO.	RATE	NO.	RATE	NO.	RATE	NO.	RATE	NO.	RATE
1	3.86E-02	2	3.86E-02	3	3.47E-02	22	3.88E-03	13	3.13E-03
18	2.84E-03	17	2.22E-03	14	1.91E-03	21	1.68E-03	16	1.66E-03
4	1.51E-03	34	1.44E-03	37	1.05E-03	38	1.03E-03	20	7.84E-04
6	4.08E-04	7	4.04E-04	12	3.16E-04	15	1.90E-04	5	6.99E-05
24	5.47E-05	9	4.54E-05	32	4.14E-05	33	3.86E-05	11	3.14E-05
10	2.63E-05	28	1.84E-05	36	1.78E-05	19	1.30E-05	8	2.99E-06
23	1.43E-06	35	9.17E-07	31	0.0	30	0.0	29	0.0
27	0.0	26	0.0	25	0.0				

INCOMING N02 CONCENTRATION CHANGED TO 4.800E-02 AT 1.185E 02 MIN.

INCOMING N0 CONCENTRATION CHANGED TO 4.300E-01 AT 1.185E 02 MIN.

TIME = 1.204E 02 MINUTES

SPECIES VALUE SPECIES VALUE SPECIES VALUE SPECIES VALUE

## DIFFERENTIAL (PPM)

N02	1.458E-01	N0	7.718E-03	O3	2.208E-01	N205	1.468E-05
H02	5.840E-04	R02	3.974E-04	RC03	1.112E-04	HN02	2.422E-03
H202	1.802E-01	ALD	6.492E-01	S02	1.554E-01	OLEF	3.173E-01
HN03	3.225E-02						

## EXHIBIT A-9. SAMPLE MODKIN OUTPUT--SELECTED PAGES (Continued)

## STEADY STATE (PPM)

O 9.225E-09 N03 6.102E-07 OH 1.514E-07 RO 7.428E-07

## UNCOUPLED (PPM)

PAN 1.831E-01 RN02 5.857E-04 RN03 1.023E-02 S03 1.420E-01

## REPLACEMENT (PPM)

ETHY 5.951E-02 PROP 2.578E-01

## REACTION RATES (SORTED INTO DECREASING SIZE)

NO.	RATE	NO.	RATE	NO.	RATE	NO.	RATE	NO.	RATE
1	3.88E-02	2	3.87E-02	3	3.54E-02	22	3.74E-03	13	3.16E-03
18	2.79E-03	17	2.26E-03	14	1.81E-03	16	1.62E-03	21	1.62E-03
4	1.50E-03	34	1.42E-03	38	1.00E-03	37	9.70E-04	20	7.81E-04
6	4.00E-04	7	3.96E-04	12	3.31E-04	15	1.91E-04	5	7.06E-05
24	5.31E-05	9	4.73E-05	32	4.08E-05	33	3.71E-05	11	3.15E-05
10	2.64E-05	28	1.86E-05	36	1.67E-05	19	1.40E-05	8	2.93E-06
23	1.43E-06	35	9.12E-07	31	0.0	30	0.0	29	0.0
27	0.0	26	0.0	25	0.0				

INCOMING ETHY CONCENTRATION CHANGED TO 2.020E-01 AT 1.226E 02 MIN.

INCOMING PROP CONCENTRATION CHANGED TO 1.818E 00 AT 1.226E 02 MIN.

TIME = 1.298E 02 MINUTES

SPECIES	VALUE	SPECIES	VALUE	SPECIES	VALUE	SPECIES	VALUE
---------	-------	---------	-------	---------	-------	---------	-------

## DIFFERENTIAL (PPM)

N02	1.514E-01	N0	8.386E-03	O3	2.122E-01	N205	1.474E-05
H02	5.474E-04	R02	3.493E-04	RC03	1.003E-04	HN02	2.508E-03
H202	1.801E-01	ALD	6.146E-01	S02	1.600E-01	OLEF	2.763E-01
HN03	3.307E-02						

## STEADY STATE (PPM)

O 9.581E-09 N03 5.899E-07 OH 1.647E-07 RO 6.859E-07

## EXHIBIT A-9. SAMPLE MODKIN OUTPUT--SELECTED PAGES (Continued)

TIME = 3.760E 02 MINUTES

SPECIES	VALUE	SPECIES	VALUE	SPECIES	VALUE	SPECIES	VALUE
DIFFERENTIAL (PPM)							
N02	1.518E-01	NO	1.044E-01	O3	1.856E-02	N2O5	5.930E-07
H02	6.287E-06	R02	2.154E-06	RCO3	1.025E-06	HN02	1.166E-02
H2O2	3.019E-02	ALD	5.619E-02	S02	2.635E-01	OLEF	1.002E-02
HN03	6.088E-02						

## STEADY STATE (PPM)

O	9.607E-09	NO3	2.370E-08	OH	1.367E-07	RO	4.048E-08
---	-----------	-----	-----------	----	-----------	----	-----------

## UNCOUPLED (PPM)

PAN	5.204E-02	RN02	1.897E-04	RN03	2.607E-03	S03	7.403E-02
-----	-----------	------	-----------	------	-----------	-----	-----------

## REPLACEMENT (PPM)

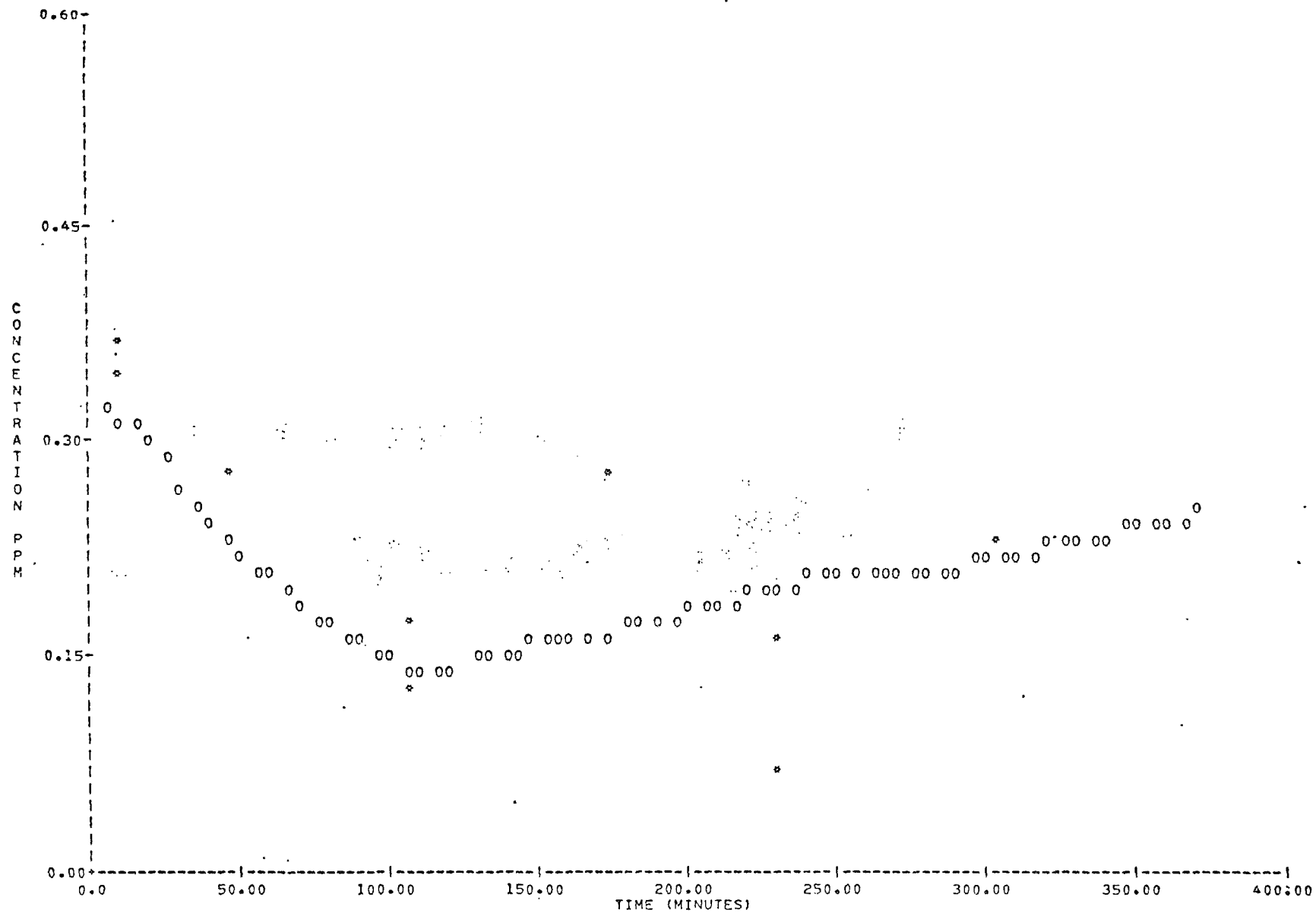
ETHY	5.277E-03	PROP	4.743E-03
------	-----------	------	-----------

## REACTION RATES (SORTED INTO DECREASING SIZE)

NO.	RATE	NO.	RATE	NO.	RATE	NO.	RATE	NO.	RATE
1	4.04E-02	2	4.03E-02	3	4.03E-02	9	6.66E-04	10	6.11E-04
13	4.62E-04	12	3.11E-04	18	2.06E-04	22	2.04E-04	17	1.77E-04
19	1.71E-04	11	1.52E-04	16	1.40E-04	4	1.31E-04	20	9.80E-05
34	9.37E-05	5	3.71E-05	15	3.20E-05	28	2.01E-05	38	1.88E-05
6	1.62E-05	7	1.60E-05	21	1.57E-05	24	3.01E-06	37	1.88E-06
23	1.06E-06	32	7.49E-07	36	3.65E-07	33	3.42E-07	14	2.11E-07
8	1.19E-07	35	6.25E-08	31	0.0	30	0.0	29	0.0
27	0.0	26	0.0	25	0.0				

THIS RUN TERMINATED WITH KFLAG = 1

EXHIBIT A-9. SAMPLE MODKIN OUTPUT--SELECTED PAGES (Concluded)



• SAMPLE DECK • SPECIES: SO2 CONCENTRATION SCALE FACTOR: 10\*0

## REFERENCES

- Bergstrom, R. W. and R. Viskanta (1973), "Modeling of the Effects of Gaseous and Particulate Pollutants in the Urban Atmosphere. Part I. Thermal Structure," J. Applied Meteor., Vol. 12, p. 901.
- Blackadar, A. K. (1962), "The Vertical Distribution of Wind and Turbulent Exchange in a Neutral Atmosphere," J. Geo. Res., Vol. 67, p. 3095.
- Boris, J. P. and D. L. Book (1973), "Flux Corrected Transport. 1. SHASTA, An Algorithm That Works," J. of Comp. Phys., Vol. 11, pp. 38-69.
- Bufalini, M. (1971), Environ. Sci. Technol., Vol. 5, p. 685.
- Calvert, J. G. (1975), to appear in Environ. Letters.
- Castleman, A. W., Jr., R. E. Davis, H. R. Munkelwitz, I. N. Tang, W. P. Wood (1974), "Symposium on Chemical Kinetics Data for the Lower and Upper Atmosphere," Warrenton, Virginia (September 1974).
- Cheng, R. T., M. Corn, and J. O. Frohlinger (1971), Atmos. Environ., Vol. 5, p. 987.
- Cox, R. A. (1974), to appear in J. Photochemistry.
- Cox, R. A., and S. A. Penkett (1972), J. Chem. Soc., Faraday Transactions I, Part 9, Vol. 68, p. 1735.
- Crowley, W. P. (1968), "Numerical Advection Experiments," Monthly Weather Review, Vol. 96, pp. 1-11.
- Davenport, A. G. (1965), "The Relationship of Wind Structures to Wind Loading," Proc. Conf. on Wind Effects on Buildings and Structures, H.M.S.O., London.
- Davis, D. D., W. Payne, and L. Stief (1973), J. Amer. Chem. Soc., Vol. 95, p. 7614.
- Deacon, E. L. (1949), "Vertical Diffusion in the Lowest Layers of the Atmosphere," Quart. J. Roy. Meteorol. Soc., Vol. 75, p. 323.
- DeMarrais, G. A. (1959), "Wind Speed Profiles at Brookhaven National Laboratory," J. Applied Meteorol., Vol. 16, p. 181.
- Egan, B. A. and J. R. Mahoney (1972), "Numerical Modeling of Advection and Diffusion of Urban Area Source Pollutants," J. of Applied Meteorol., Vol. 11, pp 312-322.
- \_\_\_\_ (1971), "Application of a Numerical Air Pollution Transport Model to Dispersion in the Atmospheric Boundary Layer," J. of Applied Meteorol., Vol. 11, pp. 1023-1039.

- Eschenroeder, A. Q., J. R. Martinez, and R. A. Nordsieck (1972), "Evaluation of a Diffusion Model for Photochemical Smog Simulation." Report CR-1-273, General Research Corporation, Santa Barbara, California.
- Fankhauser, J. C. (1974), "The Derivation of Consistent Fields of Wind and Geopotential Height from Mesoscale Rawindsonde Data," J. Applied Meteorol. Vol. 13, p. 637.
- Foster, P. M. (1969), Atmos. Environ., Vol. 3, p. 157.
- Fromm, J. E. (1969), "Practical Investigation of Corrective Difference Approximations of Reduced Dispersion," Physics of Fluids, Supplement II, pp II-3 - II-12.
- Gartrell, F. E. et al. (1963), J. Ann. Ind. Hyg. Assoc., Vol. 24, p. 113.
- Gear, C. W. (1971), "The Automatic Integration of Ordinary Differential Equations," Comm. ACM, Vol. 14, p. 176.
- Gerhard, E. G. and H. F. Johnstone (1955), Ind. Eng. Chem., Vol. 47, p. 972.
- Harlow, F. H. and J. E. Welch (1965), "Numerical Calculation of Time Dependent Viscous Incompressible Flow of Fluids with Free Surface," Physics of Fluids, Vol. 3, pp. 2182-2189.
- Hecht, T. A., J. H. Seinfeld, and M. C. Dodge (1974), "Further Development of a Generalized Mechanism for Photochemical Smog," Environ. Sci. Technol., Vol. 8, p. 327.
- Hecht, T. A., P. M. Roth, and J. H. Seinfeld (1973), "Mathematical Simulation of Photochemical Reactions: Model Development, Validation, and Applications," Report R73-28, Systems Applications, Incorporated, San Rafael, California.
- Hecht, T. A. (1972), "Further Validation of a Generalized Mechanism Suitable for Describing Atmospheric Photochemical Reactions," Report 72-SAI-26, Systems Applications, Incorporated, San Rafael, California.
- \_\_\_\_\_ (1972), "Further Validation of a Generalized Mechanism Suitable for Describing Atmospheric Photochemical Reactions," Appendix B, of "Further Development and Validation of a Simulation Model for Estimating Ground Level Concentrations of Photochemical Pollutants," Report 72-SAI-26, Systems Applications, Incorporated, San Rafael, California.
- Hecht, T. A. and J. H. Seinfeld (1972), Environ. Sci. Technol., Vol. 6, p. 47.
- Hino, M. (1968), "Computer Experiment on Smoke Diffusion over Complicated Topography," Atm. Environ., Vol. 2, p. 541.
- Hosler, C. R. (1969), "Vertical Diffusivity from Radon Profiles," J. Geophys. Res., Vol. 74, p. 7018.

- Hotchkiss, R. S. and O. S. Hirt (1972), "Particulate Transport in Highly Disturbed Three-Dimensional Flow Fields," LA-DC-72-364, Los Alamos Laboratories, Los Alamos, New Mexico.
- Jerskey, T. N. et al. (1975), "Analysis of the Data from the Three-Dimensional Gradient Study - Final Report," Systems Applications, Incorporated, San Rafael, California.
- Jones, P. M., M.A.B. de Larrinaga and C. B. Wilson (1971), "The Urban Wind Velocity Profile," Atmos. Environ., Vol. 5, p. 181.
- Johnstone, H. F., and D. R. Coughanowr (1958), Ind. Eng. Chem., Vol. 50, p. 1169.
- Johnstone, H. F., and A. J. Moll (1960), Ind. Eng. Chem., Vol. 52, p. 861.
- Jung, C. E., and T. G. Ryan (1958), Quart. J. Roy. Meteor. Soc., Vol. 84, p. 46.
- Keldysh, M. V. (1964), "On B. G. Galerkin's Method for the Solution of Boundary Value Problems," NASA Technical Translation, NASA TT F-195 (March 1964).
- Laikhtman, D. L. (1944), "Profile of Wind and Interchange in the Layer of the Atmosphere Near the Ground," Bull. Acad. Sci., U.S.S.R., Geo. and Geophys., Ser. 8, No. 1.
- Lissaman, P.B.S. (1973), "A Simple Unsteady Concentration Model Explicitly Incorporating Ground Roughness and Heat Flux," paper presented at the 66th Annual Meeting of the Air Pollution Control Association, June 24-28, Chicago, Illinois.
- Liu, M. K., P. Mundkur, and M. A. Yocke (1974), "Assessment of the Feasibility of Modeling Wind Fields Relevant to the Spread of Brush Fires," Report R74-15, Systems Applications, Incorporated, San Rafael, California.
- Lloyd, A. C. (1974), "Evaluated and Estimated Kinetic Data for Gas Phase Reactions of the Hydroperoxyl Radical," Int. J. Chem. Kinetics, Vol. 6, p. 169.
- Mahoney, J. R., and B. A. Egan (1970), "A Mesoscale Numerical Model of Atmospheric Transport Phenomena in Urban Areas," paper presented at the Second International Air Pollution Conference of the International Union of Air Pollution Prevention Association, Raleigh, North Carolina.
- Matteson, M. J., W. Stober, and H. Luther (1969), I & E. C. Fundamentals, Vol. 8, p. 677.
- McMichael, C. L., and G. W. Thomas (1973), "Reservoir Simulation by Galerkin's Method," J. of SPE, pp. 123-138 (June 1973).
- Mikusinski, J. (1959), Operational Calculus (Pergamon Press, Warsaw, Poland).
- O'Brien, J. J. (1970), "Alternative Solutions to the Classical Vertical Velocity Problem," J. Applied Meteor., Vol. 9, p. 197.
- O'Neal, H. E., and C. Blumstein (1973), Inter. J. Chem. Kinetics, Vol. V, p. 397.

- Pandolfo, J. P., M. A. Atwater, and G. E. Anderson (1971), "Prediction by Numerical Models of Transport and Diffusion in an Urban Boundary Layer," Final Report. The Center for the Environment and Man, Incorporated, Hartford, Connecticut.
- Pinder, G. F., and W. G. Gray (1974), "The Finite Element Method in Surface and Subsurface Hydrology," Notes for a summer course on hydrology, Princeton University, Princeton, New Jersey.
- Plate, E. J. (1971), "Aerodynamic Characteristics of Atmospheric Boundary Layers," U. S. Atomic Energy Commission, Oak Ridge, Tennessee.
- Price, H. S., R. S. Varga, and J. E. Warren (1966), "Applications of Oscillation Matrices to Diffusion Convection Equations," J. Math. Phys., Vol. 45, pp. 301-311.
- Ragland, K. W. (1973), "Multiple Box Model for Dispersion of Air Pollutants from Area Sources," Atm. Environ., Vol. 7, p. 1017.
- Reynolds, S. D., M. K. Liu, T. A. Hecht, P. M. Roth, and J. H. Seinfeld (1973), "Further Development and Evaluation of a Simulation Model for Estimating Ground Level Concentrations of Photochemical Pollutants." Final Report and four appendices. Systems Applications, Incorporated, San Rafael, California.
- Reynolds, S. D., P. M. Roth, and J. H. Seinfeld (1973), "Mathematical Modeling of Photochemical Air Pollution - I. Formulation of the Model," Atmos. Environ., Vol. 7., pp. 1033-1061.
- Reynolds, S. D. (1973), "Numerical Integration of the Continuity Equations. Appendix D of Further Development and Validation of a Simulation Model for Estimating Ground Level Concentrations of Photochemical Pollutants," Report R73-17, Systems Applications, Incorporated, San Rafael, California.
- Roberts, P.J.W., P. M. Roth, and C. L. Nelson (1971), "Contaminant Emissions in the Los Angeles Basin--Their Sources, Rates, and Distribution. Appendix A of "Development of a Simulation Model for Estimating Ground Level Concentrations of Photochemical Pollutants." Report 71-SAI-6, Systems Applications, Incorporated, San Rafael, California.
- Roth, P. M., S. D. Reynolds, and P.J.W. Roberts (1971), "The Treatment of Meteorological Variables. Appendix C of Development of a Simulation Model for Estimating Ground Level Concentrations of Photochemical Pollutants." Report 71-SAI-17, Systems Applications, Incorporated, San Rafael, California.
- Seinfeld, J. H. (1973), "Existing Needs in the Experimental and Observational Study of Atmospheric Chemical Reactions," Report EPA-R4-73-031, Systems Applications, Incorporated, San Rafael, California.
- Seinfeld, J. H., T. A. Hecht, and P. M. Roth (1971), "A Kinetic Mechanism for Photochemical Reactions," Report 71-SAI-9, Systems Applications, Incorporated, San Rafael, California.



- Seinfeld, J. H., T. A. Hecht, and P. M. Roth (1971), "A Kinetic Mechanism for Atmospheric Photochemical Reactions," Appendix B of "Development of a Simulation Model for Estimating Ground Level Concentration of Photochemical Pollutants," Report 71-SAI-9, Systems Applications, Incorporated, San Rafael, California.
- Shellard, H. C. (1965), "The Estimation of Design Wind Speeds," Proc. Conf. on Wind Effects on Building and Structures, H.M.S.O., London.
- Shir, C. C., and L. J. Shieh (1973), "A Generalized Urban Air Pollution Model and Its Application to the Study of SO<sub>2</sub> Distributions in the St. Louis Metropolitan Area," Report No. RJ1227 (#19588), IBM Research Laboratory, San Jose, California.
- Sklarew, R. C., A. J. Fabrick, and J. E. Prager (1971), "A Particle-In-Cell Method for Numerical Solution of the Atmospheric Diffusion Equation and Applications to Air Pollution Problems," Final Report No. 3SR-844, EPA Contract 68-02-0006, Systems, Science, and Software, La Jolla, California.
- Smith, J. P., and P. Urone (1974), Environ. Sci. Technol., Vol. 8, p. 742.
- Trijonis, J. C., and K. W. Arledge (1975), "Utility of Reactivity Criteria in Organic Emission Control Strategies for Los Angeles," TRW Environmental Services, Redondo Beach, California.
- Urone, P., and W. H. Schroeder (1969), Environ. Sci. Technol. Vol. 3, p. 436.
- Whitney, D. C. (1974), "The Automatic Construction of Chemical Kinetics Mechanisms and Solution of Their Governing Equations," Report R73-51, Systems Applications, Incorporated, San Rafael, California.
- Wilson, W. E., Jr., and A. Levy (1969), "A Study on Sulfur Dioxide in Photochemical Smog. II.," Project S-11, Battelle Memorial Institute, Columbus, Ohio.
- Wilson, W. E., Jr., A. Levy, and D. B. Wimmer (1972), J. Air Pollut. Contr. Assn., Vol. 22, p. 27.
- Wu, S. S. (1965), "A Study of Heat Transfer Coefficients in the Lowest 400 Meters of the Atmosphere," J. Geophys. Res., Vol. 70, p. 1801.
- Yanenko, N. N. (1969), Method of Fractional Steps (Springer-Verlag, New York).
- Zienkiewicz, O. C. (1971), The Finite Element Method in Engineering Science (McGraw-Hill, London, England).

TECHNICAL REPORT DATA (Please read Instructions on the reverse before completing)		
1. REPORT NO. EPA-600/4-76-016b	2.	3. RECIPIENT'S ACCESSION NO.
4. TITLE CONTINUED RESEARCH IN MESOSCALE AIR POLLUTION SIMULATION MODELING. VOLUME II. Refinements in the Treatment of Chemistry, Meteorology, and Numerical Integration Procedures	5. REPORT DATE May 1976	6. PERFORMING ORGANIZATION CODE
	8. PERFORMING ORGANIZATION REPORT NO. EF75-69	
7. AUTHOR(S) S. D. REYNOLDS, J. P. MEYER, T. A. HECHT, D. C. WHITNEY, J. AMES, AND M. A. YOCKE	10. PROGRAM ELEMENT NO. 1AA009	
	11. CONTRACT/GRANT NO. 68-02-1237	
9. PERFORMING ORGANIZATION NAME AND ADDRESS SYSTEMS APPLICATION 950 NORTHGATE DRIVE SAN RAFAEL, CALIFORNIA 94903	13. TYPE OF REPORT AND PERIOD COVERED FINAL REPORT 6/74-6/75	
	14. SPONSORING AGENCY CODE EPA-ORD	
12. SPONSORING AGENCY NAME AND ADDRESS ENVIRONMENTAL SCIENCES RESEARCH LABORATORY OFFICE OF RESEARCH AND DEVELOPMENT U. S. ENVIRONMENTAL PROTECTION AGENCY RESEARCH TRIANGLE PARK, N.C. 27711		
15. SUPPLEMENTARY NOTES		
16. ABSTRACT  This report describes the refinement of a mesoscale photochemical air quality simulation model through studies of selected chemical and meteorological phenomena that contribute to air pollution. The chemistry activities focused on the design of an automatic computer program for evaluating kinetic mechanisms, the improvement of a photochemical mechanism for incorporation in mesoscale models, and the development of a chemical mechanism for describing SO <sub>2</sub> oxidation. The meteorology studies examined the sensitivity of the model to the inclusion of wind shear, algorithms for deriving mass-consistent wind fields, and the treatment of turbulent diffusivities and elevated inversion layers. Alternative numerical techniques for solving the advection/diffusion equation in grid models are evaluated, including various finite difference, particle-in-cell, and finite element methods, in an attempt to find a suitable methodology for accurately calculating the horizontal transport of pollutants. Finally, the report considers the problem of multiday model usage and presents results from a two-day CO simulation for the Los Angeles basin.		
17. KEY WORDS AND DOCUMENT ANALYSIS		
a. DESCRIPTORS	b. IDENTIFIERS/OPEN ENDED TERMS	c. COSATI Field/Group
*Air Pollution *Photochemical Reactions *Reaction Kinetics *Numerical Analysis *Mathematical Models *Meteorological Data		13B 07E 07D 12A 14B 04B
18. DISTRIBUTION STATEMENT  RELEASE TO PUBLIC	19. SECURITY CLASS (This Report) UNCLASSIFIED	21. NO. OF PAGES 287
	20. SECURITY CLASS (This page) UNCLASSIFIED	22. PRICE